UNIVERSITI TUNKU ABDUL RAHMAN DU012(A) 拉曼大學(優大)
Wholly owned by UTAR Education Foundation Co. No. 578227-M

CMS Bulletin 2019

Publisher: Centre for Mathematical Sciences, Universiti Tunku Abdul Rahman

Publication Date: 31 December 2019 (Version 2019)

Language: English, Malay, Chinese

e-ISSN: 2710-6896

Table of Contents

Editorial Board

Publisher

Centre for Mathematical Sciences
Universiti Tunku Abdul Rahman
Jalan Sungai Long, Bandar Sungai Long,
Cheras, 43000 Kajang,
Selangor, Malaysia.

Publication Date: 31 December 2019

Language: English, Malay, Chinese

Frequency: Yearly (*This version is published specifically for the year 2019*)

All editorial correspondences can be addressed to:
Ts Dr Teoh Lay Eng
Chairperson
Centre for Mathematical Sciences
Universiti Tunku Abdul Rahman
Jalan Sungai Long, Bandar Sungai Long,
Cheras, 43000 Kajang,
Selangor, Malaysia.
Email: teohle@utar.edu.my

Website: http://cms.research.utar.edu.my/Bulletin.php

Preface

Dr Wong Voon Hee

Head of Department of Mathematical and Actuarial Sciences
Advisor of Centre for Mathematical Sciences

On behalf of the Department of Mathematical and Actuarial Sciences (DMAS), I would like to say good job and well done to all of my colleagues. Thank you very much for the time, effort and support that you put into this bulletin. From here, I can observe a great leadership from the chairperson of Centre for Mathematical Sciences (CMS) and team spirits from the committee and CMS members. Together, we make this happen.

Ts Dr Teoh Lay Eng

Chairperson of Centre for Mathematical Sciences

Conducting multi-discipline research is one of the primary goals of CMS (Centre for Mathematical Sciences). Correspondingly, this bulletin aims to provide an insightful platform for the members to share informative findings, either theoretically or practically, in various disciplines. In addition, this bulletin also summarizes numerous events organized/co-organized by CMS in the past twelve months. Although challenges are inevitable, all events became possible with the hard work, commitment and cooperation from all related parties. Thus, I would like to take this opportunity to extend my appreciation and gratitude to those involved in the events conducted by CMS throughout the year 2019. Especially to the University, faculty, organizing committee, collaborators, industries, invited speakers, participants and also student helpers, thank you very much for your contributions, supports and understanding! Let's keep our spirit high and let's strive towards a great 2020!

Centre for
Mathematical Sciences

Introduction

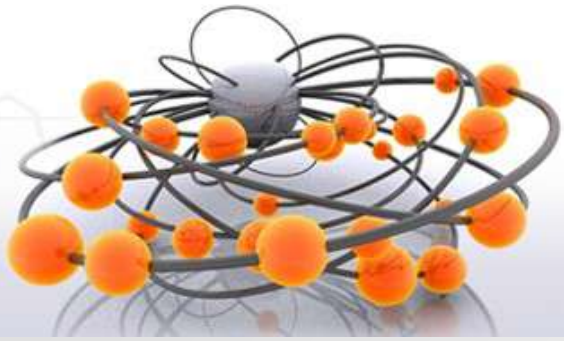

Centre for Mathematical Sciences (CMS) is an interdisciplinary centre that promotes fundamental research in mathematics and applies mathematical methods to solve problems in computational sciences, physical sciences, biological sciences, engineering and finance, leading to deeper understanding of mathematical theory and improved application of mathematics in the said areas. The goals of the research centre are stated as follows:

1. To bring together mathematicians and researchers from theoretical mathematics, computational sciences, physical sciences, life sciences, engineering and finance backgrounds to tackle fundamental problems requiring significant mathematical input.
2. To train outstanding young mathematicians to carry out research in their chosen field of mathematics and/or in interdisciplinary fields of research.
3. To provide a platform for the young and/or experienced researchers to interact on issues/research related to emerging areas of mathematics and their applications in other disciplines.
4. To act as a resource centre for the Malaysian mathematics research and/or education communities.
5. To provide consultancy in the areas of mathematical modelling, scientific visualization, survey research and mathematics education.

Research Group for the Year 2020

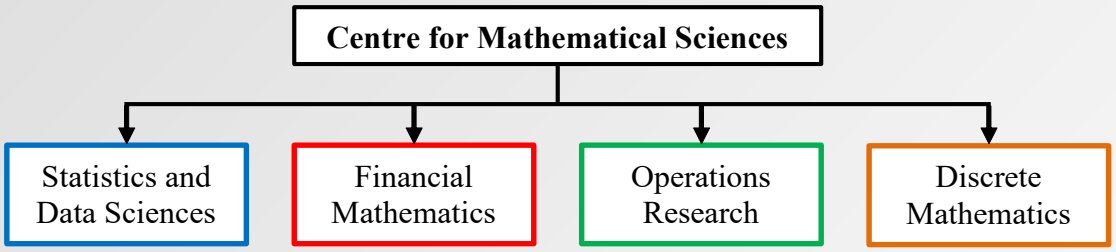

Statistics and Data Sciences research group is a UTAR-wide focal point for advancing research and education platform related to statistics and data sciences. This group undertakes research into a diverse range of fundamental and applied statistics, in particular with the emergence of the "Big Data" phenomenon. The team members specializes in a wide range of multidisciplinary researches that spans the fields of computer science, medicine, public policy, finance, quality control, and others.

Financial Mathematics research group focuses on the applications of data envelopment analysis and econometrics in portfolio/risk management, deep learning in financial networks, stochastic processes and universal portfolio, as well as pricing and valuation of natural gas related commodities.

Operation Research group focuses on various research fields, including supply chain, logistics, transportation system, optimization, inventory control, numerical modeling and analysis. The team members also provide consultancy on the related research field.

Discrete Mathematics research group forms the basis of many real-world scientific fields, especially in computer science. The primary techniques learned in a discrete mathematics course can be applied to numerous fields such as cryptography and data science.

Organization Chart 2019

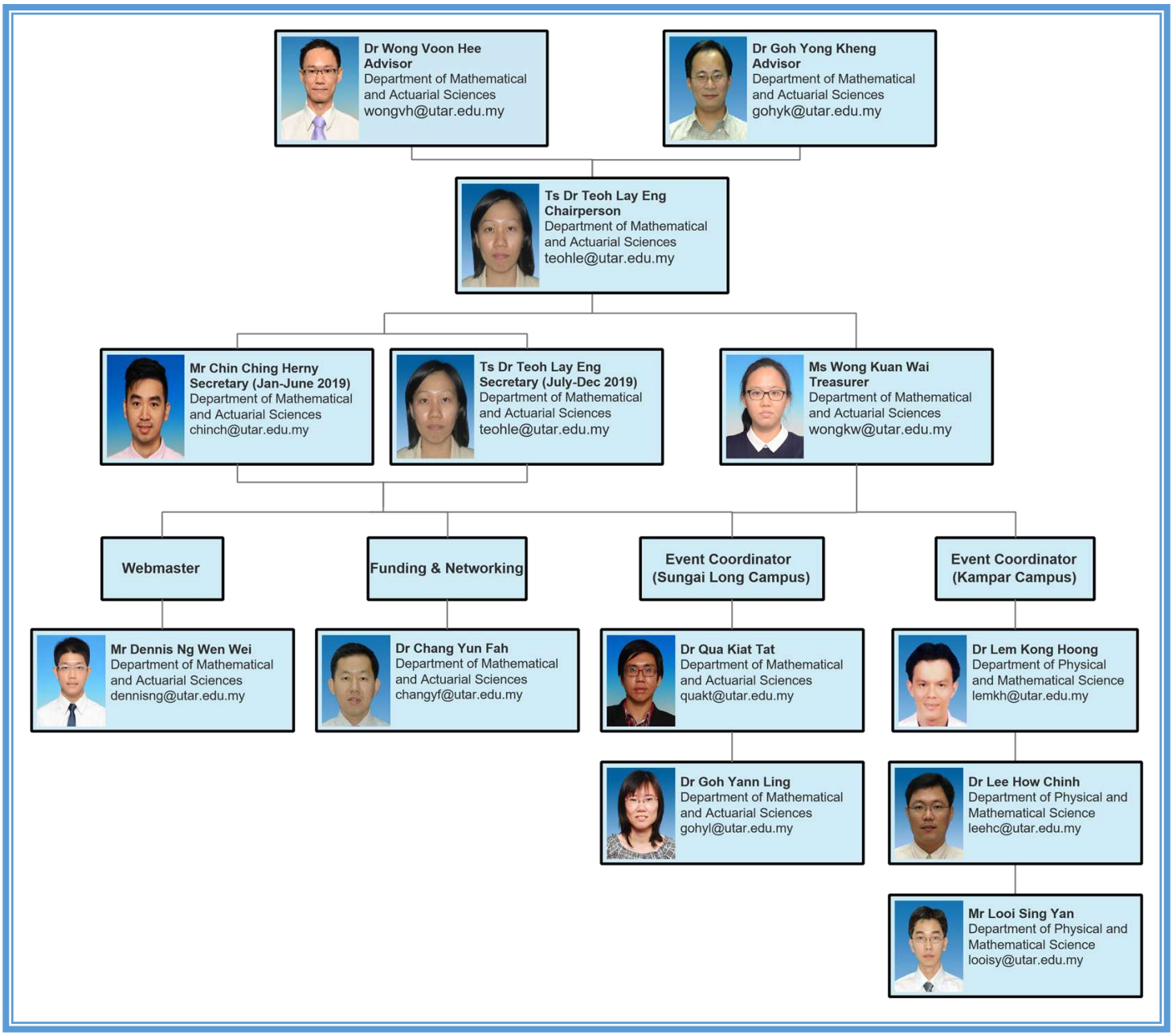

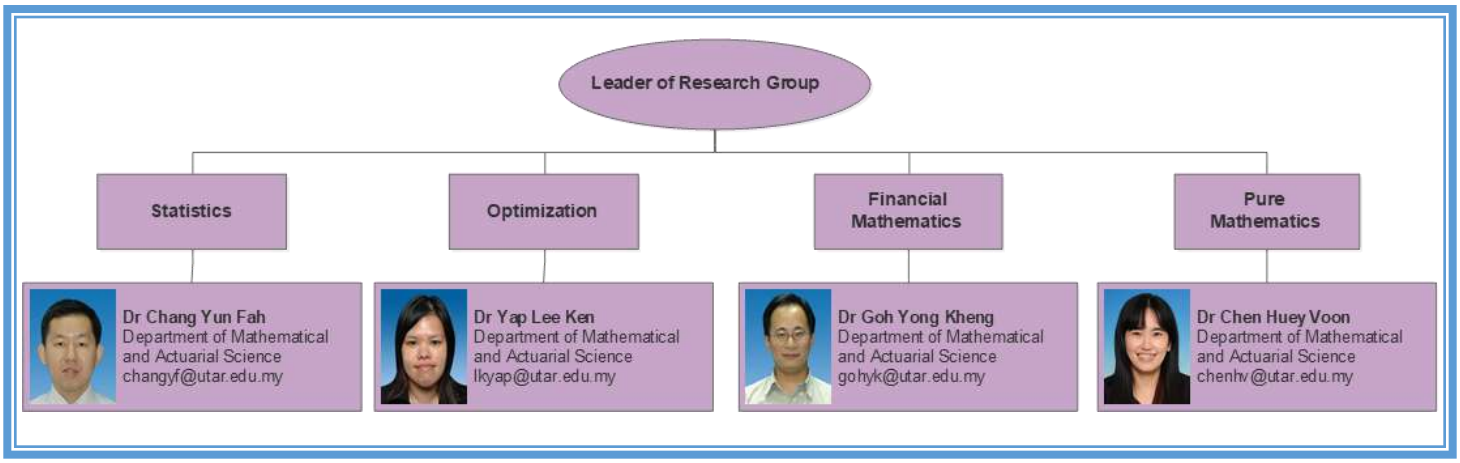

List of Articles

揭开乘法的神秘面纱: 神奇的绘图

张运华
Chang Yun Fah

Department of Mathematical and Actuarial Sciences, Lee Kong Chian Faculty of Engineering and Science, Universiti Tunku Abdul Rahman, Malaysia. Email: changyf@utar.edu.my

[Article received on 13 October 2019]

格栅法或结网计数法 (Grating Method)

在纸张甚至是数字被发明之前，人们采用结绳的方式计算。在许多地方，这种结绳方式后来演变成了算盘或用珠子计算。可是在古印度却演变成另一种精妙的计算方式称为格栅法(参考 Son, 2009)或结网计数法(参考王, 2011)。格栅法完全不需要背乘法表，只要在纸上画线条后统计交叉点就行了。这个方法从古代印度的商人一直沿用至今，是一种任何人都可以轻松上手的乘法计算方式。

让我们先看看两位数的乘法： 23×31

首先是被乘数 23；根据十位数 2 在左上的位置画两条斜线，然后个位数 3 在右下的位置画三条斜线，如下：

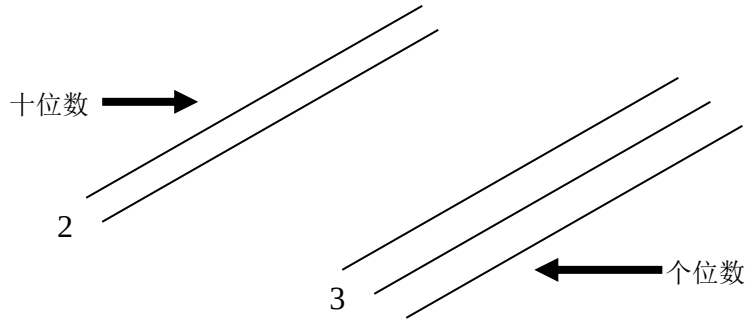

接着是乘数 31；将十位数与个位数分开来，并画上与数字相等数量的斜线。根据十位数 3 在左下的位置画三条斜线，然后个位数 1 在右上的位置画一条斜线，如下：

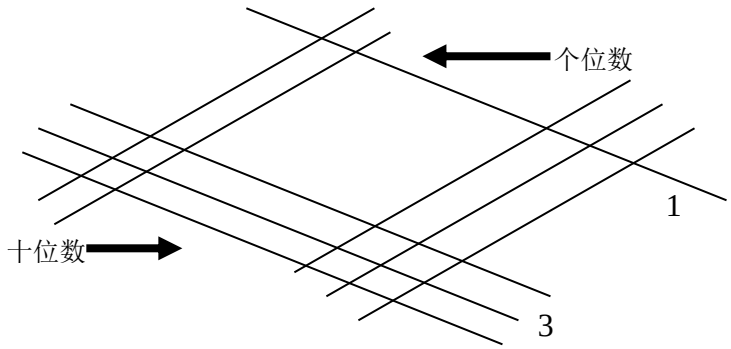

完成后就可以开始点算交叉点的数量并写在下方。

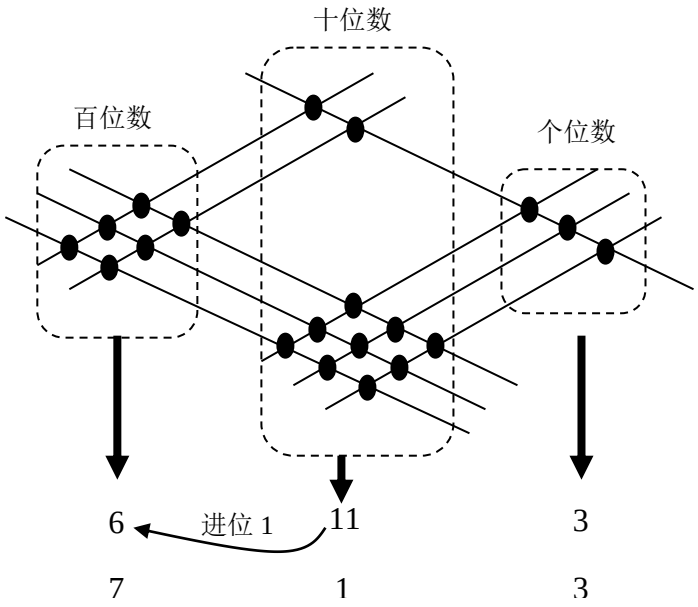

结网处共有三个部分：右边的是个位数共有 3 个交叉点；中间的是十位数共有 11 个交叉点；左边的是百位数共有 6 个交叉点。中间的 11 必须进位 1 至百位数，所以答案是 $23\times31=713$。
格栅法还可以计算三位数的乘法题。例如，你能在以下的结网中找出乘数，被乘数和答案吗？

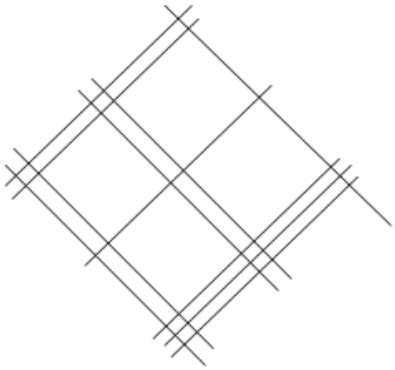

对了，答案就是 $213\times221=47073$。你可以参考下图：

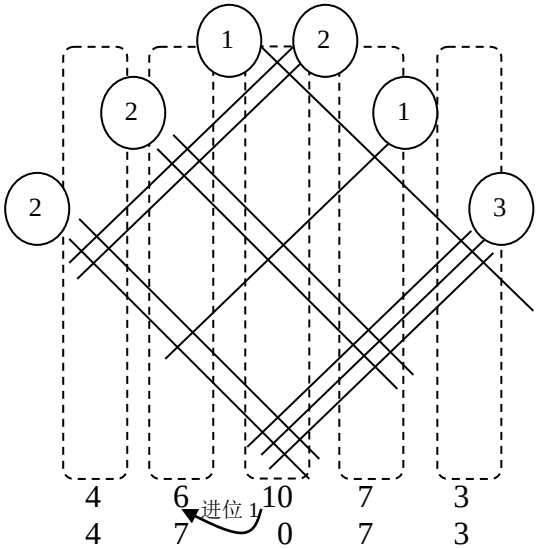

原则上，格栅法可以用来乘任何数目如四位数和五位数等。但是数目越大时它就变得越复杂，而且必须注意每一个交叉处的位置。同样地，如果乘数和被乘数中有大的数字如 7，8 和 9，线条的数量也大量地增加而使整个结网变得密密麻麻，不容易计算。例如以下的结网代表了 $217\times227=49259$，当中有一个大的数字 7。整个结网看起来密密麻麻地，有点儿复杂而且个位数，十位数和百位数的位置可能不在同一条垂直线上。

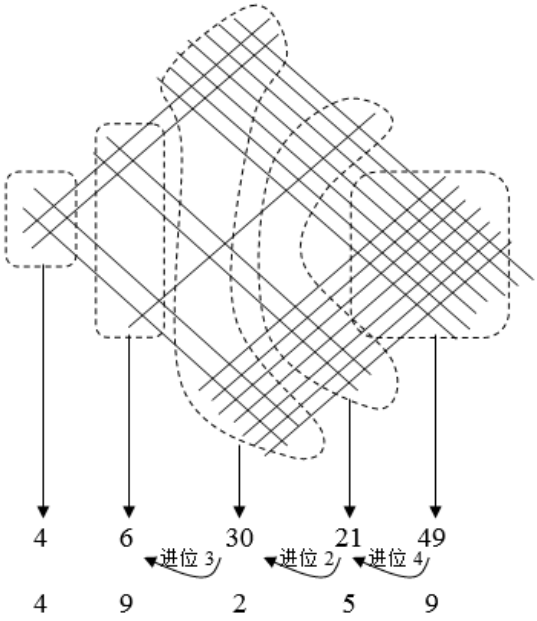

最后就是四位数 $2134\times3323=7091282$ 的乘法也是挺复杂的。

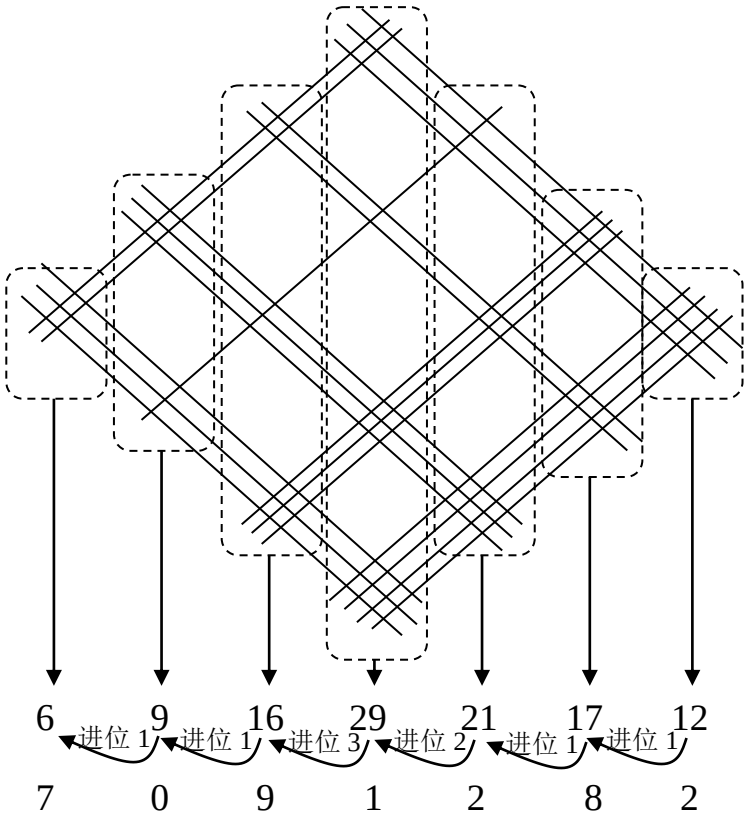

格式法 (Gelosia Method) 和骨头计算器 (Napier Bone)

公元十七世纪，来自苏格兰的数学家约翰•纳皮尔(John Napier, 1550 – 1617)发明了纳皮尔骨头计算器(Napier's Bones)。在没有计算机和电脑的年代，纳皮尔的发明为人们提供了一个非常方便和快速的计算工具并流传到世界各地。请允许我稍后再谈骨头计算器的计算方法，现在我们先来看看它的起源。

回到十六世纪的印度，虽然数学家伽尼萨(Ganeśa)在其著作《Ganita-manjarî》中评论《丽罗娃蒂》时提到了格式法(Gelosia Method 或 Lattice Method)，又称三角方块法或棋盘法，但是人们还无法确认谁是此方法的创作人，甚至无法确定到底棋盘法是印度人所发明的，还是由阿拉伯人发明并据说早在十三世纪就已经流传。大约在十四世纪，阿拉伯/波斯和欧洲的意大利都出现了格式法的应用(参考 Datta & Narayan Singh, 2001)。格式法也在中国的算术中出现，吴敬于 1450 年撰写的《九章算法比类大全》中称之为“因乘图”或“铺地锦”(参考 Ho, 1985)。

印度书籍中是如此描述格式法：
“（构造）如被乘数数位同样多的格子及在这之下如乘数数位同样多的格子；在每一个格子里各画一条斜角的线。被乘数的每一个位数乘以乘数的每一个位数后把结果写在格子里。每一个斜角所得出的总合就是答案。”

以下的例子 $934\times314=293276$ 出现在特拉维索(Traviso, 公元 1478 年)的书里。在此，我将逐步为你一一解说。

步骤一：画好格子，由于被乘数和乘数各有三个位数，因此由左至右画三个格子，由上到下也画三个格子共九个格子。每一个格子从左下角至右上角各划一条斜线。

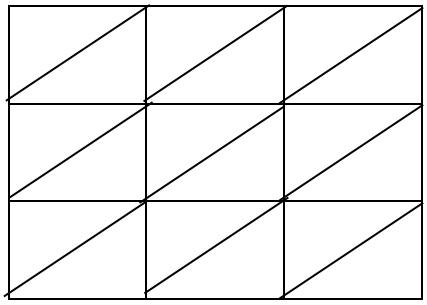

步骤二：格子顶端写上被乘数 934，右边写上乘数 314。

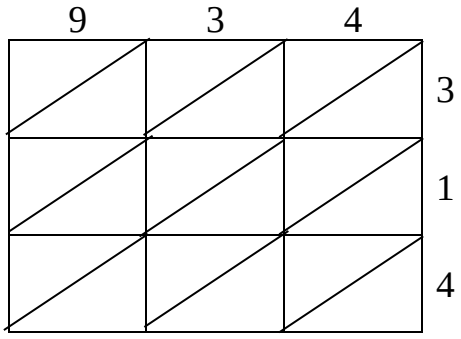

步骤三：被乘数的每一个数字和乘数的每一个数字相乘，把答案写在各自的格子内：每个三角空格只填一个数字，十位数在上，个位数在下。如 4×3=12，1 写在上面的三角形，2 写在下面的三角形。如果是单位数，那么十位数可写 0 或空着，例如1×9=09。

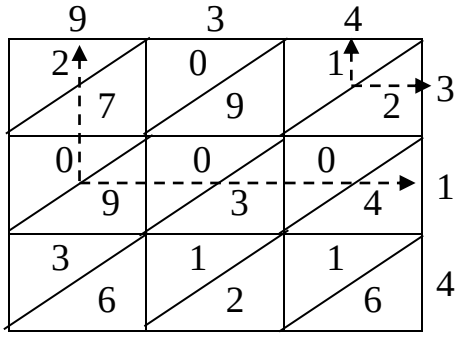

步骤四：把填入三角空格的数字斜向相加后把答案写下，例如中间的斜向总合为1+9+0+9+3=22。

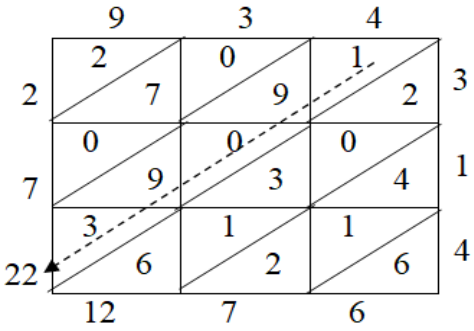

步骤五：把两位数的数目进位后（12 进位 1，进位 1+22=23，23 进位 2，进位 2 + 7=9），再从左到右看就得到答案 293276 了。

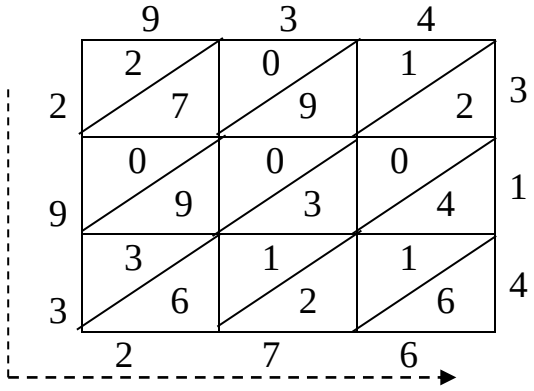

如果你已经熟悉了格式法的运作，你可以把五个步骤简化。例如乘135×12：

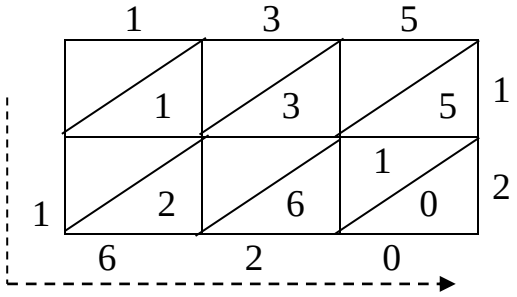

依据个人喜好，格式法可以向右倾斜（如上），也可以向左倾斜。以下是向右倾斜的例子 934×314＝293276。有一点要注意的是乘数 314 必须由上至下倒转写成 413。所有三角形内的数字也和之前的例子倒转，即个位数在上，十位数在下。

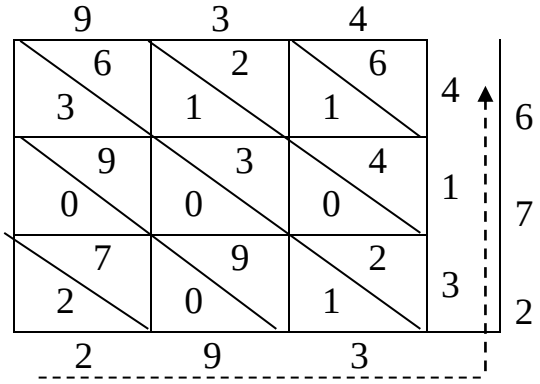

格式法的好处是它乘很大的数目时同样方便及有系统。以下是发现在一本十五世纪的手稿里：456789×987654.

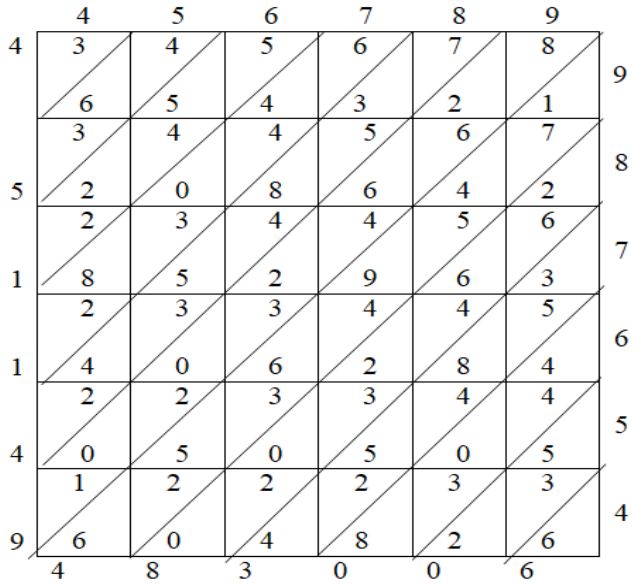

答案是 451149483006！（所有的进位过程已省略）

如前文所述，格式法传入欧洲后，来自苏格兰的数学家约翰•纳皮尔以格式法为基础发明了**纳皮尔骨头计算器**(Napier's Bones)或称为纳皮尔棒(Napier's Rods)。这么难听的名字其实不是纳皮尔自己取的，而是另一位数学家里本(W. Leybourn, 1670)于 1667 年在伦敦形容此计算法为 (参考 Smith, 1958)：

"会说话的棒的数字艺术：庸俗的称为纳皮尔骨头。"

纳皮尔在他的著作《Rabdologia》里记载了这个以排列数字棒来代表格式乘法的系统。你也不妨自己动手制作一个。

首先，准备好十支冰淇淋棒或硬纸条。冰淇淋棒的下端留一些空位做为把手（灰色格子），然后将其它部分划分为九个格子。第一个格子上写上 0 至 9 的其中一个数字；从第二个格子到第九个格子里划上对角线。下图的例子中第一个格子上是 9，然后把九的乘法表填写在三角形中，如第二格是

$2\times9=18$；将第二格的上三角形写 1 及下三角形写 8，第三格是$3\times9=27$，第四个格是$4\times9=36$，以此类推至第九个格子是$9\times9=81$ (参考 Pappas, 2004).

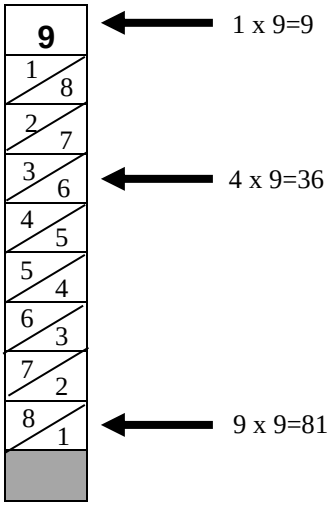

0	1	2	3	4	5	6	7	8	9
0	2	4	6	8	10	12	14	16	18
0	3	6	9	12	15	18	21	24	27
0	4	8	12	16	20	24	28	32	36
0	5	10	15	20	25	30	35	40	45
0	6	12	18	24	30	36	42	48	54
0	7	14	21	28	35	42	49	56	63
0	8	16	24	32	40	48	56	64	72
0	9	18	27	36	45	54	63	72	81

商人带着一套象牙或木制的纳皮尔骨头计算器（如上图），当需要进行乘法，除法，平方和立方的计算时就拿出来用。每一条纳皮尔棒就如第一个格子里的数字的乘法表。例如，当我们要计算$298\times7=2086$时，就把第一个格子写着 2，9 和 8 的纳皮尔棒顺序排列好：

2	9	8
4	18	16
6	27	24
8	36	32
10	45	40
12	54	48
14	63	56
16	72	64
18	81	72

然后从上而下数到第七个行，依照格式法把三角空格的数字斜向相加起来就得到答案了。

2	9	8
4	18	16
6	27	24
8	36	32
10	45	40
12	54	48
14	63	56
16	72	64
18	81	72

298
X 7
2086

→

165
+ 436
2086

纳皮尔骨头计算器不但盛行于欧洲大陆和阿拉伯世界，它甚至在十八世纪初至十九世纪这段时间分别流传到中国和日本。日语版的纳皮尔骨头计算器出现在十九世纪中，由 Hanai Kenkichi 记载在他的著作《Seisan Sokuchi》里(参考 Smith, 1958)。

纳皮尔骨头计算器的其中一个弱点是它只能进行乘数只有个位数的乘法。以上例子的乘数为个位数 7。当我们要计算 739×26 时，乘数有十位数 2 就非常麻烦了。基本上纳皮尔骨头计算器并不具备这种功能。除非你所设计的纳皮尔骨头计算器可以被折起来，就如以下的方法一（参考 Wong, 2010）：

图 1：Hanai Kenkichi 制作的纳皮尔骨头计算器

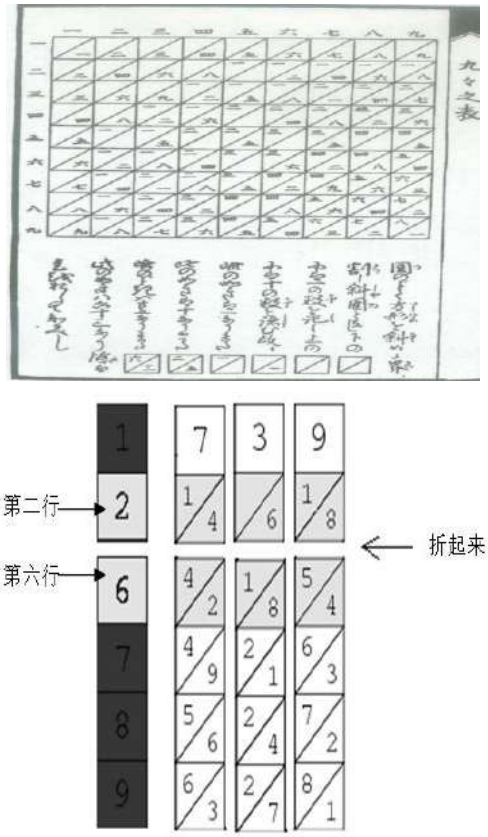

然后依照格式法把三角空格的数字斜向相加起来
4 = 4
8 + 5 + 8 = 21 = 1（2 进位到百位数）
1 + 6 + 1 + 2 + 2 （来自十位数）= 12 = 2 （1 进位到千位数）
4 + 4 + 1（来自百位数）= 9
1 = 1
答案是 19214。
折起来很麻烦是吗？不用紧，我们就试一试第二个方法吧！首先，将第二行的结果写下 $739\times2=1478$。接着把第六行的结果也写下 $739\times6=4434$，然后把两个结果相加起来就是答案了。但要记住第二行的结果要往左移一步（代表 20）：

$$\begin{array}{r} 1478 \\ +\ 4434 \\ \hline 19214 \end{array}$$

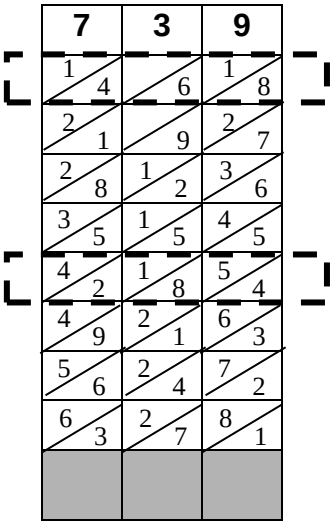

图 2：约翰●纳皮尔肖像

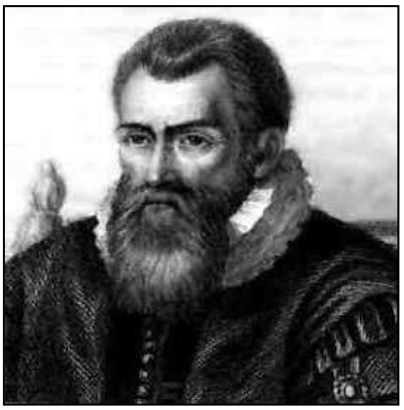

参考资料 (References):

王擎天, 2011. 印度数学，台湾：汉湘文化事业股份有限公司。

David Eugene Smith, 1958. History of Mathematics, Vol. 2 (Special Topics of Elementary Mathematics), New York: Dover Publications.

Ho Peng Yoke, 1985. Li, Qi and Shu: An Introduction to Science and Civilization in China, Hong Kong: Hong Kong University Press.

Hosung Son (孙皓诚), 2009. India Vedic Mathematics day by day Training, translated by 张琪惠 (2011), 印度吠陀数学速算训练法, Taiwan: Shymau Publication Company.

Theoni Pappas, 2004. The Joy of Mathematics: Discovering Mathematics All Around You, USA: Wide World Publishing/Tetra.

Wong Yi Vern, 2010. A Survey on Mathematical-Related Learning Products and Its Effectiveness, Petaling Jaya, Malaysia: UTAR Final Year Project Thesis.

Membongkar Rahsia Pendaraban: Lukisan Yang Ajaib

Chang Yun Fah

Department of Mathematical and Actuarial Sciences, Lee Kong Chian Faculty of Engineering and Science, Universiti Tunku Abdul Rahman, Malaysia. Email: changyf@utar.edu.my

[Article received on 13 October 2019]

Kaedah Parutan atau Kaedah Jaringan

Manusia menggunakan ikatan jaring sebagai cara pengiraan sebelum kertas dicipta mahupun nombor ditemui. Di tempat-tempat tertentu, ikatan jarring ini kemudian berkembang menjadi abacus atau pengiraan menggunakan manik. Namun di zaman purba India, ikatan jaring berkembang menjadi Kaedah Parutan (rujuk Son, 2009) atau Kaedah Jaringan (rujuk 王, 2011) yang indah. Kaedah ini tidak memerlukan penghafalan jadual pendaraban seperti kaedah-kaedah yang lain, tetapi ia hanya perlu melukiskan garis-garis lurus di atas kertas dan mengira bilangan titik persilangannya. Kaedah Jaringan ini digunakan oleh peniaga India pada zaman purba sehingga zaman moden dan ia amat mudah dipelajari .

Sekarang kita lihat kepada contoh yang melibatkan pendaraban dua digit: 23×31

Perhatikan nombor didarab 23 dahulu; angka di tempat kedudukan sepuluh ialah 2, maka lukiskan dua garis lurus yang selari di bahagianatas kiri. Kemudian angka di tempat kedudukan unit ialah 3, lukiskan tiga garis lurus selari di bahagian bawah kanan seperti di bawah:

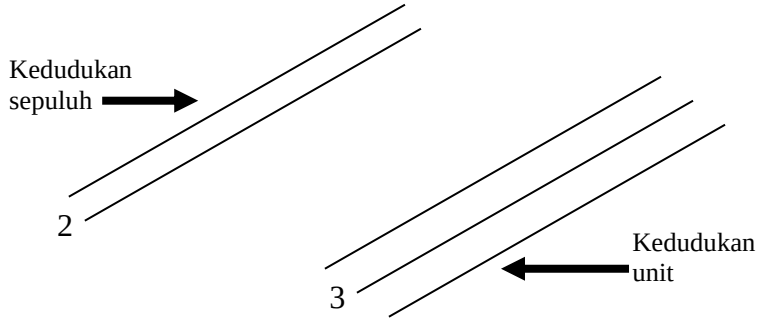

Seterusnya perhatikan pendarab 31; asingkan kedua-dua angka di tempat kedudukan sepuluh dan unit, kemudian lukiskan garis lurus selari yang sama bilangannya dengan angka yang diperolehi masing-masing.Iaitu lukiskan 3 garis lurus selari di bahagian bawah kiri dan 1 garis lurus di bahagian atas kanan seperti di bawah:

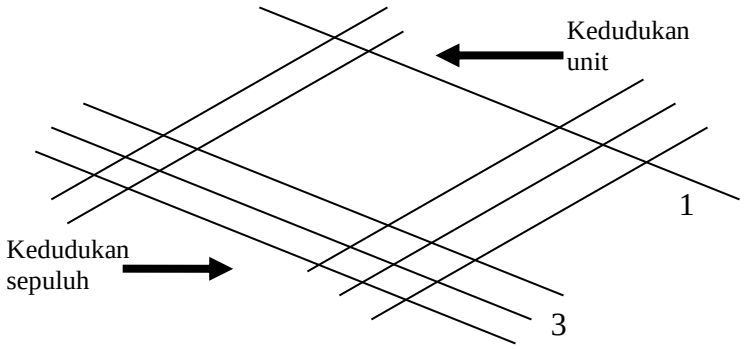

Sebaik sahaja lukis di atas selesai, kamu boleh mula mengira bilangan titik persilangan antara garis-garis lurus tersebut dan catatkan jawapan pengiraan anda di bawah.

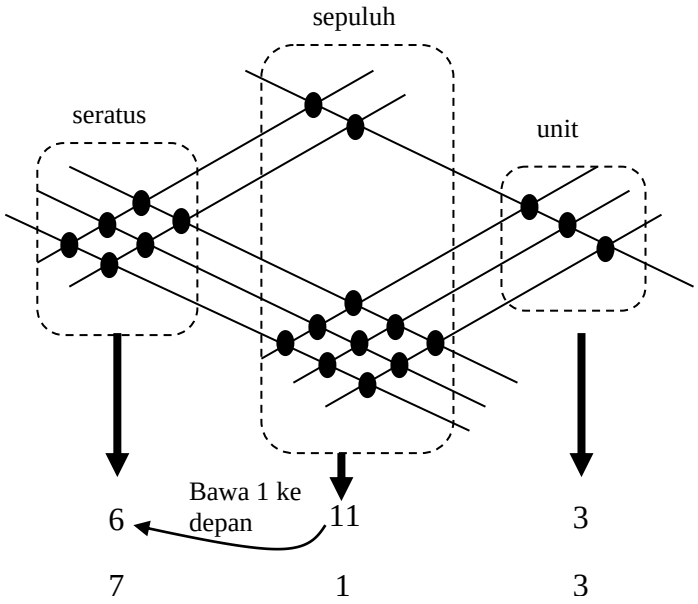

Jaringan yang dilukis dapat dibahagi kepada tiga bahagian: bahagian kanan mewakili kedudukan unit dan ia mempunyai 3 titik persilangan; bahagian tengah mewakili kedudukan sepuluh dan ia mempunyai 11 titik persilangan; bahagian kiri mewakili kedudukan seratus dan ia terdapat 6 titik persilangan. Oleh sebab bilangan titik persilangan di bahagian tengah lebih daripada 10, kita perlu bawa sepuluh ke tempat kedudukan seratus, maka bahagian tengah tinggal 1 sahaja dan bahagian kiri menjadi 7 sekarang. Justeru, jawapan akhir ialah $23\times31=713$.

Kaedah Parutan juga boleh digunakan untuk mencari hasil pendaraban bagi nilai yang mempunyai tiga angka. Sebagai contoh, dapatkah anda carikan nilai pendarab, nombor didarab dan jawapan pendaraban dari jaringan yang disediakan di bawah ini?

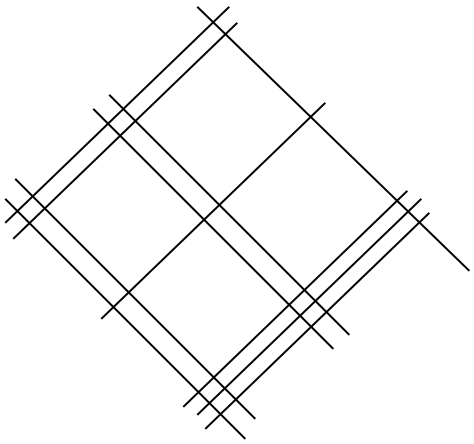

Jawapannya ialah $213\times221=47073$. Anda boleh rujuk kepada rajah di bawah sekiranya tidak dapat jawapan tersebut:

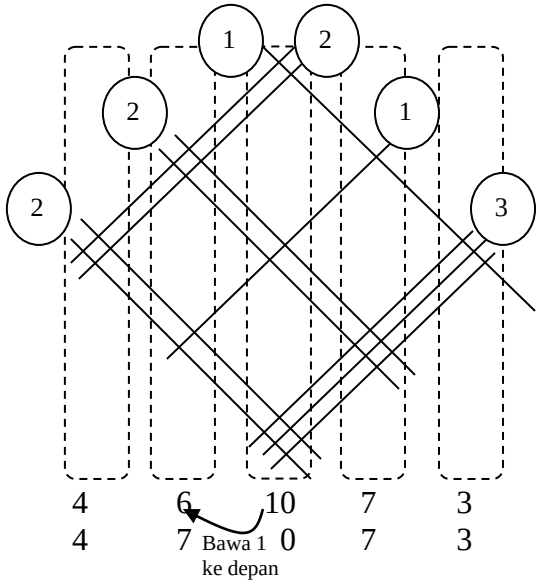

Pada prinsipnya, Kaedah Parutan boleh digunakan untuk pendaraban angka yang besar seperti empat dan lima angka. Namun jaringan yang dibentuk akan menjadi semakin rumit apabila nilai pendaraban tersebut terlalu besar dan anda harus berhati-hati apabila mengira titik persilangannya pada tempat yang sebenar. Selain itu, apabila terdapat angka yang besar seperti 7, 8 dan 9 dalam pendarab atau nombor didarab, bilangan garis lurus juga berganda menyebabkan jaringan tersebut terlalu kecil dan sukar dikira. Misalnya, jaringan di bawah mewakili pendaraban $217 \times 227 = 49259$, antaranya terdapat satu angka yang besar iaitu angka 7. Keseluruh jaringan kelihatan rumit dan titik-titik persilangan tidak lagi terletak di tempat kedudukan yang sebenar.

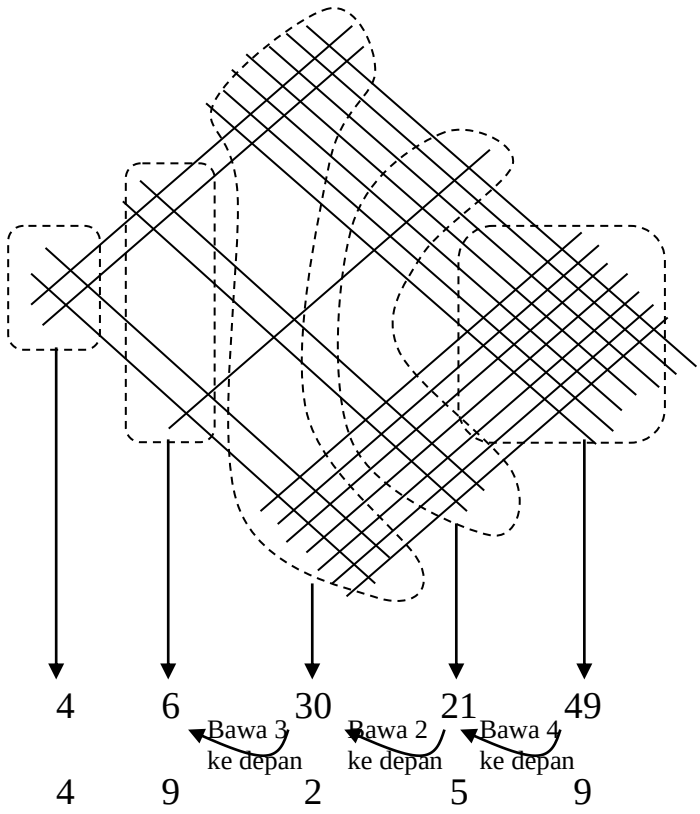

Contoh terakhir melibatkan pendaraban nilai yang mempunyai empat angka $2134 \times 3323 = 7091282$.

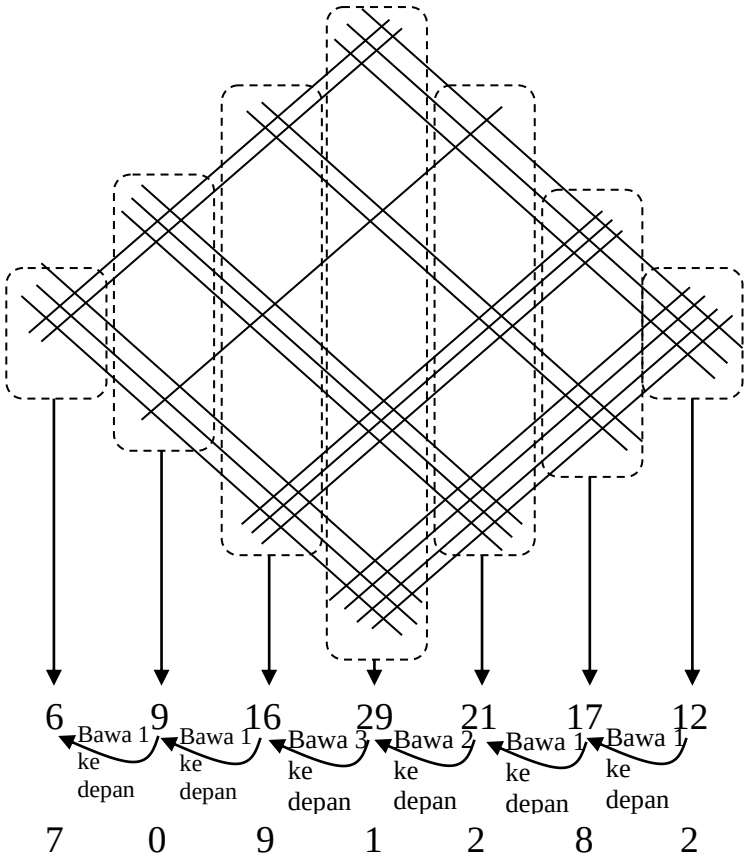

Kaedah Gelosia dan Alat Tulang Napier

John Napier (1550 – 1617) merupakan seorang ahli Matematik unggul dari Scotland pada abad ke-17. Beliau telah mencipta satu alat membuat pendaraban yang dikenali sebagai alat pengiraan Tulang Napier. Alat ini mendapat sambutan yang baik dari orang ramai dan diperkenalkan ke negara-negara lain kerana ia mudah diguna dan pengiraannya pantas. Mari kita lihat kepada asal-usulnya sebelum membincangkan lebih mendalam alat tersebut.

Menurut catatan dalam buku bertajuk "Ganita-manjarî" yang ditulis oleh seorang ahli Matematik India bernama Ganeśapada abad ke-16, Kaedah Gelosiatelahpun wujud dalam karya Matematik purba "Lîlâvatî" dan ia juga dikenali sebagai Kaedah Kekisi (Lattice Method), Kaedah Segitiga ataupun Kaedah Papan Catur.Malangnya, pencipta kaedah ini tidak dapat dikenalpasti dan perbahasan wujud samada kaedah ini dicipta oleh orang India ataupun orang Arab yang dikatakan telah menggunakannya sejak abad ke-13. Lebih kurang pada abad ke-14, Kaedah Gelosia telah wujud di negara-negara Arab/Parsi dan Itali (Datta & Narayan Singh, 2001). Kaedah Gelosia juga wujud di negara Cina di mana ahli Matematik bernama Wu Jing mengelarnya sebagai 'Ying Cheng Tu' (Rajah Pendaraban Faktor) atau 'Pu Di Jing' dalam karyanya "Kitab Perbandingan Pengiraan Sembilan Bab" pada tahun 1450 (Ho,1985).

Berikut adalah contoh ulasan Kaedah Gelosia yang terdapat dalam karya dari India:

"*(Strukturnya) bilangan kekisi adalah sama banyak dengan bilangan angka dalam nombor didarab dan di bawahnya pula mempunyai jumlah kekisi yang sama bilangannya dengan angka pendarab; lukiskan satu garis pepenjuru di dalam setiap kekisi. Tuliskan hasil darab antara setiap angka dalam nombor didarab dengan setiap angka dalam pendarab ke dalam kekisi-kekisi berkenaan. Jawapannya diperolehi dari hasil tambah bagi setiap pepenjuru.*"

Berikut adalah contoh $934 \times 314 = 293276$ yang wujud dalam buku Traviso pada tahun 1478. Di sini, kami akan menjelaskanlangkah demi langkah proses pendaraban Kaedah Gelosi.

Langkah 1: lukiskan kekisi mengikut bilangan angka dalam nombor didarab dan pendarab. Oleh sebab nombor didarab 934 dan pendarab 314 masing-masing mempunyai tiga angka, maka kita lukis tiga petak dari kiri ke kanan dan tiga petak dari atas ke bawah, keseluruhannya sembilan petak. Lukiskan satu garis pepenjuru di dalam setiap petak mula dari penjuru kanan atas hingga ke penjuru kiri bawah seperti rajah di bawah.

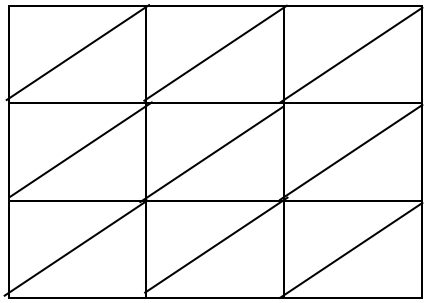

Langkah 2: tuliskan nombor didarab 934 di atas rajah yang siap sedia, dan tuliskan pendarab 314 di sebelah kanan rajah seperti berikut.

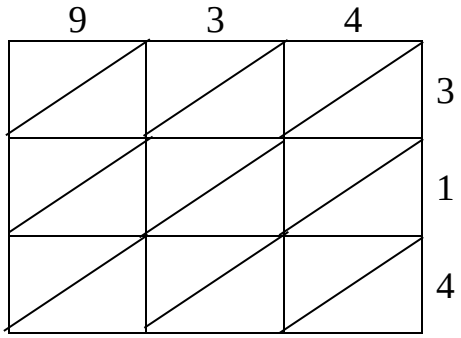

Langkah 3: darabkan setiap angka dalam nombor didarab dengan angka-angka dalam pendarab, dan tuliskan hasil pendaraban tersebut dalam petak yang berkenaan. Setiap segitiga hanya membenarkan satu angka sahaja iaitu nombor unit ditulis di dalam segitiga bawah, manakala nombor tempat sepuluh ditulis dalam segitiga atas. Misalnya $4 \times 3 = 12$, angka 1 ditulis dalam segitiga atas dan angka 2 ditulis dalam segitiga bawah. Jika terdapat hasil darab yang kurang daripada sepuluh, maka segitiga atas dibiarkan kosong atau tuliskan nombor sifar, seperti $1 \times 9 = 09$.

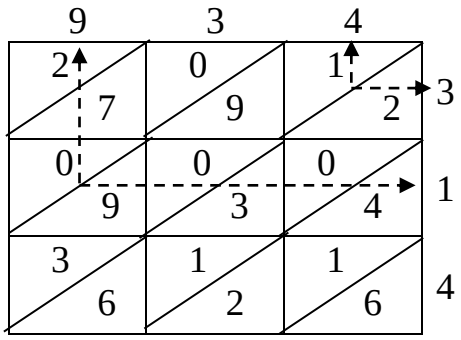

Langkah 4: tambahkan semua nombor yang terdapat dalam pepenjuru yang sama dan tuliskan hasilnya di bawah pepenjuru berkenaan. Misalnya hasil tamabah nombor-nombor di pepenjuru tengah ialah $1+9+0+9+3=22$.

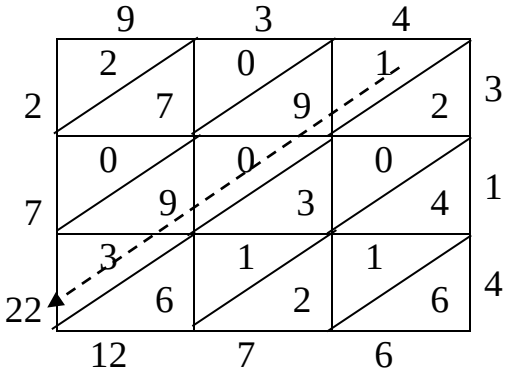

Langkah 5: semua hasil tambah yang mempunyai dua digit (melebihi sepuluh) hendaklah dibawa ke tempat kedudukan seterusnya (contohnya hasil tambah 12, angka 1 akan dibawa ke depan dan tambah dengan 22 menjadi1+22=23, seterusnya angka 2 dari 23 dibawa ke depan dan tambah dengan 7 memperolehi 2+7=9). Selepas itu, membaca hasil-hasil tambah tersebut dari arah kiri hingga kanan memberikan jawapan akhir iaitu 293276.

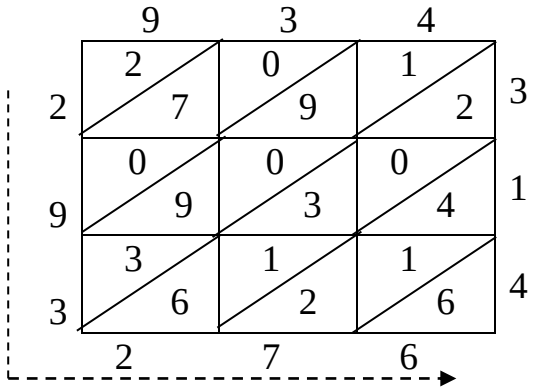

Setelah mahir dengan Kaedah Gelosia, anda boleh cuba ringkaskan langkah-langkah yang disebutkan tadi. Misalnya darabkan 135×12:

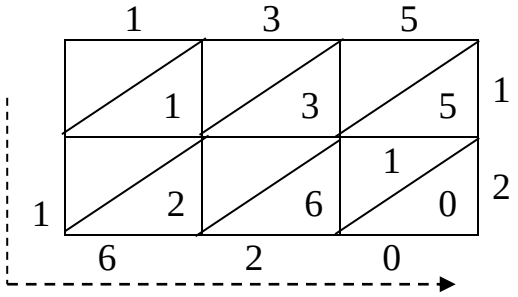

Cara melukis garis pepenjuru di dalam petak boleh tukar mengikut kebiasaan seseorang. Pepenjuru tersebut boleh cenderung ke kanan (seperti yang dijelaskan di atas) ataupun cenderung ke kiri seperti contoh $934\times314=293276$ di bawah.Harus diingati bahawa angka pendarab 314 hendaklah ditulis terbalik sebagai '413' sekiranya pepenjuru tersebut cenderung ke kiri. Semua nombor di dalam segitiga juga harus diterbalikan iaitu nombor unit ditulis di dalam segitiga atas, manakala nombor tempat sepuluh ditulis dalam segitiga bawah.

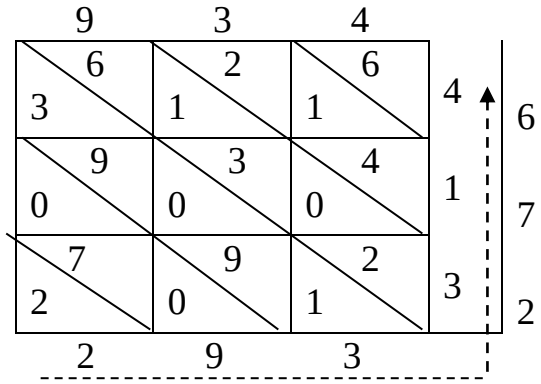

Kaedah Gelosia ialah satu cara yang mudah dan bersistematik walaupun melibatkan pendaraban nombor yang besar. Berikut adalah satu contoh pendaraban Kaedah Gelosia yang tercatat dalam sebuah skrip Matematik pada abad ke-15: 456789×987654.

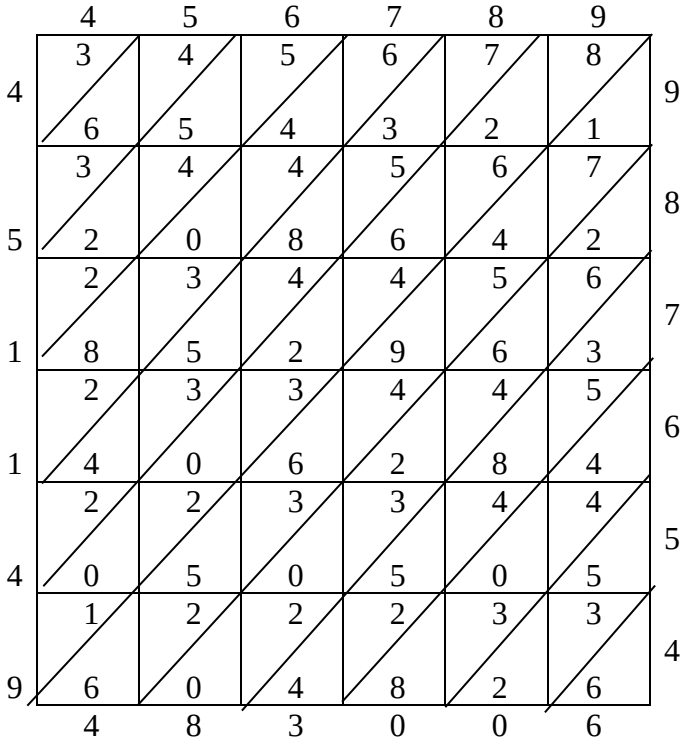

Jawapannya ialah 451149483006! (langkah-langkah membawa angka ke hadapan telah dijalankan tanpa penjelasan).

Sepertimana yang dikatakan pada permulaan kaedah ini, John Napier, seorang ahli Matematik dari Scotland telah mencipta satu alat pengiraan berdasarkan konsep Kaedah Gelosia.Alat ini kemudian diberi nama sebagai alat pengiraan Tulang Napier ataupun Rod Napier oleh seorang ahli Matematik yang bernama W. Leybourn (1670) pada tahun 1667 di London. Beliau memperkenalkan Tulang Napier sebagai (Smith, 1958):

"*Satu seni Matematik menggunakan rod yang boleh bercakap: dengan kasarnya ia dinamakan sebagai Tulang Napier.*"

John Napier dalam bukunya “Rabdologia” telah memperkenalkan sistem pendaraban Kaedah Gelosia melalui susunan rod-rod bernombor. Inginkah anda membuat satu alat pengiraan Tulang Napier sendiri? Berikut adalah caranya.

Sebagaipermulaan, sediakan sepuluh batang rod aiskrim atau kertas yang keras dengan saiz yang sama. Tinggalkan sedikit ruang kosong di bawah rod aiskrim untuk dipegang (seperti kawasan warna kelabu di rajah bawah), kemudian bahagikan bahagian rod aiskrim yang lain kepada sembilan petak yang sama saiz. Pilih satu angka dari 0 hingga 9 dan tuliskannya pada petak pertama setiap rod aiskrim; kemudian lukiskan satu garis pepenjuru dari petak kedua hingga petak ke sembilan. Rajah di bawah menunjukkan contoh rod aiskrim dengan petak pertamanya bernombor 9, seterusnya isikan jawapan pendaraban angka 9 ke dalam segitiga-segitiga tersebut mengikut susunan, misalnya petak kedua ialah pendaraban $2\times9=18$; tuliskan 1 ke dalam segitiga atas pada petak kedua dan tuliskan 8 ke dalam segitiga bawah pada petak kedua, petak ketiga ialah $3\times9=27$, petak keemat ialah $4\times9=36$, dan seterusnya sehingga ke petak sembilan ialah $9\times9=81$(Pappas, 2004).

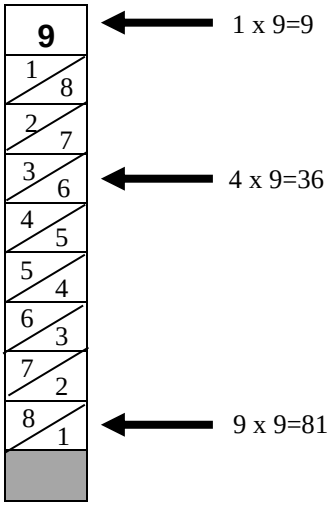

0	1	2	3	4	5	6	7	8	9
0	2	4	6	8	10	12	14	16	18
0	3	6	9	12	15	18	21	24	27
0	4	8	12	16	20	24	28	32	36
0	5	10	15	20	25	30	35	40	45
0	6	12	18	24	30	36	42	48	54
0	7	14	21	28	35	42	49	56	63
0	8	16	24	32	40	48	56	64	72
0	9	18	27	36	45	54	63	72	81

Rajah di atas merupakan alat pengiraan Tulang Napier yang lengkap. Pada zaman dahulu, peniaga-peniaga akan membawa dan menggunakan alat pengiraan Tulang Napier yang dibuat daripada kayu atau gading bagi menjalankan pengiraan seperti pendaraban, pembahagian, kuasa dua dan kuasa tiga. Setiap rod Tulang Napier sebenarnya adalah jadual pendaraban bagi nombor pertama rod tersebut. Misalnya, keluarkan rod-rod

yang menandakan nombor 2, 9 dan 8 pada petak pertama dan susunkan rod-rod ini ikut susunan apabila kita menjalankan pendaraban $298 \times 7 = 2086$:

2	9	8
4	1 / 8	1 / 6
6	2 / 7	2 / 4
8	3 / 6	3 / 2
1 / 0	4 / 5	4 / 0
1 / 2	5 / 4	4 / 8
1 / 4	6 / 3	5 / 6
1 / 6	7 / 2	6 / 4
1 / 8	8 / 1	7 / 2

Kemudian perhatikan baris yang ketujuh (mula dari atas) dan tambahkan nombor-nombor pada pepenjuru yang sama seperti Kaedah Gelosia, hasilnya adalah jawapan bagi pendaraban yang dikehendaki.

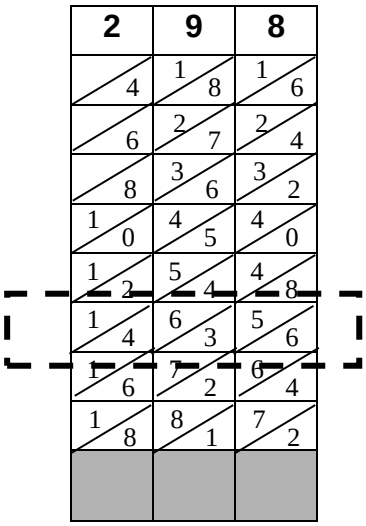

298
X 7
2086

→

165
+436
2086

Alat pengiraan Tulang Napier bukan sahaja mendapat sambutan dari benua Eropah dan Arab, malah ia telah diperkenalkan ke negara Cina dan Jepun pada awal abad ke-18 hingga abad ke-19. Alat pengiraan Tulang Napier berbahasa Jepun telah wujud pada pertengahan abad ke-19 seperti yang tercatat dalam buku Hanai Kenkichi yang bertajuk "Seisan Sokuchi" (Smith, 1958).

Rajah 1: Alat Pengiraan Tulang Napier yang dibuat oleh Hanai Kenkichi

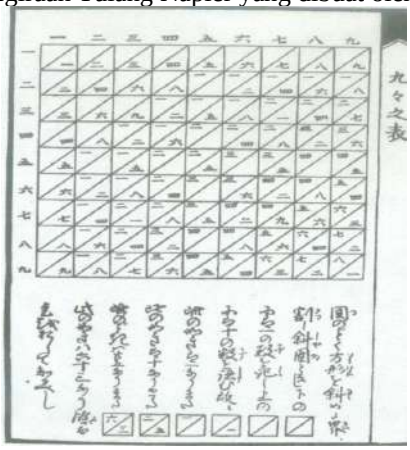

Salah satu kelemahan alat pengiraan Tulang Napier ialah ia hanya dapat menjalankan pendaraban bagi pendarab yang hanya mempunyai satu angka. Dalam contoh di atas $298 \times 7 = 2086$, pendarabnya ialah 7. Masalah akan timbul apabila pendarabnya mempunyai dua atau lebih angka seperti 739×26. Alat pengiraan Tulang Napier tidak dapat melakukannya melainkan anda boleh mencipta satu alat baru yang boleh dilipat seperti rajah berikut (Wong, 2010):

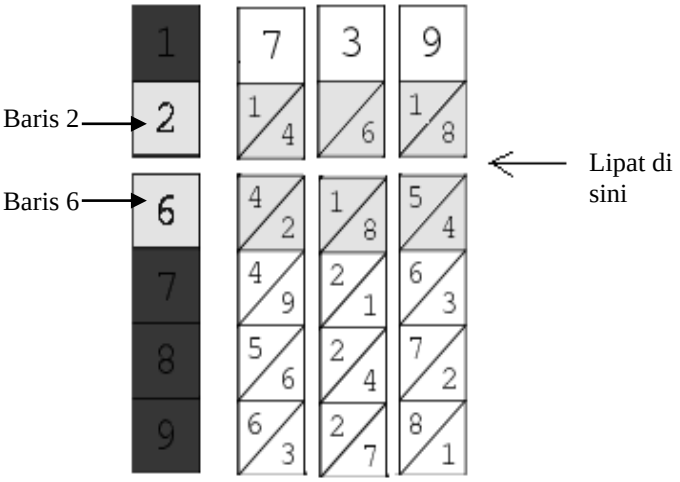

Selepas baris ke-3 hingga baris ke-5 dilipatkan, tambahkan semua nombor di dalam pepenjuru yang sama di antara baris ke-2 dan baris ke-6 seperti Kaedah Gelosia
Unit: 4 = 4
Sepuluh: 8 + 5 + 8 = 21 = 1 (membawa 2 ke hadapan)
Seratus: 1 + 6 + 1 + 2 + 2 (dari tempat sepuluh) = 12 = 2 (membawa 1 ke hadapan)
Seribu: 4 + 4 + 1 (dari tempat seratus) = 9
Sepuluh ribu: 1 = 1
Jawapan ialah 19214.

Jika anda rasa susah melipat, cubalah cara yang kedua! Tuliskan jawapan baris kedua iaitu $739 \times 2 = 1478$, diikuti dengan jawapan baris keenam $739 \times 6 = 4434$. Kemudian tambahkan kedua-dua jawapan tersebut dengan mengalih 1478 satu langkah ke kiri (sebab ia mewakili 20):

$$\begin{array}{r} 1478 \\ +\ 4434 \\ \hline 19214 \end{array}$$

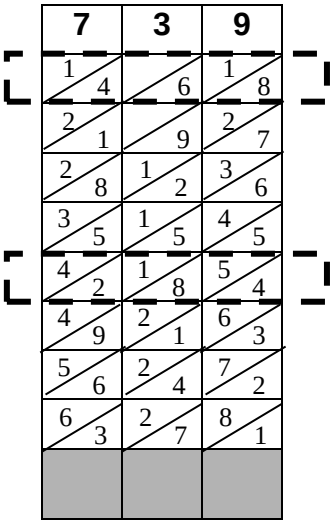

Rajah 2: Gambar John Napier

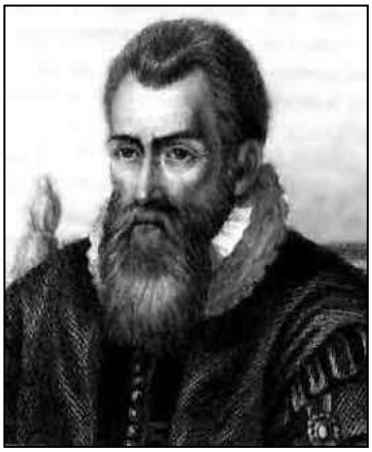

Rujukan:

王擎天, 2011. 印度数学，台湾：汉湘文化事业股份有限公司。

David Eugene Smith, 1958. History of Mathematics, Vol. 2 (Special Topics of Elementary Mathematics), New York: Dover Publications.

Ho Peng Yoke, 1985. Li, Qi and Shu: An Introduction to Science and Civilization in China, Hong Kong: Hong Kong University Press.

Hosung Son (孙皓诚), 2009. India Vedic Mathematics day by day Training, translated by 张琪惠 (2011), 印度吠陀数学速算训练法, Taiwan: Shymau Publication Company.

Theoni Pappas, 2004. The Joy of Mathematics: Discovering Mathematics All Around You, USA: Wide World Publishing/Tetra.

Wong Yi Vern, 2010. A Survey on Mathematical-Related Learning Products and Its Effectiveness, Petaling Jaya, Malaysia: UTAR Final Year Project Thesis.

Importing and Analyzing Data from A Web Page Using Power BI Desktop

Chong Fook Seng

Department of Physical and Mathematical Science, Faculty of Science, Universiti Tunku Abdul Rahman, Malaysia. Email: chongfs@utar.edu.my

[Article received on 16 August 2019]

Abstract

Power BI (Business Intelligence) is a suite of business analytics tool that create stunning reports with interactive data visualization. Power BI enable business users to excavate further into data and find outlines they may have otherwise missed, with Power BI features like quick measures, grouping, forecasting, and clustering. Therefore, we were able using Power BI to see whether we were significantly behind the reginal trend, focus on the problem, and create a solution to overcome the problem. Besides, Power BI always allow us to connect hundreds of data sources and bring the data to life with interaction dashboard and reports. In this article, some common ideas on importing and analyzing data from a web page (IMF World Economic Outlook database –Asia country) will be illustrate and the useful informations will be perform using dashboard.

1. Introduction

The World Economic Outlook (WEO) database, issued by the International Monetary Fund (IMF), covers certain macroeconomic data series from the statistical appendix of the World Economic Outlook report, which offerings the IMF staff's analysis and predictions of economic developments at the global level, in many major and individual country groups.

The WEO database replicates information from both national source and international organizations. The data are maintained jointly by the IMF's Research Department and regional departments, with the latest updating country projections based on reliable global assumptions regularly. It is published biannually and partly updated two times a year. Data are available from 1980 to the present, and projections are given for the next two years. Additionally, medium-term projections are available for selected indicators as well.

2. Connect to A Web Data Source

Web connections are only established using basic authetication. Web sites requiring authentication may not work properly with the web connector. To import the World Economic Outlook (WEO) data for Asia country using Power BI desktop, open the **Home** ribbon tab and drop down the arrow next to **Get Data**, and then select **Web**.

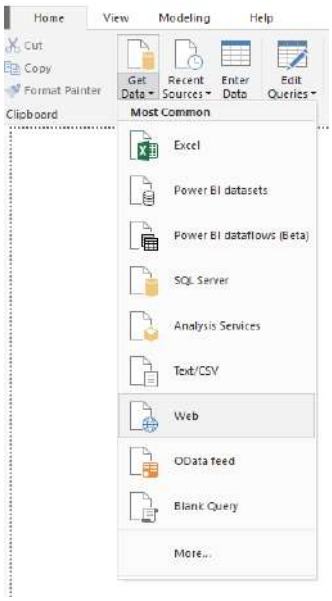

In the **From Web** dialog box, paste the URL for World Economic Outlook (WEO) database for Asia country into the URL text box, and then select **OK**.

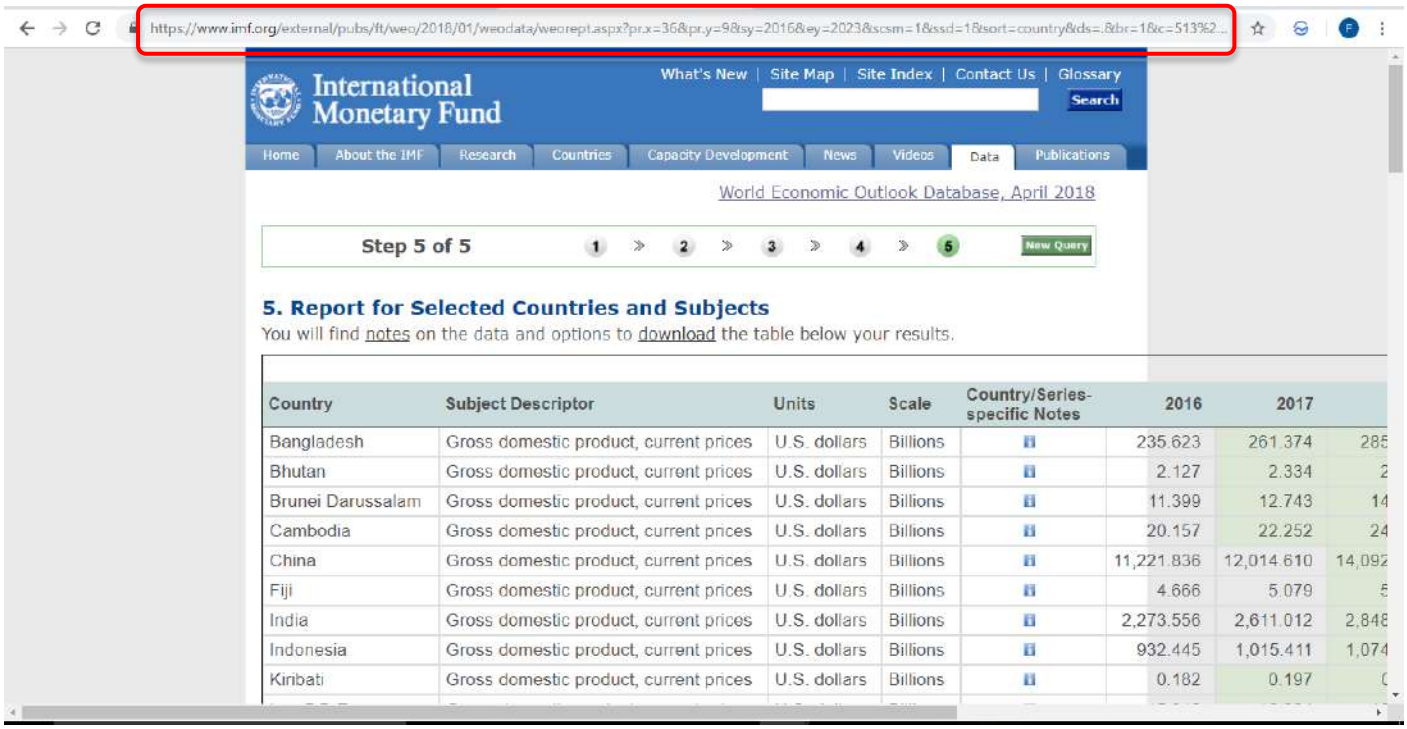

Country	Subject Descriptor	Units	Scale	Country/Series-specific Notes	2016	2017	
Bangladesh	Gross domestic product, current prices	U.S. dollars	Billions		235.623	261.374	285
Bhutan	Gross domestic product, current prices	U.S. dollars	Billions		2.127	2.334	2
Brunei Darussalam	Gross domestic product, current prices	U.S. dollars	Billions		11.399	12.743	14
Cambodia	Gross domestic product, current prices	U.S. dollars	Billions		20.157	22.252	24
China	Gross domestic product, current prices	U.S. dollars	Billions		11,221.836	12,014.610	14,092
Fiji	Gross domestic product, current prices	U.S. dollars	Billions		4.666	5.079	5
India	Gross domestic product, current prices	U.S. dollars	Billions		2,273.556	2,611.012	2,848
Indonesia	Gross domestic product, current prices	U.S. dollars	Billions		932.445	1,015.411	1,074
Kiribati	Gross domestic product, current prices	U.S. dollars	Billions		0.182	0.197	0

After connecting to the web page, the Power BI **Navigator** dialog box shows a list of avaliable tables on the page and we just need to select the correct table (although it is not exactly in the correct formatting) and load the data into Power BI desktop. Later, we can apply transformations to reshape and clean up the data.

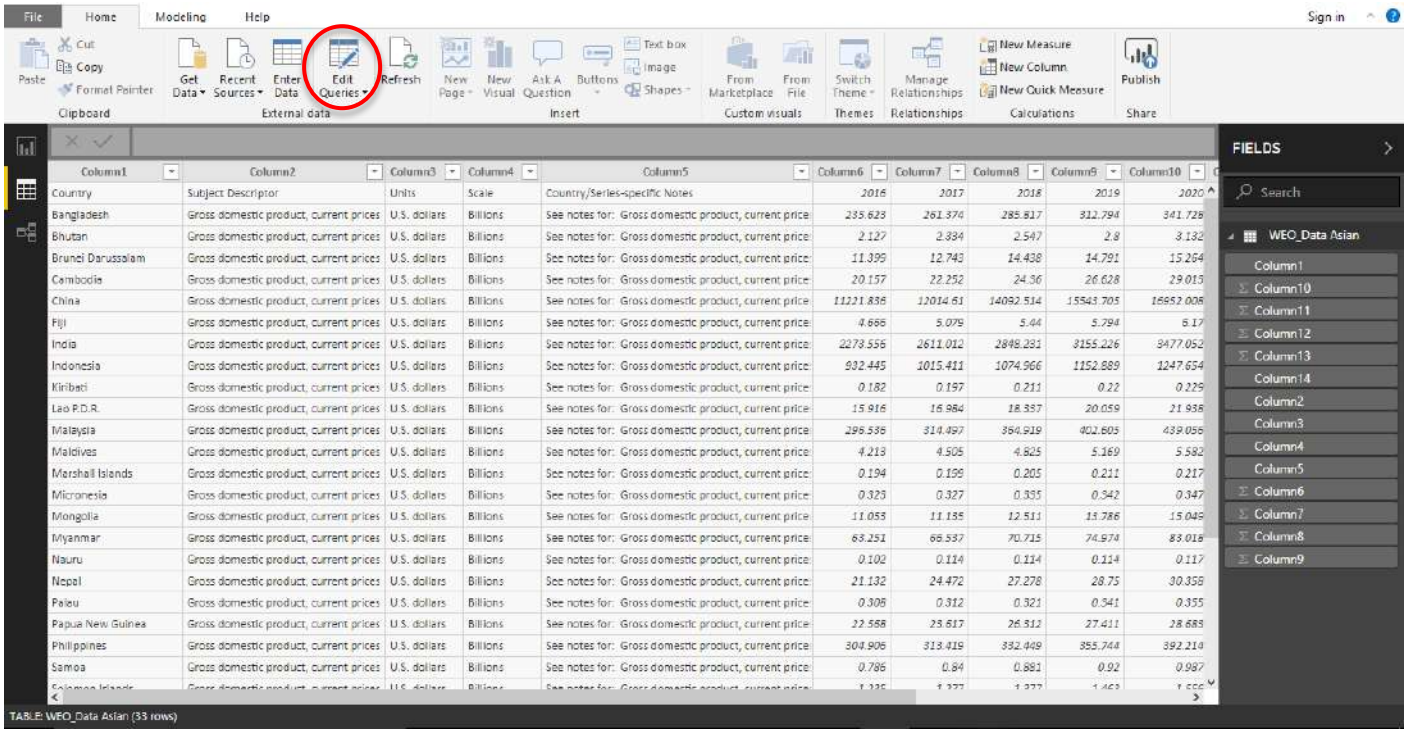

3. Data Shaping and Cleansing

For the unformatting data, we can use the **Power Query Editor** (click on **Edit Queries** tab → **Edit Queries** selection) to perform these data shaping and cleansing stages.

First, remove the unwanted column like "Country/Series-specific Notes" and "Estimates Start After" columns. In the **Power Query Editor** grid, select these two columns (hold down the **Ctrl** key for multiple selections) and right-click and select **Remove Other Columns** from the dropdown to remove the columns.

Secondly, to define header correctly, click on **Use First Row as Header** tab to change the first row descriptions become header of table.

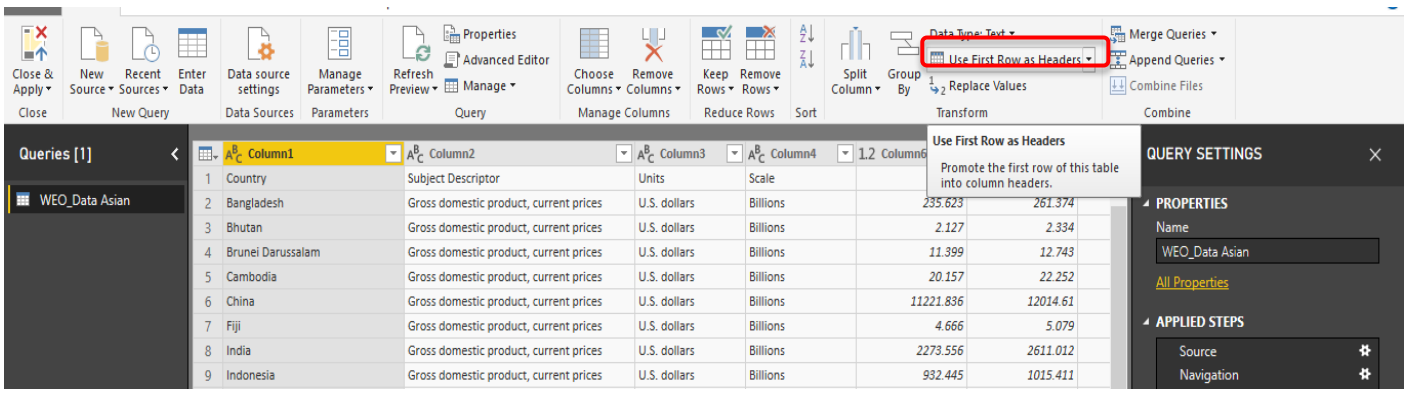

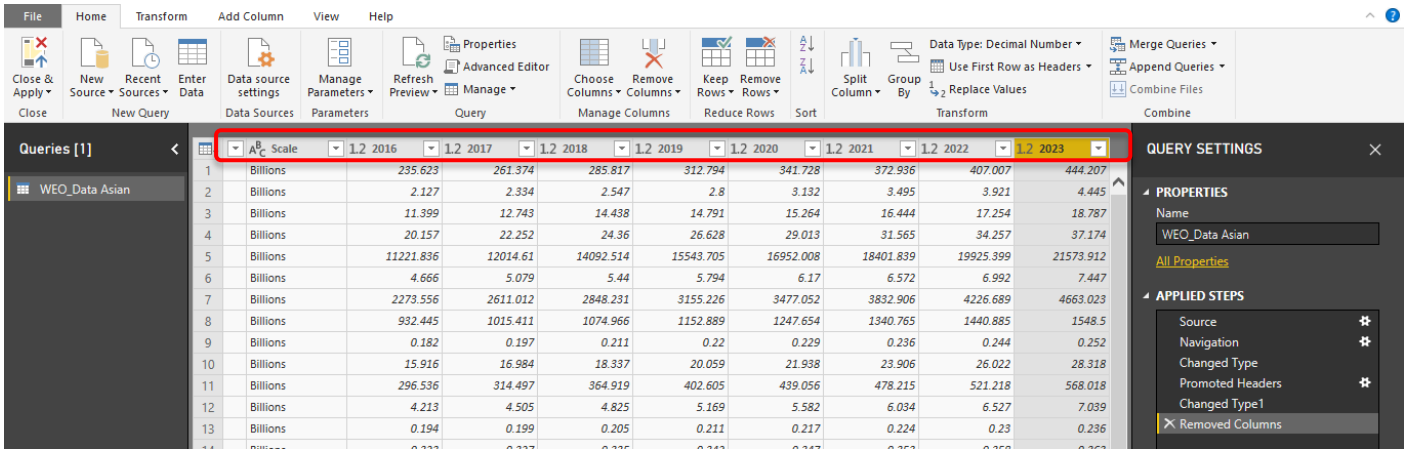

Consider to the multiple year columns (2016 to 2023), it will be better to change the years data to two columns, one for the years column and the other represent the Gross Domestic Product, GDP column. First, we highlight all multiple years columns and then changing the **Home** tab to **Transform** tab. Next, click on **Unpivot Column** to change multiples year columns to two column as shown as below.

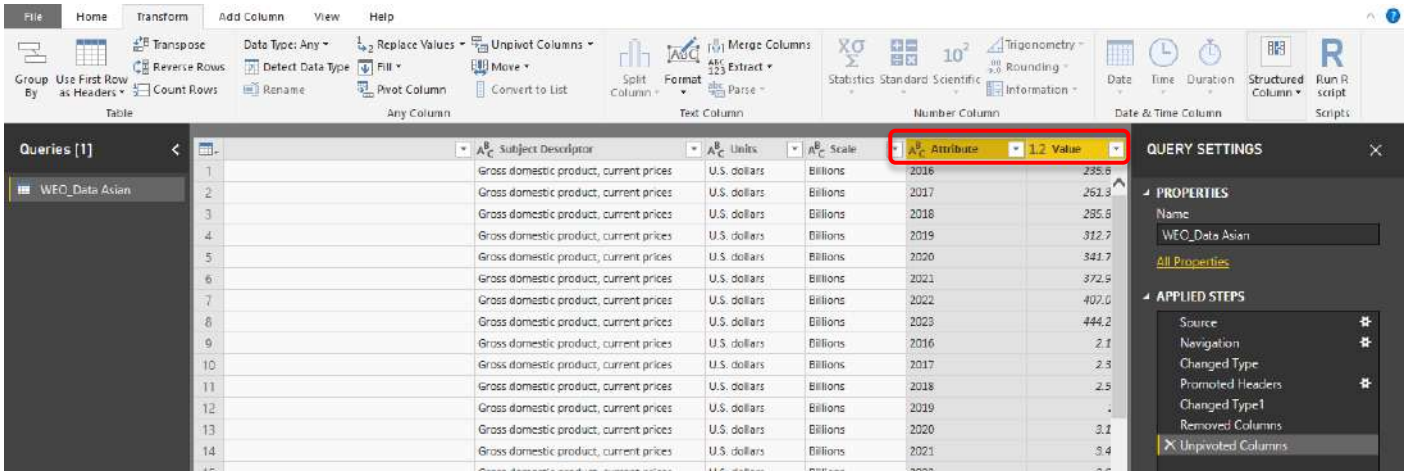

Rename the **Attribute** column as **Year** column and **Value** column as **GDP** column. Use the **Detect Data Type** button from **Transform** tab to detect the data type is defined correctly for each columns.

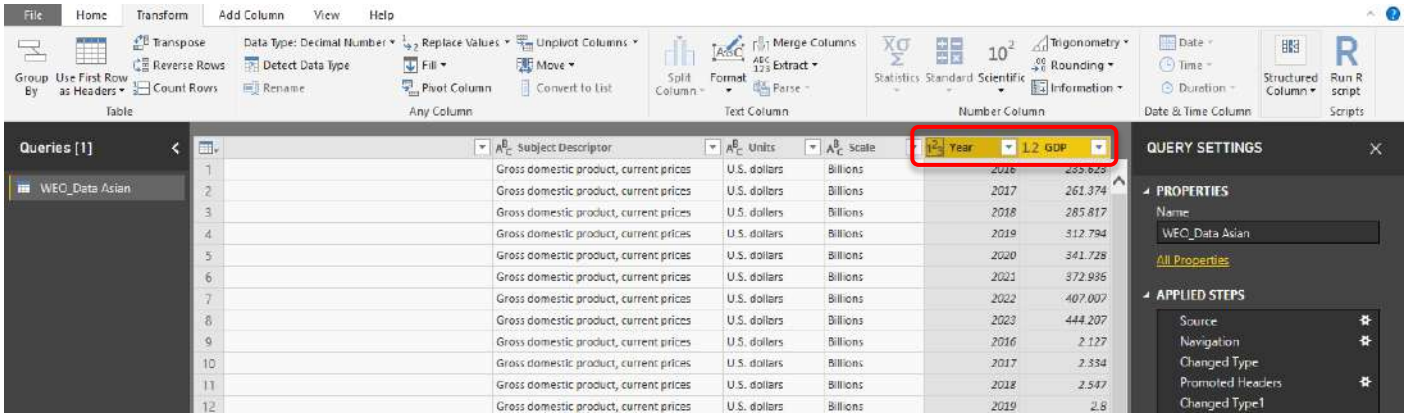

Finally, close the **Power Query Editor** by clicking on **Close & Apply** tab. Now our data is a clean data set and ready for analyzing and modeling in the report field at Power BI.

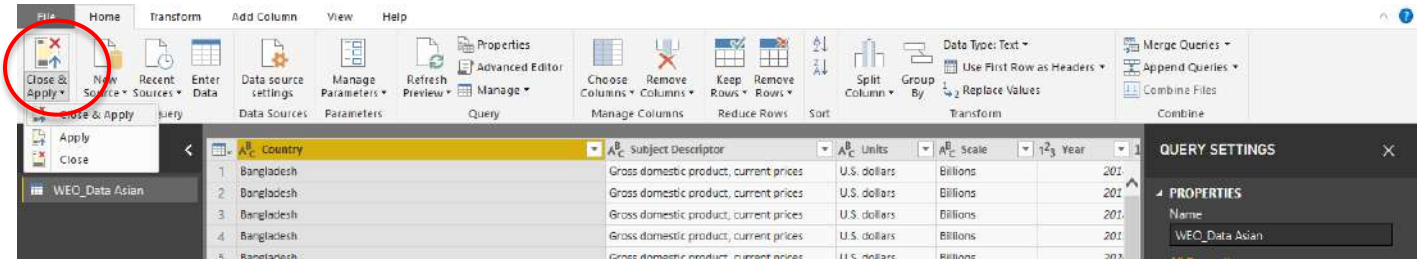

4. Create Visualization using Data Set

For the analyzing and modeling purpose, we change the **Report** field to **Data** field and turn the **Country** column formatting from "Text" to "Country". Power BI had a strong visualization data using map analysis. First, we change the **Home** tab to **Modeling** tab, click on **Data Category** and change the **Uncategorized** to **Country/Region** type.

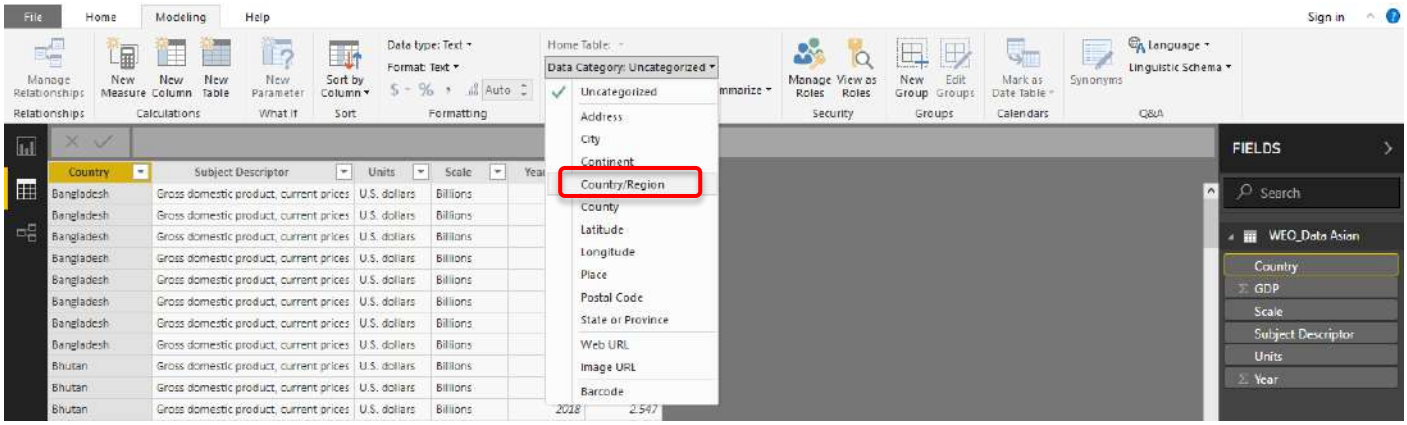

Now go back to the report filed and we can start to do visualization on data sets using **VISUALIZATIONS** column. For example, we click on the Stacked Column Chart, drag the GDP information (from **FIELDS** column) to value field, Year info to Axis field, Country info to the Legend field to get the following visualization:

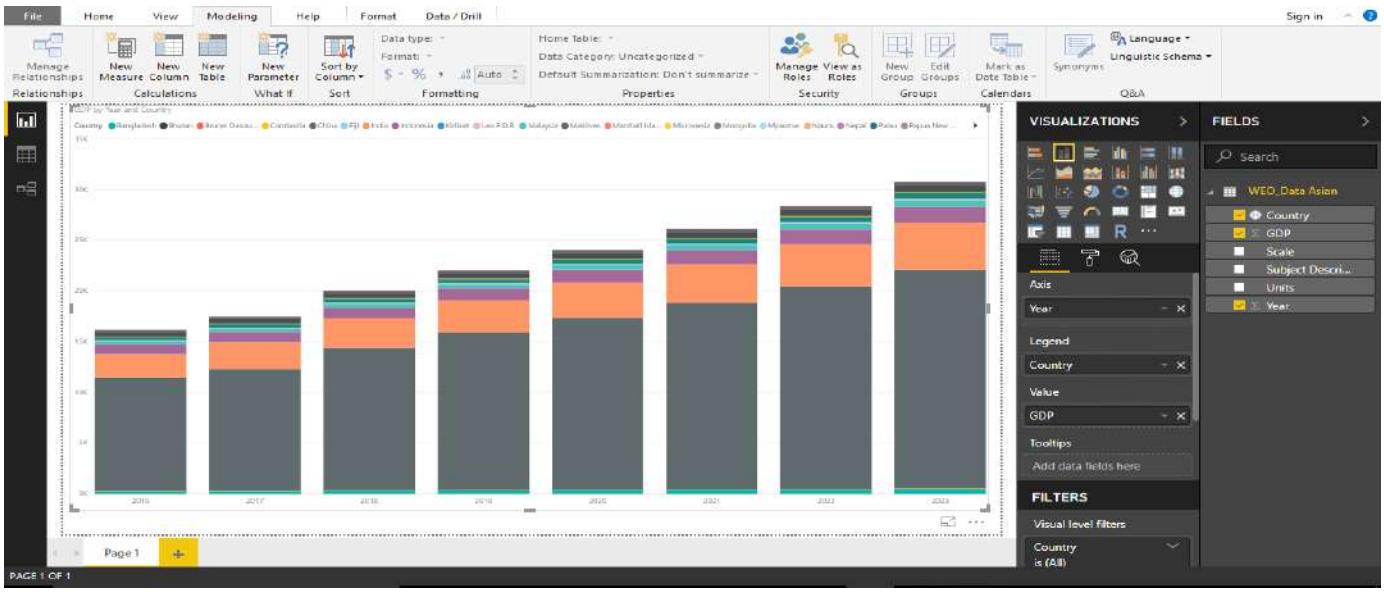

As there are too many countries on the chart, we can just analyze the top ten GDP countries using filtering function. To do so, we move to FILTERS area and click on **Country** to change the **Basic Filtering** to **Top N** filtering. We choose the number of N as 10 and drag the GDP to By value column to look for top ten GDP at Asia countries.

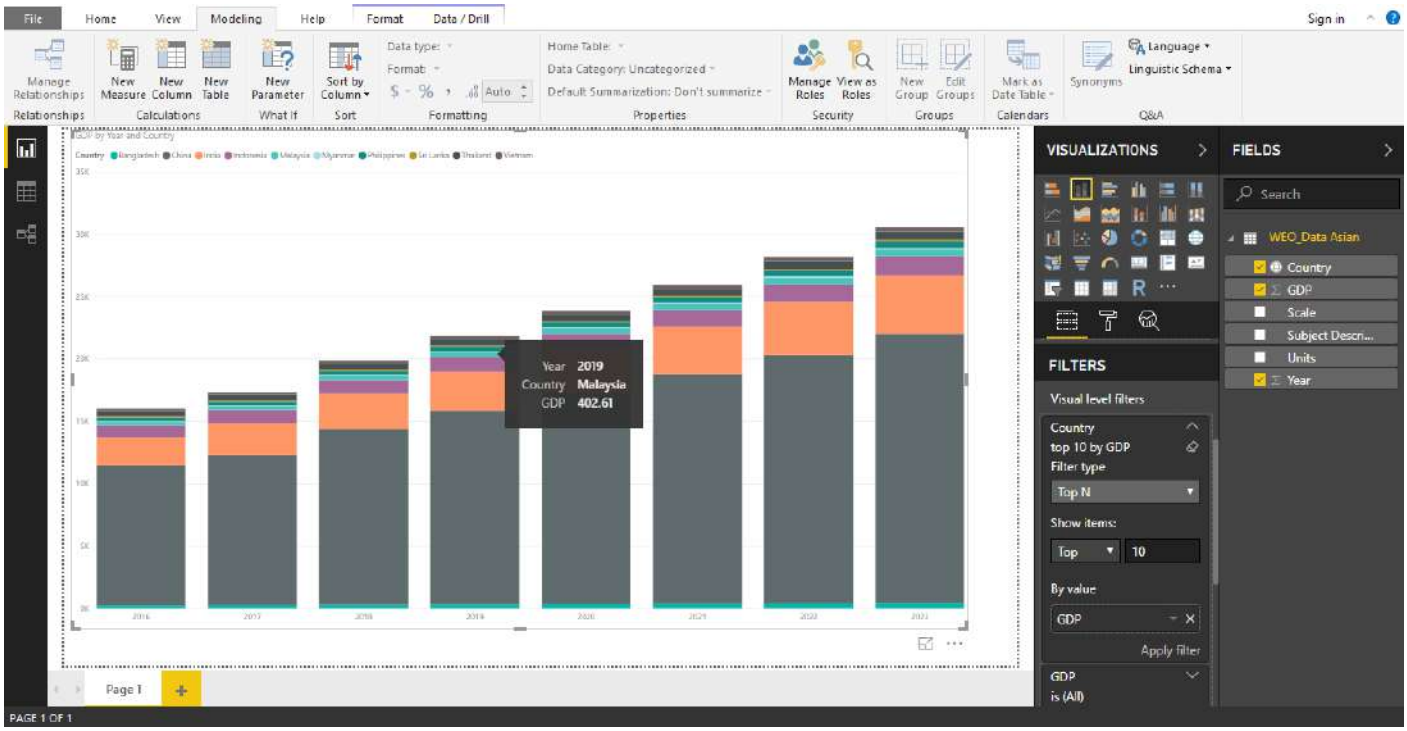

We can always change the visualization chart to others by just clicking other option charts on **VISUALIZATIONS** column.

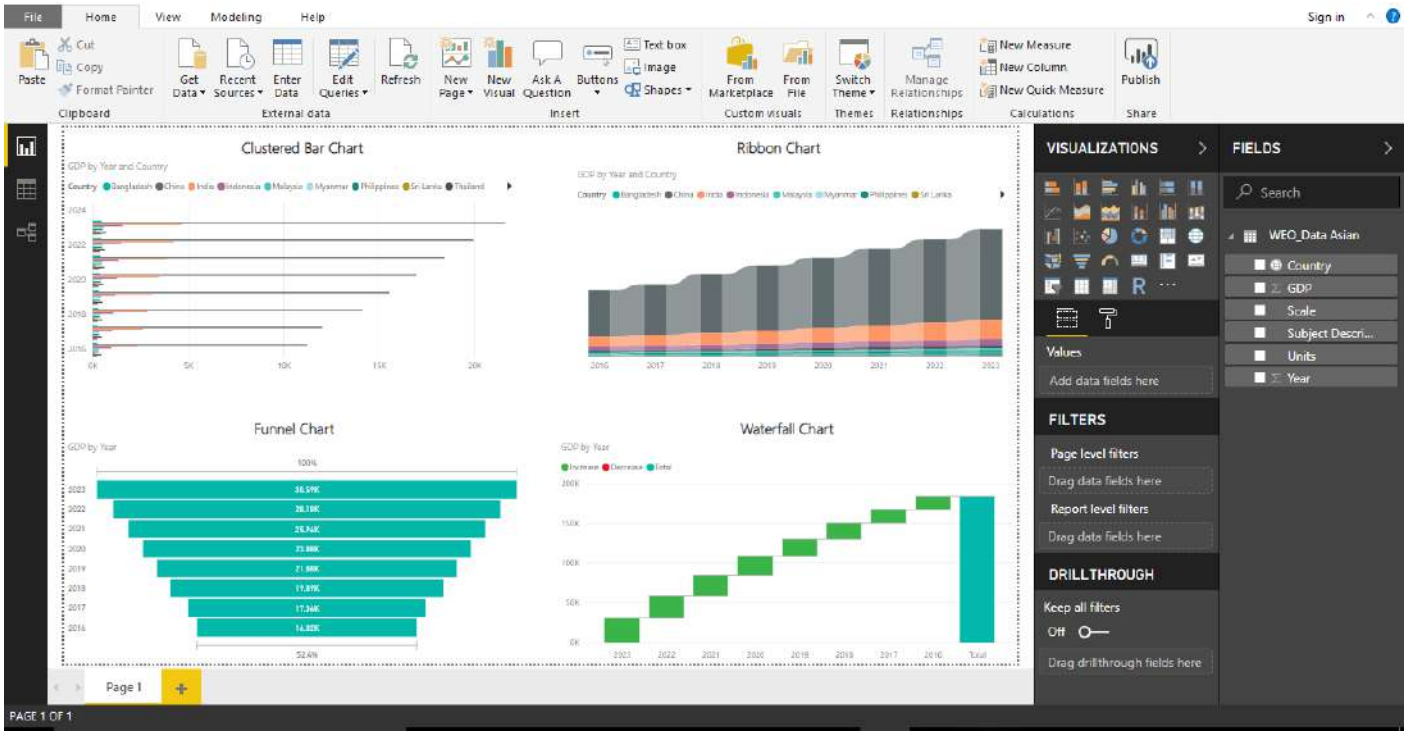

5. Conclusions

Visualization of data is a very important mechanism in every organization and business development. The user can read and understand the data easily with a good data presentation. In this paper, World Economic Outlook (WEO) data for Asia country had been visualized using different types of charts. Besides, the dashboards which are created using Power BI tool can be viewed by means of Mobile Applications such as Power Apps and Mobile Power BI. The dashboards information also can be shared on Power BI cloud service to let other users interact the data among each other using the cloud based concept. Finally, we can conclude that Power BI is a radical approach to simplifying the business intelligence data and individuals can easily provide data, create reports or aggregate them in dashboards, and share the datas with minimal investment of time and effort.

References

Miguel Martinez, 2017. *Gartner positions Microsoft as a leader in BI and Analytics Platforms for ten consecutive years* [Online]. Available at:https://powerbi.microsoft.com/en-us/blog/gartner-positions-microsoft-as-a-leader-inbi-and-analytics-platforms-for-ten-consecutiveyears/

Michael Hart, 2017. *Quick Insights with Power BI* [Online]. Available at: https://powerbi.microsoft.com/en-us/documentation/powerbi-service-auto-insights/

Microsoft Documentation, 2017. *What is Power BI* [Online]. Available at:https://powerbi.microsoft.com/en-us/what-is-power-bi/

Michelle Hoda Wilkerson, Vasiliki Laina, 2017. Youth Reasoning with Interactive Data Visualizations: A preliminary study, IDC'17 Proceedings of the 2017 conference on Interaction Design and Children 2017, 411-416.

Microsoft Power BI Organization, Microsoft Power BI Website, 2017. https://powerbi.microsoft.com/en-us/whatis-power-bi/. Accessed September 2017.

Syed Mohd Ali, Noopur Gupta, Gopala Krishna Nayak, Rakesh Kumar Lenka, 2016. Big data Visualization: Tools and Challenges, Contemporary Computing and Informatics (IC31), pp. 656-660.

On Year 1 Undergraduate Python Programming

Liew How Hui[a]

[a]*Department of Mathematical and Actuarial Sciences, Lee Kong Chian Faculty of Engineering and Science, Universiti Tunku Abdul Rahman, Malaysia.*
**Email (corresponding author):* liewhh@utar.edu.my

Abstract

Despite its age, the philosophy behind the textbook "Algorithms + Data Structures = Programs" is still important for beginner programmers. How we store data determines the kind of algorithms we need to handle the data. Getting familiar with the basic data structures is crucial to the building up of a good foundation for undergraduate programming. Despite the many programming languages in industry, Python, being a simple language, may be one of the best language for beginners.

1. Undergraduate Programming Language

They are many ways of doing programming, there is the functional approach, the traditional imperative approach and the modern object-oriented approach. Computer scientists have been arguing the best programming languages for undergraduate teaching.

The proponents of functional approach will claim that an extension of Scheme called Racket (Felleisen et al., 2010) is the best programming language for undergraduate teaching. They have tried to illustrate their points in various talks such as "How to Teach Programming to Your Loved Ones" (https://www.youtube.com/watch?v=BleOgPhsdfc), "YOW! Lambda Jam 2019 - George Wilson - Functional Programming in Education" (https://www.youtube.com/watch?v=yLTgPuOrUmI) and "Lambda Jam 2015 - Robby Findler - Racket - A Programming-Language Programming Language" as well as the availability of free textbooks such as https://htdp.org/2018-01-06/Book/. Despite the power of Racket, it is rarely used in the IT industry and therefore very few universities adopted it as an undergraduate programming language.

In the 1980s, BASIC, COBOL, C, Pascal and Fortran were popular undergraduate programming languages. They are based on the imperative approach. In the 1990s, object-oriented programming started to rise and Java started to become the undergraduate programming language for training undergraduates to master the object-oriented approach.

When there are so many programming languages, which one of them is the best pedagogical programming language? The criteria that a university should follow should be pedagogical rather than the popularity of the language in the industry.

A good pedagogical programming language should meet the following requirements:

1. The syntax of the language should not be simple and easy to learn and write;
2. It should support the basic data structures such as integers, floating-point numbers, I/O and file handling; the derived data structures such as list or array; and user-defined data structures such as "class" or "record";
3. The program written in the language should be easy to run;

4. The language should be useful in "problem-solving" by providing useful modules for data processing, web handling, and graph plotting.

The current popular programming languages which are found in the industry and some universities (such as UTAR) are C, C++, Java, C#, JavaScript, Php, Python, R, etc.

All the mentioned programming languages meet criterion 2, so we will only investigate criteria 1, 3 and 4. They are compiled into the table below.

Programming Language	Criterion 1	Criterion 3	Criterion 4
C	Simple	compile, link, run	Installing an additional "library" can be complex
C++	Complex	compile, link, run	Installing an additional "library" or a "module" is very complex
Java	Medium	compile, run	Need to put the right jar libraries
C#	Medium	compile, run	Need to put DLL library in the right place
JavaScript	Medium	run	Installing modules require NPM and Internet connection
Php	Medium	run	Php libraries need to be put in the right place
Python	Simple	run	Anaconda Python has all the essential modules
R	Medium	run	Installing modules require Internet connection

Python is a simple programming language with a relatively complete modules and is gaining popularity in universities and IT industry. Therefore, Python will be used in this article but some other language may be used as a comparison.

2. Identifiers, Keywords and Basic Data Structures

An identifier is a string (normally a "name") of English alphabets 'a' to 'z' (in capital or small letters), underscore character and digits 0 to 9 which is used in a programming language to refer to a "data".

A keyword is a string that has been reserved by the programming language and cannot be used as an identifier. The keywords in Python are listed below.

```
False     class      finally    is         return
None      continue   for        lambda     try
True      def        from       nonlocal   while
and       del        global     not        with
as        elif       if         or         yield
assert    else       import     pass
break     except     in         raise
```

A basic data structure (or basic data type) is a "class" of "data". For example, `True` and `False` are data of the class Boolean; 0,1,2, etc. are data of the class Integer.

Boolean, integer, float, complex float, string, file are the basic data structures in Python. An example illustrating how we can construct various basic data structures and use identifiers in Python to refer to them is shown below.

```
1  aBoolean1 = True
2  aBoolean2 = False
3  aBoolean3 = aBoolean1 and aBoolean2
4  anInteger = 12345678901234567890123456789012345678901234567899
5  # Floats will be introduced in UECM3034 Numerical Methods
6  aFloat =    123456789012345678901234567890123456789012345678900.0
7  aFloat2 = aFloat - anInteger
8  aComplex = 12345 + 67890j
9  aString = "Hello Python"
10 aFile = open("filename.txt", "rt")
```

In the above example, the "#" is used to denoted a comment, i.e. anything after # in that line will be ignored by Python; the equal sign "=" represents and assignment of the basic data to a "name". For example, in line number one, we have created a data "True" and then use the "identifier" `aBoolean1` to refer to the data "True".

Apart from the assignment operation "=", we also spotted other operations such as "`and`", "`-`", "`+`" which are associated with the basic data structures.

With the basic data structures, we can do many things such as writing a simple program to perform calculation using the Heron's formula which we learned in our high school. For example, suppose there is a triangle with three sides of length 4, 5 and 6 units, find the area of the triangle. A mathematical solution is illustrated below.

Let $a = 4$, $b = 5$, $c = 6$. Then

$$s = \frac{a+b+c}{2} = \frac{15}{2} = 7.5$$

and the area of the triangle, A, is

$$A = \sqrt{s(s-a)(s-b)(s-c)} = \sqrt{7.5 \times 3.5 \times 2.5 \times 1.5} \approx 9.921567$$

It is not difficult to translate the problem to a Python program as illustrated below.

```
1 a = 4.0; b = 5.0; c = 6.0
2 s = (a+b+c)/2
3 from math import sqrt
4 A = sqrt(s*(s-a)*(s-b)*(s-c))
5 print("The area of the triangle, A, is", A)
```

What one needs to know in the above program is that the standard mathematical functions in Python are collected in the library called `math`. To use the functions such as `sqrt` (square root), sine (`sin`), cosine (`cos`), etc. we need to `import` them using the syntax mentioned above.

3. Imperative Programming and Control Flow

According to Wikipedia, *imperative programming* is a programming paradigm based on *statements* that change *states* in order to perform computation. In the previous section, we have used identifiers to refer to data. The identifiers change be changed. For example, if we have "`a=1`", then after the following statement is executed, the identifier of `a` has a value of 2.

```
a = a + 1   # a = 1 + 1 = 2
```

Most programming languages (include all the programming languages we mentioned above) support the imperative programming paradigm. The "opposite" of imperative programming paradigm is declarative programming paradigm. There are very few programming languages which are purely declarative, Prolog is one of them.

It is impossible to write all programs using just the assignment and mathematical functions mentioned in the previous section. For example, the solution of a quadratic equation

$$ax^2 + bx + c = 0$$

requires the checking of value of $b^2 - 4ac$. When $b^2 - 4ac > 0$, we have two real solutions; When $b^2 - 4ac = 0$, we have a real solution; And when $b^2 - 4ac < 0$, we do not have a real solution.

To handle an instruction involving "checking" or "condition", Python provides the "if-else" statement shown below.

```
if b**2 - 4*a*c > 0:
    msg = "two real solutions."
elif b**2 - 4*a*c == 0:
    msg = "a real solution."
else:
    msg = "no real solution."
print(f"The quadratic equation {a}x^2 + {b}x + {c} has " + msg)
```

Note that many programming languages has similar syntax (e.g. C, C++, Java, C#, etc.) but some programming languages such as Scala provides the notion of "guard" for pattern matching for "checking".

```
def eqn(a:Float,b:Float,c:Float) = {
  val msg = b*b-4*a*c match {
    case x if x > 0 => "two real solutions."
    case 0.0 => "a real solution."
    case _ => "no real solution."
  }
  println(s"The quadratic equation ${a}x^2 + ${b}x + ${c} has " + msg)
}
```

When we need to repeat instructions, a loop is required. Python provides a "for" loop and a "while" loop for the handling of loops.

An example involving loops is the generation of truth table for a proposition with n atomic statements in discrete mathematics. When $n = 3$ and p, q, r are atomic statements, a proposition $(p \wedge q) \rightarrow r$ has the following truth table.

p	q	r	$(p \wedge q) \rightarrow r$
T	T	T	T
T	T	F	F
T	F	T	T
T	F	F	T
F	T	T	T
F	T	F	T
F	F	T	T
F	F	F	T

The Python program using for loops to generate the above truth table is shown below.

```
for p in [True, False]:
    for q in [True, False]:
        for r in [True, False]:
            statement = (not (p and q)) or r
            print(f"{p} & {q} & {r} & {statement}")
```

An example involving loops is the generation of standard normal distribution table (Table 3.). The Python program using for loops to generate Table 3. is shown below.

```
from scipy import stats
print(" "*3,end="")
for j in range(10):
    print(f"{j:6d} ",end="")
print()
for i in range(30):
    print(f"{0.1*i:2.1f} ",end="")
    for j in range(10):
        x = 0.1*i + 0.01*j
        y = stats.norm.cdf(x)
        print(f"{y:6.4f} ",end="")
    print()
```

Should we stop with conditional statements and loops? The answer is negative because modern programming emphasise "reusability". The truth table example is closely related to combinatorics and Python has included standard combinatorial algorithms into the `itertools` module. Therefore, it is important in undergraduate programming to expose students to "reuse" functions from standard modules.

```
import itertools
for p,q,r in itertools.product([True,False],[True,False],[True,False]):
    statement = (not (p and q)) or r
    print(f"{p} & {q} & {r} & {statement}")
```

For a one-dimensional array, the notions of "stream" and "map"–"reduce" are becoming standard "reusable" components. For example, the computation of (zero-degree-of-freedom) variance of a sequence $x_1, \cdots, x_n$ is mathematically defined as

$$\text{Var}[x] = \sum_{i=1}^{n} \frac{(x_i - \overline{x})^2}{n}, \quad \overline{x} = \frac{1}{n} \sum_{i=1}^{n} x_i.$$

The implementation in Python will involve "map-reduce" as follows.

```
mean = lambda xs: sum(xs)/len(xs)
variance = lambda xs: sum([(x-mean(xs))**2 for x in xs])/len(xs)
```

Many programming languages are introducing the "map-reduce" functions in various ways.

4. Things for Year 1 in Programming

So far, we can see that Python can be used as a calculator to help us "solve" some secondary school level and even some university level mathematical problems involving "numbers".

What are the things that we should include in the year 1 undergraduate programming to demonstrate how programming is used in the real-world?

Table 1: Standard Normal Distribution Table

	0	1	2	3	4	5	6	7	8	9
0.0	0.5000	0.5040	0.5080	0.5120	0.5160	0.5199	0.5239	0.5279	0.5319	0.5359
0.1	0.5398	0.5438	0.5478	0.5517	0.5557	0.5596	0.5636	0.5675	0.5714	0.5753
0.2	0.5793	0.5832	0.5871	0.5910	0.5948	0.5987	0.6026	0.6064	0.6103	0.6141
0.3	0.6179	0.6217	0.6255	0.6293	0.6331	0.6368	0.6406	0.6443	0.6480	0.6517
0.4	0.6554	0.6591	0.6628	0.6664	0.6700	0.6736	0.6772	0.6808	0.6844	0.6879
0.5	0.6915	0.6950	0.6985	0.7019	0.7054	0.7088	0.7123	0.7157	0.7190	0.7224
0.6	0.7257	0.7291	0.7324	0.7357	0.7389	0.7422	0.7454	0.7486	0.7517	0.7549
0.7	0.7580	0.7611	0.7642	0.7673	0.7704	0.7734	0.7764	0.7794	0.7823	0.7852
0.8	0.7881	0.7910	0.7939	0.7967	0.7995	0.8023	0.8051	0.8078	0.8106	0.8133
0.9	0.8159	0.8186	0.8212	0.8238	0.8264	0.8289	0.8315	0.8340	0.8365	0.8389
1.0	0.8413	0.8438	0.8461	0.8485	0.8508	0.8531	0.8554	0.8577	0.8599	0.8621
1.1	0.8643	0.8665	0.8686	0.8708	0.8729	0.8749	0.8770	0.8790	0.8810	0.8830
1.2	0.8849	0.8869	0.8888	0.8907	0.8925	0.8944	0.8962	0.8980	0.8997	0.9015
1.3	0.9032	0.9049	0.9066	0.9082	0.9099	0.9115	0.9131	0.9147	0.9162	0.9177
1.4	0.9192	0.9207	0.9222	0.9236	0.9251	0.9265	0.9279	0.9292	0.9306	0.9319
1.5	0.9332	0.9345	0.9357	0.9370	0.9382	0.9394	0.9406	0.9418	0.9429	0.9441
1.6	0.9452	0.9463	0.9474	0.9484	0.9495	0.9505	0.9515	0.9525	0.9535	0.9545
1.7	0.9554	0.9564	0.9573	0.9582	0.9591	0.9599	0.9608	0.9616	0.9625	0.9633
1.8	0.9641	0.9649	0.9656	0.9664	0.9671	0.9678	0.9686	0.9693	0.9699	0.9706
1.9	0.9713	0.9719	0.9726	0.9732	0.9738	0.9744	0.9750	0.9756	0.9761	0.9767
2.0	0.9772	0.9778	0.9783	0.9788	0.9793	0.9798	0.9803	0.9808	0.9812	0.9817
2.1	0.9821	0.9826	0.9830	0.9834	0.9838	0.9842	0.9846	0.9850	0.9854	0.9857
2.2	0.9861	0.9864	0.9868	0.9871	0.9875	0.9878	0.9881	0.9884	0.9887	0.9890
2.3	0.9893	0.9896	0.9898	0.9901	0.9904	0.9906	0.9909	0.9911	0.9913	0.9916
2.4	0.9918	0.9920	0.9922	0.9925	0.9927	0.9929	0.9931	0.9932	0.9934	0.9936
2.5	0.9938	0.9940	0.9941	0.9943	0.9945	0.9946	0.9948	0.9949	0.9951	0.9952
2.6	0.9953	0.9955	0.9956	0.9957	0.9959	0.9960	0.9961	0.9962	0.9963	0.9964
2.7	0.9965	0.9966	0.9967	0.9968	0.9969	0.9970	0.9971	0.9972	0.9973	0.9974
2.8	0.9974	0.9975	0.9976	0.9977	0.9977	0.9978	0.9979	0.9979	0.9980	0.9981
2.9	0.9981	0.9982	0.9982	0.9983	0.9984	0.9984	0.9985	0.9985	0.9986	0.9986

If we look at the undergraduate software engineering final year projects, we will find that they can be classified into “online training system”, “online booking/reservation system”, “content/data management system”, etc. These projects are too complex for year 1 undergraduate programming to undertake.

I would argue that the thing that a first year software engineering undergraduate student should learn is the development of a simple data management system which allows users to add, delete, query and summarise data. Many students have learned about Microsoft Word and Excel in secondary schools and asking them to develop a simple data management system from scratch will help them appreciate the complexity of modern application software.

However, for science and engineering students, what a first-year undergraduate student needs to learn is the development of a simple geometric modelling system (GMS) system. The GMS system should probably include the addition, removal, query and rendering of simple 2D and 3D geometrical objects.

By using imperative programming, a year 1 student will find that they will be using global variables and many functions in the design of a system. In addition, a science or an engineering student will find the need to learn how to translate a physical object to mathematical representation.

A year 1 assignment should probably include the functionality of the estimation of the cost of constructing "houses" using simple geometry. The year 1 project can be polished year 2 or 3 by adding in more scientific functionalities such as more sophisticated equation solvers, statics modelling, etc. For example, it should be polished into the estimation of waste generation and processing modelling and simulation in view of the importance of the development of sustainable and green cities.

The design of software is costly, suppose there are 800 to 1200 potential customers who are willing to buy a certain computer game and the development cost of the computer game is as follows:

- The computer game takes three years and at least 5 staffs to develop;
- Each staff gets a monthly salary of RM3,500 for the first year and then every year the monthly salary will be increased by 3% to retain experience staff.

Write a computer program to estimate how much should the computer game be sold at the beginning of the fourth year to have a return on investment of 20%.

A sample Python implementation goes like this:

```
number_of_dev_year = 3
number_of_staff = 5
potential_customers = 800
starting_monthly_salary = 3500
annual_increment = 1.03
roi = 0.2
total_cost = sum([
   number_of_staff * starting_monthly_salary * 12 * annual_increment**i
   for i in range(number_of_dev_year)
])
print("Total Cost          =", total_cost)
computer_game_price = total_cost * (1 + roi) / potential_customers
print("Computer Game Price =", computer_game_price)
```

The above program may not be of good quality but a well-written program will always be better than using Excel, which is the most "popular programming language" in the business world. Firstly, it is difficult to document an Excel program and it is easy to document a computer program. Secondly, the computer program can be properly extended to perform simulations for various uncertain situations and Excel is still less convenient for carrying out simulations without the use of VBA.

5. Errors and Programming Environments

Everyone will come across errors when writing a computer program. There are two types of errors — "syntax error" and "running time error".

We come across the "syntax error" when we try to use some syntax that a programming language cannot understand. For example, in Python, we cannot write "int i=1;" because this is C language syntax and not Python syntax. Just copying something from other programming language will result in syntax error.

We come across the "running time error" when the computer program come across values that it cannot handle. For example, the statement `a/b` will result in an error when **b=0**. In Python, this leads to a `ZeroDivisionError`.

Year 1 students will have to practise and to learn from "errors" to write computer program with minimum to no errors.

When it comes to the programming environments, there are experts who swear by the integrated development environment (IDE). Majority of the year 1 students will also prefer the IDE because the

interface seems fancier and more professional. Anaconda Python package has a list of programming environments for Python:

1. Spyder IDE
2. Jupyter Notebook
3. Anaconda Prompt

The first item is a very nice IDE but the Python command prompt in the IDE can sometimes crashed and the whole IDE has to be restarted.

The Jupyter Notebook is popular with trainers because they can prepare the "Python slide" directly with it.

Both environments do not separate the editing of a Python program and running a Python program. Therefore, if the students are exposed Anaconda Prompt, it is difficult for them to see what is really happening: A Python program is only a text file read and executed by a Python interpreter.

6. Conclusion

Year 1 undergraduate programming should be limited to the teaching of imperative programming which has been the most widely used programming technique. Twyla Tharp said that "before you can think out of the box, you have to start with a box." I believed that imperative programming, together with a rather rich of data structures in Python and the skill to translate a real-world problem to mathematical and programming representation, serve as the right "box" for year 1 programming skills.

Programming skills will not be useful if young programmers are not exposed to how the skills are applied. The data management system and the GMS system are two good examples that help young people engage in the learning of skills which are relevant to solving real-world problems.

References

Felleisen, M., Findler, R. B., Flatt, M., Krishnamurthi, S., Barzilay, E., McCarthy, J. and Tobin-Hochstadt, S. 2010, *The Racket Manifesto*, *in* 'Leibniz International Proceedings in Informatic', pp. 1–16.

Building Phylogenomic Tree with N-gram Contrast Value Vector

Lim Foo Weng[a], Goh Yong Kheng[b]

[a]*Department of Physical and Mathematical Science, Faculty of Science, Universiti Tunku Abdul Rahman, Malaysia. Email (corresponding author): limfw@utar.edu.my*

[b]*Department of Mathematical and Actuarial Sciences, Lee Kong Chian Faculty of Engineering and Science, Universiti Tunku Abdul Rahman, Malaysia. Email: gohyk@utar.edu.my*

Abstract

Traditional phylogenetic tree are build based on the alignment of fragment of annotated sequences of the interested genomes. In this paper, we will present an alternative algorithm of building phylogenetic tree based on the characteristic "signature" word usage in genomes analogous to the natural language processing. Here, we apply statistical N-gram analysis on whole genome sequences of several organisms. We calculated the occurrences of difference N-grams and the contrast value and departure values, which are the deviations of N-grams occurrences from their expectations, for every chromosome of 28 organisms. It could be shown that a few particular genome N-grams are found in abundance in one organism but occurring very rarely in other organisms, there by serving as genome signatures. Later, we consolidate the signature information on each organism to a features vector that consists of the average of the contrast value and departure values for 2-gram, 3-gram, 4-gram and 5-gram. From the features vector, we build the phylogenetic tree using correlations as the similarity measures, we could reproduce the taxonomy tree of 28 organisms.

1. Introduction

Every living organism possesses a genomic signature which does not depend on knowledge of individual genes or alignment of homologous sequences. In general, genomic signature profile is invariant across the genome of an organism and is similar for closely related species, and show a dissimilarity pattern between non related species. By analyzing the similarity of genomic signature among organism, we could construct a phylogenetic tree. Most common used techniques in building phylogenetic tree are based on sequence alignment, which compare the similarity of fragment from different organisms, and the observed similarity measures were used to constructing phylogenetic tree that shows the probable evolution of various organisms.

Although the sequence alignment methods were successful on building various phylogenetic trees, most are only use a small portion of the organisms. Various methods on characterization and classification of the organisms by utilizing the whole-genome have been developed. In the work of Andrewand Karlin(2001), the dinucleotide relative abundances values have shown very similar within mammalian mitochondrial genomes and animal and fungal mitochondrial are generally moderately similar but it diverge significantly from plant and protest mitochondrial set.

Also, Stuartet al. (2002)and Edgar (2004)used N-gram composition method for classification of both protein and nucleotide sequences. Other alignment free sequences comparison such as Volkovichet al. (2005) applied N-grams to the classification of genome sequences considered as text over the four-letter alphabet {A, C, G, T}. Different N-gram based methods for identification of compositionally distinct region, functional sites were proposed by Rajan et al.(2007), Srividhya et al. (2007) and Tobi andBahar (2007).

In this paper, instead of using various size of N-gram, we use the different compositional features or genomic signature such as contrast value and departure values to analyze the genetic text and later to construct a relationship tree for several organisms.

2. Methods

Let *S* be a genome sequence over the four-letter alphabet *A* = {A, T, G, C}. We define an *N*-gram (ξ) of length *N* as a string of *N* characters over the given alphabet *A*. A genome sequence can be viewed as a stream of overlapping *N*-grams one after another. In the sequence, *S* there is total | *S* | - *N* + 1, *N*-gram of length *N*, where | S | is the length of sequence.

In order to map a long genome or sequence to a point in a high dimension space for comparison, one would need a way to describe the characteristic signature of a sequence and a similarity measure to rank the relatedness of different sequences. A simple characterization and comparison of these sequences are calculating the correlation for the frequency vectors.

For any *N*-gram, let denote *f* (ξ, *S*) be the observed frequency of *N*-gram ξ in the text *S*. The frequency of ξ is the number of occurrences of ξ in the sequence *S* divided by (| S | – N + 1).

Given the observed frequencies of the *N*-grams of size (*N* – 2) and of size (*N* – 1), we can calculate the expected frequency of the *N*-grams in genome sequence *S* as

$$E(a_1..a_N, S) = \frac{f(a_1..a_{N-1}, S) \times f(a_2..a_N, S)}{f(a_2..a_{N-1}, S)} \tag{1}$$

In the case of *N* = 2, the formula (1) is reduced to

$$E(a_1a_2, S) = f(a_1, S) \times f(a_2, S) \tag{2}$$

There exist 4^N different *N*-grams of length *N*. For example, if *N* = 2, there exist 16 *N*-grams: AA, AT,..., TT. Thus, the *N*-gram bias in *S* could be defined by the contrast value

$$q(\xi, S) = f(\xi, S) - E(\xi, S) \tag{3}$$

and the departure value

$$d(\xi, S) = \frac{f(\xi, S)}{E(\xi, S)} \tag{4}$$

The *N*-vocabulary vector of the genome is the set of the characteristic values for all the *N*-grams of length *N*. In particular, we denote $\mathbf{q}(S) = \{q(\xi_1 S), \ldots, q(\xi_n S)\}$ be the contrast *N*-vocabulary and the departure *N*-vocabulary as $\mathbf{d}(S) = \{d(\xi_1, S),..d(\xi_n, S)\}$ .Since the size of the genome alphabet is four, then the size of the *N*-vocabulary is $n = 4^N$. Thus, a genome with any length is mapped into a point in the 4^N dimensional space. To compare the similarity between two genomes S_1 and S_2, we use the correlation as the similarity measures:

$$C(S_1, S_2) = \frac{\mathbf{q}^T(S_1)\mathbf{q}(S_2)}{\|\mathbf{q}(S_1)\|\|\mathbf{q}(S_2)\|} \tag{5}$$

3. Results

In this study, 28 different organisms were chosen to test the clustering of the genetic texts based on contrast value and departure value. For each of the organisms, we calculated the contrast value and departure value for N-grams with N = 2, 3, 4 and 5. Figure 1 shows the dendogram construct by using correlation coefficient CN as the similarity measure and single linkage clustering method. From the observation, it shown that departure value vector performs better in clustering the organism.

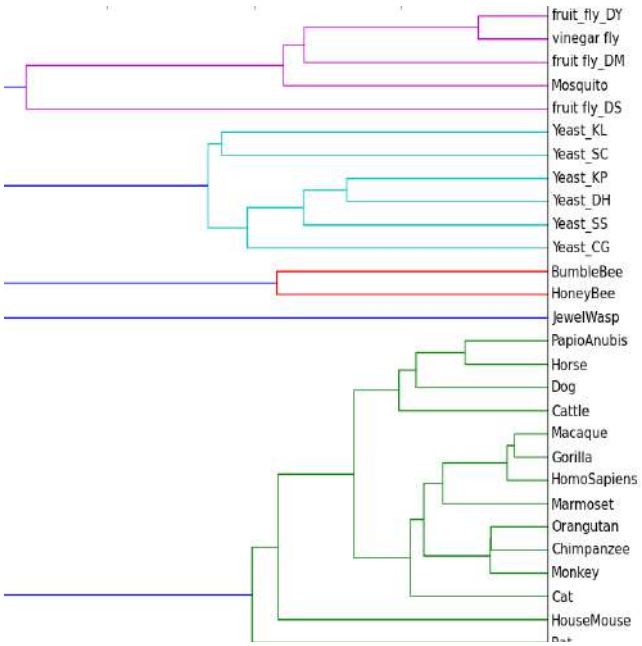

Figure 1(a): The figure shows dendrogram built from the genetic texts based on contrast value.

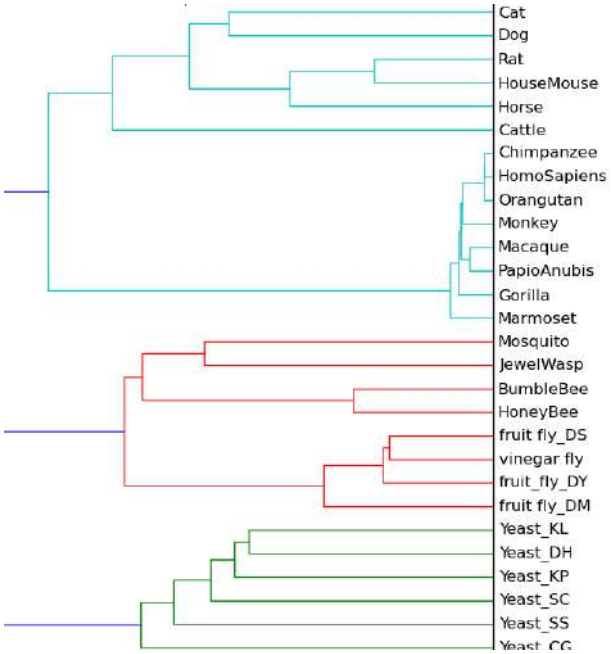

Figure 1(b): The figure shows dendrograms built from the genetic texts based on departure value.

From Figure 1(a), we can observe that the organisms are grouped together to the large group. However go to the branches of each large group, the organisms which are closely related are placed ambiguously. And the details of classification still remain a challenge.

4. Conclusions

The approach of departure value vector and contrast value from *N*-gram analysis is a relatively simple and yet effective approach for clustering genetic texts. In terms of effectiveness, departure value performs better than the contrast value. As shown in Figure 1(b), not only the organisms are successfully

group into a larger group like mammal, yeast and insect, it also able to branches of mammal like monkey, Orangutan, Gorilla, Chimpanzee under same types of organisms. However, the positions of each organism under same type of group still remain a challenge. Here, the departure value and correlation measure are robust to identify the larger family.

References

Andrew, J.G. and Karlin S., 2001. Genome-Scale Compositional Comparisonsin Eukaryotes. *Genome Research*, 11, pp. 540–546.

Edgar, R.C., 2004. Local homology recognition and distance measures in linear time using compressed amino acid alphabets. *Nucleic Acids Research*, 32(1), pp.380–384.

Rajan, I., Aravamuthan, S. and Mande, S.S., 2007. Identification of compositionally distinct regions in genomes using the centroid method. *Bioinformatics*, 23(20), pp. 2672–2677.

Srividhya, K.V. et al., 2007. Identification of prophages in bacterial genomes by dinucleotide relative abundance difference. *PLoS One*, 2(11), e1193.

Stuart, G.W., Moffett, K. and Baker, S., 2002. Integrated gene and species phylogenies from unaligned whole genome protein sequences. *Bioinformatics*, 18, pp.100–108.

Tobi, D. and Bahar, I., 2007. Recruitment of rare 3-grams at functional sites: Is this a mechanism for increasing enzyme specificity?. *BMC Bioinformatics*, 8, pp. 226.

Volkovich, Z., Kirzhner, V., Bolshoy, A., Nevo, E. and Korol, A., 2005. The method of N-grams in large scale clustering of DNA texts. *Pattern Recognition,* 38(11), pp. 1902-1912.

Minimum Redundancy and Maximum Relevance Feature Selection for Microarray Data

Chin Fung Yuen[a], **Tan Ze Ying**[b]

[a]*Department of Physical and Mathematical Science, Faculty of Science, Universiti Tunku Abdul Rahman, Malaysia.* [*]*Email (corresponding author): chinfy@utar.edu.my*

[b]*Graduated Student (BSc (Hons) Statistical Computing and Operations Research), Faculty of Science, Universiti Tunku Abdul Rahman, Malaysia.*

Abstract

Microarray analysis has developed and widely accepted for diagnosis and classification of human cancer. However, the high dimensionality of microarray data with a small sample size has made classification more difficult. Feature selection aims to reduce the dimensionality of microarray data and enhance the accuracy of the classification task by eliminating redundant features. In this paper, the feature selection method by mutual information uses to select informative genes from the microarray profile. We also use this method to find the most suitable number of selected features, *k*, and build relationships among the *k* features. Furthermore, we compare our results with previously known techniques on the performance of classification accuracy using the small number of genes. Lastly, we also dissect the regulatory relationships between genes and classify correlated gene pairs. In the end, this method plays a complementary tool in predicting and annotating relevant features, and the findings of key features with high impacts on the disease prediction might provide useful insights or clues for further experimental investigations in the medical area.

1. Introduction

The colon and rectum are constituents of the large intestine, which is the final part of the digestive tract. Colorectal cancer is the term commonly used for the cancer of colon or rectum (Muhammad, 2016). Colon cancer occurs when tumors start to develop in the lining of the colon. In cancer classification, one of the challenges is the high dimensionality of microarray data. Redundant and irrelevant information on microarray gene expression complicates the process of cancer classification. Hence, researchers need to find appropriate ways to eliminate redundant features and select informative genes for a better identification of cancer (Sun, 2016). Efficient analytical techniques reduce computing time and improve accuracy and performance prediction. In this paper, a feature selection method by mutual information uses to select informative genes from the microarray profile.

2. Methodology

The dataset used in the study is the colon cancer dataset, which describes a colon cancer study in which gene expression levels measured on 40 normal tissues and 22 tumor colon tissues, 2000 attributes corresponding to 2000 different genes (Mohamed, 2017). In this study, we use Matlab as the main testing tool.

The Minimum redundancy and maximum relevance (mRMR) method was proposed by Ding and Peng (Ding & Peng, 2003). In their experiments, they stated that the mRMR method improves predictions in experiments on six gene expression data sets. They used mutual information to measure the similarity between genes. The idea of minimum redundancy is to select the genes which are mutually maximally

dissimilar. The minimum redundancy condition is: $\min W_{i,} W_i = \frac{1}{|S|^2} \sum_{i,j \in S} I(i,j)$. The S denotes the subset of features we are looking for in this study. *I(i, j)* represents the mutual information of two genes, and $|S|$ is the number of features in *S*.

Thus, the maximum relevance condition is to maximize the total relevance of all genes. Mutual information *I(h, g)* measures the similarity between target classes *h* and the gene expression *g;* therefore, *I(h,g)* quantifies the relevance of the gene expression *g*. The maximum relevance condition is: $\max V_{i,} V_i = \frac{1}{|S|} \sum_{i \in S} I(h,i)$. The mRMR feature set obtained by optimizing the condition in minimal redundancy and maximum relevance simultaneously. This method treats the two conditions equally important, so they give two combination criteria based on Difference and Quotient: $\max(V_i - W_i)$.

The feature vectors are delivered to the classifier so that it can group the subjects in different classes. In this study, a support vector machine (SVM) uses as a classification algorithm. Furthermore, we compare our results with previously known techniques on the performance of classification accuracy using the small number of genes. Lastly, we also dissect regulatory relationships between genes and classify correlated gene pairs.

3. Results and Discussion

The performance of gene features employed in this study depends on the size of the features selected. In this work, we generate seven subsets by varying the size of features in the range of 5, 10, 20, 30, 50, 100, 200, and 500 features and measure the classification performance on the extracted feature set. The results for various feature sets are shown in Figure 1.

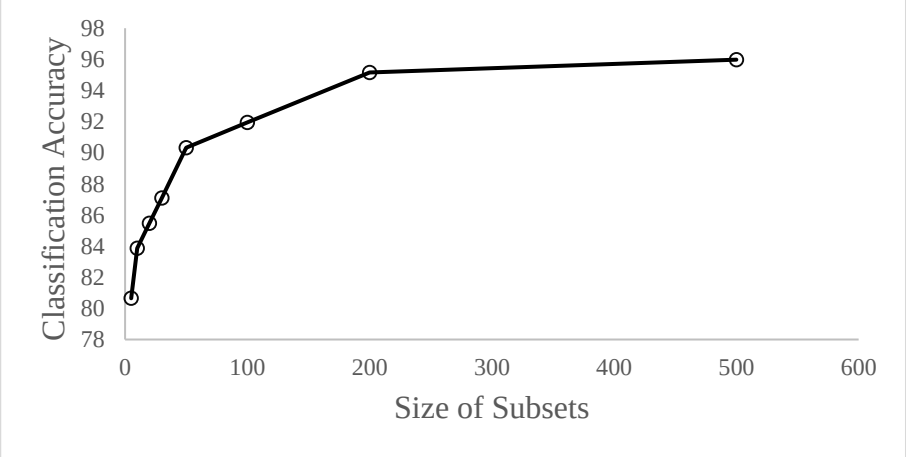

Figure 1: Performances of the method for microarray data.

By using SVM classifier, mRMR method gives the maximum accuracy of 80.65% in 5 genes, 83.87% in 10 genes, 85.48% in 20 genes, 87.10% in 30 genes, 90.32% in 50 genes, 91.94% in 100 genes, 95.16% in 200 genes and 95.98% in 500 genes. The good classification results in Figure 1 prove the fact that the mRMR method can capture the underlying differences among genes and has proven to be an effective solution for feature selection. The effectiveness of mRMR seen in the aspects of small feature set sizes. If we use the feature sets of 500 genes, the difference between 200 genes and 500 genes will not be large.

We have also made a performance comparison of the mRMR method with regression analysis. In the experiments, we compare the accuracy of mRMR feature sets against the feature sets obtained using the regression coefficient's ranking to pick up the top *m* features with *m* being 5, 10, 20, 30, 50, 100, 200 and 500. In the beginning, both methods exhibit similar accuracy at approximately 5 to 20 genes. Afterward, mRMR presents a higher classification accuracy when the number of genes increases. The result was shown in Figure 2.

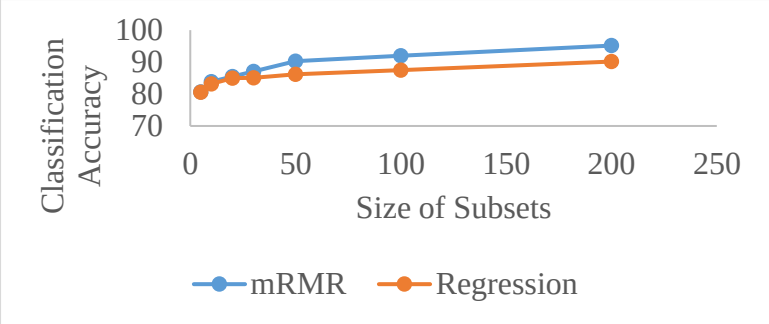

Figure 2: Comparison of accuracy in terms of mRMR and regression.

Lastly, we calculate the correlation coefficient among the selected 200 genes and select ten genes with the highest correlation. The relationship between the ten selected genes had shown in Figure 3. The network shows that there are two communication classes for the ten selected genes.

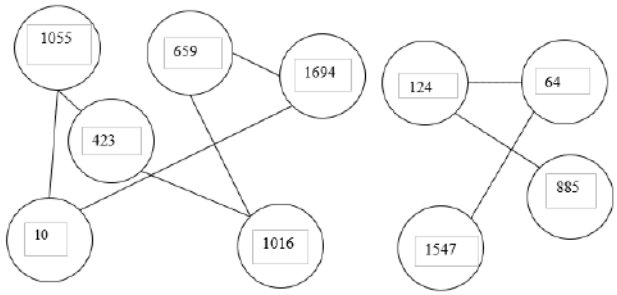

Figure 3: Relationship among ten selected genes.

4. Conclusions

Dealing with high dimensional datasets, high quality of the analytical techniques is required to build an efficient classification model. In this paper, mRMR feature selection applied to select discerning features from the dataset. From the results, it has proven that the method can lead to an effective computer-aided diagnostic system. Furthermore, we also show that the mRMR method improves accuracy compared to regression analysis. In the future, there are several positive directions for this study, such as the implementation of different classifiers used for classification.

References

Ding, C. and Peng, H. C., 2003. Minimum redundancy feature selection from microarray gene expression data. *Journal of bioinformatics and computational biology*, 3(2), pp. 185-205.

Sun, J., Passi, K. and Jain, C. K., 2016. Improved microarray data analysis using feature selection methods with machine learning methods. *2016 IEEE International Conference on Bioinformatics and Biomedicine (BIBM)*, pp. 1527-1534.

Muhammad, A. I., Hassan, M. and Alquhayz, H., 2016. A colon cancer grade prediction model using texture and statistical features, SMOTE and mRMR. *2016 19th International Multi-Topic Conference (INMIC)*, pp. 1-7.

Mohamed, N. S., Zainudin, S. and Othman, Z. A., 2017. Metaheuristic approach for an enhanced mRMR filter method for classification using drug response microarray data. *Expert systems with applications*, 90, pp. 224-231.

On $x(x-2)$-Clean Graph Rings

Lau Zhou Sheng[a], Qua Kiat Tat[b]

[a]*Graduated Student (BSc (Hons) Applied Mathematics with Computing), Lee Kong Chian Faculty of Engineering and Science, Universiti Tunku Abdul Rahman, Malaysia.*

[b]*Department of Mathematical and Actuarial Sciences, Lee Kong Chian Faculty of Engineering and Science, Universiti Tunku Abdul Rahman, Malaysia. Email (corresponding author): quakt@utar.edu.my*

Abstract

In this article, we have defined $g(x)$-nil clean graph of a ring R, where $g(x) \in Z(R)[x]$. The vertex set in the ring R is defined as two ring elements a and b are adjacent if and only if $a+b$ is $g(x)$-nil clean in R. We present some examples of $x(x-2)$-clean graph rings in this paper.

1. Introduction

Throughout this paper R is denoted as a finite commutative ring with identity. The group of units, the set of idempotents and the set of nilpotent elements in R are denoted as $U(R)$, $Id(R)$ and $N(R)$, respectively. Let G be an undirected graph, let $V(G)$ be the set of vertices and let $E(G)$ be the set of edges. If x and y in $V(G)$, and represent elements in R and an edge exists if and only if $xy = 0$. The relationships between a commutative ring and graph theory are first introduced by Beck (1988). In that paper, Beck (1988) has firstly introduced the idea of coloring of a commutative rings.

Let $G(R)$ denotes as a unit graph with a set of vertices comes from the set elements of R. Let x and y be arbitrary distinct vertices from R, such that x and y are adjacent if and only if $x+y$ is a unit in R. In 2010, Ashrafi (2010) has carried a research on unit graphs associated with rings. He obtained some properties of graph such as connectedness, chromatic index, diameter, girth and planarity of $G(R)$.

Nicholson (1977) has defined that an element x in a ring R is said to be clean if there exist an $e \in Id(R)$ such that $x - e \in U(R)$. Later in 2013, Diesel (2013) introduced a new variants, nil clean rings and strongly nil clean rings. A ring R is called nil clean ring if for each $x \in R$ such that $x = n + e$, for some $n \in N(R)$ and $e \in Id(R)$.

Let $G_N(R)$ denotes a nil clean graph with a set of vertices comes from the set elements of R. Let x and y to be distinct vertices of the elements from nil clean ring R, such that x adjacent to y if and only if $x + y \in N(R)$. In 2017, Basnet (2017a) denoted a nil clean graph by $G_N(R)$. He further investigated the properties of graph of $G_N(R)$, such as girth, diameter, dominating sets and other related properties.

In the same year, Basnet (2017b) carried out another research on the relationship between weakly nil clean ring and graph. The weakly nil clean graph denoted by $G_{WN}(R)$ and let a set of weakly nil clean elements denote by $WN(R)$. If x and y to be the distinct vertices of the elements from the weakly nil clean ring R such that x adjacent to y if and only if $x + y \in WN(R)$ or $x - y \in WN(R)$.

There are some notations and definition used in this paper. Let G denote the graph, for any $x \in V(G)$, the degree of x denotes by $deg(x)$ which defined as the number of edges that connected to x. Besides, the neighbours set of x is denoted as $NG(x) = \{y \in V(G) \mid y \text{ is adjacent to } x\}$ and the set $NG[x] = NG(x) \cup \{x\}$.

Let R be a ring and let $g(x)$ be a polynomial in $Z(R)[x]$, where $Z(R)$ denote as center of R. In 2016, Khashan (2016) denoted an element $r \in R$ is called $g(x)$-nil clean if $r = n + s$ for some $n \in Nil(R)$ and

$s \in R$ such that $g(s) = 0$. The ring R is $g(x)$-nil clean if every element in R is $g(x)$-nil clean. Clearly, if $g(x) = x(x-2)$, then $g(x)$-nil clean rings are nil clean. However, in general, $g(x)$-nil clean rings are not necessarily nil clean. For example, $\mathbb{Z}_3$ is an $(x^3 + 2x)$-nil clean rings but it is not nil clean.

Let $g(x)$-nil clean graph of ring R denote by $GN^*(R)$ and a set of $g(x)$-nil clean elements of ring R denote by $N^*(R)$. Let x and y to be distinct vertices of the elements from $g(x)$-nil clean ring R, such that x adjacent to y if and only if $x + y \in N^*(R)$.

2. Examples on $x(x-2)$-Nil Clean Graphs

In this section, we mainly focus on the polynomial $g(x) = x(x-2) \in Z(R)[x]$. We provide the examples on $x(x-2)$-nil clean graphs.

Example 2.1: We denoted that $GF(25)$ is a finite field with 25 elements. We show that the $GF(25)$ is a $x(x-2)$-nil clean graph.

$$GF(25) \cong \mathbb{Z}_5[x] \,/\, \langle x^2 + x + 1 \rangle = \{\, ax + b + \langle x^2 + x + 1 \rangle \mid a, b \in \mathbb{Z}_5 \,\}$$

Let $\beta = x + \langle x^2 + x + 1 \rangle$. Then $GF(25) = \{\bar{0}, \bar{1}, \bar{2}, \bar{3}, \bar{4},\ \beta, 2\beta, 3\beta, 4\beta, 1 + \beta, 2 + \beta, 3 + \beta, 4 + \beta, 1 + 2\beta, 2 + 2\beta, 3 + 2\beta, 4 + 2\beta, 1 + 3\beta, 2 + 3\beta, 3 + 3\beta, 4 + 3\beta, 1 + 4\beta, 2 + 4\beta, 3 + 4\beta, 4 + 4\beta \}$.

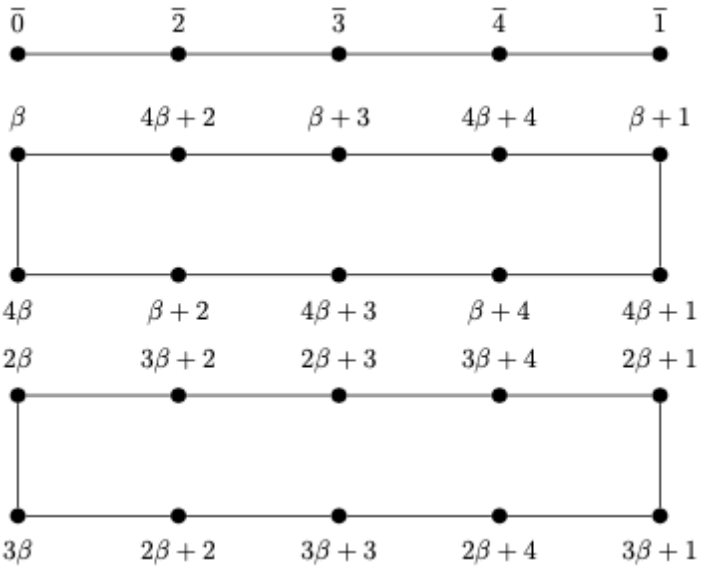

Figure 1: $x(x-2)$-nil clean graph for $GF(25)$.

Example 2.2: We denoted that $GF(27)$ is a finite field with 27 elements. We show that the $GF(27)$ is a $x(x-2)$-nil clean graph.

$$GF(27) \cong \mathbb{Z}_3[x] \,/\, \langle x^3 + 2x^2 + 1 \rangle = \{\, ax^2 + bx + c + \langle x^3 + 2x^2 + 1 \rangle \mid a, b, c \in \mathbb{Z}_3 \,\}$$

Let $\gamma = x^2 + \langle x^3 + 2x^2 + 1 \rangle$ and $\delta = x + \langle x^3 + 2x^2 + 1 \rangle$. Then $GF(27) = \{\bar{0}, \bar{1}, \bar{2}, \delta, \delta + 1, \delta + 2, 2\delta, 2\delta + 1, 2\delta + 2, \gamma, \gamma + 1, \gamma + 2, \gamma + \delta, \gamma + \delta + 1, \gamma + \delta + 2, \gamma + 2\delta, \gamma + 2\delta + 1, \gamma + 2\delta + 2, 2\gamma, 2\gamma + 1, 2\gamma + 2, 2\gamma + \delta, 2\gamma + \delta + 1, 2\gamma + \delta + 2, 2\gamma + 2\delta, 2\gamma + 2\delta + 1, 2\gamma + 2\delta + 2 \}$.

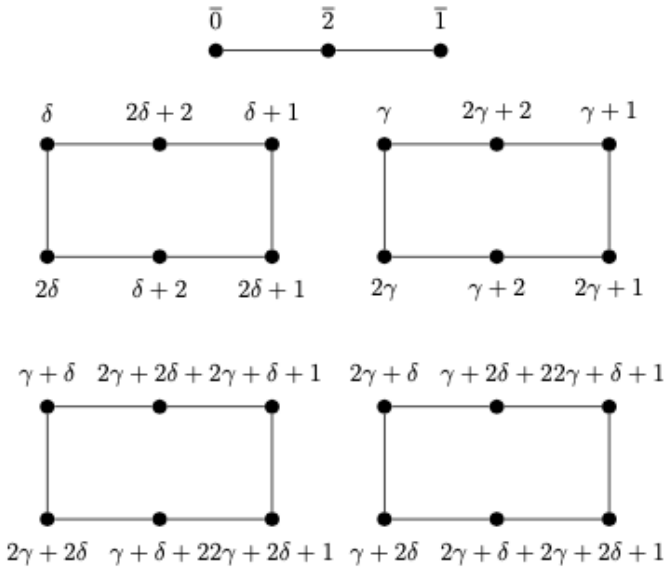

Figure 2: $x(x-2)$-nil clean graph for $GF(27)$.

Example 2.3: We denoted that $GF(49)$ is a finite field with 49 elements. We show that the $GF(49)$ is a $x(x-2)$-nil clean graph.

$$GF(27) \cong \mathbb{Z}_7[x] \,/\, \langle x^2+x+1 \rangle = \{\, ax+b+\langle x^2+x+1\rangle \mid a,b \in \mathbb{Z}_7 \,\}.$$

Let $\beta = x + \langle x^2+x+1\rangle$. Then $GF(49) = \{\overline{0}, \overline{1}, \overline{2}, \overline{3}, \overline{4}, \overline{5}, \overline{6}, \beta, 2\beta, 3\beta, 4\beta, 5\beta, 6\beta, 1+\beta, 2+\beta, 3+\beta, 4+\beta, 5+\beta, 6+\beta, 1+2\beta, 2+2\beta, 3+2\beta, 4+2\beta, 5+2\beta, 6+2\beta, 1+3\beta, 2+3\beta, 3+3\beta, 4+3\beta, 5+3\beta, 6+3\beta, 1+4\beta, 2+4\beta, 3+4\beta, 4+4\beta, 5+4\beta, 6+4\beta, 1+5\beta, 2+5\beta, 3+5\beta, 4+5\beta, 5+5\beta, 6+5\beta, 1+6\beta, 2+6\beta, 3+6\beta, 4+6\beta, 5+6\beta, 6+6\beta\}$.

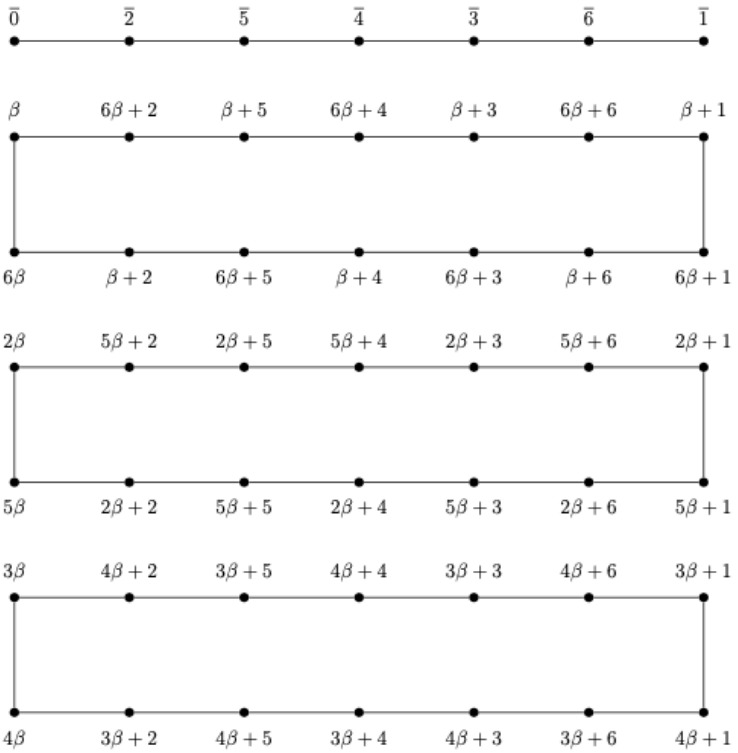

Figure 3: $x(x-2)$-nil clean graph for $GF(49)$.

Example 2.4: We show that $\mathbb{Z}_3, \mathbb{Z}_4, \ldots, \mathbb{Z}_{34}$ are $x(x-2)$-nil clean graphs by illustrate its $x(x-2)$-nil clean graph.

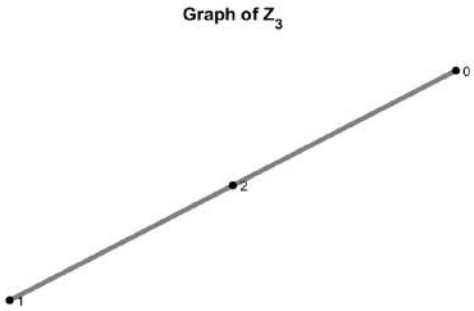

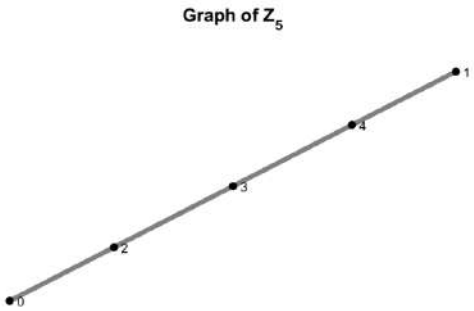

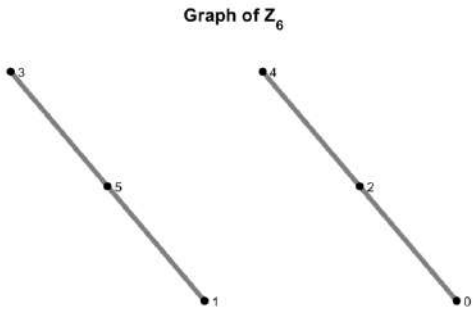

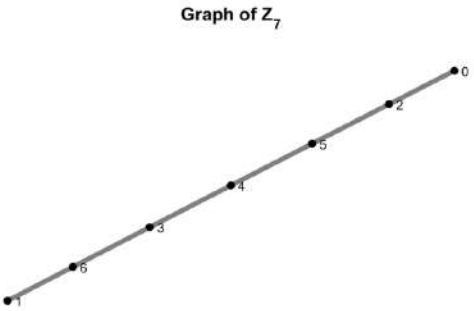

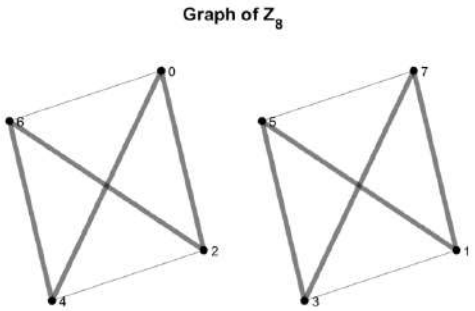

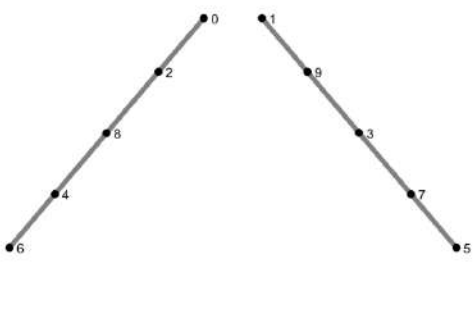

Graph of Z_{11}

Graph of Z_{12}

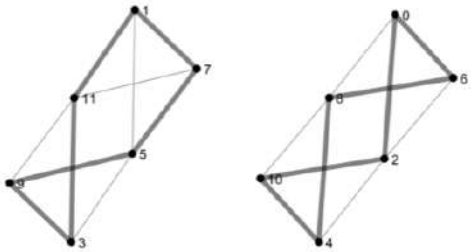

Graph of Z_{13}

Graph of Z_{14}

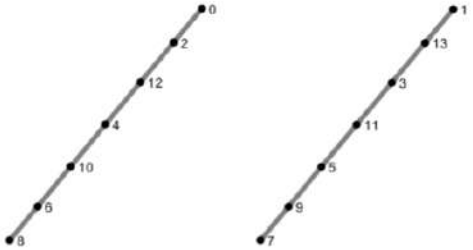

Graph of Z_{15}

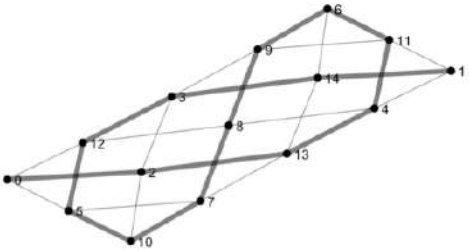

Graph of Z_{16}

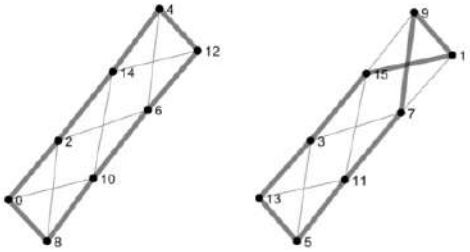

Graph of Z_{17}

Graph of Z_{18}

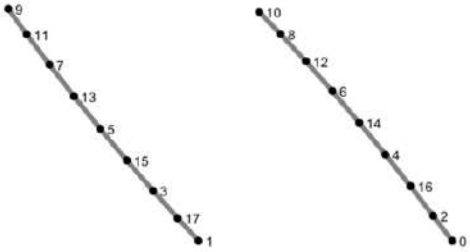

Graph of Z_{19}

Graph of Z_{20}

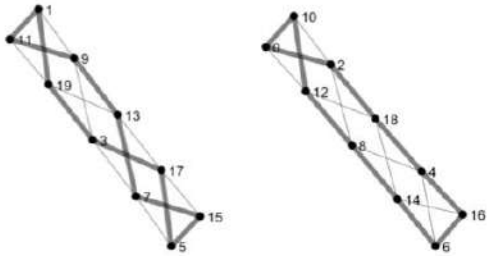

Graph of Z_{21}

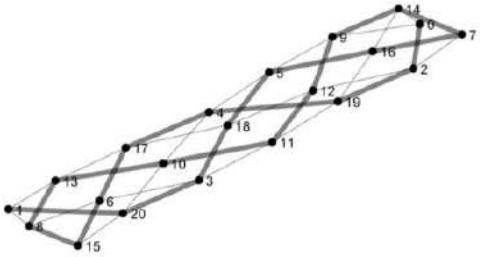

Graph of Z_{22}

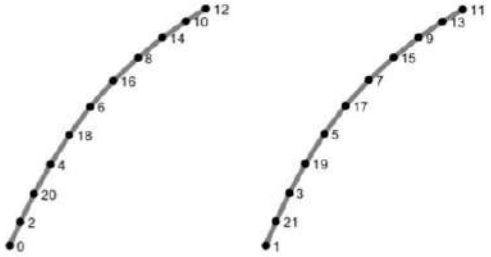

Graph of Z_{23}

Graph of Z_{24}

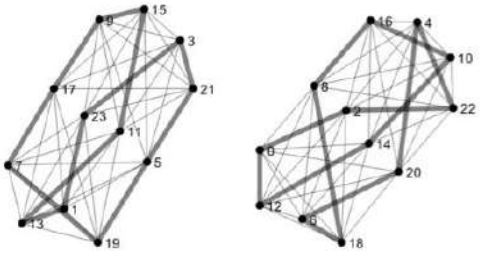

Graph of Z_{25}

Graph of Z_{26}

Graph of Z_{27}

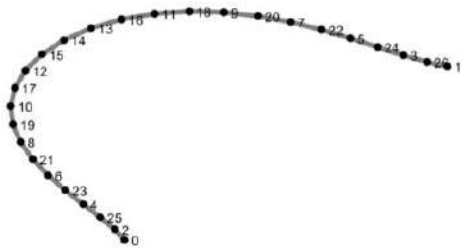

Graph of Z_{28}

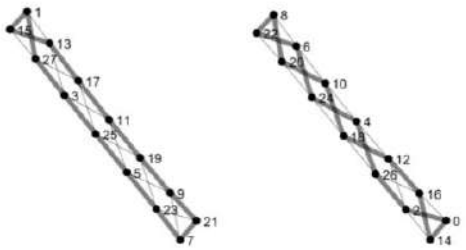

Graph of Z_{29}

Graph of Z_{30}

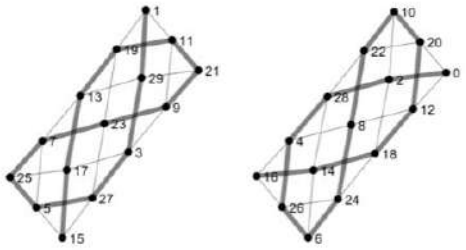

Graph of Z_{31}

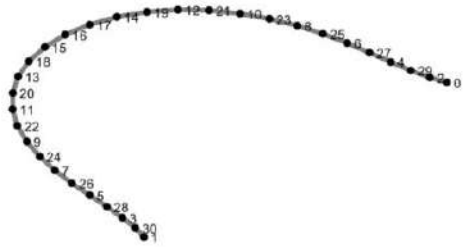

Graph of Z_{32}

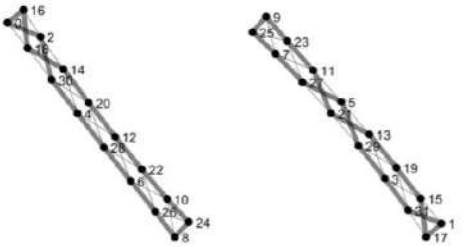

Graph of Z_{33}

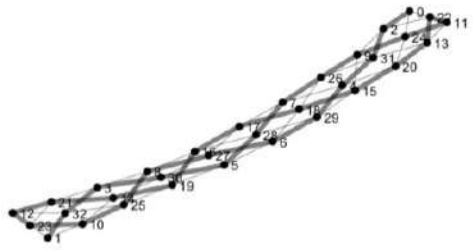

Graph of Z_{34}

3. Conclusions

By using Basnet (2017a) as our main reference, we are able to find some examples of $x(x-2)$-nil clean graph rings. In Lau (2018), Lau has also included some results on $x(x-2)$-nil clean graph rings.

Acknowledements

The authors are grateful to the referee for helpful comments and suggestions.

References

Ashraf, N., Maimani, H.R., Pournaki, M.R. and Yassemi, S., 2010. Unit graphs associated with rings, *Communications in Algebra*, 38, pp. 2851- 2871.

Basnet, D.K. and Bhattacharyya, J., 2017a. Nil clean graphs of rings, *Algebra Colloquium*, 24, pp. 481-492.

Basnet, D.K. and Bhattacharyya, J., 2017b. Weakly nil clean graphs of rings, *preprint*.

Beck, I., 1988. Coloring of commutative rings, *Journal of Algebra*, 116, pp. 208–226.

Danchev, P.V. and McGovern W., 2015. Commutative weakly nil clean unital rings, *Journal of Algebra*, 425, pp. 410 - 422.

Diesel, A.J., 2013. Nil clean rings, *Journal of Algebra*, 383, pp. 197-211.

Khashan, H. A. and Handam, A. H., 2016. $g(x)$-nil clean rings, *Scientiac Mathematicae Japonicae*, 79, pp. 145–154.

Lau, Z.S., 2018. *A study on Clean Graph Rings*. Final Year Project, Universiti Tunku Abdul Rahman, Malaysia.

Nicholson, W.K., 1977. Lifting idempotents and exchange rings, *Transactions of the America Mathematical Society*, 229, pp. 269-278.

Some Properties of Compound Preservers

Ng Wei Shean[a], **Wong Chui Hong**[b]

[a]*Department of Mathematical and Actuarial Sciences, Lee Kong Chian Faculty of Engineering and Science, Universiti Tunku Abdul Rahman, Malaysia. Email: ngws@utar.edu.my*

[b]*Pin Hwa High School Klang, Malaysia. Email: mike.wongchuihong@gmail.com*

Abstract

Let $\mathbb{F}$ be a field and let m and n be integers with $m, n \geqslant 3$. Let $\mathcal{M}_n$ denote the matrix space of $n \times n$ matrices over $\mathbb{F}$. In this note, we study some properties of mappings $\psi : \mathcal{M}_n \to \mathcal{M}_m$ that satisfy

$$|\mathbb{F}| = 2 \text{ or } |\mathbb{F}| > n+1, \text{ and } \psi(C_{n-1}(A + \alpha B)) = C_{m-1}(\psi(A) + \alpha\psi(B))$$

for all $A, B \in \mathcal{M}_n$ and $\alpha \in \mathbb{F}$ where ψ is injective. Here, $C_{n-1}(A)$ denotes the $(n-1)$-th compound matrix of A.

1. Introduction

Let $\mathbb{F}$ be a field and let $\mathcal{M}_n$ denote the matrix space of $n \times n$ matrices over $\mathbb{F}$. Let E_{ij} be the matrix in $\mathcal{M}_n$ whose (i,j)-th entry is one and the other entries are zeros. For $A \in \mathcal{M}_n$, A^t denotes the transpose matrix of A and $A^\sim$ denotes the $n \times n$ matrix whose (i,j)-th entry is $a_{m+1-j,n+1-i}$. Let $\sigma : \mathbb{F} \to \mathbb{F}$ be a field homomorphism. For $A \in \mathcal{M}_n$, A^σ is the $n \times n$ matrix whose (i,j)-th entry is $\sigma(a_{ij})$. Z_n denotes the diagonal matrix in $\mathcal{M}_n$ where $Z_n = \sum_{i=1}^{n} (-1)^{i+1} E_{ii}$. Given a matrix $A \in \mathcal{M}_n$, the $(n-1)$-th *compound matrix* or simply *compound matrix* of A, denoted by $C_{n-1}(A)$, is defined by an $n \times n$ matrix which (i,j)-th entry is

$$C_{n-1}(A)_{ij} = \det\left(A[n+1-i|n+1-j]\right),$$

with $1 \leqslant i, j \leqslant n$, where $A[i|j]$ is the $(n-1) \times (n-1)$ submatrix of A obtained by deleting i-th row and j-th column.

2. Preserver Problems

"Linear Preserver Problems" is one of the active and continuing topics in matrix theory which the classification of linear transformations on spaces of matrices that leave certain subsets, functions, relations, etc unchanged is studied. Frobenius (1897) possibly produced the earliest result in linear preserver problems which preserves the determinant of a matrix over complex field. Thereafter, matrix invertibility was classified by Marcus and Purves (1959). Hiai (1987) classified linear operators that preserve similarity of matrices.

Let $\mathcal{U}_1$ and $\mathcal{U}_2$ be matrix spaces over the same field. Then $f : \mathcal{U}_1 \to \mathcal{U}_2$ is *a classical adjoint preserver* (sometimes is called adjugate preserver) if

$$f(\text{adj } A) = \text{adj } (f(A)) \text{ for all } A \in \mathcal{U}_1.$$

Sinkhorn (1982) started the study of the classification of the classical adjoint linear preservers. He produced a general form of the classical adjoint linear preservers on $n \times n$ complex matrices and showed that if $n > 3$, then the mapping is of the form

$$A \to \lambda PAP{-}1 \text{ or } A \to \lambda PA^tP^{-1},$$

where $\lambda \in \mathbb{C}$ with $\lambda^{n-2} = 1$, P is an invertible complex matrix of order n, and A^t denotes the transpose of A.

Since then, classical adjoint linear preservers and classical adjoint additive preservers on various matrix spaces have been studied. Chan et al. (1987) studied the classical adjoint linear preservers on $\mathcal{M}_n$ over any infinite field and $n > 2$. The classical adjoint linear preserver as well as additive preservers on various matrix spaces have been studied in some papers (see Chooi and Lim (1998); Chooi (2010); Chooi and Lim (2003); Tang (2003, 2005); Tang and Zhang (2006); Tang et al. (1999)). Chooi and Ng (2010, 2011, 2014) have extended the study of the classical adjoint preservers. They studied the mappings $\psi : \mathcal{U}_1 \to \mathcal{U}_2$ where $\mathcal{U}_1$ and $\mathcal{U}_2$ are matrix spaces over the same field, $\mathbb{F}$, that satisfy one of the following conditions:

1. $\psi(\text{adj } (A + \alpha B) = \text{adj } (\psi(A) + \alpha\psi(B))$,
2. $\psi(\text{adj } (A - B) = \text{adj } (\psi(A) - \psi(B))$,

for all $A, B \in \mathcal{U}_1$ and $\alpha \in \mathbb{F}$.

Other than the classical adjoint preservers, compound preservers was also studied. Chooi (2011) studied compound additive preservers in 2011. Let $\mathcal{U}_1$ and $\mathcal{U}_2$ be matrix spaces over the same field. Then $f : \mathcal{U}_1 \to \mathcal{U}_2$ is *a classical adjoint preserver* (sometimes is called adjugate preserver) if

$$f(C_{n-1}A) = C_{m-1}(f(A)) \text{ for all } A \in \mathcal{U}_1.$$

In Chooi (2011), Chooi classified compound additive preservers on four types of matrices: triangular matrices, square matrices, symmetric matrices and Hermitian matrices. The following proposition is one of the main results in his paper.

Proposition 1. (Chooi, 2011, Theorem 2.12) *Let m, n be integers greater than 2 and $\mathbb{F}$ be a field. Let $\psi : \mathcal{M}_n \to \mathcal{M}_m$ be a nonzero mapping. Then ψ is an additive compound-commuting mapping if and only if $m = n$ and there exist nonsingular matrices $P, Q \in \mathcal{M}_n$ with $C_{n-1}(P) = \mu P$ and $C_{n-1}(Q) = \mu^{-1}Q$ for some nonzero $\mu \in \mathbb{F}$, and a field homomorphism $\sigma : \mathbb{F} \to \mathbb{F}$, such that*

$$\psi(A) = PA^\sigma Q \text{ or } \psi(A) = P(A^\sigma)^tQ$$

for every $A \in \mathcal{M}_n$.

3. Compound Preservers

Motivated by the studies of Chooi and Ng (2010, 2011, 2014) and Chooi (2011), we study some properties of mappings $\psi : \mathcal{M}_n \to \mathcal{M}_m$ that satisfy

$$\psi(C_{n-1}(A + \alpha B)) = C_{m-1}(\psi(A) + \alpha\psi(B)). \tag{C}$$

Lemma 2 (Properties of Compound Matrices (Chooi, 2011, Lemma 2.2 & Lemma 2.3))**.** *Let n be an integer greater than 1 and $\mathbb{F}$ be a field. Let $A, B \in \mathcal{M}_n$ and $\alpha \in \mathbb{F}$. Then the following hold true.*

(a) $C_{n-1}(I_n) = I_n$ *and* $C_{n-1}(0) = 0$.

(b) $C_{n-1}(\alpha A) = \alpha^{n-1} C_{n-1}(A)$.

(c) ***(Binet-Cauchy theorem)*** $C_{n-1}(AB) = C_{n-1}(A)C_{n-1}(B)$.

(d) *If A is nonsingular, then* $C_{n-1}(A^{-1}) = (C_{n-1}(A))^{-1}$.

(e) $C_{n-1}(A^t) = (C_{n-1}(A))^t$.

(f) $C_{n-1}(A^\sigma) = (C_{n-1}(A))^\sigma$.

(g) $C_{n-1}(A^\sim) = (C_{n-1}(A))^\sim$.

(h) $C_{n-1}(A) = Z_n((\text{adj } A)^\sim)Z_n$.

(i) $C_{n-1}(Z_n) = \begin{cases} -Z_n, & \text{when } n = 4k-1, 4k, \text{ for } k = 1, 2, \cdots, \\ Z_n, & \text{otherwise.} \end{cases}$

The following lemma shows that if $\psi : \mathcal{M}_n \to \mathcal{M}_m$ satisfies Condition (C), then ψ is a compound preserver.

Lemma 3. *Let m, n be integers and $\mathbb{F}$ be a field. If $\psi : \mathcal{M}_n \to \mathcal{M}_m$ is a mapping satisfying $\psi(C_{n-1}(A + \alpha B)) = C_{m-1}(\psi(A) + \alpha\psi(B))$ for every $\alpha \in \mathbb{F}$ and $A, B \in \mathcal{M}_n$, then*

(a) $\psi(0) = 0$,

(b) *ψ is a compound preserver.*

Proof.

(a) $\psi(0) = \psi(C_{n-1}(0+(-1)0)) = C_{m-1}(\psi(0)+(-1)\psi(0)) = C_{m-1}(\psi(0)-\psi(0)) = C_{m-1}(0) = 0$.

(b) Let $A \in \mathcal{M}_n$. Then $\psi(C_{n-1}(A)) = \psi(C_{n-1}(A+0A)) = C_{m-1}(\psi(A)+0\psi(A)) = C_{m-1}(\psi(A)+O) = C_{m-1}(\psi(A))$. Hence, ψ is a compound preserver.

Lemma 4. (Chooi, 2011, Lemma 2.3) *Let n be an integer greater than 1 and $\mathbb{F}$ be a field. Then for $A \in \mathcal{M}_n$, then*

(a) $\text{rank } C_{n-1}(A) = n$ *whenever* $\text{rank } A = n$,

(b) $\text{rank } C_{n-1}(A) = 1$ *whenever* $\text{rank } A = n-1$,

(c) $\text{rank } C_{n-1}(A) = 0$ *whenever* $\text{rank } A \leq n-2$.

Lemma 5. (Chooi, 2011, Lemma 2.4) *Let n be an integer greater than* 1 *and $\mathbb{F}$ be a field. If $A \in \mathcal{M}_n$ with* $\text{rank } A = 1$*, then there exist a matrix $X \in \mathcal{M}_n$ with* $\text{rank } X = n-1$ *such that $A = C_{n-1}(X)$.*

When the Condition (C) is satisfied, we found that the rank of $\psi(A)$ depends on the rank of A.

Lemma 6. *Let m, n be integers greater than* 2 *and $\mathbb{F}$ be a field. Let $\psi : \mathcal{M}_n \to \mathcal{M}_m$ be a mapping satisfying Condition (C). Then for $A \in \mathcal{M}_n$,*

(a) *if* $\text{rank } A = 1$, *then* $\text{rank } \psi(A) \leq 1$,

(b) *if* $\text{rank } A = n-1$, *then* $\text{rank } \psi(A) \leq m-1$,

(c) *if* $\text{rank } A \leq n-2$, *then* $\text{rank } \psi(A) \leq m-2$,

(d) $\text{rank } A = n$ *whenever* $\text{rank } \psi(A) = m$.

Proof.

(a) Let $A \in \mathcal{M}_n$ be a rank 1 matrix. By Lemma 5, there exists $B \in \mathcal{M}_n$ with $\text{rank } B = n-1$ such that $A = C_{n-1}(B)$. Then by Lemma 4, $C_{m-1}(\psi(A)) = \psi(C_{n-1}(A)) = \psi(0) = 0$. Hence, we know that $\text{rank } \psi(A) \leq m-2$. Since $\psi(A) = \psi(C_{n-1}(B)) = C_{m-1}(\psi(B))$, and $\text{rank } \psi(A) < m$, by Lemma 4, we know that $\text{rank } \psi(B) < m$ and hence, $\text{rank } \psi(A) = \text{rank } C_{m-1}(\psi(B)) \leq 1$.

(b) Let $A \in \mathcal{M}_n$ be a rank $n-1$ matrix. By Lemma 4, $\text{rank } C_{n-1}(A) = 1$, and hence $C_{n-1}(C_{n-1}(A)) = O$. Then $C_{m-1}(C_{m-1}(\psi(A))) = \psi(C_{n-1}(C_{n-1}(A))) = \psi(0) = 0$. By Lemma 4, $\text{rank } C_{m-1}(\psi(A)) \leq m-2$, and hence $\text{rank } \psi(A) \leq m-1$.

(c) Let $A \in \mathcal{M}_n$ with $\text{rank } A \leq n-2$. By Lemma 4, $C_{n-1}(A) = O$. Hence, $C_{m-1}(\psi(A)) = \psi(C_{n-1}(A)) = \psi(0) = 0$. Therefore, by Lemma 4, we get $\text{rank } \psi(A) \leq m-2$.

(d) Let $A \in \mathcal{M}_n$ with $\text{rank } \psi(A) = m$. Suppose $\text{rank } A < n$. By part (b) and (c), we know that $\text{rank } \psi(A) \leq m-1$, which contradicts with $\text{rank } \psi(A) = m$. Therefore, $\text{rank } A = n$.

Lemma 7 (Chooi and Ng (2010))**.** *Let n be an integer greater than 2 and $\mathbb{F}$ be a field.*

(a) *For $A \in \mathcal{M}_n$ with $\text{rank } A = r$, there exists $X \in \mathcal{M}_n$ with $\text{rank } X = n-r$ such that $\text{rank } (A+X) = n$.*

(b) *For $A, B \in \mathcal{M}_n$, there exist a matrix $X \in \mathcal{M}_n$ such that $\text{rank } (A+X) = \text{rank } (B+X) = n$.*

(c) *For $A \in \mathcal{M}_n$, there exist a nonzero matrix $X \in \mathcal{M}_n$ such that either A or X is nonsingular but not both, and $\text{rank } (A+X) = n$.*

(d) *Let $|\mathbb{F}| \geq n+2$. For $A, B \in \mathcal{M}_n$ with $\text{rank } (A+B) = n$, there exist a nonzero $\lambda \in \mathbb{F}$ such that $\text{rank } (A+(1+\lambda)B) = n$.*

Moreover, we found that if ψ is injective, the mapping has nice properties that lead us to find the form of the mapping.

Lemma 8. *Let m, n be integers greater than 2 and $\mathbb{F}$ be a field. If $\psi : \mathcal{M}_n \to \mathcal{M}_m$ is a mapping satisfying Condition (C) for every $\alpha \in \mathbb{F}$ and $A, B \in \mathcal{M}_n$, then the following statements are equivalent.*

(a) *ψ is injective.*

(b) $\ker \psi = \{0\}$.

(c) *For every $A \in \mathcal{M}_n$,* $\text{rank } A = n$ *if and only if* $\text{rank } \psi(A) = m$.

(d) *For every $\alpha \in \mathbb{F}$ and $A, B \in \mathcal{M}_n$,* $\text{rank } (A+\alpha B) = n$ *if and only if* $\text{rank } (\psi(A)+\alpha\psi(B)) = m$.

Proof. (a)⇒(b). Let ψ is injective. Suppose $A \in \ker \psi$, then $\psi(A) = O$. Since $\psi(O) = O$, and hence $\psi(A) = \psi(0)$, then $A = 0$ by the injectivity of ψ. Therefore, $\ker \psi = \{O\}$.
(b)⇒(c). By Lemma 6, we see that when $\text{rank } \psi(A) = m$, then $\text{rank } A = n$ holds true. Conversely, let $A \in \mathcal{M}_n$ with $\text{rank } A = n$. Suppose $\text{rank } \psi(A) < m$. By 4, $\text{rank } C_{m-1}(\psi(A)) \leq 1$ and hence $C_{m-1}(C_{m-1}(\psi(A))) = O$. Then, $\psi(C_{n-1}(C_{n-1}(A))) = O$. Since $\ker f = \{O\}$, $C_{n-1}(C_{n-1}(A)) = O$. Then by Lemma 4, $\text{rank } C_{n-1}(A) \leq n-2$ and hence $\text{rank } A \leq n-1$, which leads to a contradiction. Therefore, $\text{rank } \psi(A) = m$. Hence, $\text{rank } A = n$ if and only if $\text{rank } \psi(A) = m$
(c)⇒(a). Let $A, B \in \mathcal{M}_n$ with $\psi(A) = \psi(B)$. Assume that $\text{rank } (A - B) = r$. By Lemma 7(a), there exists $C \in \mathcal{M}_n$ with $\text{rank } C = n - r$ such that $\text{rank } (A - B + C) = n$. Hence,

$$\begin{aligned}
C_{m-1}(\psi(C)) &= C_{m-1}(\psi(B - (B - C))) \\
&= \psi(C_{n-1}(B - (B - C))) \\
&= \psi(C_{n-1}(B + (-1)(B - C))) \\
&= C_{m-1}(\psi(B) + (-1)\psi(B - C)) \\
&= C_{m-1}(\psi(A) + (-1)\psi(B - C)) \\
&= \psi(C_{n-1}(A + (-1)(B - C))) \\
&= \psi(C_{n-1}(A - (B - C))) \\
&= \psi(C_{n-1}(A - B + C)) \\
&= C_{m-1}(\psi(A - B + C))
\end{aligned}$$

Since $\text{rank } (A - B + C) = n$, hence $\text{rank } \psi(A - B + C)) = m$. By Lemma 4, we know that $\text{rank } C_{m-1}(\psi(A-B+C)) = m$, and hence $\text{rank } C_{m-1}(\psi(C)) = m$. Then it follows by $\text{rank } \psi(C) = m$, and hence $\text{rank } C = n$. Since $\text{rank } C = n - r$, we know that $r = 0$, that means $A - B = O$, which followed by $A = B$. Hence, ψ is injective.
(c)⇒(d). Let $A, B \in \mathcal{M}_n$ and $\alpha \in \mathbb{F}$. Then $\text{rank } (A+\alpha B) = n$ if and only if $\text{rank } \psi(A+\alpha B) = m$. Since $C_{m-1}(\psi(A) + \alpha\psi(B)) = \psi(C_{n-1}(A + \alpha B)) = C_{m-1}(\psi(A + \alpha B))$, by Lemma 4, hence $\text{rank } \psi(A + \alpha B) = m$ if and only if $\text{rank } C_{m-1}(\psi(A) + \alpha\psi(B)) = m$, which is equivalent to $\text{rank } (\psi(A) + \alpha\psi(B)) = m$.
(d)⇒(c). When $\alpha = 0$, condition (c) is fulfilled.
Here we complete the proof.

4. Conclusion

More properties of compound preservers are to be obtained in future. All the properties obtained are to be used as tools to classify the mappings that satisfy Condition (C).

References

Chan, G.H., Lim, M.H. and Tan, K.K., 1987. Linear preservers on matrices. *Linear Algebra and Its Applications*, 93, pp. 67–80.

Chooi, W.L., 2010. Rank-one nonincreasing additive maps between triangular matrix algebras. *Linear and Multilinear Algebra*, 58, pp. 715–740.

Chooi, W.L., 2011. Compound-commuting additive maps on matrix spaces. *Journal of the Korean Mathematical Society*, 48, pp. 83–104.

Chooi, W.L. and Lim, M.H., 1998. Linear preservers on triangular matrices. *Linear Algebra and Its Applications*, 269, pp. 241–255.

Chooi, W.L. and Lim, M.H., 2003. Some linear preserver problems on block triangular matrix algebras. *Linear Algebra and Its Applications*, 370, pp. 25–39.

Chooi, W.L. and Ng, W.S., 2010. On classical adjoint-commuting mappings betweed matrix algebras. *Linear Algebra and Its Applications*, 432, pp. 2589–2599.

Chooi, W.L. and Ng, W.S., 2011. Classical adjoint-commuting mappings on Hermitian and symmetric matrices. *Linear Algebra and Its Applications*, 435, pp. 202–223.

Chooi, W.L. and Ng, W.S., 2014. Classical adjoint-commuting mappings on alternate and skew-Hermitian matrices. *Operators and Matrices*, 8, pp. 485–512.

Frobenius, G., 1897. Über die Darstellung der endlichen Gruppen durch lineare Substitutionen. *Sitzungsberichte der Deutschen Akademie der Wissenschaften Berlin*, pp. 994–1015.

Hiai, F., 1987. Similarity preserving maps on matrices. *Linear Algebra and Its Applications*, 97, pp. 127–139.

Marcus, M. and Purves, R., 1959. Linear transformations on algebras of matrices II: The invariance of the elementary symmetric functions. *Canadian Journal of Mathematics*, 11, pp. 383–396.

Sinkhorn, R., 1982. Linear adjugate preservers on the complex matrices. *Linear and Multilinear Algebra*, 12, pp. 215–222.

Tang, X. M., 2003. Linear operators preserving adjoint matrix between matrix spaces. *Linear Algebra and Its Applications*. 372, pp. 287–293.

Tang, X. M., 2005. Additive rank-1 preservers between hermitian matrix spaces and applications. *Linear Algebra and Its Applications*, 395, pp. 333–342.

Tang, X.M. and Zhang, X., 2006. Additive adjoint preservers between matrix spaces. *Linear and Multilinear Algebra*, 54, pp. 285–300.

Tang, X.M., Zhang, X. and Cao, C.G., 1999. Additive adjugate preservers on the matrices over Fields. *Northeastern Mathematical Journal*, 15, pp. 246–252.

Empirical Research of Malaysia Stocks using Three-Parameter Dirichlet Universal Portfolio

Pang Sook Theng[a], George Tan Shing Hong[b]

[a]*Department of Mathematical and Actuarial Sciences, Lee Kong Chian Faculty of Engineering and Science, Universiti Tunku Abdul Rahman, Malaysia. Email (corresponding author): pangst@utar.edu.my*

[b]*Graduated Student (BSc (Hons) Applied Mathematics with Computing), Lee Kong Chian Faculty of Engineering and Science, Universiti Tunku Abdul Rahman, Malaysia.*

Abstract

Finding a good strategy to seek the greatest wealth has been the aim of investors. Cover has shown that for a reasonable financial market, investors can use the Three-Parameter Dirichlet Universal Portfolio to gain a good return on an investment on chosen stocks. In this study, three particular malaysia stocks: Astro, Nestle and Top Glove are selected to study the performance of Three-Parameter Dirichlet Universal Portfolio with different periods, namely one year, two years and four years. Empirically, a higher return in capital can be achieved by investing a large portion of wealth for Top Glove in one year period. However, Astro shows a good return for two years and four years period.

1. Introduction

The universal porttolio is a sequential portfolio selection procedure studied by Cover (1991) for the use of investing in the stock market with the efficiency of performance if the empirical distribution of future stock market was considered. Futhermore, it is mathematically shown to outperform the best stock in the portfolio. This universal portfolio is a strategy which is independent of the underlying probability distribution or any stochastic model of the stock markets. The current portfolio depends solely on past data. One popular universal portfolio is the Dirichlet universal portfolio which have been studied by Cover (1991) and Cover and Ordentlich (1996) with the aim of obtaining a higher investment return than that of the buy-and-hold portfolio.

Helmbold et al. (1998) introduced the exponential-gradient-update universal portfolio and provided some empirical evidence based on the same stock-price data studied by Cover (1991) that the Helmbold portfolio can outperform the Dirichlet (1,1,...,1) universal portfolio. In Tan and Tang (2003), it was shown that the Helmbold portfolio is sensitive to the initial starting portfolio of the algorithm for ordinary stock-price data and has the approximate behaviour of a constant rebalanced portfolio. Helmbold et al. (1998) did not elaborate on the proper choice of the initial starting portfolio for a good Helmbold portfolio to achieve high returns. Based on some stock-price data from the Kuala Lumpur Stock Exchange, Tan and Tang (2003) have shown that there are Dirichlet (α_1, α_2) universal portfolios that can outperform the Helmbold portfolio based on the observation that it is an approximate constant rebalanced portfolio. Therefore, this paper will apply the Three-Paremeter Dirichlet Universal Portfolio to study the performance of three selected Malaysia stocks.

2. Some Basic Theory

We begin with some preliminaries. Consider a market of m stocks. The price relative of a stock is the ratio of the closing price of the stock to the opening price on a particular trading day. A portfolio vector $\mathbf{b} = (b_1, b_2, ..., b_m)$ is a vector such that $b_i \geq 0$ for $i = 1, 2, ...m$ and $\sum_{i=1}^{m} b_i = 1$. The component b_i can be

interpreted as the proportion of the current wealth of the investor that is invested on the i^{th} stock for $i = 1, 2, ..., m$. The simplex B is the set of all portfolio vectors $\mathbf{b}$, i.e. $i = 1, 2, ..., m$,

$$B = \{\mathbf{b} = (b_1, ..., b_m) : b_i \geq 0 \text{ for } \sum_{i=1}^{m} b_i = 1\} \tag{1}$$

Let $\mathbf{x}_1, \mathbf{x}_2, ..., \mathbf{x}_k$ be a sequence of price-relative vectors corresponding to k trading days. The sequence $\{\hat{\mathbf{b}}_k\}$ of the portfolio vectors is said to be a μ-weighted universal portfolio if

$$\hat{\mathbf{b}}_k = \frac{[\int_B \mathbf{b}[\prod_{i=1}^{k-1} \mathbf{b}^t \mathbf{x}_i]\, d\mu(\mathbf{b})]}{[\int_B \prod_{i=1}^{k-1} \mathbf{b}^t \mathbf{x}_i\, d\mu(\mathbf{b})]} \tag{2}$$

for $k = 1, 2, ...$, where μ is a probability measure over the simplex B defined by (1). We note that the portfolio $\hat{\mathbf{b}}_k$ depends only on the past price-relative vectors $\mathbf{x}_1, \mathbf{x}_2, ..., \mathbf{x}_{k-1}$. The universal capital or wealth achieved at the end of the n^{th} trading day is given by

$$\hat{S}_n(\mathbf{x}^n) = (\prod_{k=1}^{n} \hat{\mathbf{b}}_k^t \mathbf{x}_k) \tag{3}$$

where $\mathbf{x}^n$ is the sequence of price-relative vectors $\mathbf{x}_1, \mathbf{x}_2, ..., \mathbf{x}_n$ and the initial capital or wealth is assumed to be 1 unit.

The Dirichlet($\alpha_1, \alpha_2, ..., \alpha_m$) universal portfolio is the universal portfolio where

$$d\mu(\mathbf{b}) = \frac{\Gamma(\alpha_1 + \alpha_2 + ... + \alpha_m)}{\Gamma(\alpha_1)\Gamma(\alpha_2).....\Gamma(\alpha_m)} \prod_{j=1}^{m} b_j^{\alpha_j - 1} d\mathbf{b} \tag{4}$$

where $\alpha_j > 0$ for $j = 1, 2, ..., m$ and $d\mathbf{b}$ refers to the differential with respect to any $m - 1$ independent variables from $b_1, b_2, ..., b_m$, say $b_1, b_2, ..., b_{m-1}$ due to the constraint $\sum_{i=1}^{m} b_i = 1$. The integration of any function $f(\mathbf{b})$ with respect to $db_1, db_2, ..., db_{m-1}$ is the integration of $f(\mathrm{b})$ over the region $\overline{B}$, where

$$\overline{B} = \{\mathbf{b} = (b_1, ..., b_{m-1}) : 0 \leq \sum_{i=1}^{m-1} b_i \leq 1, \\ b_i \geq 0 \text{ for } i = 1, 2, ..., m-1\} \tag{5}$$

3. Methodology

Cover and Ordentlich (1996) presented an algorithm for generating the Dirichlet $(\frac{1}{2}, \frac{1}{2})$ two stock universal portfolio. Chan (2002) modified this algorithm for generating any Dirichlet $(\alpha_1, \alpha_2, ..., \alpha_m)$ universal portfolio for $m = 2, 3$ and 4 stocks. The modified algorithm to generate the m-stock Dirichlet ($\alpha_1, \alpha_2, ..., \alpha_m$) universal portfolio was obtained by Tan (2004b).

We now present the modified algorithm of Chan (2002) for computing the three-stock universal portfolio generated by the Dirichlet $(\alpha_1, \alpha_2, \alpha_3)$ distribution where $\alpha_j > 0$ for $i = 1, 2, 3$. Consider a sequence of price-relative vectors $\mathbf{x}_1, \mathbf{x}_2, ..., \mathbf{x}_n$ corresponding to n trading days in a three-stock market, where $\mathbf{x}_i = (x_{i1}, x_{i2}, x_{i3})$ for $i = 1, 2, ..., n$. We shall define three recursive functions $X_n(l_1, l_2)$, $C_n(l_1, l_2)$ and $Q_n(l_1, l_2)$.

Firstly, we define

$$X_n(l_1, l_2) = \sum_{j^n \in T_n(l_1, l_2)} \prod_{i=1}^{n} x_{ij} \tag{6}$$

where $T_n(l_1, l_2)$ is the set of all sequences $j^n = (j_1, j_2, ..., j_n) \in \{1, 2, 3\}^n$ with l_1 1's and l_2 2's and $n - l_1 - l_2$ 3's and

Secondly, we defined,

$$C_n(l_1,l_2)=\int_{\overline{B}} b_1^{l_1}b_2^{l_2}b_3^{n-l_1-l_2}d\mu(\mathbf{b}) \tag{7}$$

where

$$d\mu(\mathbf{b})=\frac{\Gamma(\alpha_1+\alpha_2+\alpha_3)}{\Gamma(\alpha_1)\Gamma(\alpha_2)\Gamma(\alpha_3)}b_1^{\alpha_1-1}b_2^{\alpha_2-1}b_3^{\alpha_3-1}db_1db_2 \tag{8}$$

Finally,

$$Q_n(l_1,l_2)=X_n(l_1,l_2)C_n(l_1,l_2) \tag{9}$$

The universal portfolio $\{\hat{\mathbf{b}}_n\}$ can then be computed as follows:

$$\hat{\mathbf{b}}_n=\frac{1}{\sum_{l_1=0}^{n-1}\sum_{l_2=0}^{n-l_1-1}Q_{n-1}(l_1,l_2)}\begin{pmatrix}\sum_{l_1=0}^{n-1}\sum_{l_2=0}^{n-l_1-1}\frac{(l_1+\alpha_1)}{(n+\alpha_1+\alpha_2+\alpha_3-1)}Q_{n-1}(l_1,l_2)\\ \sum_{l_1=0}^{n-1}\sum_{l_2=0}^{n-l_1-1}\frac{(l_2+\alpha_2)}{(n+\alpha_1+\alpha_2+\alpha_3-1)}Q_{n-1}(l_1,l_2)\\ \sum_{l_1=0}^{n-1}\sum_{l_2=0}^{n-l_1-1}\frac{(n-l_1-l_2+\alpha_3-1)}{(n+\alpha_1+\alpha_2+\alpha_3-1)}Q_{n-1}(l_1,l_2)\end{pmatrix} \tag{10}$$

and the universal capital achieved by $\hat{\mathbf{b}}_n$ is computed as:

$$\hat{S_n}=\sum_{l=0}^{n}Q_n(l_1,l_2) \tag{11}$$

Next, we give the recursive relationships of the functions $X_n(l_1,l_2)$, $C_n(1_1,l_2)$ and $Q_n(l_1,l_2)$ and their end-point conditions.

1. The recursion for $X_n(l_1,l_2)$ is given by:

$$\begin{aligned}X_n(l_1,l_2)=&x_{n1}X_{n-1}(l_1-1,l_2)\\&+x_{n2}X_{n-1}(l_1,l_2-1)\\&+x_{n3}X_{n-1}(l_1,l_2)\end{aligned} \tag{12}$$

for $1\le l_1\le n-1$ and $1\le l_2\le n-l_1-1$ and the endpoint condition are given by:

$$\begin{aligned}X_n(l_1,0)=&x_{n1}X_{n-1}(l_1,0)\\&+x_{n3}X_{n-1}(l_1,0)\end{aligned} \tag{13}$$

$$\begin{aligned}X_n(0,l_2)=&x_{n2}X_{n-1}(0,l_2-1)\\&+x_{n3}X_{n-1}(0,l_2)\end{aligned} \tag{14}$$

2. The recursion for $C_n(l_1,l_2)$ given by:

$$\begin{aligned}&C_n(l_1,l_2)\\&=\frac{l_1+\alpha_1-1}{n+\alpha_1+\alpha_2+\alpha_3-1}C_{n-1}(l_1-1,l_2)\end{aligned} \tag{15}$$

for $1\le l_1\le n$ and $0\le l_2\le n-l_1$.

$$\begin{aligned}&C_n(l_1,l_2)\\&=\frac{l_2+\alpha_2-1}{n+\alpha_1+\alpha_2+\alpha_3-1}C_{n-1}(l_1,l_2-1)\end{aligned} \tag{16}$$

for $0\le l_1\le n-1$ and $1\le l_2\le n-l_1$.

$$\begin{aligned}&C_n(l_1,l_2)\\&=\frac{n-l_1-l_2+\alpha_3-1}{n+\alpha_1+\alpha_2+\alpha_3-1}C_{n-1}(l_1,l_2)\end{aligned} \tag{17}$$

for $0 \leq l_1 \leq n-1$ and $0 \leq l_2 \leq n-l_1-1$.

The initial condition is

$$C_o(0,0) = 1. \tag{18}$$

The recursion for $Q_n(l_1, l_2)$ given by:

$$\begin{aligned} & Q_n(l_1, l_2) \\ & = x_{n1} \tfrac{l_1+\alpha_1-1}{n+\alpha_1+\alpha_2+\alpha_3-1} Q_{n-1}(l_1-1, l_2) \\ & \quad + x_{n2} \tfrac{l_2+\alpha_2-1}{n+\alpha_1+\alpha_2+\alpha_3-1} Q_{n-1}(l_1, l_2-1) \\ & \quad + x_{n3} \tfrac{n-l_1-l_2+\alpha_3-1}{n+\alpha_1+\alpha_2+\alpha_3-1} Q_{n-1}(l_1, l_2) \end{aligned} \tag{19}$$

for $1 \leq l_1 \leq n-1$ and $1 \leq l_2 \leq n-l_1$. The six endpoint conditions are given by:

$$\begin{aligned} & Q_n(l_1, 0) \\ & = x_{n1} \tfrac{l_1+\alpha_1-1}{n+\alpha_1+\alpha_2+\alpha_3-1} Q_{n-1}(l_1-1, 0) \\ & \quad + x_{n3} \tfrac{n-l_1-l_2+\alpha_3-1}{n+\alpha_1+\alpha_2+\alpha_3-1} Q_{n-1}(l_1, 0) \end{aligned} \tag{20}$$

for $1 \leq l_1 \leq n-1$.

$$\begin{aligned} & Q_n(0, l_2) \\ & = x_{n2} \tfrac{l_2+\alpha_2-1}{n+\alpha_1+\alpha_2+\alpha_3-1} Q_{n-1}(0, l_2-1) \\ & \quad + x_{n3} \tfrac{n-l_1-l_2+\alpha_3-1}{n+\alpha_1+\alpha_2+\alpha_3-1} Q_{n-1}(0, l_2) \end{aligned} \tag{21}$$

for $1 \leq l_2 \leq n-l_1-1$.

$$\begin{aligned} & Q_n(l_1, l_2) \\ & = x_{n1} \tfrac{l_1+\alpha_1-1}{n+\alpha_1+\alpha_2+\alpha_3-1} Q_{n-1}(l_1-1, l_2) \\ & \quad + x_{n2} \tfrac{l_2+\alpha_2-1}{n+\alpha_1+\alpha_2+\alpha_3-1} Q_{n-1}(l_1, l_2-1) \end{aligned} \tag{22}$$

for $1 \leq l_1,\ 1 \leq l_2$ and $l_1 + l_2 = n$.

$$\begin{aligned} Q_n(n, 0) &= x_{n1} \tfrac{n+\alpha_1-1}{n+\alpha_1+\alpha_2+\alpha_3-1} \\ &\quad \times Q_{n-1}(n-1, 0) \\ Q_n(0, n) &= x_{n2} \tfrac{n+\alpha_2-1}{n+\alpha_1+\alpha_2+\alpha_3-1} \\ &\quad \times Q_{n-1}(0, n-1) \\ Q_n(0, 0) &= x_{n3} \tfrac{n+\alpha_3-1}{n+\alpha_1+\alpha_2+\alpha_3-1} \\ &\quad \times Q_{n-1}(0, 0) \end{aligned} \tag{23}$$

The initial condition is

$$Q_0(0,0) = 1. \tag{24}$$

The computation of the universal portfolio $\hat{\mathbf{b}}_n$ and the universal capital $\hat{S}_n$ through (10) and (11) respectively can be done solely by computing the quantities $Q_n(l_1, l_2)$ recursively through (19)-(24) or by computing both $X_n(l_1, l_2)$ and $C_n(l_1, l_2)$ recursively through (12)–(18). The detailed derivations of the formulae are given in Chan (2002).

3.1 Data Collection

Stock price data (opening price and closing price) of three Malaysia stocks namely Top Glove,

Nestle and Astro are collected from Bloomberg with the duration of one year (year 2017), two years (year 2016 to year 2017) and four years (year 2014 to year 2017). Python programming language are used to write a code based on the modified algorithm of Chan (2002) for computing the three-stock universal portfolio generated by the Dirichlet ($\alpha_1, \alpha_2, \alpha_3$) distribution where $\alpha_j > 0$ for $i = 1, 2, 3$.

4. Empirical Results

The Three-parameter Dirichlet $(\alpha_1, \alpha_2, \alpha_3)$ universal portfolio on 3 stocks data with trading period of one year from 2 January 2014 to 31 December 2014, two years from 2 January 2014 to 31 December 2015 and four years from 2 January 2014 to 29 December 2017 are selected. The three stocks data are Top Glove, Nestle and Astro.

Using the modified algorithm described in the previous section with the starting capital S_0 to be 1 unit and the initial portfolio $\mathbf{b}_0 = \left(\frac{1}{3}, \frac{1}{3}, \frac{1}{3}\right)$, we can compute the investment capitals achieved by ten different Dirichlet$(\alpha_1, \alpha_2, \alpha_3)$ Cover-Ordentlich universal portfolios for the above 3 stock data with three different periods. Tables 1, 2 and 3 show the wealths obtained by varying the Three-parameter of Dirichlet $(\alpha_1, \alpha_2, \alpha_3)$ universal portfolios.

From Table 1, Three-Parameter Dirichlet universal portfolio showed that investor can yield the good return at the end of one year period by investing as large portion as possible into Top Glove instead on the other two stocks. However, Astro showed the good return in Table 2 and Table 3 for 2 years and 4 years investment period.

Table 1: Empirical results for one-year period (year 2017).

$(\alpha_1, \alpha_2 \alpha_2)$	(b_1, b_2, b_3)	Wealth obtained S_n
(1,1,1)	(0.333300,0.333300,0.333400)	1.110328419
(10,1,1)	(0.833400,0.083300,0.083300)	1.1029922948
(1,10,1)	(0.083300,0.833400,0.083300)	1.002264375
(1,1,10)	(0.083300,0.083300,0.833400)	1.299865425
(1,1,20)	(0.045455,0.045455,0.90909)	1.329443054
(1,1,50)	(0.019231,0.019231,0.961538)	1.350058993
(1,1,100)	(0.009804,0.009804,0.980932)	1.357496929
(1,1,200)	(0.00495,0.00495,0.9900990)	1.361331761
(1,1,500)	(0.001992,0.001992,0.996016)	1.363671099

Table 2: Empirical results for two-year period (year 2016- 2017).

$(\alpha_1, \alpha_2 \alpha_2)$	(b_1, b_2, b_3)	Wealth obtained S_n
(1,1,1)	(0.333300,0.333300,0.333400)	1.085371358
(10,1,1)	(0.833400,0.083300,0.083300)	1.345534339
(1,10,1)	(0.083300,0.833400,0.083300)	0.882980156
(1,1,10)	(0.083300,0.083300,0.833400)	1.025231349
(20,1,1)	(0.909090,0.045455,0.045455)	1.385589859
(50,1,1)	(0.961538,0.019231,0.019231)	1.413312174
(100,1,1)	(0.980392,0.009804,0.009804)	1.423264668
(200,1,1)	(0.990099,0.004950,0.004950)	1.428384415

Table 3: Empirical results for four-year period (year 2014-2017).

$(\alpha_1, \alpha_2 \alpha_2)$	(b_1, b_2, b_3)	Wealth obtained S_n
(1,1,1)	(0.333300,0.333300,0.333400)	1.633188323
(10,1,1)	(0.833400,0.083300,0.083300)	2.224179241
(1,10,1)	(0.083300,0.833400,0.083300)	1.047713158
(1,1,10)	(0.083300,0.083300,0.833400)	1.660165174
(20,1,1)	(0.909090,0.045455,0.045455)	2.316591672
(50,1,1)	(0.961538,0.019231,0.019231)	2.380595372
(100,1,1)	(0.980932,0.009804,0.009804)	2.403562919
(200,1,1)	(0.990099,0.004950,0.004950)	2.415372985
(300,1,1)	(0.993377,0.003311,0.003312)	2.419359097

5. Conclusions

These results empirically verified that the Three-Parameter Dirichlet universal portfolio is useful in determining a portfolio for investor to obtain the good return based on a certain stocks and periods. Stock Top-Glove holds the highest priority to be invested in one year period and Astro shows a good return for a two years and four years period investment independent of the parameters.

References

Cover, T.M., 1991. Universal portfolios, *Mathematical Finance*, 1, pp. 1–29.

Cover, T.M. and Ordentlich, E., 1996. Universal portfolios with side information, *IEEE Transactions on*

Information Theory, 42(2), pp. 348–363.

Helmbol D.P., Shapire,R.E., Singer,Y. and Warmuth, M.K., 1998. On-line portfolio selection using multiplicative updates, *Mathematical Finance*, 8(4), pp. 325–347.

Tan, C.P. and Tang, S.F., 2003. A comparison of two types of universal portfolios based on some stock-price data, *Malaysia Journal of Sciences*, 22(2), pp. 127–224.

Chan, C.T., 2002. *Universal portfolios and relative entropy bounds in investment*, Master's thesis, University of Malaya, Kuala Lumpur.

Further Empirical Study of the Universal Portfolio Generated by the Reverse Kullback-Leibler Divergence

Choon Peng Tan[a], Kee Seng Kuang[b], Yap Jia Lee[c]

[a,b,c]Department of Mathematical and Actuarial Sciences, Lee Kong Chian Faculty of Engineering and Science, Universiti Tunku Abdul Rahman, Malaysia. [c]Email (corresponding author): yjlee@utar.edu.my

Abstract

The universal portfolio generated by the Kullback-Leibler divergence (also known as the Helmbold universal portfolio) is a well-studied portfolio. This paper considers the portfolio generated by the reverse Kullback-Leibler divergence and studies its performance on the selected stock-price data sets from the local stock exchange. The number of trading days extends to two thousand and fifty. The performance of this portfolio is compared to that of the universal portfolios generated by the Hölder ratios.

1. Introduction

The Markowitz model is a mean-variance model based on some assumptions to construct the portfolio (Markowitz, 1952). Cover (1991) presents a universal portfolio adaptive algorithm that can perform well even if the stochastic model of the stock market is unknown. The universal portfolio strategy is a weighted average of invested stock proportions where no statistical assumption is made about the model of the market. Cover and Ordentlich (1996) generalize their algorithm by using the Dirichlet distribution moments as weights. Helmbold et. al. (1998) present a universal portfolio algorithm with an attempt to reduce the tremendous computational time and memory amount in the Cover and Ordentlich's algorithm by employing a framework introduced by Kivinen and Warmuth (1997). The exponentiated-gradient-update universal portfolio of Helmbold uses the multiplicative update rule, suitable for on-line implementation.

Tan and Tang (2003) show that for small parametric values of the learning parameter, the performance of the Helmbold universal portfolio is close to a constant rebalanced portfolio. Tan and Lim (2011) introduce large parametric values including some negative values to further improve the performance of Helmbold universal portfolio. The use of the distance function is studied extensively in the literature, especially in information theory and statistical inference (Basu et. al., 2011). Tan and Kuang (2015) present the connection between the Renyi and the Kullback-Leibler-divergence universal portfolios. The extension of the Helmbold universal portfolio by scaling the Kullback-Leibler divergence generating the portfolio is studied in Tan and Kuang (2015). Tan and Lee (2018) propose a special Bregman-divergence universal portfolio associated with a convex polynomial.

This paper is a further empirical study of the reverse-Kullback-Leibler-divergence generated universal portfolio in Tan, Kuang and Lee (2017) by extending the number of trading days to two thousand and fifty. This paper concludes with a comparison of the performance of the reverse Kullback-Leibler divergence universal portfolio with that of the Hölder ratio universal portfolio (Tan and Lee, 2019).

2. Some Preliminaries

Consider investing in a market described by m stocks for a period of n trading days. Let $\boldsymbol{x}_n = (x_{ni})$ denotes the i^{th} stock price-relative vector, where

$$x_{ni} = \frac{closing\ price}{opening\ price}, i = 1,2, \dots, m$$

on the n^{th} trading day. The portfolio vector $\boldsymbol{b}_n = (b_{ni})$ is a set of the proportions of investor's wealth distributed over m stocks on day n, where

$$0 \le b_{ni} \le 1, i = 1,2, \dots, m$$

and

$$\sum_{j=1}^{m} b_{nj} = 1, n = 1,2, \dots.$$

The porfolio return S_n at the end of the n^{th} trading day is computed according to

$$\boldsymbol{S}_n = \prod_{j=1}^{n} \boldsymbol{b}_j^t \boldsymbol{x}_j.$$

The porfolios $\{b_n\}$ used are universal if no statistical assumption is made about the behaviour of the market.

3. Theory

The initial wealth of the investor is assumed to be 1 unit, given by $S_0 = 1$. The portfolio on day 1 is computed as the uniform weighted average of all stock proportions, namely,

$$\boldsymbol{b}_1 = \left(\frac{1}{m}, \frac{1}{m}, \dots, \frac{1}{m}\right).$$

The next-day portfolio $\boldsymbol{b}_{n+1}$ is to be determined by maximizing an objective funtion of $\boldsymbol{b}_{n+1}$ given the current portfolio $\boldsymbol{b}_n$ and the current price-relative $\boldsymbol{x}_n$. The objective function $\hat{F}(\boldsymbol{b}_{n+1}, \lambda)$ is a linear combination of the estimated rate of daily wealth increase and the distance function $D(\boldsymbol{b}_{n+1}, \boldsymbol{b}_n)$ subject to the constraint that the sum of b_{ni} for the i^{th} stock on the n^{th} trading day is equal to 1. The objective function is given by

$$\hat{F}(\boldsymbol{b}_{n+1}, \lambda) = \xi \left[\log(\boldsymbol{b}_n^t \boldsymbol{x}_n) + \frac{\boldsymbol{b}_{n+1}^t \boldsymbol{x}_n}{\boldsymbol{b}_n^t \boldsymbol{x}_n} - 1\right] - D(\boldsymbol{b}_{n+1}, \boldsymbol{b}_n) + \lambda\left[\sum_{j=1}^{m} b_{nj} - 1\right] \quad (1)$$

where $\xi > 0$ and λ is the Lagrange multiplier.

For two probability disributions $\boldsymbol{p} = (p_i)$ and $\boldsymbol{q} = (q_i)$, the Kullback-Leibler order-α divergence is defined as

$$D_\alpha(\boldsymbol{p}||\boldsymbol{q}) = \alpha \sum_{j=1}^{m} p_j \log\left(\frac{p_j}{q_j}\right) \quad (2)$$

for $\alpha > 0$. The parameter $\alpha = 1$ corresponds to the well-known Kullback-Leibler divergence which generates the Helmbold universal portfolio with parameter ξ defined as:

$$b_{n+1,i} = \frac{b_{ni} e^{\frac{\xi x_{ni}}{\boldsymbol{b}_n^t \boldsymbol{x}_n}}}{\sum_{j=1}^{m} b_{nj} e^{\frac{\xi x_{nj}}{\boldsymbol{b}_n^t \boldsymbol{x}_n}}} \text{ for } i = 1,2, \dots, m. \quad (3)$$

The reverse Kullback-Leibler order-α divergence of $\boldsymbol{p} = (p_i)$ and $\boldsymbol{q} = (q_i)$ is defined as

$$D_\alpha^*(\boldsymbol{p}||\boldsymbol{q}) = D_\alpha(\boldsymbol{q}||\boldsymbol{p}) = \alpha \sum_{j=1}^{m} q_j \log\left(\frac{q_j}{p_j}\right) \quad (4)$$

for $\alpha > 0$. The universal portfolio generated by (4) will be known as the *reverse order-α Helmbold portfolio*. In the derivation of the reverse order-α universal portfolio, a system of linear equations needs to be solved. The solution is given in the following proposition.

Proposition 1. Let $\boldsymbol{v} = (v_i)$ be a given vector, where

$$v_i = \frac{\xi}{\alpha}\left[\frac{x_{ni}}{\boldsymbol{b}_n^t \boldsymbol{x}_n} - 1\right], \text{ for } i = 1,2, \dots, m, \quad (5)$$

$\xi > 0$ and $\alpha > 0$ are given scalars. Consider the set of linear equations

$$C\boldsymbol{u} = \boldsymbol{v}, \quad (6)$$

where $C = (c_{ij})$ is a known matrix given by

$$c_{ij} = \begin{cases} b_{nj}^2 & for\ i \neq j \\ b_{ni}^2 - b_{ni} & for\ i = j \end{cases}. \tag{7}$$

The solution to the set of equations (6) is

$$u_i = \frac{1}{b_{ni}}(\eta - v_i) \text{ for } i = 1,2,\dots,m \tag{8}$$

where η is any real scalar.

Proposition 2. Consider the objective function

$$\hat{F}(\boldsymbol{b}_{n+1}, \lambda) = \xi\left[\log(\boldsymbol{b}_n^t \boldsymbol{x}_n) + \frac{\boldsymbol{b}_{n+1}^t \boldsymbol{x}_n}{\boldsymbol{b}_n^t \boldsymbol{x}_n} - 1\right] - \alpha \sum_{j=1}^m b_{nj} \log\left(\frac{b_{nj}}{b_{n+1,j}}\right) + \lambda\left[\sum_{j=1}^m b_{nj} - 1\right] \tag{9}$$

for $\xi > 0$ and $\alpha > 0$ are given, where λ is the Lagrange multiplier. The reverse order-α Helmbold universal portfolio generated by the reverse Kullback-Leibler order-α divergence (4) is given by

$$b_{n+1,i} = \frac{b_{ni}[\beta(\boldsymbol{b}_n^t \boldsymbol{x}_n) - x_{ni}]^{-1}}{\sum_{j=1}^m b_{nj}[\beta(\boldsymbol{b}_n^t \boldsymbol{x}_n) - x_{nj}]^{-1}} \text{ for } i = 1,2,\dots,m \tag{10}$$

where $\beta = \frac{\alpha\eta}{\xi} + 1$ for any real scalar η and is chosen such that $\beta(\boldsymbol{b}_n^t \boldsymbol{x}_n) - x_{ni} > 0$ for all $i = 1,2,\dots,m$.

For the proofs of proposition 1 and 2, refer to Tan, Kuang and Lee (2017).

Proposition 3. Let

$$h(\boldsymbol{b}_{n+1}, \boldsymbol{b}_n) = \frac{\left(\sum_{j=1}^m b_{n+1,j}^r\right)^{\frac{1}{r}}\left(\sum_{j=1}^m b_{nj}^s\right)^{\frac{1}{s}}}{\sum_{j=1}^m (b_{n+1,j} b_{nj})} \geq 1 \tag{11}$$

be the Hölder ratio for $1 \leq r < \infty$, $1 \leq s < \infty$, $\frac{1}{r} + \frac{1}{s} = 1$ and $g(h)$ is an increasing function of h. The universal portfolio generated by (1) and (11) is

$$b_{n+1,i} = \frac{\left\{b_{ni}^{\frac{1}{r-1}} + \beta_{r,n} b_{ni}^{\frac{2-r}{r-1}}\left[\frac{x_{ni} - \alpha_n(\boldsymbol{b}_n^t \boldsymbol{x}_n)}{\boldsymbol{b}_n^t \boldsymbol{x}_n}\right]\right\}}{\sum_{j=1}^m \left\{b_{nj}^{\frac{1}{r-1}} + \beta_{r,n} b_{nj}^{\frac{2-r}{r-1}}\left[\frac{x_{nj} - \alpha_n(\boldsymbol{b}_n^t \boldsymbol{x}_n)}{\boldsymbol{b}_n^t \boldsymbol{x}_n}\right]\right\}}, \quad i = 1,2,\dots,m \tag{12}$$

where

$$\beta_{r,n} = \frac{\left[\sum_{j=1}^m (b_{n+1,j} b_{nj})\right]\delta^{-1}\xi\left(\frac{dg}{dh}\right)^{-1}}{(r-1)h(\boldsymbol{b}_{n+1}, \boldsymbol{b}_n)} > 0 \tag{13}$$

for $r > 1$, $\delta > 0$, $\xi > 0$, $\frac{dg}{dh} > 0$, $\alpha_n > 0$. Note that $D(\boldsymbol{b}_{n+1}, \boldsymbol{b}_n)$ in (1) is replaced by $g(h)$.

For a pseudo Hölder-ratio universal portfolio with parametric vector (r, α, β), assume that $\alpha_n = \alpha$ does not depend on n, and $\beta_{r,n} = \beta$ does not depend on r and n. Hence (12) becomes

$$b_{n+1,i} = \frac{\left\{b_{ni}^{\frac{1}{r-1}} + \beta b_{ni}^{\frac{2-r}{r-1}}\left[\frac{x_{ni} - \alpha(\boldsymbol{b}_n^t \boldsymbol{x}_n)}{\boldsymbol{b}_n^t \boldsymbol{x}_n}\right]\right\}}{\sum_{j=1}^m \left\{b_{nj}^{\frac{1}{r-1}} + \beta b_{nj}^{\frac{2-r}{r-1}}\left[\frac{x_{nj} - \alpha(\boldsymbol{b}_n^t \boldsymbol{x}_n)}{\boldsymbol{b}_n^t \boldsymbol{x}_n}\right]\right\}} \tag{14}$$

for $i = 1,2,\dots,m$, where $r > 1$, $\alpha > 0$, $\beta > 0$. The numerator of (14) must be positive for chosen (r, α, β).

For the proof of proposition 3, refer to Tan and Lee (2019).

4. Empirical Results

The performance of the reverse order-α Helmbold universal portfolio in (10) is tested on the historical stock data from the Kuala Lumpur Stock Exchange and compared with that of the performance of the Hölder-ratio universal portfolio in (14). The trading period of the stock data is from 3rd January 2005 to 4th September 2015, accumulated over 2500 trading days. The list of the Malaysian companies is given in Table 1. These Malaysian companies are randomly selected from different sectors of the market industry to ensure diversification in investments for the purpose of empirical study.

Table 1: List of Malaysian companies in the data sets J, K, L, M and N.

Data Set	Malaysian Companies in Each Portfolio
J	Public Bank, Nestle Malaysia, Telekom Malaysia, Eco World Development Group, Gamuda
K	AMMB Holding, Air Asia, Encorp, IJM Corp, Genting Plantations
L	Alliance Financial Group, DiGi.com, KSL Holdings, IJM Corp, Kulim Malaysia
M	Hong Leong Bank, DiGi.com, Eco World Development Group, Zecon, United Malacca
N	RHB Capital, Carlsberg Brewery Malaysia, KSL Holdings, Crest Building Holdings, Kulim Malaysia

Table 2 shows the accumulated portfolio return over 2500 trading days (S_{2500}) and the next-day portfolios ($\boldsymbol{b}_{2501}$) for selected values of parameter β by running the reverse order-α Helmbold universal portfolio in (10) over the company data sets J, K, L, M and N. From the computational results, data sets J and M are good portfolios achieving 19.2781 and 23.3541 units in return, respectively. Surprisingly, data sets J and M both achieve local maximum wealth for parameter value $\beta = 3.2$. Further observation reveals that Eco World Development Group plays an important role in the universal portfolio where higher weights are assigned to the company for both data sets J and M. On the other hand, portfolios K, L and N exhibit a lack-luster performance by achieving 4.5486, 5.476 and 3.6644 units in return, respectively. For data sets K and L, higher weight is assgned to the companies Encorp and Digi.com, respectively. It is observed that the porportions of wealth allocated for data set N is still close to 0.2 which is also the initial portfolio proportion on day 1.

Table 2: The wealth S_{2500} obtained after 2500 trading days by running the reverse order-α Helmbold universal portfolio (10) and the next-day portfolios after 2500 trading days for selected values of β.

Set	β	S_{2500}	$b_{2501,1}$	$b_{2501,2}$	$b_{2501,3}$	$b_{2501,4}$	$b_{2501,5}$
J	3.2	19.2781	0.0772	0.0793	0.0683	0.7022	0.073
K	1.204	4.5486	0.0003	0.0154	0.8907	0.0479	0.0457
L	1.1813	5.476	0.0002	0.7256	0.2529	0.0007	0.0206
M	3.2	23.3541	0.0636	0.1154	0.6717	0.0827	0.0666
N	30	3.6644	0.2019	0.198	0.197	0.1988	0.2042

The accumulated wealth S_n over n trading days for data sets J and M are given in Figure 1. Figure 2 shows the accumulated wealth S_n over n trading days for data sets K, L and N. The parameter values of β used in plotting the graph is fixed for each data set throughout the period of 2500 trading days as given in Table 2. In Figure 1, the accumulated wealth grows exponentially for both data sets J and M. Generally, the wealth achieved by portfolio M is larger than portfolio J. It is clear from Figure 2 that the accumulated wealth by portfolios L and N increase gradually in a similar manner while the performance of portfolio K exhibits some interesting behaviour. There is a rapid increase in the accumulated wealth around day-620 and the accumulated wealth stays around 3 to 4 units for approximately 300 days. The accumulated wealth then dramastically decreases to 1.4 units on day-1000. The accumulated wealth for portfolio K achieves 4.5486 units after 2500 trading days.

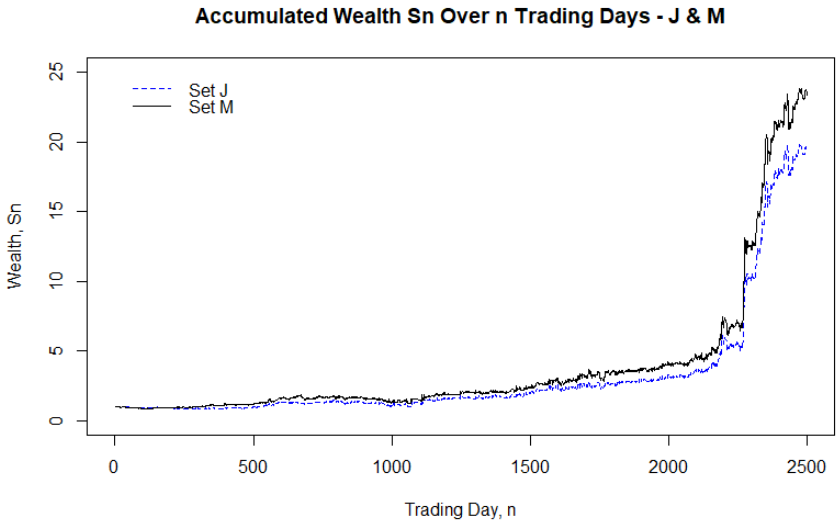

Figure 1: Accumulated wealth S_n over n trading days for data sets J and M.

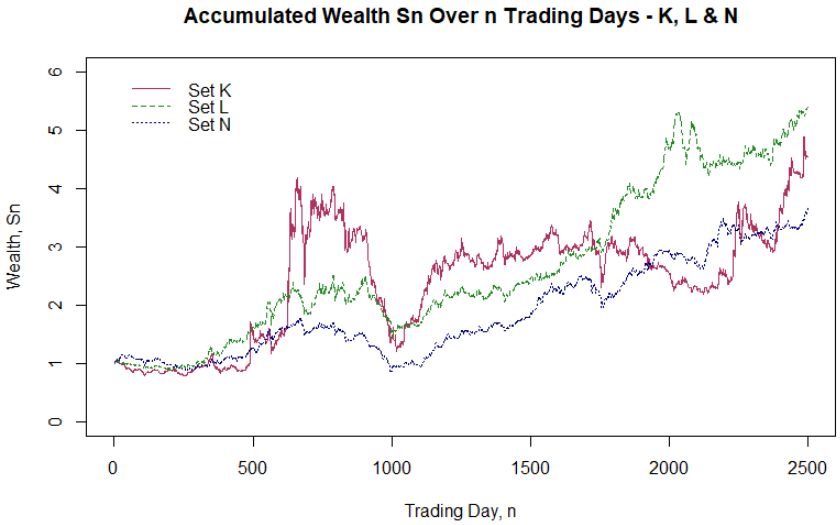

Figure 2: Accumulated wealth S_n over n trading days for data sets K, L and N.

Table 3 gives the comparison of the accumulated portfolio return over 2500 trading days (S_{2500}) achieved by the reverse order-α Helmbold universal portfolio in (10) and the Hölder-ratio universal portfolio in (14). There is no significant difference in the wealth achieved. The reverse order-α Helmbold portfolio strategy can perform better for data sets J and M while the Hölder-ratio universal portfolio can generate a higher wealth for data sets K, L and N. It is evident that the performance of the portfolios is parameter-dependent.

Table 3: The comparison of wealth S_{2500} obtained after 2500 trading days by the Hölder-ratio universal portfolio and the reverse order-α Helmbold universal portfolio over the data sets J, K, L, M and N.

Set	Hölder-ratio	Reverse Helmbold
	S_{2500}	S_{2500}
J	17.845	19.2781
K	5.0198	4.5486
L	6.8694	5.476
M	19.9976	23.3541
N	5.3035	3.6644

5. Conclusions

The ability of the universal portfolio investment strategy to allocate proper weights to the investment stocks to achieve higher investment return is demonstrated in this empirical study. It can be observed in Table 3 that the wealth achievable for the same data set is different according to the portfolio investment strategy used, namely, the Hölder-ratio universal portfolio or the reverse Helmbold universal portfolio. Apart from that, it can be shown in Figure 1 and 2 that long term investment strategy works well for all portfolio data sets except for portfolio K, in which the accumulated wealth on day-660, $S_{660} = 4.1791$ units, is merely slightly lower compared to the accumulated wealth on day-2500, $S_{2500} = 4.5486$ units. The performance of a universal portfolio can be affected by a few factors such as the selected values of the parameters and the combination of the constituent stocks in the investment portfolio.

References

Basu, A., Shioya, H. and Park, C., 2011. *Statistical inference: the minimum distance approach*. Chapman and Hall/CRC.

Cover, T.M. and Ordentlich, E., 1996. Universal portfolios with side information. *IEEE Transactions on Information Theory*, 42(2), pp. 348 – 363.

Cover, T.M., 1991. Universal portfolios. *Mathematical Finance*, 1, pp. 1 – 29.

Helmbold, D.P., Schapire, R.E., Singer, Y. and Warmuth, M.K., 1998. On-line portfolio selection using multiplicative updates. *Mathematical Finance*, 8(4), pp. 325 – 347.

Kivinen, J. and Warmuth, M.K., 1997. Exponentiated gradient versus gradient descent for linear predictors. *Information and Computation*, 132(1), pp. 1 – 63.

Markowitz, H., 1952. Portfolio Selection. *The Journal of Finance*, 7(1), pp. 77 – 91.

Tan, C.P. and Kuang, K.S., 2015. Universal portfolios generated by the Renyi and generalized Kullback-Leibler divergences. *AIP Conference Proceedings*. AIP Publishing, 1691(1), 040025. URL: https://doi.org/10.1063/1.4937075.

Tan, C.P. and Lee, Y.J., 2018. The Bregman-divergence universal portfolio associated with a convex polynomial. *Journal of Physics: Conference Series*. IOP Publishing, 1132(1), 012073. DOI: 10.1088/1742-6596/1132/1/012073.

Tan, C.P. and Lee, Y.J., 2019. Universal portfolios generated by the inequality ratios. *IOSR Journal of Mathematics*, 15(3), pp. 24 – 28. DOI: 10.9790/5728-1503032428.

Tan, C.P. and Lim, W.X., 2011. The two parameters affecting the performance of the Helmbold universal portfolio. *Canadian Journal on Computing in Mathematics, Natural Sciences, Engineering and Medicine*, 2(6), pp. 158 – 165.

Tan, C.P. and Tang, S.F., 2003. Relationship between the Fisher index of discrimination and the minimum test sample size. *Malaysian Journal of Science*, 22(1), pp. 111 – 119.

Tan, C.P., Kuang, K.S. and Lee, Y.J., 2017. Performance of the reverse Helmbold universal portfolio. *AIP Conference Proceedings*. AIP Publishing, 1830(1), 020023. URL: https://doi.org/10.1063/1.4980886.

Control Chart for Monitoring Stock Price and Trading Volume in Malaysia Stock Market

Tan Zong Ming

Department of Mathematical and Actuarial Sciences, Lee Kong Chian Faculty of Engineering and Science, Universiti Tunku Abdul Rahman, Malaysia. Email: tanzm@utar.edu.my

Abstract

Statistical control charts are rarely explored as a charting technique in stock tradingdue to high rate of possible false alarms as the stock price is non-normally distributed and auto correlated.ARIMA model is used to build the control chart as it is widely used in modelling auto correlated data. Some research also shows that there is a strong relationship between stock price and trading volume. In this research, control chart with ARIMA model is used on both the stock price and trading volume to detect trading signal. A demonstration of application by using the real time data is done and comparison with weighted moving average technical charts is carried out.

1. Introduction

Stock market is representing a country's economy, financial status and growth. Stock market traders always want to get a broad picture on the movement of the market or on particular stocks. It is crucial for market trader to detect an upward or downward price trend in making trading decision. Most of the market traders use technical charts, for example candle stick, relative strength index, moving average convergence divergence, smoothing moving average etc., to detect such trends to determine their trading strategy. In fact, market traders and quality controllers are relied on charts and both of them use chart to identify signals. Quality controllers use statistical control charts to detect a signal whenever the quality of a product is out of control meanwhile the market traders use technical charts to detect a trend in making trading decision (buy, hold or sell the stock) in the market.

Statistical control charts are rarely explored as a charting technique in stock trading and portfolio analysis (Gandy, 2012;Rebisz, 2015). The main reason control charts not to be used in monitoring financial data is because of the lack of important information (McNeese *et al*., 2002). Robert (1959) was first to suggest the use of control chart in studying market price levels and changes. In order to construct control charts, Hubbard (1967) used logarithmic monthly values to determine the price trend and compare with the gross national product and personal income trends. He identified ways to recognize signal for buying or holding stocks. According to Hubbard (1967), small price fluctuates between the center line have no recognizable pattern and do not give any buy or sell signals to the market traders. Meanwhile, significant departures from the center line signals stock price overvaluation or undervaluation.Gandy (2012) used a wide range of different CUSUM control charts to detect changes in the performance of a credit portfolio. Dumiĉić and Žmuk (2015) used control chart for individual units, MR, EWMA and CUSUM control charts in monitoring the performance of short-term stock trading in Croatia based.

2. Literature Review

Alexander (1961, 1964) introduce the filter trading rules. The filter trading rules is a sequence of buy-sell signals. He uses the rules to investigate stock price trends. These buy-sell signals for an observed stock are based on the daily closing price. Buy signal is given if the closing price increases more than certain percentage from a subsequent low, while sell signal is given if the closing price decreases more than certain percentage from a subsequent high. The rules further developed by Fama and Blume (1965), Dryden (1969),

Sweeney (1988), Corrado and Lee (1992) and Sullivan *et al.* (1999). However, the filter trading rules only take stock price into consideration. These rules can be enhanced by include the trading volume. Trading volume provide a measure of number of shares traded in a specific period of time. It is often overlooked but will be a powerful tool to maximize profit and minimize risk. The analysis of the relationship between trading volume and stock returns has received increasing attention from investors and researchers (Kaizoji, 2013). This is because many of them consider that stock returns might be predicted by trading volume. Kaizoji (2013) define return as the logarithmic daily price change whereas trading volume is defined as number of shares traded in a particular trading day.

Classical Shewhart control charts are measuring data without autocorrelation. Even a low degree of autocorrelation data will cause the Classical Shewhart control charts to be failed. Stochastic modelling of time series analysis is one of the ways to tackle the autocorrelation problem.Time series analysis is a theory of using mathematical statistic theory and random process in analyzing time series data. It is applying comprehensively in the area of financial market. However, time series analyses are mainly used in forecasting and residuals testing in the area of financial market.

Rebisz (2015) and Dumiĉić and Žmuk (2015) claim that the control charts are not widely used in stock trading and portfolio analysis due to high rate of possible false alarms. They also claim that stock price is non-normally distributed and auto correlated. However, Žmuk (2016) introduce and develop additional statistical tools to support the decision-making process in stock trading. Žmuk (2016) overcome the autocorrelation problem by applying the ARIMA(*p,d,q*) model on the residual-based control chart. He shows that the residual-based EWMA and residual-based CUSUM control charts approach resulted higher portfolio profit in stock trading compare to pick and hold strategy. Zhang *et al.* (2009) use time series model to build the stock price forecast model for Shanghai Composite Index. Mondal *et al*. (2014) use ARIMA model to forecast the Indian stock for various sector and examine the accuracy based on different span of period data. They achieve more than 85% accuracy by using ARIMA model in forecasting the stock price for all the sectors. Ariyo *et al*. (2014) show that the ARIMA models are useful in predicting stock price on short term basis. Meanwhile, Žmuk (2016) apply ARIMA model on the residual-based control chart for residuals testing.

3. Methodology

In this research, we will apply ARIMA model on both the stock price and trading volume respectively. Dumiĉić and Žmuk (2015) claim that the stock prices are non-normally distributed and auto correlated. Mohamad and Nassir (1995) find out that absolute price changes have a strong relationship with trading volume. They also claimthat there is a lagged relationship interaction between price change and trading volume. Ying (1966) and Tauchen and Pitts (1983) findings also suggest that the absolute price changes are positively correlated to trading volume. In order to overcome the shortages, we used ARIMA model to build the control chart for stock price. This is because ARIMA model is widely used in modelling auto correlated data. ARIMA (*p, d, q*) model has the following general structure:

$$\boldsymbol{\Phi}_p(\boldsymbol{B}) \cdot \boldsymbol{\nabla}^d x_t = \boldsymbol{\theta}_q(\boldsymbol{B})\varepsilon_t, \tag{1}$$

where

$\boldsymbol{\Phi}_p(\boldsymbol{B}) = \left(1 - \varphi_1 B - \varphi_2 B^2 \ldots - \varphi_p B^p\right)$ is *p*-th order autoregressive polynomial,

$\boldsymbol{\theta}_q(\boldsymbol{B}) = \left(1 - \theta_1 B - \theta_2 B^2 \ldots - \theta_q B^q\right)$ is *q*-th order moving averages polynomial,

$\boldsymbol{\nabla}^d = (1 - B)^d$is the *d*-th difference operator,

B is back shift operator as $B \cdot x_t = x_{t-1}$,

$\varphi_1,\ \varphi_2,\ \ldots,\ \varphi_p$ is the parameters of autoregressive model,

$\theta_1,\ \theta_2,\ \ldots,\ \theta_q$ is the parameters of moving averages model,

ε_t is an error term, usually a white noise with normal distribution, $N(0, \sigma^2)$.

The 100(1 – *k*) % prediction interval for *h* period ahead is given by

$$\hat{x}_{t+h|T} \pm z_{k/2}\hat{\sigma}_h, \tag{2}$$

where
$0 < k < 1$,
$\hat{x}_{t+h|T}$ is the forecast value for *h* period ahead,
$z_{k/2}$ is the two tailed *k* percentage point of a standard normal distribution,
$\hat{\sigma}_h$ is the estimated forecast standard deviation.

We use the 100(1 – *k*) %prediction interval of 1 period ahead as the upper and lower control limits (UCL, LCL) for our ARIMA control chart. Thus, the UCL and LCL are respectively have the form:

$$UCL = \hat{x}_{t+1|T} + z_{k/2}\hat{\sigma}, \tag{3}$$

$$LCL = \hat{x}_{t+1|T} - z_{k/2}\hat{\sigma}, \tag{4}$$

where
$\hat{x}_{t+1|T}$ is the 1 period ahead forecast value,
$\hat{\sigma}$ is the standard deviation of the residuals,
$z_{k/2}$ is the two tailed *k* percentage point of a standard normal distribution,

The value of *k* could be set as the sensitivity of the ARIMA control chart. The sensitivity of ARIMA control chart decrease as *k* increase.

4. Result and Discussion

FBM KLCI constituent companies' stock pricehas be chosen for analysis. This is because FBM KLCI composed the 30 largest capital listed companies on Bursa Malaysia. The stock price for large-cap or blue-chip companies normally having smaller volatility and stable trading volume. Thus, any sudden change in stock price or volume might indicate an alert to investor. Besides, all the KLCI component companies have minimum of 15% free float and liquid enough to be traded as stated in the Ground Rules set by Bursa Malaysia.

The UCL and LCL in constructing the control charts are using 99% prediction interval. The chart of the stock price, trading volume, UCL and LCL of Genting Malaysia Berhad has shown below. The control charts show that most of the time the stock prices and trading volumes are between the UCL and LCL. The stock price move above the UCL or move below the LCL will be consider as assignable causes. This assignable causes could be trading signals.When the stock price is above UCL indicate a buy signal and when the stock price is below the LCL indicate a sell signal. When trading volume is above the UCL indicate as unusual market behavior. Stock prices for year 2017 are use as training set to build the model while the stock prices for year 2018 are used as validation set in monitoring process. Below are the steps in building the control chart:

1. Firstly, use the stock prices (or trading volume) for year 2017 to build an ARIMA model using *auto.arima* function in R-program. *Auto.arima* function will return the ARIMA model with the least AIC values as the model.

2. Next, using the *forecast* function in R-program, compute the 99% prediction interval of the forecast value for 1 period ahead based on the selected ARIMA model.

3. The upper and lower bound of the prediction interval will be the UCL and LCL.

4. The stock price of next trading day is examine based on the UCL and LCL.

5. Trading signal is said to be detected when the stock price is above UCL or below the LCL.

6. Repeat Step 2 to Step 5 until the end of the validation set.

Figure 1 and Figure 2 show the ARIMA control chart for stock price and trading volume of Genting Malaysia Berhad in year 2018. Both Figure 1 and Figure 2 showa few trading signals. There issome news in year 2018 associated with the signals and the ARIMA control charts able to identify them.Signal 2 is a sell signal and detected in both Figure 1 and Figure 2. The news associated with this signal is Malaysia Government announced in the Budget 2019 that casino license will be increased from RM120 million to RM150 million annually and casino duty will be raised to 35% on gross income starting year 2019. This will negatively impact the bottom line of the company. In fact, one month before the announcement (trading day 188), there is a selling signal and market might already predict and price in the tax raised factor and create a sell signal (Signal 1) before the announcement.Meanwhile, another selling signal (signal 3) is detected when Genting Malaysia filed a USD1.75 billion lawsuits against The Walt Disney Co. and 20th Century Fox World due to Fox trying to terminate the deal for licensing the Genting theme park after The Walt Disney Co. has completed its acquisition of 20th Century Fox World. This will delay the grand opening of the Genting Malaysia theme park which has invested and planed for almost 10 years. The revenue and profit of the company might not increase as expected and most of the investment institutes have lower down their target price on Genting Malaysia.

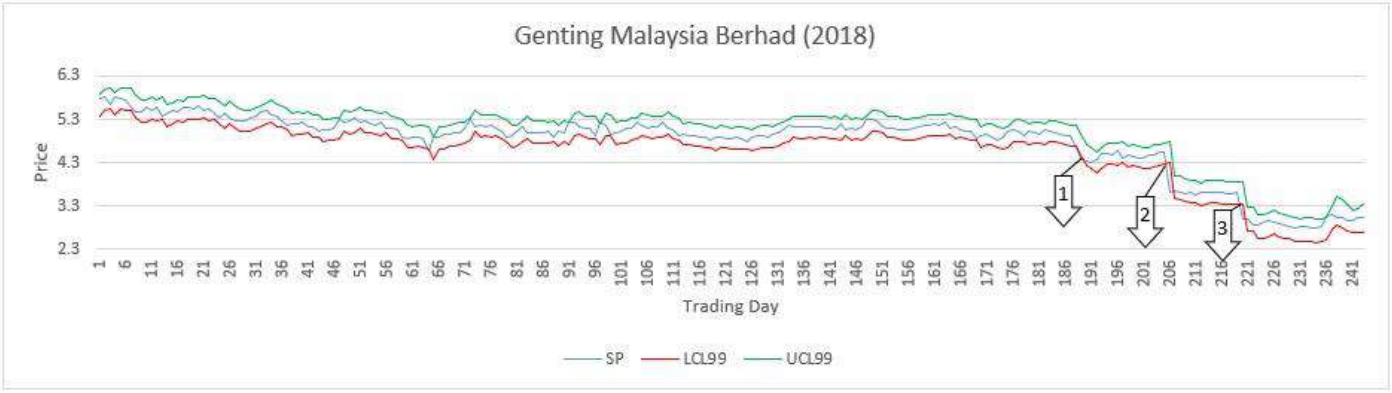

Figure 1: ARIMA control chart for stock price of Genting Malaysia Berhad in year 2018.

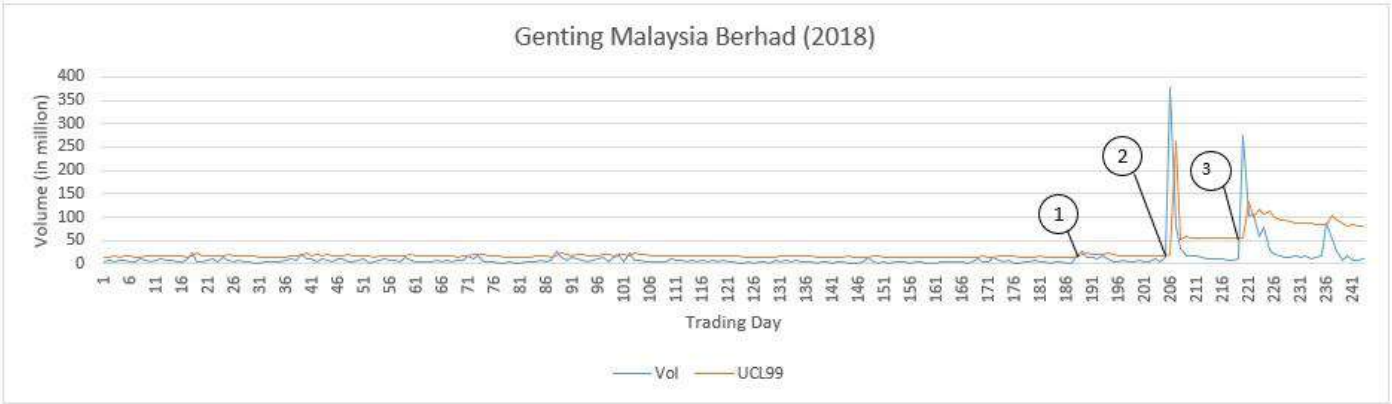

Figure 2: ARIMA control chart for trading volume of Genting Malaysia Berhad in year 2018.

Although the rest of the signals are not associate to any news, those signals are also important as trading signal for investors accordance to market force. Besides that, the 9-days weighted moving average (blue line) and 26-days weighted moving average (purple line) technical charts are show in Figure 3 as a comparison.Weighted moving average chart is chosen because it is a popular and easy chart in technical analysis. For weighted moving average chart, signal is identified when the blue line and the purple line crossover. It is a sell signal if the blue line cross below the purple line. Meanwhile it is a buy signal if the blue line crosses above the purple line.

In Figure 3, weighted moving average chart shows more signal compare to Arima control chart. There are too much of signal observed in weighted moving average chart. This might lead to frequent trading and increase the cost. Besides that, the weighted moving average chart cannot detect a signal which incorporate with those important news (Signal 2 and Signal 3). Meanwhile Arima control chart reflect immediately after the news was announced.In addition, weighted moving average chart unable produced any signal during the downtrend. For example, during the down trend from Oct to Dec, Arima control chart able to produce signal during the trends but for weighted moving average chart the purple line and blue line did not crossover to generate a signal.

Figure 3: Weighted moving average for stock price of Genting Malaysia Berhad in year 2018

5. Conclusions

In conclusion, both stock price and trading volume ARIMA control chart shows a good result in generating trading signals. ARIMA control chart can serve as an alternative charting tool in monitoring and generating signal in stock market. Interactive control chart by combining stock price and trading volume incorporate into a single control chart could be considered. Besides, this research can be further enhanced by applying multivariate ARIMA model in to the control chart and monitor stock price and trading volume together in one control chart.

References

Alexander, S.S., 1961. Price movements in speculative markets: Trends or random walk. *Industrial Management Review*, 2(2), pp. 7–26.

Alexander, S.S., 1964. Price movements in speculative markets: Trends or random walk, number 2. *Industrial Management Review*,5(2), pp. 25–46.

Ariyo, A.A., Adewumi, A.O. and Ayo, C.K., 2014. Stock Price Prediction Using the ARIMA Model. *UKSim-AMSS 16th IEEE International Conference on Computer Modelling and Simulation*, pp. 106–112.

Corrado, J.C. and Lee, S.H., 1992. Filter rule tests of the economic significance of serial dependencies in daily stock returns. *Journal of Financial Research*, 15(4), pp. 369–387.

Dumičić, K. and Žmuk, B., 2015. Statistical control charts: Performances of short term stock trading in Croatia. *Business Systems Research*, 6(1), pp. 22–35.

Dryden, M.M., 1969. A source of bias in filter tests of share prices. *Journal of Business*, 42(3), pp. 321–325.

Fama, E.F. and Blume, M.E., 1965. Filter rules and stock-market trading. *Journal of Business*, 39(1), pp. 226–241.

Gandy, A., 2012. Performance monitoring of credit portfolios using survival analysis.*International Journal of Forecasting*, 28(1), pp.139–144.

Hubbard, C.L., 1967. A control chart for postwar stock price levels. *Financial Analysts Journal*, 23(6), pp.139–145.

Kaizoji, T., 2013. Modeling of Stock Returns and Trading Volume. *IIM Kozhikode Society & Management Review*, 2(2), pp. 147–155.

McNeese, W. and Wilson, W., 2002. *Using time series charts to analyse financial data* [Online]. Available at: http://www.spcforexcel.com/files/timeseriesfinancial.pdf [Accessed: 1 July 2019].

Mohamad, S. and Nassir, M.D.A., 1995. Price changes and trading volume relationship: Some preliminary evidence from Kuala Lumpur stock exchange. *Pertanika Journal of Social Sciences and Humanities*, 3(2), pp.147–154.

Mondal, P., Shit, L. and Goswami, S., 2014. Study of effectiveness of time series modeling (ARIMA) in forecasting stock prices. *International Journal of Computer Science, Engineering and Application*, 4(2), pp. 13–29.

Rebisz, B., 2015. Appliance of quality control charts for sovereign risk modelling. *Journal of Applied Economics and Business Research*, 5(3), pp.148–160.

Roberts, H.V., 1959. Stock market "patterns" and financial analysis: Methodological suggestions. *Journal of Finance*, 14(1), pp.1–10.

Sullivan, R., Timmermann, A. and White, H., 1999. Data-snooping, technical trading rule performance and the bootstrap. *The Journal of Finance*, 54(5), pp. 1647–1691.

Sweeney, J.R., 1988. Some new filter rule tests: Methods and results. *Journal of Financial and Quantitative Analysis*, 23(3), pp. 285–300.

Tauchen, G. and Pitts, M., 1983. The price variability-volume relationship on speculative markets. *Econometrica*, 51(2), pp.485–505.

Ying, C.C., 1966. Stock market prices and volumes of sales. *Econometrica*, 34(3), pp.676–686.

Zhang, J., Shan, R. and Su, W., 2009. Applying time series analysis builds stock price forecast model. *Modern Applied Science*, 3(5), pp. 152–157.

Žmuk, B., 2016. Capabilities of Statistical Residual-Based Control Charts in Short- and Long-Term Stock Trading. *Našegospodarstvo/Our Economy*, 62(1), pp.12–26.

Percentiles of the Run-Length Distribution of the Group Runs $\bar{X}$ Chart

Chong Zhi Lin[a], Michael Khoo Boon Chong[b], Teoh Wei Lin[c], Yeong Wai Chung[d], Lim Sok Li[e]

[a]*Department of Physical and Mathematical Science, Faculty of Science, Universiti Tunku Abdul Rahman, Malaysia.* [*]*Email (corresponding author):chongzl@utar.edu.my*

[b]*School of Mathematical Sciences, Universiti Sains Malaysia, Malaysia.*

[c]*School of Mathematical and Computer Sciences, Heriot-Watt University Malaysia, Malaysia.*

[d]*Department of Operations and Management Information Systems, Faculty of Business and Accountancy, Universiti Malaya, Malaysia.*

[e]*Institute of Mathematical Sciences, Faculty of Science, Universiti Malaya, Malaysia.*

Abstract

Nowadays, quality is essential in every field. Producing quality products or services can help to increase the competitiveness, reputation and customer loyalty of a company as this ensures that the products or services meet customers' expectations. However, for a product or service to have a satisfactory quality level, the underlying process manufacturing the product or providing the service should be in statistical control. The Group Runs (GR) $\bar{X}$ chart is proposed as an improvement of the synthetic $\bar{X}$ chart for the detection of process mean shifts. The GR $\bar{X}$ chart integrates the Shewhart $\bar{X}$ sub-chart and an extended version of the conforming run length (CRL) sub-chart. To have a better understanding of the behavior of the GR chart, in this paper, we study the percentage points (or percentiles) of the run-length distribution of the GR chart, instead of depending entirely on the average run length (ARL) criterion. Before computing the percentiles of the GR $\bar{X}$ chart, we need to obtain the optimal parameters of the GR $\bar{X}$ chart. This can be achieved by writing a computer program to search for a set of optimal L and k values that minimize the out-of-control ARL, while maintaining the in-control ARL at a desired value. Then, the percentiles of the run-length distribution of the GR $\bar{X}$ chart can be investigated using this set of L and k values.

1. Introduction

Statistical Process Control (SPC) refers to a set of statistical techniques that is widely used to monitor and enhance the quality characteristics of both the manufacturing and service industries (Montgomery, 2012). In practical situations, no process is able to remain stable forever. Control chart is the primary technique of SPC applied to control the quality of a process. A high-quality process will result in an improvement in production yield, reduction in production costs and ensure the product or service is able to satisfy customer expectations.

Walter A. Shewhart proposed the Shewhart $\bar{X}$ chart in the 1920s. The Shewhart $\bar{X}$ chart is commonly applied to monitor the performance and stability of the mean of any process. The Shewhart $\bar{X}$ chart is very sensitive in the detection of large process mean shifts, but it is ineffective towards the detection of small and moderate process mean shifts. The Shewhart $\bar{X}$ chart has this performance because it is a memoryless chart that only considers the latest sample in determining the status of the process mean, whether it is in statistical control or out of statistical control.

Bourke (1991) introduced an attributes conforming run length (CRL) chart to monitor the fraction non-conforming, p of a process. Based on the total number of conforming samples between two non-conforming samples, the CRL chart is able to categorize the process as either in-control (IC) or out-of-control (OOC). This indicates that similar to a variables chart, an attributes chart is also easy to be implemented. Many researchers have studied the CRL chart due to its simplicity, see, for example, Aparisi (2009), Khoo (2010), and Haq (2016).

The CRL value denotes the number of examined units between two successive non-conforming units, inclusive of the ending non-conforming unit. Since the CRL's distribution varies based on p, i.e. the CRL increases when p decreases and the CRL decreases when p increases, the CRL chart can detect the changes in p promptly. To improve the performance of the CRL chart, Wu and Spedding (2000) proposed the synthetic $\bar{X}$ chart by integrating the Shewhart $\bar{X}$ sub-chart and a CRL sub-chart.

Gadre and Rattihalli (2004) mentioned that a signal may be either caused by a false alarm or by a shift in the process mean. Hence, it is necessary to examine the process further by waiting for successive samples to identify the true cause for the signal. Based on this idea, Gadre and Rattihalli (2004) presented the Group Runs (GR) control chart by merging the Shewhart $\bar{X}$ sub-chart with an extended version of the CRL sub-chart. Gadre and Rattihalli (2004) proved that the GR chart is superior to the Shewhart $\bar{X}$ chart and synthetic $\bar{X}$ chart. Chong et al. (2016) proposed the GR revised m-of-k runs rules chart based on the generalized synthetic charting principle developed by Scariano and Calzada (2009). They showed that the performance of the proposed chart is significantly better than the revised m-of-k runs rules and the GR charts.

The average run length (ARL) is widely considered as a performance measure of a chart. However, interpretation of a control chart based only on the ARL can be confusing to practitioners (Bischak and Trietsh 2007; Teoh et al. 2015). This is because the ARL merely gives information about the average number of samples before a signal, without any information regarding the probability of obtaining an IC signal by a particular number of samples. To solve this problem, Palm (1990) and Radson and Boyd (2005) proposed a better performance measure, i.e. the percentiles of the run-length distribution, to evaluate the performance of a chart.

Chakraborti (2000) mentioned that the run-length distribution follows a right-skewed geometric distribution. In fact, the shape of the run-length distribution alters along with the size of the shifts in the process mean. It changes from highly skewed to the right when there is no shift or small shift, to nearly symmetric when the shift is large. Therefore, to fully understand the performance of a chart, we should investigate the full run-length distribution of the chart. By studying the chart's run-length distribution, we can comprehensively understand the characteristic of a process. Palm (1990) presented the tables of the run-length percentiles to investigate the efficacy of the Shewhart $\bar{X}$ chart with supplementary runs rules.

The run-length distribution can be represented by the percentiles (or percentage points) of its distribution, where the 50^{th} percentile is the median. The percentiles give more information compared to the ARL. This is because the lower percentiles of the run-length distribution for an IC process provide information regarding the initial false alarm rates. Moreover, the percentiles of the run-length distribution also give information about the probability of receiving a signal by a particular number of samples. An in-depth study of the percentiles gives comprehensive information about the skewness of the run-length distribution.

The rest of this paper is structured as follows: Section 2 introduces the charting statistics of the GR $\bar{X}$ chart. Section 3 presents the optimal design of the GR $\bar{X}$ chart. This is followed by a simulated performance study. Finally, concluding remarks are drawn in Section 4.

2. The Group Runs $\bar{X}$ Chart

The GR $\bar{X}$ chart declares that the process is OOC, if either the first CRL value, i.e. $\text{CRL}_1 \leq L$ or two consecutive values of $\text{CRL}_i \leq L$ and $\text{CRL}_{i+1} \leq L$, for $i = 2, 3, \ldots$, where L is the lower control limit

(LCL) of the CRL sub-chart. The operation of the GR chart can be justified as follows: If the process mean is shifted greatly at the start of a process monitoring, it is expected that the first CRL is small ($\leq L$). If $\mathrm{CRL}_1 \leq L$, the process is regarded as OOC. However, if $\mathrm{CRL}_1 > L$, it is a sign that the process is stable and the process monitoring continue. Moreover, for subsequent process monitoring, the process is not declared as OOC by just taking a single CRL greater than L, but by considering the next CRL is also greater than L. This is because the previous small CRL value may be caused by sampling fluctuation and thus the process is continued.

The GR $\bar{X}$ chart's operation is given in the following steps:

Step 1. Take n continuous samples to form a subgroup.

Step 2. Applying the Shewhart $\bar{X}$ sub-chart to decide whether the subgroup is conforming (the samples plot inside the sub-chart's limits) or non-conforming (the samples plot outside the sub-chart's limits). The $\mathrm{LCL}_{\bar{X}}$ and upper control limit ($\mathrm{UCL}_{\bar{X}}$) of the $\bar{X}$ sub-chart is:

$$\mathrm{LCL}_{\bar{X}} = \mu_0 - k\frac{\sigma_0}{\sqrt{n}} \tag{1}$$

and

$$\mathrm{UCL}_{\bar{X}} = \mu_0 + k\frac{\sigma_0}{\sqrt{n}}, \tag{2}$$

where μ_0, k and σ_0 represent the IC mean, control limit charting constant and the IC standard deviation, respectively.

Step 3. If the subgroup is categorized as conforming, the control flow goes back to Step 1. Otherwise, the control flow proceeds to the next step.

Step 4. The process is considered as OOC if $\mathrm{CRL}_1 \leq L$ or two successive $\mathrm{CRL}_i \leq L$ and $\mathrm{CRL}_{i+1} \leq L$, for i = 2, 3, ….Then, the control flow proceeds to the next step. Otherwise, the control flow returns to Step 1.

Step 5. Necessary action is taken to investigate and eliminate the assignable cause(s). Then, return to Step 1.

3. Optimal Design of the Group Runs $\bar{X}$ Chart

In this section, we will discuss the optimal design of the GR $\bar{X}$ chart. This can be done by obtaining the optimal parameters (L, k) of the GR $\bar{X}$ chart. The optimal parameters (L, k) of the GR $\bar{X}$ chart can be obtained by minimizing the OOC ARL (ARL_1), subject to the constraint $\mathrm{ARL}_0 = \tau$. In this paper, $\tau = 370$ is used. The optimal parameters can be obtained by using the Matlab program.

Prior to computing the optimal parameters (L, k) of the GR $\bar{X}$ chart, the users need to set the optimal shift size of interest (δ_{opt}), sample size (n), and τ values. However, the user does not need to specify the target values of μ and σ as the calculation of the optimal parameters (L, k) does not involve these values.

We use the Matlab program to conduct a simulation study for the GR $\bar{X}$ chart. We set δ_d = 1, sample size, $n \in \{3, 5, 7, 10\}$ and$\tau = 370$. The optimization algorithm will initialize L as 1. Hence, L is considered to be an independent charting parameter. By solving the following equation:

$$\mathrm{ARL}_0 = \frac{1}{P(0)} \times \frac{1}{\left(1-(1-P(0))\right)^2} \tag{3}$$

we can obtain the value of *k*, where probability $P(0) = 2\Phi(-k)$ and Φ is the cumulative density function of the standard normal distribution. In this equation, *L* is defined as the independent charting parameter that is allowed to vary. First, the program will initialize *L* as 1, followed by increasing *L* one at a time up to sixty. From this sixty combinations of parameters (*L*, *k*) and their respective ARL_1 values, the combination that gives the minimum ARL_1 is considered as the optimal parameters combination. Since *L* is generally small, it is sufficient for us to set the maximum *L* as sixty.

For any pair of (*L*, *k*), the ARL_1 value can be calculated using the following equation:

$$\mathrm{ARL}_1 = \frac{1}{P(\delta)} \times \frac{1}{\left(1-(1-P(\delta))\right)^2}, \tag{4}$$

where δ is the shift size and probability $P(\delta)$ is given as:

$$P(\delta) = 1 - \Phi\left(k - \delta\sqrt{n}\right) + \Phi\left(-k - \delta\sqrt{n}\right). \tag{5}$$

Then, based on the optimal parameters (*L*, *k*), a simulation program written in the Statistical Analysis System (SAS) is applied to calculate the percentiles of the run-length distribution of the GR $\bar{X}$ chart. As the run-length distribution is highly skewed to the right, examining the full run-length distribution gives a complete knowledge about the performance of the GR $\bar{X}$ chart. In this simulation program, we consider both decreasing and increasing shifts in the process mean. A decreasing shift happens when the underlying distribution of the process mean decreases from μ_0 to $\mu_0 - \delta\sigma$, whereas an increasing shift happens when the distribution of the process mean increases from μ_0 to $\mu_0 + \delta\sigma$.

In this paper, we study the 0.1^{th}, 1^{st}, 5^{th}, 10^{th}, 20^{th}, 30^{th}, 40^{th}, 50^{th}, 60^{th}, 70^{th}, 80^{th} and 90^{th} percentiles of the run-length distribution for both the IC ($\delta = 0$) and OOC ($\delta > 0$) processes, where $\delta \in \{0.00, 0.25, 0.50, 0.75, 1.00, 1.50, 2.00, 2.50, 3.00\}$ and $n \in \{3, 5, 7, 10\}$. It is important to note that the underlying distribution of the GR $\bar{X}$ chart is assumed to be normal.

4. Results and Findings

Using the Matlab program, optimal chart's parameters are computed for the cases where $n \in \{3, 5, 7, 10\}$, and τ= 370. From Table 1, it is noticed that the optimal parameters (*L*, *k*) generally decrease as *n* increases. Based on the optimal parameters obtained in Table 1, the percentiles of the run-length distribution of the GR $\bar{X}$ chart is computed using the SAS program. The percentiles for *n* = 3, 5, 7 and 10 are given in Tables 2 to 5, respectively.

Table 1: Optimal charting parameters (*L*, *k*), for $\delta_{\mathrm{opt}} = 1$, sample size $n \in \{3,\ 5,\ 7,\ 10\}$ and $\tau = 370$.

n	*L*	*k*
3	5	1.9517
5	3	1.8107
7	3	1.8107
10	2	1.6929

For ARL_0 = 370, users may falsely think that a false alarm should happen at the 370^{th} sample with 50% chance or 50% of the time. However, in real scenario, the value of ARL_0 = 370 falls between the 60^{th}

and 70th percentage points (see Tables 2 to 5) of the run-length distribution, and in practice, the false alarm happens much quicker at the 214~230th samples, for 50% of the time (see 50th percentile of Tables 2 to 5). From this example, it is clear that the IC run-length distribution of the GR $\bar{X}$ chart is right-skewed and the 50th percentiles (median) of the run-length distribution is a better representation of central tendency of the run-length distribution compared to the average.

From Tables 2 to 5, it can be seen that as the size of mean shift, δ increases, the skewness of the run-length distribution of the GR $\bar{X}$ chart decreases. This is because the skewness of the run-length distribution of the GR $\bar{X}$ chart varies according to the size of the mean shift. Therefore, sole dependence on the ARL as a performance measure of a control chart can be misleading. For a complete understanding of a control chart performance, it is important to study the percentiles of the run-length distribution.

The lower percentiles (i.e. 0.1th, 1th, 5th and 10th percentiles) of the run-length distribution when δ = 0 give information about the early false alarm in the process. For instance, by considering δ = 0 in Table 2, we can state that there is an approximately 10% probability that a false alarm will happen by the 3rd sample. Moreover, the percentage points of the run-length distribution enable a practitioner to state with confidence the exact probability for a chart to signal by a certain number of sample. Moreover, the higher percentiles, that is, the 70th, 80th and 90th percentiles of the run-length distribution give some useful information to users. For example, consider the case where δ = 0.5 in Table 2, one can conclude with 90% confidence that an OOC signal will be identified by the 73th sample point.

Table 2: Simulation results for the Group Runs (GR) $\bar{X}$ chart when n = 3, L = 5, k = 1.9517.

δ	Percentage points of the run-length distribution (%)											
	0.1	1	5	10	20	30	40	50	60	70	80	90
0.00	1	1	1	3	5	56	128	214	318	451	637	962
0.25	1	1	1	2	3	5	36	71	113	167	245	378
0.50	1	1	1	1	2	3	4	5	16	28	44	73
0.75	1	1	1	1	1	2	2	3	4	4	10	18
1.00	1	1	1	1	1	1	1	2	2	3	4	5
1.50	1	1	1	1	1	1	1	1	1	1	2	2
2.00	1	1	1	1	1	1	1	1	1	1	1	1
2.50	1	1	1	1	1	1	1	1	1	1	1	1
3.00	1	1	1	1	1	1	1	1	1	1	1	1

Table 3: Simulation results for the GR $\bar{X}$ chart when n = 5, L = 3, k = 1.8107.

δ	Percentage points of the run-length distribution (%)											
	0.1	1	5	10	20	30	40	50	60	70	80	90
0.00	1	1	1	2	8	70	139	222	324	453	636	946
0.25	1	1	1	1	2	3	26	49	78	116	168	257
0.50	1	1	1	1	1	2	2	3	8	14	22	36
0.75	1	1	1	1	1	1	1	2	2	3	3	9
1.00	1	1	1	1	1	1	1	1	1	2	2	3
1.50	1	1	1	1	1	1	1	1	1	1	1	1
2.00	1	1	1	1	1	1	1	1	1	1	1	1
2.50	1	1	1	1	1	1	1	1	1	1	1	1
3.00	1	1	1	1	1	1	1	1	1	1	1	1

Table 4: Simulation results for the GR $\bar{X}$ chart when n=7, L=3, k= 1.8107.

δ	Percentage points of the run-length distribution (%)											
	0.1	1	5	10	20	30	40	50	60	70	80	90
0.00	1	1	1	2	9	69	138	219	322	451	636	946
0.25	1	1	1	1	2	3	15	31	51	77	113	176
0.50	1	1	1	1	1	1	2	2	3	7	12	20
0.75	1	1	1	1	1	1	1	1	2	2	2	3
1.00	1	1	1	1	1	1	1	1	1	1	2	2
1.50	1	1	1	1	1	1	1	1	1	1	1	1
2.00	1	1	1	1	1	1	1	1	1	1	1	1
2.50	1	1	1	1	1	1	1	1	1	1	1	1
3.00	1	1	1	1	1	1	1	1	1	1	1	1

Table 5: Simulation results for the GR $\bar{X}$ chart when n=10, L=2, k= 1.6929.

δ	Percentage points of the run-length distribution (%)											
	0.1	1	5	10	20	30	40	50	60	70	80	90
0.00	1	1	1	2	20	80	149	230	325	449	626	921
0.25	1	1	1	1	2	2	11	22	36	54	79	123
0.50	1	1	1	1	1	1	1	2	2	2	7	12
0.75	1	1	1	1	1	1	1	1	1	1	2	2
1.00	1	1	1	1	1	1	1	1	1	1	1	1
1.50	1	1	1	1	1	1	1	1	1	1	1	1
2.00	1	1	1	1	1	1	1	1	1	1	1	1
2.50	1	1	1	1	1	1	1	1	1	1	1	1
3.00	1	1	1	1	1	1	1	1	1	1	1	1

5. Conclusions

In this study, it is observed that for an IC process, the ARL_0 is allocated within the range of 60^{th} and 70^{th} percentiles of the run-length distribution. This indicates that there is a huge discrepancy between the ARL_0 and IC median run length (MRL_0) (50^{th} percentiles of the run-length distribution when $\delta = 0$). Nevertheless, the difference between the ARL_0 and MRL_0 reduces as the size of the mean shift increases. This shows that the skewness of the run-length distribution of the GR $\bar{X}$ chart decreases as the size of mean shift, δ increases, ranging from highly right-skewed for an IC process to almost symmetric when $\delta$is large. Here, it is shown that the ARL is a confusing performance measure and the percentiles of the run-length distribution give more information regarding the behaviour of the GR $\bar{X}$ chart. In conclusion, the performance of the GR $\bar{X}$ chart should be investigated via the percentiles of the run-length distribution instead of a sole dependence on the ARL. Future research can consider the optimal design of the GR chart based on MRL instead of ARL.

Acknowledements

This research is supported by the Universiti Tunku Abdul Rahman, Fundamental Research Grant Scheme (FRGS), no. FRGS/1/2016/STG06/UTAR/02/1.

References

Aparisi, F. and de Luna, M.A., 2009. Synthetic-$\bar{X}$control charts optimized for in-control and out-of-control regions. *Computers & Operations Research*, 36(12), pp. 3204 – 3214.

Bischak, D.P. and Trietsch D., 2007. The rate of false signals in X-bar control charts with estimated limits. *Journal of Quality Technology*, 39(1), pp. 54 – 65.

Bourke, P.D., 1991. Detecting a shift in fraction nonconforming using run-length control charts with 100% inspection. *Journal of Quality Technology*, 23(3), pp. 225 – 238.

Chakraborti, S., 2000. Run Length, average run length and false alarm rate of Shewhart X-bar chart: exact derivations by conditioning. *Communications in Statistics-Simulation and Computation*, 29(1), pp. 61 – 81.

Chong, Z.L., Khoo, M.B.C., Lee, M.H. and Chen, C.H., 2016. Group runs revised *m*-of-*k* runs rule control chart. *Communications in Statistics-Theory and Methods*, 46(14), pp. 6916 – 6935.

Gadre, M.P. and Rattihalli, R.N., 2004. A group runs control chart for detecting shifts in the process mean. *Economic Quality Control*, 19(1), pp. 29– 43.

Haq, A. and Khoo, M.B.C., 2016. A new synthetic control chart for monitoring process mean using auxiliary information. *Journal of Statistical Computation and Simulation*, 86(15), pp. 3068 – 3092.

Khoo, M.B.C., Lee, H.C., Wu, Z., Chen, C.H., Castagliola, P., 2010. A synthetic double sampling control chart for the process mean. *IIE Transactions*, 43(1), pp. 23 – 38.

Montgomery, D.C., 2012. *Introduction to statistical process control.* New York, NY: John Wily & Sons.

Palm, A.C., 1990. Tables of run length percentiles for determining the sensitivity of Shewhart control charts for averages with supplementary runs rules. *Journal of Quality Technology*, 22(4), pp. 289 – 298.

Radson, D. and Boyd, A.H., 2005. Graphical representation of run-length distributions. *Quality Engineering*, 17(2), pp. 301–308.

Scariano, S.M. and Calzada, M.E., 2009. The generalized synthetic chart. *Sequential Analysis*, 28(1), pp. 54 – 68.

Teoh, W.L., Khoo, M.B.C., Castagliola, P. and Chakraborti, S., 2015. A median run length-based double-sampling $\bar{X}$ chart with estimated parameters for minimizing the average sample size. *International Journal of Advanced Manufacturing Technology*, 80(1), pp. 411 – 426.

Wu, Z. and Spedding, T.A., 2000. A synthetic control chart for detecting small shifts in the process mean. *Journal of Quality Engineering*, 32(1), pp. 32 – 38.

A Production-inventory Model with Repair and Time-varying Rates

Yeo Heng Giap Ivan

Department of Mathematical and Actuarial Sciences, Lee Kong Chian Faculty of Engineering & Science, Universiti Tunku Abdul Rahman, Malaysia. Email: yeohg@utar.edu.my

Abstract

In this paper, we proposed a model for an inventory system that satisfies demand for a finished product by supplying both new items and repaired items. New items are fabricated from a single type of raw material procured from an external supplier, while used items are collected from the customers and then repaired to a condition that is as-good-as-new. The demand, production, and repair rates are assumed to be deterministic time-varying functions. The problem is to determine a joint policy for raw materials procurement, new items fabrication, and used items repair such that the total relevant cost of the model is minimized. We proposed a numerical solution procedure and we tested the procedure with two numerical examples. We also gave conditions that ensure the global optimality of the solution.

1. Introduction

Reuse is not a new phenomenon. Recycling of metal scrap, waste paper and soft drink bottles are examples that have been around for some time. In these cases, recovery of the used items is more economically appealing than disposal. However, the growth of environmental concerns has gave reuse increasing attention (Fleischmann et al., 1997). Reuse slows down the growth of landfills, and consequently slows down the accumulation of toxic solid waste in the environment. Reuse of old items often uses less resources than producing brand new items, and one result of this is lower carbon emissions. Today, environmental costs during a product's entire life cycle play an important role in the calculation of the product's total production costs (Spengler, 1997).

The study of repairable inventory models began with authors modifying the economic order quantity (EOQ) model by Harris (1913). As far as we are aware, the first author to propose an EOQ model of a repairable inventory system is Schrady (1967). He considered a single-item system in which demand is satisfied by the procurement of new items and the repair of used items. He jointly determined the EOQ formulas for procurement and repair. He assumed that all used items are reparable and procurement and repair have infinite rates. He considered policies that alternate one procurement setup with R repair setups ($(1, R)$ policies).

Nahmias and Rivera (1979) extended the work of Schrady (1967) to the case of finite repair rate. They derived EOQ formulas for $(1, R)$ policies as well. Mabini et al. (1992) also extended the work of Schrady (1967) by considering the case of a multi-item system, where items share the same repair facility. They allowed shortages to occur and proposed numerical solution procedures.

Koh et al. (2002) considered two types of policies: (1) $(1, R)$ policies, and (2) policies that alternate one recovery setup with P production setups ($(P, 1)$), as well as two cases for each policy: (1) the case where the repair rate is greater than the demand rate, and (2) the case where the repair rate is less than or equal to the demand rate. They also assumed infinite production rate and finite repair rate. They derived EOQ formulas and

found the optimal R and P through an exhaustive search procedure. In a follow up work, Konstantaras and Papachristos (2008a) obtained closed form expressions for the optimal setup numbers of the model by Koh et al. (2002).

Teunter (2004) generalized preceding works by considering the case of finite production and recovery rates for $(1, R)$ and $(P, 1)$ policies. He simplified the associated integer programming problem by treating R and P as real values, and used the nearest positive integers in the solution. His algorithm gave an approximate policy, although numerical tests showed that the results are fairly good in most cases. In follow up works, Konstantaras and Papachristos (2008b) and Wee and Widyadana (2010) proposed exact solution algorithms for the model by Teunter (2004).

The above works assumed that all returned items are recoverable. However, Richter (1996a,b) proposed EOQ waste disposal models, in which some of the returned items are scrapped at a cost. Richter assumed that the production and repair rates are infinite, and one production setup and one repair setup occur during each time interval (Richter, 1996a), or n production setups and m repair setups occur during each time interval (Richter, 1996b). Richter and Dobos (1999) and Dobos and Richter (2000) extended the works of Richter (1996a,b) by considering part of the problem as an integer programming problem, and in a similar work, Teunter (2001) examined an EOQ waste disposal model where repaired items and manufactured items have different holding costs. Dobos and Richter (2003) considered finite production and repair rates and a single production and a single repair setup per time interval. Later, Dobos and Richter (2004) generalized their former work for the case of P production setups and R repair setups per time interval ((P, R) policy).

Alamri (2011) proposed a global optimal solution to a general production-repair inventory model with time-varying rates for demand, return, production, repair, and deterioration. They considered one remanufacturing setup and one production setup per time interval ((1,1) policy) over an infinite planning horizon. In this paper, we use Alamri's work as base to propose a production-repair inventory model that incorporates returned items, serviceable items, and raw material inventories. A general framework of the item flow through these inventories is given in Figure 1. We assumed that the production, repair, demand, and return rates are deterministic functions of time. Our model ran a (1,1) policy, for which we proposed a unit time cost function, and showed that under certain conditions, the associated problem has a global optimal solution.

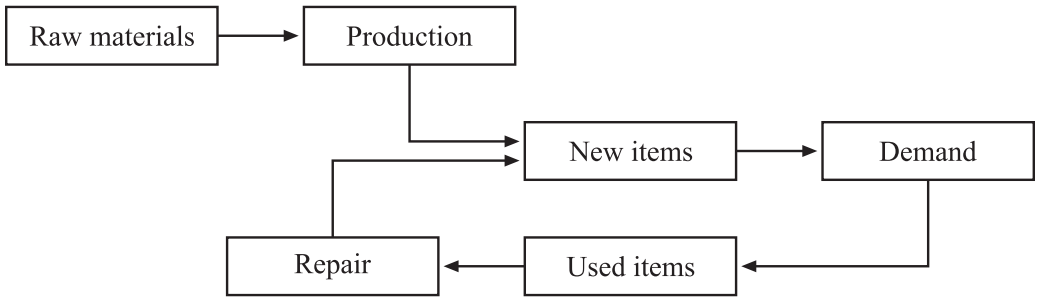

Figure 1: Framework of item flow of the proposed model.

2. Mathematical Formulation

The following assumptions and notations are used to formulate the proposed production-repair model:

1. The demand rate, production rate, and repair rate are deterministic functions of time, and are denoted by $D(t)$, $P(t)$, and $R(t)$ respectively. These functions satisfy the conditions $D(t) > 0$, $P(t) > D(t)$, and $R(t) > D(t)$.

2. The return rate is $\theta D(t)$, where θ is constant and $0 < \theta < 1$.

3. Returned items are repaired to an as-good-as-new condition.

4. Each unit of the finished product requires either m units of raw material or one returned item.

5. Raw material replenishment is instantaneous.

6. Shortages are not allowed.

7. The following costs are included in the model:

k_p	production setup cost/setup
k_r	repair setup cost/setup
k_m	raw material replenishment cost/replenishment
h_p	holding cost of serviceable items/item/time
h_r	holding cost of returned items/item/time
h_m	holding cost of the raw material/item/time
s_p	production cost/item
s_r	repair cost/item

Let $I_p(t)$ represent the serviceable items inventory level at time t, $I_r(t)$ represent the returned items inventory level at time t, and $I_m(t)$ represent the raw material inventory level at time t. Each cycle starts operating at time T_0. The repair run starts at time T_0, which increases $I_p(t)$ at the rate $R(t) - D(t)$ until time T_1, at which the repair run ends. Then $I_p(t)$ declines due to demand at the rate $D(t)$ until time T_2, at which it falls to zero. For ease of reference, we shall call the period (T_0, T_1) the repair uptime period, (T_1, T_2) the repair downtime period, and (T_0, T_2) the repair period.

The production run starts at time T_2, which increases $I_p(t)$ at the rate $P(t) - D(t)$ until time T_3, at which the production run ends. Then $I_p(t)$ declines due to demand at the rate $D(t)$ until time T_4, at which it falls to zero. We shall call the period (T_2, T_3) the production uptime period, (T_3, T_4) the production downtime period, and (T_2, T_4) the production period.

At time T_2, a shipment of raw material is received, and is consumed at the rate $mP(t)$ over the production uptime period. On the other hand, the consumption of returned items over the repair uptime period causes $I_r(t)$ to decrease at the rate $R(t) - \theta D(t)$ from $I_r(t) = Q$ to $I_r(t) = 0$. Then $I_r(t)$ increases at the rate $\theta D(t)$ due to more returned items entering the system, until time T_4, at which $I_r(t) = Q$ again. The inventory movement of such a system is illustrated in Figure 2 for increasing rates.

The movements of the inventory levels depicted in Figure 2 are described by the following differential equations and boundary values:

$$\frac{dI_p(t)}{dt} = R(t) - D(t), \qquad T_0 \le t \le T_1, \qquad I_p(T_0) = 0, \tag{1}$$

$$\frac{dI_p(t)}{dt} = -D(t), \qquad T_1 \le t \le T_2, \qquad I_p(T_2) = 0, \tag{2}$$

$$\frac{dI_p(t)}{dt} = P(t) - D(t), \qquad T_2 \le t \le T_3, \qquad I_p(T_2) = 0, \tag{3}$$

$$\frac{dI_p(t)}{dt} = -D(t), \qquad T_3 \le t \le T_4, \qquad I_p(T_4) = 0, \tag{4}$$

$$\frac{dI_r(t)}{dt} = -R(t) + \theta D(t), \qquad T_0 \le t \le T_1, \qquad I_r(T_1) = 0, \tag{5}$$

$$\frac{dI_r(t)}{dt} = \theta D(t), \qquad T_1 \le t \le T_4, \qquad I_r(T_1) = 0, \tag{6}$$

$$\frac{dI_m(t)}{dt} = -mP(t), \qquad T_2 \le t \le T_3, \qquad I_m(T_3) = 0. \tag{7}$$

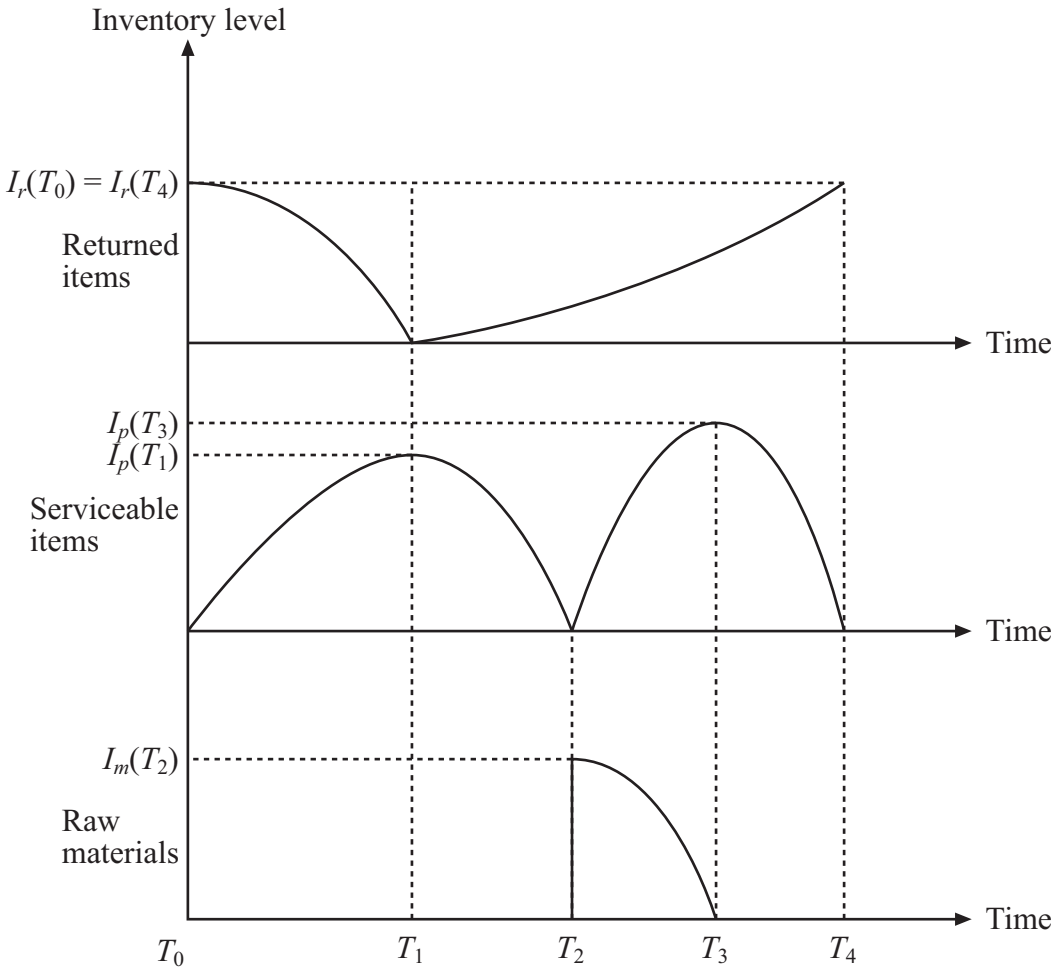

Figure 2: Inventory behavior of the proposed production-repair system in a time interval.

The solutions to Equations (1)−(7) are given by

$$I_p(t) = \int_{T_0}^{t} [R(u) - D(u)]\ du, \qquad T_0 \le t \le T_1, \tag{8}$$

$$I_p(t) = \int_{t}^{T_2} D(u)\ du, \qquad T_1 \le t \le T_2, \tag{9}$$

$$I_p(t) = \int_{T_2}^{t} [P(u) - D(u)]\ du, \qquad T_2 \le t \le T_3, \tag{10}$$

$$I_p(t) = \int_{t}^{T_4} D(u)\ du, \qquad T_3 \le t \le T_4, \tag{11}$$

$$I_r(t) = \int_{t}^{T_1} [R(u) - \theta D(u)]\ du, \qquad T_0 \le t \le T_1, \tag{12}$$

$$I_r(t) = \int_{T_1}^{t} \theta D(u)\ du, \qquad T_1 \le t \le T_4, \tag{13}$$

$$I_m(t) = \int_{t}^{T_3} mP(u)\ du, \qquad T_2 \le t \le T_3. \tag{14}$$

Let $I_j(c,d)$ denote the area under the graph (of Figure 2) during the period $c \le t \le d$, where $I_j(c,d) = \int_c^d I_j(u)\ du$ $(j = p, r, m)$. Then from Equations (8)−(14), we get

$$I_p(T_0,T_1) = \int_{T_0}^{T_1} \left(\int_{T_0}^{t} [R(u) - D(u)]\ du \right)\ dt, \tag{15}$$

$$I_p(T_1,T_2) = \int_{T_1}^{T_2} \left(\int_{t}^{T_2} D(u)\ du \right)\ dt, \tag{16}$$

$$I_p(T_2,T_3) = \int_{T_2}^{T_3} \left(\int_{T_2}^{t} [P(u) - D(u)]\ du \right)\ dt, \tag{17}$$

$$I_p(T_3,T_4) = \int_{T_3}^{T_4} \left(\int_{t}^{T_4} D(u)\ du \right)\ dt, \tag{18}$$

$$I_r(T_0,T_1) = \int_{T_0}^{T_1} \left(\int_{t}^{T_1} [R(u) - \theta D(u)]\ du \right)\ dt, \tag{19}$$

$$I_r(T_1,T_4) = \int_{T_1}^{T_4} \left(\int_{T_1}^{t} \theta D(u)\ du \right)\ dt, \tag{20}$$

$$I_m(T_2,T_3) = \int_{T_2}^{T_3} \left(\int_{t}^{T_3} mP(u)\ du \right)\ dt. \tag{21}$$

Using integration by parts, we get

$$I_p(T_0, T_1) = \int_{T_0}^{T_1} (T_1 - u)[R(u) - D(u)]\ dt. \tag{22}$$

$$I_p(T_1, T_2) = \int_{T_1}^{T_2} (u - T_1)D(u)\ du, \tag{23}$$

$$I_p(T_2, T_3) = \int_{T_2}^{T_3} (T_3 - u)[P(u) - D(u)]\ du, \tag{24}$$

$$I_p(T_3, T_4) = \int_{T_3}^{T_4} (u - T_3)D(u)\ du, \tag{25}$$

$$I_r(T_0, T_1) = \int_{T_0}^{T_1} (u - T_0)[R(u) - \theta D(u)]\ du, \tag{26}$$

$$I_r(T_1, T_4) = \int_{T_1}^{T_4} (T_4 - u)\theta D(u)\ du, \tag{27}$$

$$I_m(T_2, T_3) = \int_{T_2}^{T_3} (u - T_2)mP(t)\ du. \tag{28}$$

We can set $T_0 = 0$ without any loss of generality. Then the time-dependant cost components of a cycle are given by

$$\begin{aligned}\text{Holding cost} = {} & h_p[I_p(0, T_1) + I_p(T_1, T_2) + I_p(T_2, T_3) + I_p(T_3, T_4)] \\ & + h_r[I_r(0, T_1) + I_r(T_1, T_4)] + h_m I_m(T_2, T_3),\end{aligned} \tag{29}$$

$$\text{Repair cost} = s_r \int_0^{T_1} R(u)\ du, \tag{30}$$

$$\text{Production cost} = s_p \int_{T_2}^{T_3} P(u)\ du. \tag{31}$$

Then the total cost per unit time, TC, is given by

$$\begin{aligned}TC(T_1, T_2, T_3, T_4) = \frac{1}{T_4}\Bigg\{ & s_r \int_0^{T_1} R(u)\ du + s_p \int_{T_2}^{T_3} P(u)\ du + k_p + k_r + k_m \\ & + h_p\Bigg[\int_0^{T_1} (T_1 - u)[R(u) - D(u)]\ du + \int_{T_1}^{T_2} (u - T_1)D(u)\ du \\ & + \int_{T_2}^{T_3} (T_3 - u)[P(u) - D(u)]\ du + \int_{T_3}^{T_4} (u - T_3)D(u)\ du\Bigg] \\ & + h_r\Bigg[\int_0^{T_1} u[R(u) - \theta D(u)]\ du + \int_{T_1}^{T_4} (T_4 - u)\theta D(u)\ du\Bigg] \\ & + h_m \int_{T_2}^{T_3} (u - T_2)mP(u)\ du\Bigg\}.\end{aligned} \tag{32}$$

The problem is to find the T_1, T_2, T_3, and T_4 that minimize $TC(T_1, T_2, T_3, T_4)$, subject

to the following constraints:

$$0 < T_1 < T_2 < T_3 < T_4, \tag{33}$$

$$\int_0^{T_1} [R(u) - D(u)]\ du = \int_{T_1}^{T_2} D(u)\ du, \tag{34}$$

$$\int_{T_2}^{T_3} [P(u) - D(u)]\ du = \int_{T_3}^{T_4} D(u)\ du, \tag{35}$$

$$\int_0^{T_1} [R(u) - \theta D(u)]\ du = \int_{T_1}^{T_4} \theta D(u)\ du, \tag{36}$$

Inequality (33) ensures the feasibility of the given problem. Equations (34) and (35) ensure that all demands are satisfied by either repair or production. Equation (36) ensures that the inventory levels of the returned items at $t = 0$ and at $t = T_4$ are equal.

3. Solution Procedure

Let Q be the amount of used items that are returned in the period $(0, T_4)$. Then Q is given by

$$Q = \int_0^{T_4} \theta D(u)\ du, \tag{37}$$

from which it is apparent that T_4 is a function of Q. Let us write

$$T_4 = f_4(Q). \tag{38}$$

From Equations (36) and (38), T_1 is a function of T_4, and hence of Q. Let us write

$$T_1 = f_1(Q). \tag{39}$$

From Equations (34) and (39), T_2 is a function of T_1, and hence of Q. Let us write

$$T_2 = f_2(Q). \tag{40}$$

And from Equations (35), (38) and (40), T_3 is a function of T_2 and T_4, and hence of Q. Let us write

$$T_3 = f_3(Q). \tag{41}$$

Upon substituting Equations (38)−(41) into Equation (32), our constrained problem is converted to an unconstrained problem involving only one decision variable, Q:

$$\begin{aligned}\text{Minimize } TC(Q) = \frac{1}{f_4}\Bigg\{ & s_r \int_0^{f_2} D(u)\ du + s_p \int_{f_2}^{f_4} D(u)\ du + k_p + k_r + k_m \\ & + h_p \left[\int_0^{f_4} uD(u)\ du - \int_0^{f_1} uR(u)\ du - \int_{f_2}^{f_3} uP(u)\ du \right] \\ & + h_r \left[\int_0^{f_1} (u + f_4)[R(u) - \theta D(u)]\ du - \int_{f_1}^{f_4} u\theta D(u)\ du \right] \\ & + mh_m \int_{f_2}^{f_3} (u - f_2)P(u)\ du \Bigg\}. \end{aligned} \tag{42}$$

Note that $f_i(Q)$ $(i = 1, 2, 3, 4)$ does not require an explicit form, since whenever necessary, its value can be evaluated numerically.

The necessary condition for the solution to the given problem is

$$d(TC)/dQ = 0. \tag{43}$$

Let $w =$ the expression inside the curly brackets in Equation (42), so that

$$TC = w/f_4. \tag{44}$$

Then Equation (43) gives us the optimality condition

$$f_4 w' - w f_4' = 0. \tag{45}$$

Differentiating w with respect to Q gives

$$\begin{aligned} w' = {} & s_r f_2' D(f_2) + s_p[f_4' D(f_4) - f_2' D(f_2)] \\ & + h_p[f_4' f_4 D(f_4) - f_1' f_1 R(f_1) - f_3' f_3 P(f_3) + f_2' f_2 P(f_2)] \\ & + h_r\left[f_1' f_1 R(f_1) + f_4' \int_0^{f_1} [R(u) - \theta D(u)]\, du + f_4[f_1' R(f_1) \right. \\ & \left. - f_1' \theta D(f_1) - f_4' \theta D(f_4)]\right] + m h_m\left[f_3'(f_3 - f_2) P(f_3) - f_2' \int_{f_2}^{f_3} P(u)\, du\right]. \end{aligned} \tag{46}$$

Then from Equations (45) and (46), we get

$$\begin{aligned} w = \frac{f_4}{f_4'}\Big\{ & s_r f_2' D(f_2) + s_p[f_4' D(f_4) - f_2' D(f_2)] \\ & + h_p[f_4' f_4 D(f_4) - f_2' f_1 D(f_2) - f_3' f_3 P(f_3) + f_2' f_2 P(f_2)] \\ & + h_r\left[f_2' f_1 D(f_2) + f_4' \int_0^{f_1} [R(u) - \theta D(u)]\, du - f_1' f_4 \theta D(f_1)\right] \\ & + m h_m\left[f_3'(f_3 - f_2) P(f_3) - f_2' \int_{f_2}^{f_3} P(u)\, du\right]\Big\}, \end{aligned} \tag{47}$$

where the derivatives f_1', f_2', f_3', and f_4' are given by

$$f_1' = \frac{1}{R(f_1)}, \tag{48}$$

$$f_2' = \frac{1}{D(f_2)}, \tag{49}$$

$$f_3' = \left[\theta^{-1} - 1 + \frac{P(f_2)}{D(f_2)}\right] \frac{1}{P(f_3)}, \tag{50}$$

$$f_4' = \frac{1}{\theta D(f_4)}. \tag{51}$$

To determine the optimal value of Q, Equation (45) is solved. Then the optimal values of T_1, T_2, T_3, and T_4 are found from Equations (38)$-$(41). Finally, the minimum total cost per unit time is determined from the equation

$$TC = w'/f_4'. \tag{52}$$

4. Numerical Examples

Example 1

Consider the following functions:

$$P(t) = \pi_p t + \phi_p, \qquad R(t) = \pi_r t + \phi_r, \qquad D(t) = at + b,$$

where $\phi_p,\ \phi_r,\ b > 0$, and $\pi_p,\ \pi_r,\ a \geq 0$. From Equation (37), we get

$$f_4 = \frac{-\theta b + \sqrt{\theta^2 b^2 + 2\theta a Q}}{\theta a}. \tag{53}$$

From Equations (36) and (53), we get

$$f_1 = \frac{-\phi_r + \sqrt{\phi_r^2 + \pi_r \theta (a f_4^2 + 2 b f_4)}}{\pi_r}. \tag{54}$$

From Equations (34) and (54), we get

$$f_2 = \frac{-b + \sqrt{b^2 + a(\pi_r f_1^2 + 2\phi_r f_1)}}{a}. \tag{55}$$

From Equations (35), (53), and (55), we get

$$f_3 = \frac{-\phi_p + [\phi_p^2 + \pi_p \sqrt{(\pi_p - a) f_2^2 + 2(\phi_p - b) f_2 + a f_4^2 + 2 b f_4}}{\pi_p}. \tag{56}$$

Moreover, from Equation (53), we get

$$f_4' = 1/\sqrt{\theta^2 b^2 + 2\theta a Q}. \tag{57}$$

After some algebraic manipulation, Equation (42) gives

$$\begin{aligned} w = {} & k_p + k_r + k_m + s_r \left(\frac{a f_2^2}{2} + b f_2 \right) + s_p \left[\frac{a(f_4^2 - f_2^2)}{2} + b(f_4 - f_2) \right] \\ & + \left(\frac{a f_4^3}{3} + \frac{b f_4^2}{2} \right) (h_p - \theta h_r) + \left(\frac{\pi_r f_1^3}{3} + \frac{\phi_r f_1^2}{2} \right) (h_r - h_p) \\ & + \left[\frac{\pi_p (f_3^3 - f_2^3)}{3} + \frac{\phi_p (f_3^2 - f_2^2)}{2} \right] (m h_m - h_p) \\ & + h_r f_4 \left[\frac{\theta a (f_4^2 - f_1^2)}{2} + \theta b (f_4 - f_1) \right] - m h_m f_2 \left[\frac{\pi_p (f_3^2 - f_2^2)}{2} + \phi_p (f_3 - f_2) \right]. \end{aligned} \tag{58}$$

and Equation (46) gives

$$\begin{aligned} w' = {} & s_r + s_p(\theta^{-1} - 1) + h_p \left[\frac{f_4 - f_3}{\theta} + f_3 - f_1 - \frac{\pi_p f_2 + \phi_p}{a f_2 + b} (f_3 - f_2) \right] \\ & + h_r \left[f_1 + \frac{(a/2)(f_4^2 - f_1^2) + b(f_4 - f_1)}{a f_4 + b} - \frac{f_4 \theta (a f_1 + b)}{\pi_r f_1 + \phi_r} \right] \\ & + m h_m \left[\left(\theta^{-1} - 1 + \frac{\pi_p f_2 + \phi_p}{a f_2 + b} \right) (f_3 - f_2) + \frac{(a/2)(f_4^2 - f_2^2) + b(f_4 - f_2)}{a f_2 + b} \right]. \end{aligned} \tag{59}$$

Table 1: Parameter values for Example 1.

k_p	k_r	k_m	h_p	h_r	h_m	s_p	s_r
2400	1600	1200	1.6	1.2	0.8	2	1.2

π_p	ϕ_p	π_r	ϕ_r	a	b	θ	m
30	1250	50	2000	30	1000	0.8	1

Then the solution to the problem is found by equating the RHS of Equation (58) with the RHS of Equation (47) and then solving for Q.

We illustrate the solution procedure with a numerical example that uses the parameter values in Table 1. The best return quantity, Q^*, is computed to be 2396 units. Q^* units of used items are repaired over the repair uptime period $(0, 1.1807)$, and fully consumed by time $T_2 = 2.3157$. The best production quantity is $Q_p^* = 599$, which is produced over the production uptime period $(2.3157, 2.7674)$, and fully consumed by time $T_4 = 2.8715$. The best total cost per unit time is $TC^* = \$4914$.

Example 2

Consider the following functions:

$$P(t) = \phi_p \exp(\pi_p t), \qquad R(t) = \phi_r \exp(\pi_r t), \qquad D(t) = b \exp(at),$$

where $\phi_p,\ \phi_r,\ b > 0$, and $\pi_p,\ \pi_r,\ a \geq 0$. From Equation (37), we get

$$f_4 = \frac{1}{a} \ln \left(\frac{aQ}{b\theta} + 1 \right). \tag{60}$$

From Equations (36) and (60), we get

$$f_1 = \frac{1}{\pi_r} \ln \left[\frac{b\theta\pi_r}{a\phi_r} (\exp(af_4) - 1) + 1 \right]. \tag{61}$$

From Equations (34) and (61), we get

$$f_2 = \frac{1}{a} \ln \left[\frac{a\phi_r}{b\pi_r} (\exp(\pi_r f_1) - 1) + 1 \right]. \tag{62}$$

From Equations (35), (60), and (62), we get

$$f_3 = \frac{1}{\pi_p} \ln \left\{ \frac{b\pi_p}{a\phi_p} [\exp(af_4) - \exp(af_2)] + \exp(\pi_p f_2) \right\}. \tag{63}$$

Moreover, from Equation (60), we get

$$f_4' = \frac{1}{a} \left[\frac{a/(b\theta)}{(aQ)/(b\theta) + 1} \right] = \frac{1}{aQ + b\theta}. \tag{64}$$

After some algebraic manipulation, Equation (42) gives

$$\begin{aligned} w = {} & k_p + k_r + k_m + \frac{s_r b}{a}[\exp(af_2) - 1] + \frac{s_p b}{a}[\exp(af_4) - \exp(af_2)] \\ & + \frac{(h_p - \theta h_r)b}{a^2}[\exp(af_4)(af_4 - 1) + 1] + \frac{(h_r - h_p)\phi_r}{\pi_r^2}[\exp(\pi_r f_1)(\pi_r f_1 - 1) + 1] \\ & \frac{(mh_m - h_p)\phi_p}{\pi_p^2}[\exp(\pi_p f_3)(\pi_p f_3 - 1) - \exp(\pi_p f_2)(\pi_p f_2 - 1)] \\ & + \frac{h_r \theta b f_4}{a}[\exp(af_4) - \exp(af_1)] - \frac{mh_m \phi_p f_2}{\pi_p}[\exp(\pi_p f_3) - \exp(\pi_p f_2)], \end{aligned} \tag{65}$$

and Equation (46) gives us

$$\begin{aligned} w' = {} & s_r + s_p(\theta^{-1} - 1) + h_p \left[\frac{f_4 - f_3}{\theta} + f_3 - f_1 - \frac{\phi_p}{b} \exp((\pi_p f_2 - af_2)(f_3 - f_2) \right] \\ & + h_r \left[f_1 + \frac{1 - \exp(af_1 - af_4)}{a} - \frac{b\theta}{\phi_r} \exp(af_1 - \pi_r f_1) f_4 \right] \\ & + mh_m \left[\left(\theta^{-1} - 1 + \frac{\phi_p}{b} \exp(\pi_p f_2 - af_2) \right) (f_3 - f_2) + \frac{1 - \exp(af_4 - af_2)}{a} \right]. \end{aligned} \tag{66}$$

Then the solution to the given problem is found by equating the RHS of Equation (65) with the RHS of Equation (47) and then solving for Q.

For this example, we use the parameter values from Example 1 as well, with the exception that $\phi_p = 100$, $\pi_p = 0.05$, $\phi_r = 80$, $\pi_r = 0.015$, $b = 60$, and $a = 0.01$. The best return quantity, Q^*, is computed to be 723.58 units. Q^* units of used items are repaired over the repair uptime period $(0, 8.4816)$, and fully consumed by time $T_2 = 11.3862$. The best production quantity is $Q_p^* = 180.90$, which is produced over the production uptime period $(11.3862, 12.3845)$, and fully consumed by time $T_4 = 14.0411$. The best total cost per unit time is $TC^* = \$783.43$.

5. The Global Optimality of the Solution

The goal of this section is to give conditions that guarantee that the solution to the given problem, if it exists, is unique and global optimal. From Equations (34)−(36), $f_1 = 0$ implies that $f_2 = f_3 = f_4 = 0$, since $D(t) > 0$, $0 \leq \theta \leq 1$, $P(t) > D(t)$, and $R(t) > D(t)$. In addition, $f_1 > 0$ implies that $f_1 < f_2 < f_3 < f_4$. Thus Inequality (33) is implied from Equations (34)−(36).

Let the LHS of Equation (45) be expressed as the function

$$L(Q) = f_4 w' - w f_4'. \tag{67}$$

From Equation (37), since $Q = 0$ implies that $f_4 = 0$, we get

$$L(0) = -w f_4' < 0,$$

since $w, f_4' > 0$. Thus Equation (45) has solution(s) if $L(Q) = 0$ for some $Q > 0$.

The uniqueness of the solution to problem can be guaranteed if $L(Q)$ is an increasing function of Q, or

$$L'(Q) > 0. \tag{68}$$

To illuminate, suppose that $Q_1 > 0$ and $Q_2 > 0$ are two solutions to the problem, with $Q_1 < Q_2$. Then $L(Q_1) = 0$ and $L(Q_2) = 0$. If $L(Q)$ is a continuous and differentiable function of Q, then from Rolle's Theorem, there exists a number $c > 0$ such that $L'(c) = 0$. Since this is impossible because $L'(Q) > 0$ for all $Q > 0$, then our supposition is wrong, and thus, the solution to the problem, if it exists, is unique.

From Equations (45) and (67), we get

$$\frac{d(TC)^2}{d^2Q} = \frac{L'(Q)f_4 - 2L(Q)f_4'}{f_4^3}. \tag{69}$$

The global optimality of the solution to the problem can be guaranteed if the condition $d(TC)^2/d^2Q > 0$ is satisfied, which in turn, is guaranteed by $L'(Q) > 0$. This is because if the solution to Equation (45), say Q^*, gives $L(Q^*) = 0$, then the value of $d(TC)^2/d^2Q$ is $L'(Q^*)/f_4^2$, which is positive when $L'(Q^*)$ is positive.

Now we give the conditions under which $L'(Q) > 0$ can be obtained. Let $f_i'' = d^2f_i/dQ^2$, $D_i = D(f_i)$, $R_i = R(f_i)$, $P_i = P(f_i)$, $D_i' = dD(f_i)/dQ$, $R_i' = dR(f_i)/dQ$, and $P_i' = dP(f_i)/dQ$ $(i = 1, 2, 3, 4)$. From Equation (51), we obtain

$$f_4'' = -\frac{D_4}{\theta D_4^2}. \tag{70}$$

Let $w'' = d^2w/dQ^2$. Differentiating Equation (46) with respect to Q, and using Equations (51)−(50), we obtain

$$\begin{aligned} w'' = {} & (mh_m - h_p)\left[\frac{(P_2'D_2 - P_2D_2')(f_3 - f_2)}{D_2^2} + \left(\frac{1}{\theta} - 1 + \frac{P_2}{D_2}\right)\frac{1}{P_3}\right] \\ & + h_p\left[\frac{1}{\theta^2 D_4} + \frac{P_2}{D_2^2} - \frac{1}{R_1}\right] \\ & + h_r\left[\frac{1}{\theta D_4} + \frac{1}{R_1}\left(1 - \frac{2D_1}{D_4} - f_4\theta D_1'\right) + \frac{f_4\theta R_1' D_1}{R_1} - \frac{D_4'}{D_4^2}\int_{f_1}^{f_4} D(u)\ du\right] \\ & + mh_m\left[\frac{D_2'}{D_2^2}\int_{f_2}^{f_4} D(u)\ du - \left(\frac{1}{\theta} - 1 + \frac{P_2}{D_2}\right)\frac{1}{P_2}\right]. \end{aligned} \tag{71}$$

Differentiating $L(Q)$ from Equation (67) with respect to Q gives us

$$L'(Q) = w''f_4 - f_4''w, \tag{72}$$

The conditions under which $L'(Q) > 0$ are complicated, but let us distinguish two cases: (1) $f_4'' \leq 0$, and (2) $f_4'' > 0$.

Case 1. $f_4'' \leq 0$. Suppose that $w'' > 0$. Then the optimality condition $L'(Q) = w''f_4 - f_4''w > 0$ holds, which guarantees the existence and uniqueness of the solution to Equation (45). Conversely, let $w'' \leq 0$ and recall that $L(0) < 0$. Then we have two possibilities:

1. $w''f_4 - f_4''w \leq 0$, which happens when $|w''f_4|$ dominates $|f_4''w|$. Then $L(Q)$ is a non-increasing function of Q, and hence $L(Q) < 0$ for $Q > 0$. Thus Equation (45) is infeasible, in which case the problem has no solution.

2. $w''f_4 - f_4''w > 0$, which happens when $|f_4''w|$ dominates $|w''f_4|$. Then $L(Q)$ is an increasing function of Q, and hence $L(Q) \geq 0$ for $Q > 0$. Thus Equation (45) has a unique solution, in which case the problem has a unique global optimal solution.

Case 2. $f_4'' > 0$. A declining demand function $D(t)$, where $D'(t) < 0$, and consequently, $f_4'' > 0$, demonstrates the application of the theoretical assumption $f_4'' > 0$. We also have two possibilities:

1. $w'' f_4 - f_4'' w \leq 0$, which happens when $w'' < 0$ or $|f_4'' w|$ dominates $|w'' f_4|$. Then $L(Q)$ is a non-increasing function of Q, and hence $L(Q) < 0$ for $Q > 0$. Thus Equation (45) is infeasible, in which case the problem has no solution.

2. $w'' f_4 - f_4'' w > 0$, which happens when $w'' > 0$ and $|w'' f_4|$ dominates $|f_4'' w|$. Then $L(Q)$ is an increasing function of Q, and hence $L(Q) \geq 0$ for $Q > 0$. Thus Equation (45) has a unique solution, in which case the problem has a unique global optimal solution.

Finally, we propose the theorems that describe the uniqueness and global optimality of the solution to the given problem.

Theorem 1. *If a solution to the given problem exists and if Condition* (68) *is satisfied, then the solution is unique.*

Proof. The solution to the problem must satisfy Equation (45). Let $L(Q)$ be the LHS of Equation (45). Thus any solution to Equation (45) must satisfy $L(Q) = 0$. Since $L(0) < 0$, if $L'(Q) > 0$ for $Q > 0$ (Condition (68)), then $L(Q) = 0$ will occur once, if it occurs at all, with the corresponding Q being positive.

Theorem 2. *If a solution to the given problem exists and if Condition* (68) *is satisfied, then the solution is a global minimum solution.*

Proof. Suppose that $Q^* > 0$ is a solution to the problem. The global minimum condition to the problem is $d^2(TC)/dQ^2 > 0$ at $Q = Q^*$. From Equation (69),

$$\frac{d^2(TC)}{dQ^2} = \frac{L'(Q) f_4 - 2L(Q) f_4'}{f_4^3}.$$

Hence if $L'(Q) > 0$ for $Q > 0$ (Condition (68)), then at $Q = Q^*$,

$$\frac{d^2(TC)}{dQ^2} = \frac{L'(Q^*)}{f_4^2} > 0,$$

because $L(Q^*) = 0$.

6. Conclusion

In this paper, an integrated inventory model of production and repair is proposed. This model considers three types of inventories: returned items, serviceable items, and raw material. The returned items are repaired to a quality level that is indistinguishable from newly produced items. The demand rate, repair rate, and production rate are assumed to be known and continuous functions of time. Shortages are not considered. Throughout the planning horizon, one production setup alternates with one repair setup. A joint total cost per unit time function is derived, using the repair batch size Q as the decision variable. An analytical solution procedure is proposed, which is illustrated using two numerical examples. Finally, conditions that guarantee the uniqueness and global optimality of the solution are given. One possible extension of this work is to generalize the model further by considering the case where deterioration and shortages occur.

References

Alamri, A.A., 2011. Theory and methodology on the global optimal solution to a General Reverse Logistics Inventory Model for deteriorating items and time-varying rates. *Computers & Industrial Engineering*, 60(2), pp. 236−247.

Dobos, I., Richter, K., 2000. The integer EOQ repair and waste disposal model - further analysis. *Central European Journal of Operations Research*, 8(2), pp. 173-194.

Dobos, I., Richter, K., 2003. A production/recycling model with stationary demand and return rates. *Central European Journal of Operations Research*, 11(1), pp. 35-46.

Dobos, I., Richter, K., 2004. An extended production/recycling model with stationary demand and return rates. *International Journal of Production Economics*, 90(3), pp. 311-323.

Fleischmann, M., Bloemhof-Ruwaard, J.M., Dekker, R., van der Laan, R., van Nunen, J.A., van Wassenhove, L.N., 1997. Quantitative models for reverse logistics: A review. *European Journal of Operational Research*, 103(1), pp. 1-17.

Harris, F.W., 1913. How many parts to make at once. *Factory, The Magazine of Management*, 10(2), pp. 135-136, & 152.

Koh, S.G., Hwang, H., Sohn, K.I., Ko, C.S., 2002. An optimal ordering and recovery policy for reuseable items. *Computers & Industrial Engineering*, 43(1-2), pp. 59-73.

Konstantaras, I., Papachristos, S., 2008a. Note on: An optimal ordering and recovery policy for reusable items. *Computers & Industrial Engineering*, 55(3), pp. 729-734.

Konstantaras, I., Papachristos, S., 2008b. A note on: Developing an exact solution for an inventory system with product recovery. *International Journal of Production Economics*, 111(2), pp. 707-712.

Mabini, M.C., Pintelon, L.M., Gelders, L.F., 1992. EOQ type formulations for controlling repairable inventories. *International Journal of Production Economics*, 28(1), pp. 21-33.

Nahmias, N., Rivera, H., 1979. A deterministic model for repairable item inventory system with a finite repair rate. *International Journal of Production Research*, 17(3), pp. 215-221.

Richter, K., 1996a. The EOQ repair and waste disposal model with variable setup numbers. *European Journal of Operational Research*, 95(2), pp. 313-324.

Richter, K., 1996b. The extended EOQ repair and waste disposal model. *International Journal of Production Economics*, 45(1-3), pp. 443-448.

Richter, K., Dobos, I., 1999. Analysis of the EOQ repair and waste disposal model with integer setup numbers. *International Journal of Production Economics*, 59(1-3), pp. 463-467.

Schrady, D.A., 1967. A deterministic inventory model for repairable items. *Naval Research Logistics Quarterly*, 14(3), pp. 391-398.

Spengler, T., Püchert, H., Penkuhn, T., Rentz, O., 1997. Environmental integrated production and recycling management. *European Journal of Operational Research*, 97(2), pp. 308-326.

Teunter, R.H., 2001. Economic ordering quantities for recoverable item inventory systems. *Naval Research Logistics*, 48(6), pp. 484-495.

Teunter, R.H., 2004. Lot-sizing for inventory systems with product recovery. *Computers & Industrial Engineering*, 46(3), pp. 431-441.

Wee, H.M., Widyadana, G.A., 2010. Revisiting lot sizing for an inventory system with product recovery. *Computers & Mathematics with Applications*, 59(8), pp. 2933-2939.

Examining the Influencing Factors of Choosing Business Programme (UTAR Kampar Students): Application of Bayesian Network

Song Poh Choo[a], Chee Yen Nee[b]

[a]*Department of Physical and Mathematical Sciences, Faculty of Science, Universiti Tunku Abdul Rahman, Malaysia. [*]Email (corresponding author): songpc@utar.edu.my*

[b]*Graduated student (BSc (Hons) Statistical Computing and Operations Research), Faculty of Science, Universiti Tunku Abdul Rahman, Malaysia.*

Abstract

Business studies remain the most popular degrees regardless of whether the universities being considered are public or private. The purpose of this paper is to examine the factors that affect UTAR Kampar students' decision in choosing business programmes by using Bayesian network. Questionnaires are distributed to students who enrolled in the Faculty of Business and Finance at UTAR. Bayesian network is a directed acyclic graph which belongs to the probabilistic graphical model where it is used for reasoning under uncertainty. Each node in the graph represents a random variable whereas the arcs represent dependencies between variables. Bayesian network is considered as a representation of a joint probability distribution based on conditional probabilities. Therefore, this study aims to identify the factors influencing students' decision in choosing business programmes for tertiary education with Bayesian network.

1. Introduction

Universiti Tunku Abdul Rahman (UTAR) is a private university in Malaysia. It was established under a non-profit organization called UTAR Education Foundation in 2002. UTAR has two campuses, one located in Bandar Sungai Long, Selangor and the other one in Kampar, Perak. UTAR currently offers more than 110 programmes at foundation, undergraduate and postgraduate level. All programmes offered by UTAR are qualified by the Ministry of Education (MOE) and Malaysian Qualifications Agency (MQA). There are six faculties in UTAR Kampar campus which are Faculty of Arts and Social Science (FAS), Faculty of Business and Finance (FBF), Faculty of Engineering and Green Technology (FEGT), Faculty of Information and Communication Technology (FICT), Faculty of Science (FSc) and the Institute of Chinese Studies (ICS). FBF was launched in June 2008 for the Kampar campus. It can be considered as the biggest faculty in UTAR Kampar based on the number of enrolled students in this faculty. The number of undergraduate students who choose an undergraduate degree in business has gradually increased over the past couple of years. As of 2018/2019, 10,000 undergraduate students were enrolled in this faculty. This raises the question of why do students consider pursuing an undergraduate degree in business at UTAR Kampar? What are the factors that influence students' decision in getting an undergraduate degree in business at UTAR Kampar?

2. Literature Review

Previous studies have highlighted several factors that are likely to impact students' intention to enroll in business programmes (Malgwi, 2005; DeMarie &Young, 2003; Lowe & Simons, 1997). These factors include financial factors, personal interest, career opportunities, influence of parents or friends, and ability to gain transferable skills.

Financial factors is one of the important aspects to be considered in determining the choice for programmes in Malaysia since education cost has increased around the world (Wagner, 2009). Students who are facing financial struggles may not be able to afford the programme fees because the total programme fees

which the students are required to pay are too high. Therefore, students who are in financial need should seek for financial support to finance their studies in the university. There are a few sources of financial assistance available for students to cover both their programme and accommodation fees. Students receive the largest source of financial help from their parents to pay for university. Parents' capability to support their children's undergraduate studies depends on parents' education level and occupation (Nguyen & Taylor, 2003).

Another source of financial aid comes from government loans and scholarships. Government loan is a type of financial assistance that requires repayment of loan after graduation whereas scholarships are financial aid that does not require its recipient to repay for the award. Generally, scholarships are granted to students who demonstrate a high level of achievement (Joseph, 2003). Another source of funding for students is most likely to come from a part-time job. It is a good alternative for students to make money that can be used to cover their study and living costs. Students would usually look for part-time jobs that could fit into their schedules. It could be an hourly paid part-time job, a half day job or the weekend jobs. Most of the students prefer to work part-time during semester breaks at their hometown to make extra money.

Personal interest may be the most significant factor that affects the choice of programme (Kim et al, 2002; Kaur & Ei Leen, 2008). Personal interest is a key motivating factor for students to study hard and focus on their studies. Mustapha & Long (2010) revealed that students having a genuine interest in their degree would be more engaged, which leads to better performance. Otherwise, students would not be able to do well if they are not interested in their chosen programme.

Many studies have emphasized that majority of the students were influenced by their family and friends. Influence of parents and friends would eventually affect their choice of programme. Students' choice of undergraduate major primarily rely on advice from family and friends (Angela et al, 2010). According to Ceja (2006), the support and guidance from family can be divided into three groups, which are parents, family members and siblings. Younger siblings are more likely to follow older siblings when it comes to programme selection.

In addition, parents' occupation and education level would influence students' choice of programme as well (Looker & Lowe, 2001; Othman, 2006). Some of the students would choose business studies so as to follow in their parents' footsteps due to family-owned bsuinesses or their parents are currently working in the business industry (Simpson, 2001). According to Mauldin et al. (2000), lecturers, supervisors, advisors or mentors all play a fundamental role in students' choice of undergraduate programmes.

According to Simons et al. (2003), it has been found that future career opportunities is the most significant factor that influences the selection of business programme. Kim et al. (2002) also revealed that career opportunity is one of the dominant factors influencing programme choices of students. The selection of programmes would be affected by future career opportunities as students would usually start to plan for the career in their future. There are many career opportunities for business majors such as accounting, human resource, management, marketing, education, and banking and finance. Uyar et al. (2011) mentioned that students choose business programme as they feel that it provides a better or more job opportunity.

Students are able to develop a broad range of transferable skills through business programme. These transferable skills include interpersonal communication skills, decision making, problem solving, time management, and analytical thinking skills. Transferable skills are skills that students might need for future jobs and also skills which employers would value. As a result, students who enrolled in business studies could make use of the knowledge they have gained and the transferable skills which have been developed at university could also be put to use after graduation.

2.1. Bayesian Network

Bayesian network (BN) is also known as belief network or causal network. It is one of the classes of the probabilistic graphical models which provides a probabilistic graphical model that represents the probabilistic dependencies among a set of random variables via a directed acyclic graph (DAG). The structure $G = (V, A)$ of a DAG consists of nodes (V) and directed arcs (A). Graphically, the nodes represent random variables and are drawn as circles labelled by variable names. The directed arcs specify dependencies among

random variables and are represented by arrows between nodes. The joint probability distribution for a complete network can be written as:

$$P(x_1,\ldots,x_n)=\prod_{i=1}^{n}P(x_i \mid pa_i)$$

where pa_i is the parents of variable x_i.

Bayesian network learning involves the learning of structures (structural learning) and the estimation of the conditional probabilities (parameter learning). Structural learning is the qualitative part of the model in which it provides a graphical representation to describe the dependencies among the variables. Parameter learning is the quantitative part of the model where it provides conditional probability tables based on the graphical structure obtained. Scutari (2010) stated that there are two different algorithms in structural learning, i.e. score-based algorithm and constraint-based algorithm.

Constraint-based algorithm learns the structure of the network by analyzing the independence relations based on Markov property of BN. According to Verma and Pearl (1991), two DAGs are equivalent if they have the same skeleton and v-structures. The skeleton of a DAG is the undirected graph that disregards the edge direction whereas the v-structure is an ordered triplet of nodes. In Figure 1, it shows the v-structure in a DAG.

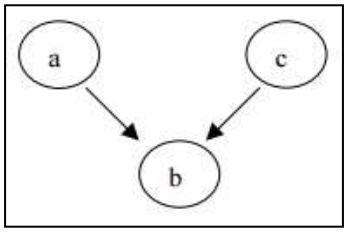

Figure 1: v-structure.

Hill-climbing (HC) and Tabu (TABU) greedy search are the examples of score-based algorithm. HC algorithm is the most popular algorithm as it has a good trade-off between computational demands and the quality of the models learned (Gámez, Mateo and Puerta, 2010). Although heuristic search does not always guarantee to provide the optimal or best result, it can generate good or acceptable results which are proven to be computationally efficient. There are several types of scoring functions in BN to estimate the fitness of network such as log-likelihood (loglik), Akaike information criterion (AIC), Bayesian information criterion (BIC), K2, Bayesian Dirichlet (BD) and its variants BDe and BDeu.

A simple scoring function, Score (*G*, *D*) for the learning of BN structure is given as follows:

$$\text{Score}(G, D) = \sum_{i=1}^{m} S(D_i, D_{G_i})$$

where *G* is the DAG and *D* refers to the data set.

The scoring functions are used to find a balance between the complexity and fitness of model in order to avoid overfitting. It is given as follows:

$$\text{Score}(G, D) = \log \hat{P}(D \mid G) - \Delta(D, G)$$

where $\hat{P}(D \mid G)$ is the conditional probability of data given the DAG and $\Delta(D, G)$ represents the complexity penalty.

Bayesian Information Criterion (BIC) is one of the commonly used scoring functions for the learning of BN structure. BIC score is expressed as a log-likelihood function of variables X_i:

$$\text{BIC} = \log L(X_1, \ldots, X_v) - \Delta_i^{BIC}.$$

The penalized score for BIC, Δ_i^{BIC} is expressed as:

$$\Delta_i = \frac{q_i(r_i - 1)}{2} \ln N ,$$

where
r_i is the number of states of the variable X_i,
q_i is the number of possible configuration of the parents set of variable X_i, and
N is the total number of instances of variable X_i takes its k-th value and its parents take their j-th configuration in the dataset D.

2.2. Learning BN from Data

Table 1 shows the four different cases of BN learning problems (Ben-Gal, 2007; Cao, 2014). As for the first case, it is the simplest and most popular learning in BN. The purpose of this learning is to obtain a value for the parameter θ that maximizes the likelihood of the data set D. Let data set $D = \{d[1], \ldots, d[M]\}$ of M instances. The MLE function is given below:

$$L(\theta : D) = P(D|\theta) = \prod_{m=1}^{M} P(d[m] \mid \theta) .$$

The most frequently used of conjugate prior distribution in compensate the zero occurrences in the data set D is the Dirichlet prior.

Table 1: Four different cases in learning BN(Ben-Gal, 2007).

Case	BN structure	Data observability	Proposed learning method
1	Known	Full	Maximum-likelihood estimation (MLE)
2	Known	Partial	Gradient ascent , Expectation maximization (EM)
3	Unknown	Full	Search through model space
4	Unknown	Partial	Structural EM

Consider the second case, there are two learning methods which are gradient ascent and expectation maximization (EM). Gradient ascent retains a set of parameters and computes the gradient in a parameter space. The parameters for maximum-likelihood will then change by a small amount in the direction of the gradient. EM is a method that can be used to compute an optimal maximum-likelihood estimate for a parameter.

The third case refers to the greedy search method where it obtains the best result by selecting parent nodes for all variable nodes. In such case, the two structural learning algorithms used within the context of BN are constraint-based algorithm and score based algorithm. This is being emphasized in this study as it aims to determine the network structure based on the collection of complete data.

The fourth case is the hardest case to be resolved among all other cases. The proposed learning method used in this case is named as structural EM method. It is an iterative algorithm that combines with the EM algorithm. The goal of this method is to maximize the score in order to construct the best scoring network.

3. Methodology and Data

The questionnaire is the research instrument employed to collect data from respondents. It is designed based on the factor influencing students' selection of a business programme. The questionnaire is divided into two sections with Part A having questions related to the demographic profile of the respondents. The demographic information include gender, age, programme, year of study, parents' highest education level, and parents' occupation. Part B comprises questions relating to the main factors that influence respondents to choose business programme such as high graduate employment rate, career opportunity, personal interest, high salary payment, influence of parents or friends, gain transferable skills, family business, financial support, and

difficulty of programme. The data were collected from students who enrolled in the FBF at UTAR Kampar Campus. A total of 168 samples were gathered through the distribution of questionnaires. All the 12 variables are in discrete form and comprise only categorical value. Table 2 shows the descriptive statistics of the respondent's demographic profile based on gender and the programmes being selected.Table 3 shows the description of variables.

Table 2: Demographic profile of respondents.

Demographic	Category	Number	Percentage (%)
Gender	Male	67	39.9
	Female	101	60.1
Programme	Accounting	29	17.3
	Business Administration	18	10.7
	Banking & Finance	25	14.9
	Entrepreneurship	16	9.5
	Marketing	26	15.5
	Financial Economics	30	17.9
	Finance	24	14.3

Table 3: Description of variables.

Variable	Possible value	Description
Father_occ	4	Father's occupation: employed in public-sector, employed in private-sector, self-employed, and retirement
Mother_occ	5	Mother's occupation: employed in public-sector, employed in private-sector, self-employed, housewife, and retirement
Employment_rate	2	Graduate employment rate is high: yes or no
Career_opp	2	Career opportunity: yes or no
Interest	2	Personal interest: yes or no
Salary	2	High salary: yes or no
Influence	2	Influence of parents or friends: yes or no
Skills	2	Able to gain transferable skills: yes or no
Family_business	2	Parents run their own business: yes or no
Financial	2	Financial support: yes or no
Difficulty	2	Is the business programme difficult?: yes or no
Business Programme	2	Is the business programme useful?: yes or no

4. Results

Figure 2 shows the network structure obtained from HC algorithm. There are 13 arcs in total. Based on the network above, it shows that students whose parents run their own family business will influence their father's occupation, and mother's occupation. This is because students' parents may be following in their parents' footsteps to succeed in a family-owned business. In addition to that, family-owned business will also influence the ability of the parents to provide financial support to their adult children. This is due to the fact that students' parents who run their own business are financially secure to support their costs of going to the university. Growing up in an environment of a family business influences students' perception towards the difficulty of a business programe. Owing to the fact that they are exposed to the business from an early age, it assists the students to have a better understanding of the business programme which makes learning easier.

Moreover, it has been found that influence of family and friends is affected by graduate employment rate. This is due to the fact that family and friends may influence students' decision in choosing a business programme as they perceive that business graduates would have higher rates of employment. On top of that, career opportunity is influenced by graduate employment rate. Students might select a programme based on

their future career where the selected programme is believed to have a high graduate employment rate. Family business is somewhat related to graduate employment rate because they might work with their parents after graduation.

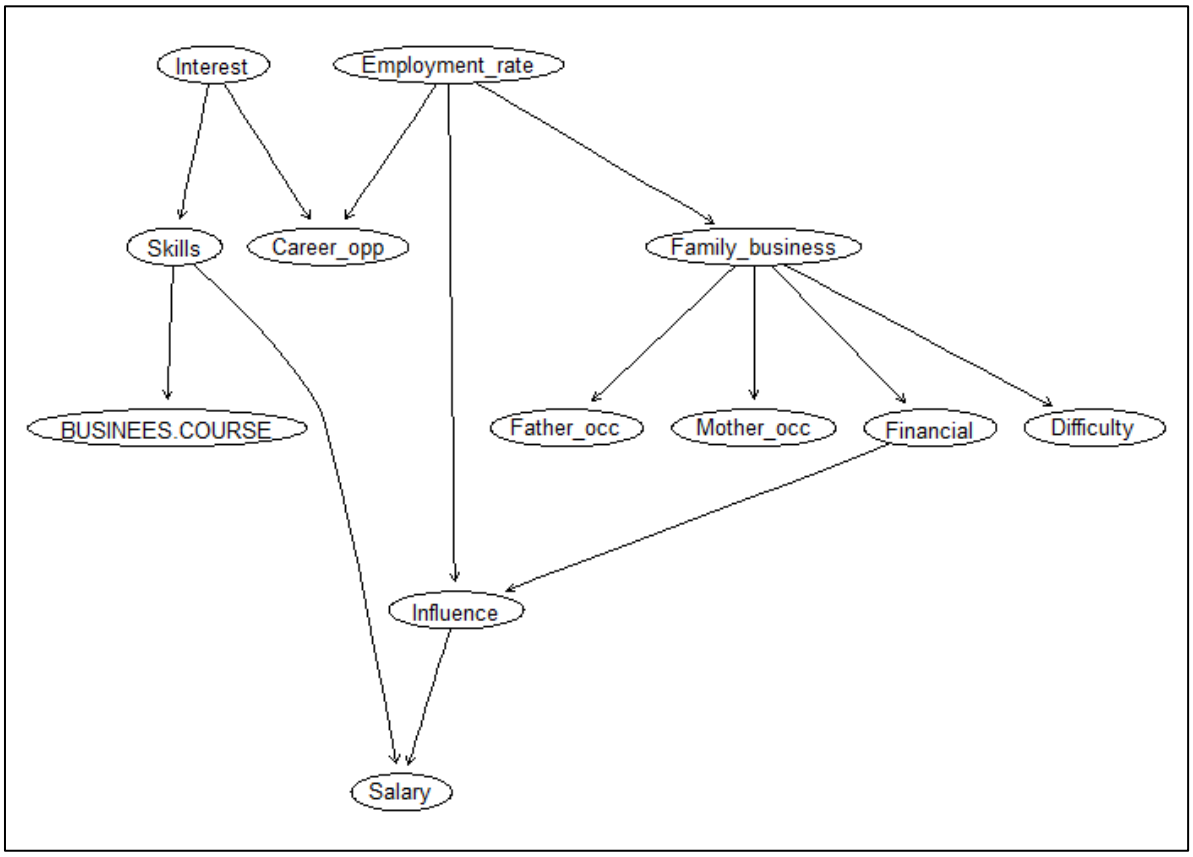

Figure 2: Hill-climbing algorithm.

Besides, personal interest powerfully drives knowledge and skill acquisition of the business education students. Students are genuinely interested in the business programme primarily due to the fact that they are able to gain transferable skills through the business programme. Aside from that, student's personal interest will impact on their choice of careers. The reason for this is that students discover their interest in business programme as they wanted to explore careers related to a business degree. Furthermore, there could be a direct relationship between salary and the skills possesed by a business graduate. Higher level of skills would contribute toward higher earnings. Skills gained has a direct impact on students's decision in choosing a business programme. Students are able to develop a broad range of transferable skills which are assured to be in high demand in the job market if they decide to take up a business major.

5. Conclusions

In this study, a questionnaire was designed and adopted as a tool for data collection. Data were collected from students who enrolled in the FBF at UTAR Kampar Campus. The questionnaire is tailored to identify factors affecting students' choice for business programme. The software used in this research for the construction of network is `R` studio. The `R` packages that have been used in this study is `bnlearn`. In addition to that, `Rgraphviz` has also been used where it yields larger graphs with better layouts. The algorithm that has been used to construct the structure of the network is Hill-climbing algorithm. The Bayesian network is made of 13 arcs. Based on the results obtained from the network, skills has a direct influence on students' decision in choosing business programme. Students decided to take up a business programme because they are able to gain transferable skills through business programmes.

References

Angela, W., Travis, W. and Courtney, M., 2010. Influences on a College Student's Major: A Development Perspective. *Journal for the Liberal Arts and Sciences*, 14(2), pp. 25-46.

Ben-Gal, I., 2007. Bayesian networks. In: F. Ruggeri, F. Faltin and R. Kenett, eds. *Encyclopedia of Statistics in Quality & Reliability*. Chichester UK: John Wiley and Sons.

Cao, Y., 2014. Study of four types of learning Bayesian networks cases. *Applied Mathematics & Information Sciences: An International Journal*, 8(1), pp.379-386.

Ceja, M., 2006. Understanding the role of parents and siblings as information sources in the college choice process of Chicana students. *Journal of College Student Development*, 47(1), pp. 78-104.

DeMarie, D. and Aloise-Young, P., 2003. College students' interest in their major. *College Student Journal*, 37, pp. 462-470.

Gámez, J., Mateo, J. and Puerta, J., 2010. Learning Bayesian networks by hill climbing: efficient methods based on progressive restriction of the neighborhood. *Data Mining and Knowledge Discovery*, 22(1), pp.106-148.

Joseph, F.B., 2013. Factors influencing the selection of business studies: A comparative study of Indian students at an Indian University and Chinese students at a Thai University. *AU-GSB E-Journal*, 6(1), pp. 32-43.

Kaur, M. and Ei Leem, Y., 2008. Factors influencing undergraduate's choice of Business Major. INTI International University College, Persiaran Perdana, Putra Nilai, 71800 Nilai, Negeri Sembilan.

Kim, D., Markham, F. and Cangelosi, J., 2002. Why students pursue the business degree: A comparison of business majors across universities. *Journal of Education for Business*, 78, pp. 28-32.

Looker, E. D. and Lowe, G. S., 2001. *Postsecondary access and student financial aid in Canada: Current* knowledge and research gaps [Online]. Available at: https://qspace.library.queensu.ca/bitstream/handle/1974/5870/cprn-bkgnd.pdf?sequence=1&isAllowed=y [Accessed: 5 June 2019].

Lowe, D. R. and Simons, K., 1997. Factors influencing choice of business majors-some additional evidence: a research note. *Accounting Education: An International Journal*, 6, pp. 39-45.

Malgwi, C., Howe, M. and Burnaby, P., 2005. Influences on students' choice of college major. *Journal of Education for Business*, 80, pp. 275-282.

Mauldin, S., Crain, J.L. and Mounce, P.H., 2000. The Accounting Principles Instructor's Influence on Student's Decision to Major in Accounting. *Journal of Education for Business*, pp. 142-148.

Mustapha, R. and Long, N.L., 2010. *Career decision process among women in technical fields* [Online]. Available at: https://www.academia.edu/31799888/Women_in_technical_fields_Career_decision_process [Accessed: 1 June 2019].

Nguyen, A., Taylor, J. and Bradley, S., 2003. *Relative pay and job satisfaction: some new evidence* [Online]. Available at: http://mpra.ub.uni-muenchen.de/1382/ [Accessed: 1 June 2019].

Othman, F., 2006. *The relationships between family socioeconomic status and student achievement of mathematic in two schools at Johor Bahru district*. Bachelor dissertation,Universiti Teknologi Malaysia, Malaysia.

Scutari, M., 2010. Learning Bayesian networks with the bnlearn R package. *Journal of Statistical Software*, 35(3), pp. 1-22.

Simons, K., Lowe, A., Dana, R. and Stout, D.E., 2003. *Comprehensive Literature Review: Factors Influencing Choice of Accounting as a Major* [Online]. Available at: https://www.researchgate.net/profile/David_Stout5/publication/253931567_Comprehensive_Literature_Review_Factors_Influencing_Choice_Of_Accounting_As_A_Major/links/547f6b420cf2ccc7f8b920c6/Comprehensive-Literature-Review-Factors-Influencing-Choice-Of-Accounting-As-A-Major.pdf [Accessed: 1 June 2019].

Simpson, J. C., 2001. Segregated differences by subject: Racial differences in the factors influencing academic major between European Americans, Asian Americans, and African, Hispanic, and native Americans. *Journal of higher education*, 72(1), pp. 63-100.

Uyar, A., Güngörmüş, A. and Kuzey, C., 2011. Factors Affecting Students' Career Choice in Accounting: The Case of a Turkish University. *American Journal of Business Education*, 4(10), pp. 29.

Verma, TS. and Pearl, J., 1991. Equivalence and Synthesis of Causal Models. *Uncertainty in Artifical Intelligence*, 6, pp. 255-268.

Wagner, K. and Fard, P. Y., 2009. *Factors influencing Malaysian students' intention to study at a higher educational institution*. New York: E Leader.

Forecasting The Rainfall Amount In Kemaman, Terengganu, Malaysia By Using State Space Time Series Model

Yeoh Soon Chean[a], Ooi Cheau Pian[b]

[a]*Final Year Project student (BSc (Hons) Statistical Computing and Operations Research), Faculty of Science, Universiti Tunku Abdul Rahman, Malaysia. Email: soonchean96@1utar.my*

[b]*Department of Physical and Mathematical Science, Faculty of Science, Universiti Tunku Abdul Rahman, Malaysia. Email: ooicp@utar.edu.my*

Abstract

The study attempts to forecast the rainfall amount in Kemaman, the city of Terengganu, Malaysia. Flash flood was one of the severe problem faced by Terengganu. Heavy structural damage caused by flash flood to homes forced refugee to move away and destroy large pieces of property easily. Hence, a reliable tool for predicting monthly rainfall amount is needed in order to provide more details and insight in precautionary strategy of flash flood matter. This paper describes the state space model (SSM) with stochastic approach for modeling and forecasting the rainfall on monthly scales from January 2009 to May 2019 in Kemaman. The stochastic level with trend component including four explanatory variables model was identified as the best model to forecast rainfall for the next 5 years by analyzing the last 10 years data (2009-2018). The results indicate that the model is able to capture the dynamics of the monthly average rainfall data and to produce consistent and satisfactory predictions.

1. Introduction

Malaysia is a country located on the north side of the equator. However, the climate of this country is categorised as equatorial which caused this region high in temperature and humidity. Every year, Malaysia experiences heavy rainfall during the northeast monsoon (November to March) and the southwest monsoon (May to September). Generally, the rainfall amount in Peninsular receives an average of 250 cm (centimetres) and the average temperature is about 27 ℃ in the most lowland areas annually. The escalating temperature of the sea surface in the eastern and central Pacific Ocean is the result of the El Nino effect. The El Nino effect occurs in an inconsistent period from two years to seven years and it can last for half to two years. As the climate in the East coast of Peninsula Malaysia exposed to the El Nino effect, it reduced the rainfall and causes large drought in the dry season. In spite of that, it brings heavy rainfall and strong wind during the wet season. Meanwhile, the impact of the heavy rains and strong wind could cause flash floods in lowland areas with poor drainage and also bring down the trees and properties. Kemaman is located in Terengganu, one of the states in Malaysia which situated in the north-eastern of Peninsula Malaysia. Terengganu experiences tropical monsoon climate throughout the year with the regular high humidity of about 80% during the day time and warm condition. Every year, the northeast monsoon season occurs from November to March and bring heavy rainfall to all areas in Terengganu, the continuous rainfall can be extended into a pessimistic condition such as the flash floods and landslides from November to January. On 15 December 2014, 4209 people in Terengganu were forced to leave their roofs, and the rivers in Terengganu reached dangerous levels on 23 December 2014 due to the heavy rains (Abu, 2016). The paper aims to design an effective state space time series model with explanatory variables to forecast the monthly average rainfall data up to five years ahead. STAMP in OxMetrics 7 is used to model and forecast the rainfall data. The rest of the paper is organized as follows. In Section 2, some related works done by various researchers are introduced. Section 3 provides a description of the data and the development of methodology

used for rainfall predictions. In Sections 4, the analysis and discussion of the experiments conducted are presented. Lastly, the conclusions and future studies are made in Section 5.

2. Literature Review

2.1. Review of Methodology to Model the Rainfall Measurement

Zainudin, Jasim and Abu Bakar (2016) compared five data mining techniques which are Decision Tree, Neural Network, Naïve Bayes, Random Forest and Support Vector Machine in analysing monthly rainfall data in Malaysia from January 2010 to April 2014. The researchers found that relative humidity, temperature, the speed of river flow, rainfall amount and water level of the river were correlated significantly. The accuracy of the model was compared by using F-measure for which a higher F-measure indicates a higher accuracy of the model. The ability of Random Forest is to train on little data and able to predict the higher portion of data with higher F-measure made the model be the best prediction model for rainfall prediction among five data mining techniques. Hung et. al. (2008) developed six different attributes Artificial Neural Network models which used generalized feedforward type network and a hyperbolic tangent function, including meteorological parameters (relative humidity, air pressure, wet bulb temperature ,and cloudiness) in forecasting hourly rainfall data in Bangkok, Thailand. The performance of the models were tested with Efficiency Index (EI), Root Mean Square Error (RMSE) and Correlation Coefficient (R^2). The result showed that Model F which adopted a Generalized feedforward network, with tanh function including rain gauge stations which is E00, E18, E19 and E26 as training set gave the highest performance in terms of efficiency and forecasting rainfall from 1 to 6 h ahead for all 75 stations. Hernandez at. al. (2016) employed a deep learning architecture model which is composed of 2 different neural networks such as Autoencoder Network and MLP (Multilayer Perceptron Network). The time frame of the data used was covering from 2002 to 2013 and including temperature, relative humidity, barometric pressure, sun brightness, speed and direction of the wind as parameters. The architecture model was compared with few models including MLP, Naive, Feed Forward Back Propagation, Layer Recurrent, Cascaded Feed Forward Back Propagation and Ensemble Empirical Mode Decomposition (EEMD). The result showed that the proposed architecture model is the best model among other models as mentioned above.

2.2. Review of State Space Time Series Model

Asemota, Bamanga and Alaribe (2016) implemented state space time series model to examine the seasonal behaviour of monthly rainfall data from 1981 to 2013 in Maiduguri and Damaturu areas of Borno and the Yobe States respectively. In this study, the local level model with stochastic seasonal and the local level model with deterministic seasonal was employed to modeling of the dynamic feature of the rainfall data. The model was compared by the AIC and BIC index and the results showed that the local level model with deterministic seasonal provided a better fit among the models. Moreover, the local level model with deterministic seasonal can model the dynamic features of the rainfall time series in Maiduguri and Damaturu. Yusof and Kane (2012) selected the SARIMA and ETS state space model to model and forecast the rainfall amount in Malacca and Kuantan. The results showed that both models found to be adequate for predicting and forecasting the rainfall amount. However, it also can provide insight to help decision makers discover strategies for proper planning in the drainage system, agriculture and other water resource application. Ravichandran and Prajneshu (2001) compared state space modelling and ARIMA time series modelling by using the all-India marine products export data. The review of the result revealed that state space modelling technique performs better than ARIMA approach.

3. Data and Methods

Monthly average rainfall data were obtained from World Weather Online, including rain day, wind speed, humidity, cloudiness, average temperature, pressure, and sun hour to be used for factor identification. 120 rainfall data from January 2009 to December 2018 were used as a training set in this research, while another 5 rainfall data from January 2019 to May 2019 were used as a testing set. Time series plots, autocorrelation functions, model identification and diagnostic checking were generated using STAMP in OxMetrics 7, while stationary test and factor identification were generated using R time series statistical software. Figure 1 shows the flowchart of the complete process in this study.

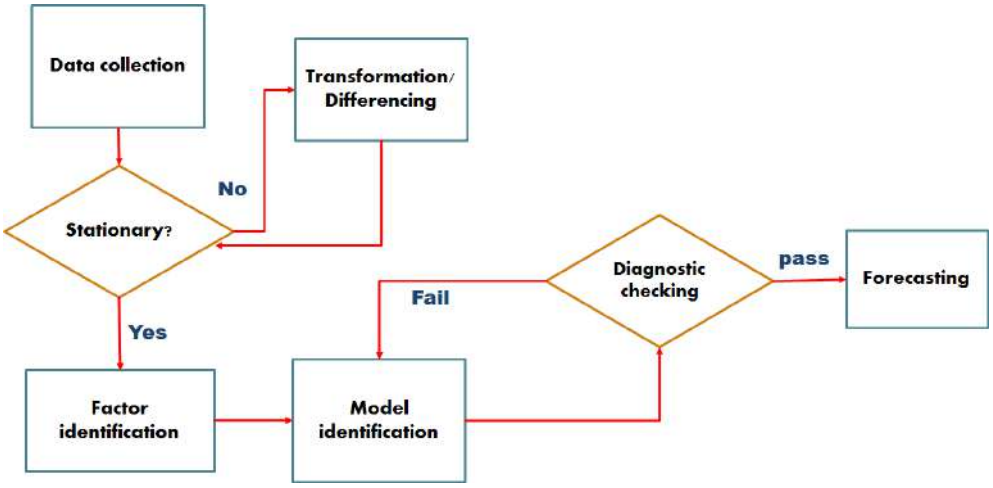

Figure 1: Basic structure of the proposed methodology.

3.1 Stationary Test

The stationarity of the data can be known by observing the Autocorrelation Function (ACF) plot and Partial Autocorrelation Function (PACF) plot. ACF and PACF can be used to estimate the direct relationship between the observations. A stable mean, variance and autocorrelation structure are said to be stationary. Other than that, stationarity of the data is also tested using Kwiatkowski–Phillips–Schmidt–Shin (KPSS) test. The null hypothesis for the test is that the data is stationary while the alternative hypothesis for the test is that the data is not stationary.

3.2 Transformation/Differencing of Data

Transformation and differencing of data are only needed when the data failed to fulfill the stationary test. Differencing can be used to reduce a homogeneous nonstationary time series to stationary. However, many of non-stationary of the time series are caused by the time-dependent variance and autocovariances but not time-dependent means. In order to reduce these types of problems, transformation is needed instead of differencing. On the other hand, if the non-stationary is caused by time-dependent means, transformation and differencing are needed to achieve stationary time series. The transformation method used in this research is power transformation introduce by Box and Cox in year 1964. Not to mention, a variance and autocovariances stabilizing transformation should be performed before differencing.

3.3 Factor Identification

The independent variables with very high inter-association are known as multicollinearity might occur in certain cases. It can be considered as a disturbance in the data and caused the model and inferences not reliable. In order to detect the intercorrelation between the independent variables in this research, the correlation matrix plot is needed to observe the correlation between the independent variables. If the

intercorrelation problem exists, backward stepwise regression will be performed to eliminate the unnecessary independent variables.

3.4 Model Identification

3.4.1 Local Level Model

The local level model or random walk-plus-noise model is a simple form of a linear Gaussian state space model. The local level model equation is shown below:

$$\begin{aligned} y_t &= \mu_t + \varepsilon_t & \varepsilon_t &\sim NID(0, \sigma_\varepsilon^2) \\ \mu_{t+1} &= \mu_t + \xi_t & \xi_t &\sim NID(0, \sigma_\xi^2) \end{aligned} \tag{1}$$

The first equation is observation equation and the second one is state equation at time *t*. The observation equation is the combination of random walk μ_t, and irregular component ε_t also known as noise at time t. Furthermore, the state equation shows how the random walk μ_{t+1}, at time $t+1$ vary with previous random walk μ_t, at time t where affect by the ξ_t, the level disturbance. The noise and the level disturbance are independent and normally distributed with mean of zero and variance of disturbance σ_ε^2 and σ_ξ^2 respectively.

3.4.2 Local Linear Trend Model

Slope component can be included in the local level model if the trend is observed from the time series data and it is called local linear trend model. The slope component is considered as the angle of the trend line and it act as the regression coefficient but the slope component in state space model is allowed to vary in time whereby regression coefficient is fixed in regression model.

$$\begin{aligned} y_t &= \mu_t + \varepsilon_t & \varepsilon_t &\sim NID(0, \sigma_\varepsilon^2) \\ \mu_{t+1} &= \mu_t + \nu_t + \xi_t & \xi_t &\sim NID(0, \sigma_\xi^2) \\ \nu_{t+1} &= \nu_t + \zeta_t & \zeta_t &\sim NID(0, \sigma_\zeta^2) \end{aligned} \tag{2}$$

The observation equation for local linear trend model is similar to local level model but the state equation is different in this case. The slope component ν_t is added in the state equation of random walk μ_t and there is one more state equation for the slope component ν_t, where independent and normally distributed with mean of zero and variance of disturbance σ_ζ^2.

3.4.3 Local Level Model with Explanatory Variable

In order to study the effect of other variables with the rainfall measurement, the explanatory variables are needed to include in the observation equation of the model. For example, if the explanatory variables are added into the local level model, it can be formulated as:

$$\begin{aligned} y_t &= \mu_t + \sum_{j=1}^{k} \beta_{jt} x_{jt} + \varepsilon_t & \varepsilon_t &\sim NID(0, \sigma_\varepsilon^2) \\ \mu_{t+1} &= \mu_t + \xi_t & \xi_t &\sim NID(0, \sigma_\xi^2) \\ \beta_{t+1} &= \beta_t + \tau_t & \tau_t &\sim NID(0, \sigma_\tau^2) \end{aligned} \tag{3}$$

3.4.4 Akaike Information Criterion (AIC)

In this study, the Akaike Information Criterion (AIC) is used as the indicator to compare the performance of each model.

$$AIC = \frac{1}{n}[-2n \log L_d + 2(q + w)] \tag{4}$$

A lower AIC value represents a better fitting model where n is the number of observation of the main data, L_d is the hyperparameter that obtained from maximum likelihood function, q is the number of the initial value in state and w is the number of estimated variance disturbance.

3.5 Diagnostic Checking

3.5.1 Independency Test

In this research, Ljung-Box Q test will be conducted to check the independence of the data. The test statistic $Q(k, d)$ is based on the r, for lag k of residual autocorrelation, n is the number of residual and d is $(k - w + 1)$ where w is the number of parameter.

$$Q(k, d) = n(n + 2) \sum_{l=1}^{k} \frac{r_l^2}{n - l} \tag{5}$$

The null hypothesis of the test stated the data is independently distributed whereby the alternative hypothesis stated the data is not independently distributed.

3.5.2 Homoscedasticity Test

The second most important assumption is the homoscedasticity of residuals. This is checked using the following test statistic:

$$H(h) = \frac{\sum_{t=n-h+1}^{n} e_t^2}{\sum_{t=d+1}^{d+h+1} e_t^2} \tag{6}$$

where h is the closest integer to $(n - d)/3$, n is the number of observation and d is the number of diffuse initial elements. The test statistic should test against F −distribution with (h, h) of degree of freedom. If the test statistic is smaller than the critical value, then the data is said to be satisfied with the homoscedasticity assumption.

3.5.3 Normality Test

The last assumption is the normality test and it can be tested by Jarque-Bera (JB) test, the test statistic of this test can be calculated as follow:

$$N = n\left(\frac{S^2}{2} + \frac{(K - 3)^2}{24}\right) \tag{7}$$

$$S = \frac{\frac{1}{n}\sum_{t=1}^{n}(e_t - \bar{e})^3}{\sqrt{\left(\frac{1}{n}\sum_{t=1}^{n}(e_t - \bar{e})^2\right)^3}} \text{ and } K = \frac{\frac{1}{n}\sum_{t=1}^{n}(e_t - \bar{e})^4}{\left(\frac{1}{n}\sum_{t=1}^{n}(e_t - \bar{e})^2\right)^2}$$

where S is the skewness and K is the kurtosis of the residuals. The test statistic should test against chi-square distribution with two degrees of freedom. If the test statistic is smaller than the critical value, then the data is said to be fulfilled with the normality assumption.

3.6 Forecasting

The model that fulfill all the assumption mentioned above with the lowest AIC value will be used to forecast the future value. In order to check the accuracy of the model, Root Mean Square Error (RMSE) and Mean Absolute Percentage Error (MAPE) will be used as the indicator of the accuracy checking test. RMSE and MAPE can be calculated as follow:

$$RMSE = \sqrt{\sum_{t=1}^{n} \frac{\left(Y_l - \hat{Y}_t\right)^2}{n}} \tag{8}$$

$$MAPE = \sum_{t=1}^{n} \left| \frac{\left(Y_l - \hat{Y}_t\right)^2}{Y_l} \right| \times 100 \tag{9}$$

4. Results and Discussion

The period of collected data is from January 2009 to May 2019, the actual series of the rainfall measurement data is plotted below (Figure 2). From the time series plot, a stationary mean can be observed along the period but the slight curve and inconstant variance might exist in the data that need the help of software to detect.

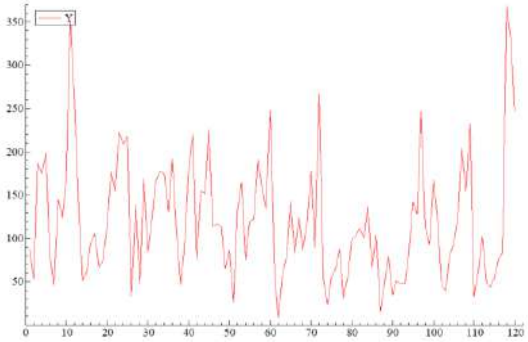

Figure 2: The actual series of the monthly rainfall data.

From Figure 3 and Figure 4 below, the ACF and PACF show a cyclic and seasonal pattern, it has a large correlation at lag 12 for both plot. Furthermore, the correlation is then decreased after a few lags are then followed by a constant wave that alternates between positive and negative correlations. In order to get a more reliable judgement, the KPSS test is then applied to test the stationarity of the data. The p-value is 0.1, the null hypothesis is failed to reject and it showed that the rainfall measurement data is stationary.

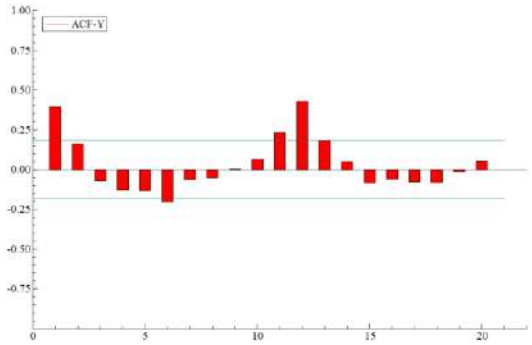

Figure 3: ACF plot of the original data

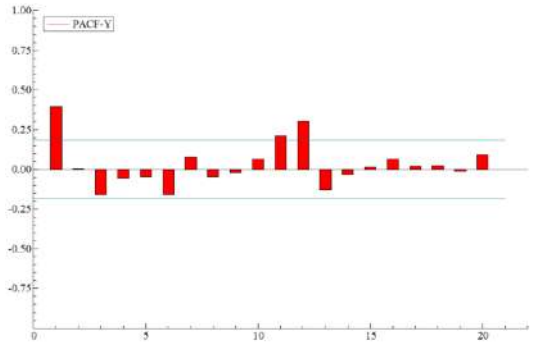

Figure 4: PACF plot of the original data.

4.1 Factor Identification

Table 1 shows that the relationship between all variables includes the *Y* variable (monthly rainfall amount) and *X* variable (rain day per month, wind speed, humidity, cloudiness, average temperature, pressure, sun hour). From Table 1, the strength of the relationship and the multicollinearity problem between each variable can be observed. The correlation between humidity and cloudiness is 0.7001 which indicates that a strong positive relationship existed among these two variables as well as the correlation between the cloudiness and the sun hour is -0.9031, which shows that a relatively strong negative relationship existed among them. The redundant factor has to remove from the pool of explanatory variables but the judgement cannot be made by only observing the high intercorrelated factor and simply remove any one of the factor. Hence, stepwise regression is then applied to remove the unnecessary factor.

Table 1: Correlation matrix plot of all variables.

	Y	***RD***	***WS***	***HM***	***CDN***	***AT***	***PS***	***SH***
Y	1.0000	0.7163	-0.2969	0.5269	0.6472	0.0112	-0.1722	-0.5345
RD	0.7163	1.0000	-0.3837	0.2857	0.3869	0.2488	-0.4206	-0.2168
WS	-0.2969	-0.3837	1.0000	-0.0641	0.1298	-0.5191	0.5203	-0.2090
HM	0.5269	0.2857	-0.0641	1.0000	0.7001	-0.6092	0.0591	-0.5955
CDN	0.6472	0.3869	0.1298	0.7001	1.0000	-0.4735	0.1872	-0.9031
AT	0.0112	0.2488	-0.5191	-0.6092	-0.4735	1.0000	-0.4550	0.4692
PS	-0.1722	-0.4206	0.5203	0.0591	0.1872	-0.4550	1.0000	-0.2981
SH	-0.5345	-0.2168	-0.2090	-0.5955	-0.9031	0.4692	-0.2981	1.0000

Y: Monthly rainfall amount (mm)
RD: Rain day per month
WS: Wind speed (kmph)
HM: Humidity (%)
CDN: Cloudiness (%)
AT: Average temperature (˚C)
PS: Pressure (mb)
SH: Sun hour

In order to remove redundant factor, backward stepwise regression is then applied that begins with a full model and eliminate the variables with least significant at each step until no insignificant variables remain. The result shows that the rain day, humidity, cloudiness and average temperature are the combination of the most significant variables. As a result, these four variables is then used to build the model with explanatory variables.

4.2 Model Identification

Table 2 shows the four models with a different combination of components, the first model is the local stochastic level model, the second model is the local stochastic level model with a stochastic trend component. The third model is similar to the first model but included explanatory variable, as well as the fourth model, is similar to the second model which also included the explanatory variable. Based on the result shown in Table 2, the fourth model which is the local stochastic level and stochastic slope with explanatory variables yield the smallest AIC value and the variance of disturbance of the irregular component is 8.2350. After done the diagnostic checking, all the assumptions were fulfilled. Hence, the fourth model is selected as the best model to forecast future rainfall data.

Table 2: Four models with a different combination and AIC value.

MODEL	LEVEL	SLOPE	EXPLANATORY	AIC
1	Stochastic	-	No	2.5228
2	Stochastic	Stochastic	No	2.5400
3	Stochastic	-	Yes	2.19180
4	Stochastic	Stochastic	Yes	2.1747

4.3 Forecasting

In this research, 5 periods of rainfall data were forecasted and then compared with the testing set. Table 3 shows the forecast result and the actual data and Figure 5 shows the forecast components output from the model.

Table 3: Actual and predicted value from period 121 to 125.

Period	*Actual value*	*Forecasted value*
121	123.5	369.9
122	82.4	518.4
123	114.8	692.6
124	186.7	893.0
125	412.7	1119.8

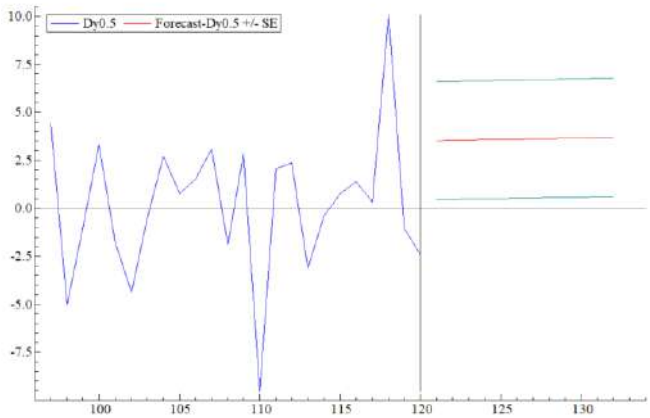

Figure 5: Forecast component plot.

Table 4 below shows the RMSE and MAPE increase gradually from period 121 to period 125, it indicates that the prediction accuracy decrease over time.

Table 4: RMSE and MAPE from period 121 to 125.

Period	*RMSE*	*MAPE*
121	22.4	1.6
122	45.3	5.9
123	68.9	10.0
124	93.4	12.9
125	112.5	14.2

5. Conclusions

The statistical analysis shows that rain day of the month, humidity, cloudiness and the average temperature of the area provide a significant impact on rainfall data. The local stochastic level and stochastic slope with explanatory variables which yielded the lowest AIC value was the best model and was used in predicting the rainfall data. However, the model is only suitable for a short-term prediction.

References

Abu, M.F. and Alias, N.E., 2016. *Extreme Rainfall Analysis on the December 2014 Flood, Terengganu* [Online]. Available at: http://engineering.utm.my/civil/wp-content/uploads/sites/29/2016/12/Extreme-Rainfall-Analysis-on-the-December-2014-Flood-Terengganu.pdf [Accesed: 18 December 2018]

Asemota, O., Bamanga, M. and Alaribe, O., 2016. Modelling seasonal behaviour of rainfall in northeast nigeria. a state space approach. *International Journal of Statistics and Applications 201*, 6(4), pp. 203-222.

Chan, N.W., 1997. Increasing flood risk in Malaysia: causes and solutions. *Disaster Prevention and Management: An International Journal*, 6(2), pp. 72–86.

Hernández E., Sanchez-Anguix V., Julian V., Palanca J., Duque N., 2016. Rainfall Prediction: A Deep Learning Approach. In: Martínez-Álvarez F., Troncoso A., Quintián H., Corchado E. (eds) Hybrid Artificial Intelligent Systems. HAIS 2016. Lecture Notes in Computer Science, 9648. Springer, Cham.

Hung, N.Q., Babel, M. S., Weesakul, S. and Tripathi, N.K., 2008. An artificial neural network model for rainfall forecasting in Bangkok, Thailand. *Hydrology and Earth System Sciences Discussions, European Geosciences Union*, 5(1), pp.183-218.

Juneng, L., Tangang, F. and Reason, C., 2007. Numerical case study of an extreme rainfall event during 9–11 December 2004 over the east coast of Peninsular Malaysia. *Meteorology and Atmospheric Physics*, 98 (1-2), pp. 81-98.

Nayan, N., Mahat, H., Hashim, M., Saleh, Y., Rahaman, Z.A. and Koh, L.S., 2017. Flood aftermath impact on business: a case study of Kuala Krai, Kelantan, Malaysia. *International Journal of Academic Research in Business and Social Sciences*, 7 (6), pp. 836-845.

Ravichandran, S. and Prajneshu, 2001. State space modelling versus arima time-series modelling. *Journal of the Indian Society of Agricultural Statistics*, 54(1), pp. 43-51.

Yusof, F., and Kane, I.L., 2012. Modelling monthly rainfall time series using ets state space and SARIMA models. *International Journal of Current Research*, 4(9), pp. 195-200.

Zainudin, S., Jasim, D.S., and Abu Bakar, A., 2016. Comparative analysis of data mining techniques for Malaysian rainfall prediction. *International Journal on Advanced Science Engineering Information Technology*, 6(6), pp. 1148-1153.

Circular Statistical Approach in Seasonality of Extreme Precipitation in Malaysia: An Analysis of Selected Stations

Aida Adha binti Mohd Jamil[a], Rossita Mohamad Yunus[b], Yong Zulina binti Zubairi[c]

[a]Department of Mathematical and Actuarial Sciences, Lee Kong Chian Faculty of Engineering and Science, Universiti Tunku Abdul Rahman, Malaysia. [*]Email (corresponding author): aidaadha@utar.edu.my

[b]Institute of Mathematical Sciences, Faculty of Science, University of Malaya, Malaysia.

[c]Mathematics Division, Centre for Foundation Studies in Science, University of Malaya, Malaysia.

Abstract

Rainfall data is analysed in the time series and linear form in most literature. Angular data, measured in degrees or radians, is useful for clear understanding the behavior and characteristics of extreme precipitation.Thus, to identify the influenced of the Southwest and Northeast Monsoon, the total amount more than 100mm of rainfall per day from 2008 until 2014 for four stations; Bayan Lepas and Subang in West Coast region, Muazam Shah and Kota Bharu in East Coast region, Malaysia have been analysed. Herein, the process of performing initial studies on data by generating circular plots, and computing hypothesis tests and the circular correlation coefficient were conducted when analysing circular data. Then, the circular mean, mean resultant length and circular standard deviation had been used to explain the variation of extreme precipitation event with the help of graphical representations in circular plots. The results shows that Northeast Monsoon has stronger seasonality compared to Southwest Monsoon. Besides that, the pattern and variation of rainfall data in circular are clearly describing the effect change of monsoon seasons.

1. Introduction

The most significant effect of climate change can cause rise of sea level, heavy rainfall and lead to drought. Natural rainfall is valuable for life in the earth, but it is a crucial element of weather. Frequent of extreme rainfall events may lead to serious flooding that cause massive loss in agriculture and fisheries. Prevention of damage to private and public property, and avoidance of health and ecological dangers are the impact of notable rainfall model.

Malaysia is located near the equator and well known for its hot and humid tropical rainfall climate all the year. Peninsular Malaysia and East Malaysia (Malaysian Borneo) are two major parts of country that located in the same latitudes and are influenced by wind, El Niño effect, and monsoon seasons. Malaysia have temperature average from 25^{o}C to 35^{o}C and faces two monsoon winds seasons. Monsoon is a significant wind system that changes its direction according to seasons. The Northeast Monsoon (NEM) is coming from China and the North Pacific, occurs between October and March has attributed heavy rainfall to East Coast of Malaysia (Ooi et al., 2019). On the other hand, West Coast of Malaysia is affected by the Southwest Monsoon (SWM) from the deserts of Australia that occurs between May and September as shown in Figure 1.

Circular statistics are useful to explore the trends of rainfall in Malaysia. The significant differences between each region are indicated by comparing the samples of circular data. The rainfall data at one station are having same distribution for each monsoon winds seasons throughout the years, but the opposite condition happens for different station locations. Lee et al. (2012) used circular statistical approach to determine the seasonality of extreme precipitation in Southern Korea. The study found that circular statistics

explicitly reflect the seasonal pattern of precipitation with maximum frequency of the timing of daily and monthly maximums.

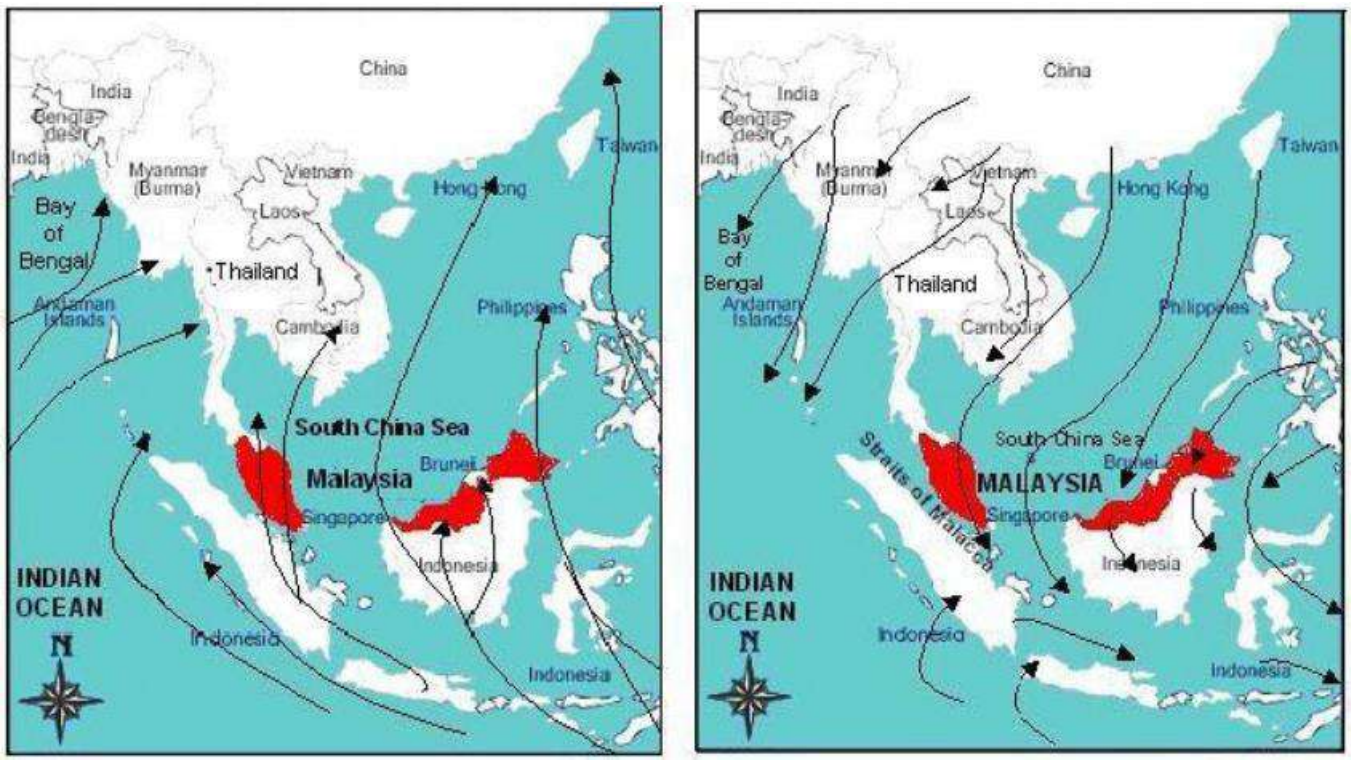

Figure 1: Southwest (left) and Northeast (right) monsoons around South-East Asia.
(Source: D/iya et al., 2014)

Inconsistency in rainfall data during long and irregular periods could produce biasness in the results of data analysis, however the rainfall data has demonstrated regional patterns. These factors can greatly influence the length and number of seasonal precipitation windows within a year. Besides that, Dhakal et al. (2015) presented a circular statistical approach for the assessment of temporal changes in seasonality of extreme precipitation in the state of Maine, United States by evaluating mean date, variability of the date of occurrence of extreme precipitation events and the tests for uniformity to check the null hypothesis of no seasonality against the alternative hypothesis of seasonality. As a result, the probability distribution of extreme event timing tends to be more often multimodal and less well aligned with calendar months and predefined seasons

The inability of the traditional summary statistics to detect and model event-timing distributions with multiple seasons remains a significant challenge. Nonparametric circular density approach, presented in this study, offers an adaptive and robust alternative. At the end, this approach can accurately characterize one or more modes representing seasonal peaks, as well as pave the way for an assessment of changes in seasonality over time.The use of statistical models of rainfall has been applied worldwide in order to give a better understanding about the rainfall pattern and its characteristics. This process involves the understanding of the past trends, identifying for any anomalies, and making projections of future climate change in Malaysia.

The aim of this study is to provide the statistical summary and interpretation of rainfall data in circular form as well as in validating the event of extreme precipitation - Southwest and Northeast monsoons. Section 2 discusses the data used in this study. The methodology of circular statistics is used to perform the studies on data in order to discover patterns, test hypothesis and check assumptions by using rainfall data in Section 3. Section 4 discusses the results based on the help of summary statistics in previous section. Concluding remarks are given in Section 5.

2. Data and Preliminaries

The sample data is provided by Malaysian Meteorological Department and is located at 4 stations - Bayan Lepas and Subangin West Coast region, Muazam Shah and Kota Bharu in West Coast, Malaysia. Daily rainfall (mm) is the amount collected over 24-hour period at 0800 from 1st January 2008 to 31 December 2014. Based on Malaysian Meteorological Department, the extreme precipitation happened when the total amount of rainfall exceeds 240mm per day. The red (danger) code warning will be issued to the residents. During the monsoon, the amount of rainfall is between 100mm to 200mm per day. The purpose of preliminary data analysis is to perform the descriptive statistics in order to study the pattern and seasonality of rainfall data in Malaysia.

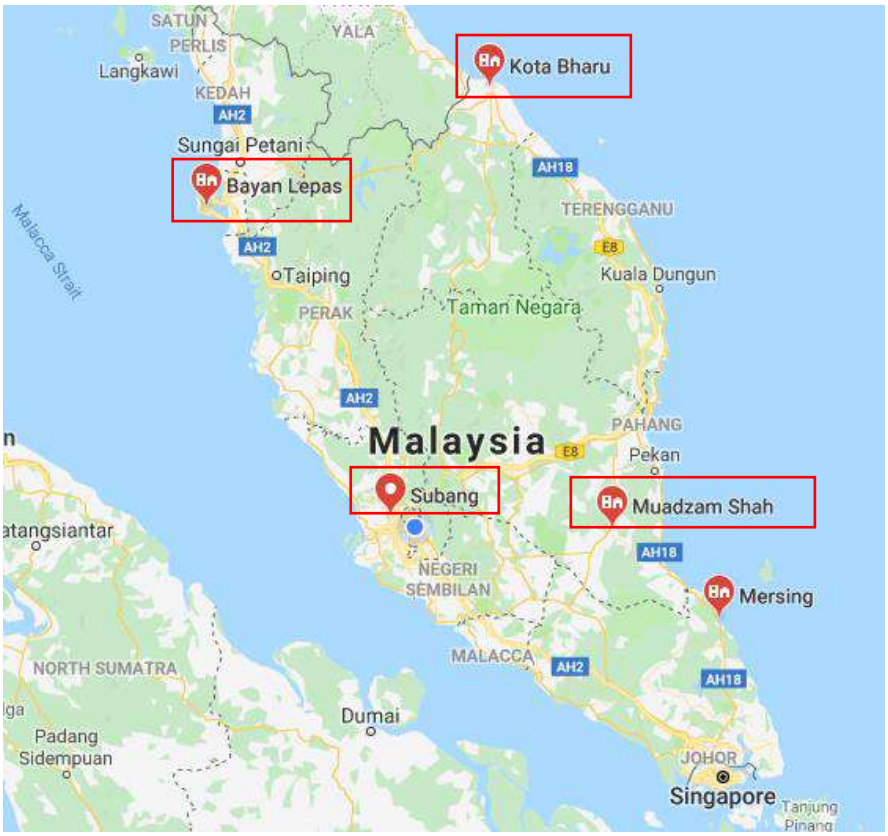

Figure 2: The Map location for 4 Stations.
(Source: Google Maps)

3. Circular Statistics

A circular distribution is a probability distribution of random variable, whose total probability is focused on the circumference of a unit circle (Jammalamadaka and Sengupta, 2001). The circular random variables is measured in degrees or radians and the values are angles in the range of $[0,2\pi)$ or $[-\pi, \pi)$. Let θ_i is the angular value (in radian) for extreme event "i", the angular position of the date of occurrence (D) for extreme precipitation event "i" is defined as (Dhakal et al., 2015):

$$\theta_i = D_i\left(\frac{2\pi}{365}\right) \tag{1}$$

D = 1 for 1st of January and D = 365 for 31st of December (D = 366 for leap year). In terms of angular value in radians, 0 radian corresponds to 1st of January and 2π radians is 31st of December.

From a sample of n extreme precipitation events, the x and y coordinates of the mean extreme precipitation date around the year are calculated based on the following equation:

$$\bar{x} = \frac{\sum_{i=1}^{n} \cos(\theta_i)}{n} \tag{2}$$

$$\bar{y} = \frac{\sum_{i=1}^{n} \sin(\theta_i)}{n} \tag{3}$$

where $\bar{x}$ and $\bar{y}$ are the coordinate of the mean extreme precipitation date. The direction representing mean date of occurrence of n extreme precipitation events is obtained using:

$$\bar{\theta} = tan^{-1}\left(\frac{\bar{x}}{\bar{y}}\right) \tag{4}$$

The variability of $n$extreme precipitation event occurrences about the mean date is obtained using themean resultant length:

$$\rho = \frac{\sqrt{\bar{x}^2 + \bar{y}^2}}{n} \tag{5}$$

ρ is a dimensionless measure of the spread of the data and the value of ρ ranges from 0 (indicating greatervariability in the date of occurrence of extreme precipitation events) to 1 (indicating all the extreme precipitation events occurred on the same day of the year). The circular standard deviation (csd) is given by (Mardia and Jupp, 2000):

$$csd = \sqrt{-2ln\rho} \tag{6}$$

Besides that, the departure from uniformity in the circular distribution is tested by Rayleigh's test. According to Dhakal et al., 2015, Rayleigh's test is powerful against unimodal (nonuniform) alternatives only. The mean resultant length, $\bar{R}$, as a measure of the concentration of data points around the circle. If $\bar{R}$ is greater than a threshold value, the data are interpreted as being too concentrated to be consistent with uniformity; and Rayleigh's test rejects the null hypothesis of uniformity. As with Rayleigh's test for unimodal departures, the p-values of the tests at least, the 1% significance level to reject the null hypothesis of uniformity (Pewsey et al., 2013).

4. Result and Discussions

Table 1 shows summary statistics of the rainfall totals of the studied stations. Parameters $\bar{\theta}$, ρ, csd, and Rayleigh's test offer simplified and accessible station-by-station summary of annual maximum daily precipitation variability for the 2008 to 2014 period.

Among the four studied stations, Muazam Shah observed the highest and Subang recorded the lowest percentages of days with no rainfall. Kota Bharu and Subang have larger mean of rainfall than Muazam Shah and Bayan Lepas. These stations observe a variety of rainfall patterns and have differences in monsoon experience. The rainy seasons are highly associated with monsoon winds that hit different parts of the country throughout the year.The Southwest Monsoon (SWM) influences the rainfall of Bayan Lepas, a station located at the northern region of the west coast of Peninsular Malaysia and contributes relatively higher rainfall to Subang. Meanwhile, Kota Bharu and Muazam Shah is located at the east coast of Peninsular Malaysia where the rainfall climate is affected by direct exposure to the Northeast Monsoon (NEM).

In the following analysis, we assume that the 365 days in a year is equivalent to a circle. The plots in the circle is represented the occurrence of amount of rainfall more than 100mm per day from 2008 until

2014. Based on circular plot in Figure 3 and 4, heavy rainfall from October until late March can be observed in East Coast regions, but the frequency of rainfall is scattering randomly in areas of West Coast around the year.

Table 1: Summary statistics of the daily rainfall for Bayan Lepas, Muazam Shah and Kota Bharu stations.

Station	Mean (mm)	Percentage of days with no rainfall	Circular Statistics			Uniformity Test	
			$\bar{\theta}$ (degree)	ρ	csd	Rayleigh Test (p-value)	Uniformity
Bayan Lepas, Penang	7.35	43.06	196.21 *(July)*	0.60	1.01	0.07	Yes
Subang, Selangor	8.58	41.36	262.36 *(Sept)*	0.84	0.58	0.28	Yes
Kota Bharu, Kelantan	8.97	50.40	340.05 *(Dec)*	0.85	0.58	0*	No
Muazam Shah, Pahang	6.89	51.70	8.53 *(Jan)*	0.68	0.87	0.01*	No

*p-values ≤ 0.01

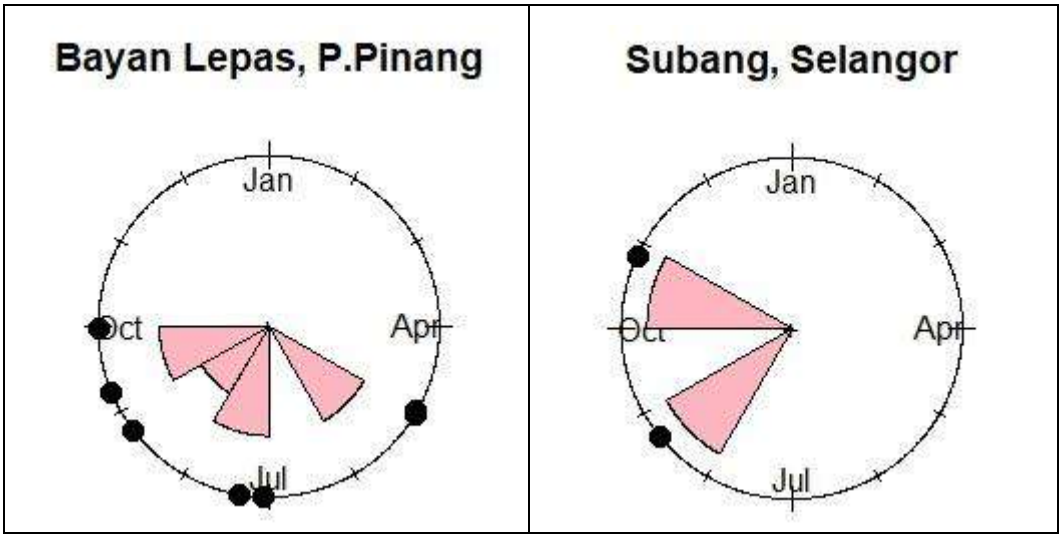

Figure 3: Circular Plot for West Coast region, Peninsular Malaysia (WCM).

Table 1 shows The values of $\bar{\theta}$, ρ, csd, and Rayleigh's test as analysis of seasonality using circular statistical measures. For West Coast region, the estimated circular mean, $\bar{\theta}$ indicating the computed means corresponding within the July-September based on the calendar day. Furthermore, the values of ρ is small, csd is high and p-values of Rayleigh's test are more than 0.01, then the null hypothesis of uniformity is accepted and demonstrating no seasonal peaks as expected. In different circumstances, ρ is high, csd is low and p-values of Rayleigh's test are less than 0.01 for East Coast region. This condition indicates strong

seasonality and the mean date of occurrence within the period of Northeast Monsoon (December and January).

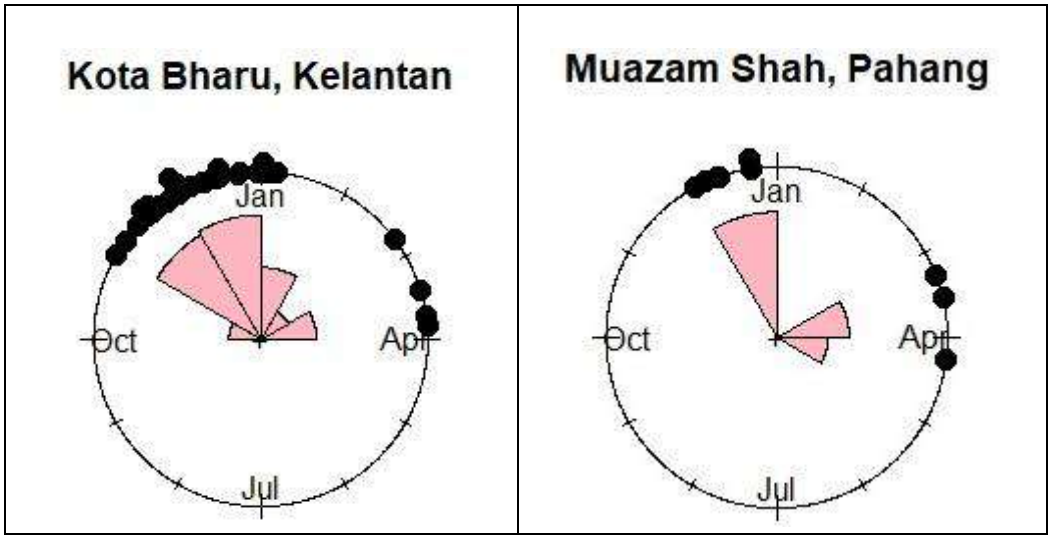

Figure 4: Circular Plot for East Coast region, Peninsular Malaysia (ECM).

Figure 3 and Figure 4 shows the ocuurence of extreme rainfall for East Coast (ECM) and West Coast (WCM), Malaysia respectively. The frequency of extreme rainfall at ECM in December has significantly higher due to the occurrence of Northeast Monsoon (NEM) and shows stronger seasonality than other areas of Malaysia. The presence of Titiwangsa Range of Peninsular Malaysia has attributed the barrier to NEM. As seen in Table 1, Rayleigh test statistics are significant for two stations in East Coast region – Kota Bharu and Muazam Shah and consistent in existence of seasonality for time periods of NEM. The contradiction happens in West Coast region - Bayan Lepas and Subang are representing no seasonal peaks and misleading indicator of the dominant Southwest Monsoon's (SWM) season, where the amount of rainfalls has relatively lower precipitation than ECM in December. The date for maximum rainfall in areas of WCM are mostly random around the year. This is because of the regions have not exposed SWM directly due barrier from North Sumatra, Indonesia (Wong et al., 2016). However, based on the circular plot in Figure 3, it displays that the extreme precipitation events occur during this monsoon season.

Results obtained are relatively well assessed by the statistical tests; the cases need a more comprehensive approach, perhaps with attention to local changes in the probability density. To sum up, methods based on three summary statistics ($\bar{\theta}$, ρ, csd) and the uniformity tests are useful for assessing seasonality for simple data like cases unimodal (strong seasonality) and uniform.

5. Conclusions

The amount of rainfall at East Coast, Malaysia (ECM) in December has significantly higher and mostly random around the year in areas of West Coast, Malaysia (WCM). The seasonal trend on rainfall is observed on ECM stations; but imprecise of seasonal trend happens on WCM stations. Therefore, ongoing work will seek the suitable of seasonality approach for Malaysian rainfall for both regions. The contradiction between the amount of rainfall at ECM and WCM need better understanding on the rainfall pattern and its characteristics. This process involves the study to attempt on highlighting the latest trends and projections of climate change in Malaysia. Early warning system can be produced based on early detection and forecasting by assessing the model from any disasters of extreme precipitation in Malaysia. Besides that, the damage scale can be reduced by situational awareness, strategy planning and logistic planning as our benefits through this research.

References

Dhakal, N., Jain, S., Gray, A., Dandy, M. and Stancioff, E., 2015. Nonstationarity in seasonality of extreme precipitation: A nonparametric circular statistical approach and its application. *Water Resources Research*, (6), pp. 4499– 4515.

D/iya, S.G., Gasim, M. B., Toriman, M.E. and Abdullahi, M.G., 2014. Floods in Malaysia: Historical Reviews, Causes, Effects and Mitigations Approach- *Scientific Figure on Research Gate.* Available from: https://www.researchgate.net/figure/Map-showing-the-study-area_fig1_268152474 [Accessed:18 Dec, 2019]

Jammalamadaka, S.R. and Sengupta, A., 2001. *Topics in Circular Statistics*. Singapore: World Scientific Press.

Lee, J.J., Kwon, H.H. and Kim, T.W., 2012. Spatio-temporal analysis of extreme precipitation regimes across South Korea and its application to regionalization. *Journal of Hydro-environment Research*, (6), pp. 101–110.

Mardia, K.V. and Jupp, P.E., 1999. *Directional Statistics*, 1st ed. John Wiley and Sons Ltd., pp. 15 – 23.

Ooi, J.B. and Zakaria, A., 2019. *Malaysia - Climate | Britannica.com*. [Online]. Available at: https://www.britannica.com/place/Malaysia/Climate [Accessed: November 12, 2019]

Pewsey, A., Neuhäuser, M. and Ruxton, G.D., 2013. *Circular Statistics in R*, Oxford and New York: Oxford University Press.

Wong, C.L., Yusop, Z., Ismail, T., Liew, J., Venneker, R. and Uhlenbrook, S., 2016. Rainfall Characteristics and Regionalization in Peninsular Malaysia Based on a High Resolution Gridded Data Set. *Water (Switzerland)*, 8(11), pp. 500.

An Overview on Run Sum Control Charts

Hii Siew Chen

Department of Mathematical and Actuarial Sciences, Lee Kong Chian Faculty of Engineering and Science, University Tunku Abdul Rahman, Malaysia. Email: hiisc@utar.edu.my

Abstract

Control charts are widely used to monitor process performance and to detect a shift in the process mean and standard deviation. Run Sum Control Charts have experienced significant developments since its birth in the early 60's. During these years, numerical researches have been carried out and achievements have been obtained. This article presents an overview about the RSCC and their relevant works previously and lately.

1. Introduction

Control charts are the most powerful and commonly used tools in statistical process control (SPC) to monitor a process for quality improvement. In the literature, several charting techniques have been proposed, in particular the Shewhart control chart, Cumulative Sum (CUSUM) control chart (Page, 1954) and the Exponentially Weighted Moving Average (EWMA) control chart (Roberts, 1959). The Shewhart control chart is effective to detect the large shifts in the process, while the CUSUM and EWMA control charts are effective to detect small and moderate shifts in the process.

Most of the charts mentioned in the previous paragraph monitor the process location and spread between upper and lower limits of the charts. Recently, lots of research works have been committed to a special type of control chart that divide the in-control interval between upper and lower limits of the charts into zones (regions). Such charts are called run sum charts which monitor the run sum of the scores. It signals an out-of-control condition when the run sum of the scores reaches or exceeds its critical score.

In this article, various types of run sum control charts are surveyed. The rest of the article is organized as follows. Section 2 presents the related works on univariate run sum control charts. The related works on multivariate run sum control charts will be presented in Section 3. Section 4 provides the summary of statistics that used in the run sum control charts. Finally concluding remarks are made in section 5.

2. Related Works on Univariate Run Sum Control Charts

The run sum control charts are simple and powerful control charts to monitor the process mean and standard deviation. The first run sum control chart was proposed by Roberts (1966) and further studied by Reynolds (1971). It was initially proposed for the monitoring of process average. The chart is divided into k regions above the central line (CL) and k regions below the CL. Then, an integer score is assigned to each region. Cumulative (run) sum of the scores are monitored and an out-of-control signal is given when this value is equal to or greater than a critical value.

Davis, et al. (1990) studied the average run length (ARL) of the run sum $\overline{X}$ chart by using the scores 0, 2, 4, and 8, or equivalently the scores 0, 1, 2, and 4 and found they are superior than the Shewhart charts with supplementary runs rules. Jaehn (1991) proposed a zone control chart with four regions each above and below CL of the chart. Davis, et al. (1994) proposed a general model of the zone control chart and a fast initial

response (FIR) feature. An economic design of zone control chart for joint monitoring of process mean and variance was proposed by Ho and Case (1994).

In 1997, Champ and Rigdon developed a Markov chain technique to study the run length distribution of the run sum $\overline{X}$ chart. They claimed that the run sum $\overline{X}$ chart is competitive with the CUSUM and EWMA charts by adding more regions and scores, in detecting process mean shifts. Aguirre-Torres and Reyes-Lopez (1999) proposed a run sum charts for both sample mean, $\overline{X}$ and sample range, *R*, while Davis and Krehbiel (2002) proposed $\overline{X}$ zone control charts that generally outperform the Shewhart charts for detecting the linear drift in process mean. The run sum *R* chart with FIR feature was proposed by Acosta-Mejia and Pignatiello (2010). The chart is more sensitive than the other *R* charts with run rules.

In the previous studies on run sum control charts, lots of run sum $\overline{X}$ chart have been developed to monitor the process mean. Since monitoring the variability of the process is as vital as monitoring its mean, some run sum *R* charts had also developed to detect small shifts in the process dispersion. Some researchers have contributed to the advancement of this control charts, such as Aguirre-Torres and Reyes-Lopez (1999) and Acosta-Mejia and Pignatiello (2010). Sitt, et al (2014) introduced a run sum *t* control chart. This chart is found to be more robust than the existing run sum $\overline{X}$ chart for small shifts and more sensitive than the other *t* type charts by having smaller ARL_1 (out-of-control detection speed) for medium to large shifts.

In 2016, Rakitzis and Antzoulakos proposed two-sided run sum *S* control charts based on *ARL* performance and compared with other competitive control charts. The charts outperform the two-sided Shewhart *S* control chart for small to moderate shifts in process standard deviation. The overall performance of the chart, in terms of the *Average Extra Quadratic Loss* (*AEQL*) for different score schemes is investigated. From the study, the performance of the score schemes is found not affected by the distribution of the shift in process standard deviation.

The *ARL* is a traditional performance indicator of the control charts. It is the average number of samples that plotted on the chart before the chart signals an out-of-control condition. However, since the run length distribution of the control charts is highly skewed and the interpretation based on *ARL* could give a false alarm, the median run length (*MRL*) is suggested in the study of run sum control charts. Gao H., et al (2019) studied the *MRL* performance of the run sum S control chart. The in-control *ARL* and in-control *MRL* is calculated for the chart with nine different score schemes. The study show that the *MRL* measurement is better explanation than the *ARL* measurement.

Monitoring the coefficient of variation (CV) is important in Statistical Process Control when the process mean and standard deviation are not constants. Therefore monitoring CV by using run sum control charts have been studied by Teoh, et al. (2017). Markov chain approach has been used to study the run-length properties of the run-sum CV (RS-γ) charts. Performance of the charts are made under both zero- and steady-state modes with the Shewhart-γ, run-rules (RR)-γ and EWMA-γ charts. From the study, it is found that by adding more regions and scores, the RS-γ chart has the potential to be improved. The results obtained in the study show that the RS-γ charts perform significantly better than Shewhart-γ, run-rules (RR)-γ and VSI-γ charts. The RS-γ charts are recommended for monitoring moderate to large shifts in the CV.

The control charts discussed above are designed based on samples from the process at fixed length sampling intervals. Research works focused on the variable sampling intervals (VSIs) have been carried out on the run sum (RS) control charts recently. Chew, et al. (2015) proposed a VSI run sum (RS) $\overline{X}$ chart. Markov chain method is used to evaluate both average time to signal (ATS) and adjusted average time to signal (AATS) of the chart. The chart is found more efficient than the basic RS $\overline{X}$ chart, in process monitoring, for quicker detection of out-of-control situations. The sensitivity of the VSI RS $\overline{X}$ chart had been increased by adding more scoring regions and a head-start feature (FIR).

3. Related Works on Multivariate Run Sum Control Charts

The Shewhart charts, CUSUM charts and EWMA charts are the control charts used to monitor a single quality variable (univariate). However, in reality, product quality cannot be justified only by one product

characteristic since it should be measured from some quality variables. Therefore, some multivariate control charts such as Hotelling χ^2 chart, MCUSUM chart and MEWMA chart have been studied among the researchers.

A Hotelling χ^2chart is the basic multivariate control chart. The chart is used for monitoring the mean vector of a process. The χ^2 chart's statistics was computed for each multivariate sample in which each contains *n* number of correlated quality characteristics. In 2003, Khoo and Quah transformed the T^2 statistics of the Hotelling χ^2 chart into the standard normal statistics and they applied the run rules to the transformed statistics. For the χ^2 chart, Aparisi, Champ and Garcia-Diaz proposed some rules using the charting statistics in original forms in 2004. For the χ^2 chart, Koutras, Bersimis and Antzoulakos (2006) also proposed the *k*-of-*k*, and combined *r*-of-*r* and *k*-of-*k* rules. The performance of the χ^2 chart supplemented with the *r*-of-*m* runs rule was studied by Rakitzis and Antzoulakos (2011) and the rules are found to perform better than the standard χ^2chart.

In recent years, the attention on the run sum charts had paid on the multivariate case. The charts are useful to monitor two or more related quality characteristics simultaneously. The standard χ^2chart detects small and moderate shifts in the mean vector relatively slower and reduces its sensitivity. Therefore, to improve the sensitivity, the run sum Hotelling's χ^2chart had been introduced and proposed by Michael, et al. (2013).

In 2013, the proposed run sum Hotelling's χ^2 chart is the most widely used multivariate chart for monitoring the mean vector of a process. The *ARL* performance is evaluated using the Markov chain approach and it can be made as competitive as that of the MEWMA control chart by increasing the number of scoring regions. The run sum Hotelling's χ^2 chart had been shown that it is superior to other run rules χ^2 charts, including the standard Hotelling's χ^2 chart. When the sample size is small, the run sum Hotelling's χ^2 chart is recommended to use to detect large shifts. However, for larger sample size, i.e. $n \geq 5$, the run sum Hotelling's χ^2 chart is used to detect moderate to large shifts in the process.

Monitoring the multivariate coefficient of variation (CV) in the run sum control chart had been studied recently by Alex, et al. (2017). They proposed a downward and upward run sum chart for monitoring decreasing and increasing shifts in the multivariate CV of the Phase-II process. They use the average run length (*ARL*), standard deviation of the run length (*SDRL*) and expected average run length (*EARL*), under the zero state and steady state cases, to compare the performance of the proposed chart with the existing multivariate CV chart. The proposed chart had been shown that it outperforms the existing multivariate chart for monitoring the CV.

4. Summary of Statistics Used in Run Sum Control Charts

Let X_{ij} be the *j*th observation in a sequence of samples of size *n* from a quality characteristic *X*. Assume that the samples are independent and identically distributed observations which follow a normal distribution where $X_{ij} \sim N(\mu_0 + a\sigma_0, b^2\sigma_0^2)$, with μ_0 and σ_0 be the nominal process mean and standard deviation respectively. The sample mean and the sample standard deviation of the *i*th sample for the control chart is defined as $\overline{X}_i = \frac{1}{n}\sum_{i=0}^{n} X_{ij}$ and $S_i = \frac{1}{n}\sqrt{\sum_{i=0}^{n}\left(X_{ij} - \overline{X}_i\right)^2}$, respectively. The process is in control if $a = 0$ and $b = 1$, otherwise the process shifted, either process mean or/and process standard deviation shifted.

For the multivariate process, let $\{X_{ij}\}$ be a sample of *n* independent multivariate normal $N(\mu_0, \Sigma_0)$ where μ_0 is the in-control mean vector and Σ_0 is the in-control covariance matrix.

Table 1 and 2 below provide the summary statistics that are used in some of the run sum control charts discussed in this article.

Table 1: Univariate run sum charts.

Charts	*Statistics*
Run Sum $\overline{X}$ chart (1999)	$\hat{\sigma}_{\overline{Y}} = \frac{A_2\overline{R}}{3}$
Run Sum *R* chart (1999)	$\hat{\sigma} = \frac{\overline{R}}{d_2}$ $R_p = \hat{\sigma}W_p = \frac{\overline{R}}{d_2}W_p = E_p\overline{R}$ where $E_p = \frac{W_p}{d_2}$
Run Sum *S* chart (2016)	$UCL_j = \sigma_0\sqrt{\frac{\chi^2_{n-1;1-\Phi(jL)}}{n-1}}$ $LCL_j = \sigma_0\sqrt{\frac{\chi^2_{n-1;\Phi(jL)}}{n-1}}$ $CU_i = \begin{cases} 0 & otherwise \\ CU_{i-1} + a_{j+1} & \text{if } UCL_j \le S_i \le UCL_{j+1} \end{cases}$ $CL_i = \begin{cases} 0 & otherwise \\ CL_{i-1} - a_{j+1} & \text{if } LCL_{j+1} \le S_i \le LCL_j \end{cases}$ $C_i = \max\{CU_i, -CL_i\}$
Run Sum *t* chart (2014)	$UCL_j = K \times F_t^{-1}(\alpha_j)$ $\alpha_j = \Phi\left(\frac{3j}{k-1}\right)$ $U_r = \begin{cases} 0 & \text{if } T_r < CL \\ U_{r-1} + S(T_r) & \text{if } T_r \ge CL \end{cases}$ $L_r = \begin{cases} 0 & \text{if } T_r > CL \\ L_{r-1} + S(T_r) & \text{if } T_r \le CL \end{cases}$ $S(T_r) = \begin{cases} S_j & \text{if } T_r \in [UCL_{j-1}, UCL_j) \\ -S_j & \text{if } T_r \in [LCL_j, LCL_{j-1}) \end{cases}$ $LCL_j = -UCL_j$ for $j = 1,2,\dots,k-1$
Run Sum γ chart (2017)	$\hat{\gamma}_i = \frac{S_i}{\overline{X}_i}$ $U_i = \begin{cases} U_{i-1} + S(\hat{\gamma}_i), & \text{if } \hat{\gamma}_i \ge CL \\ 0, & \text{if } \hat{\gamma}_i < CL \end{cases}$ $L_i = \begin{cases} L_{i-1} + S(\hat{\gamma}_i), & \text{if } \hat{\gamma}_i \le CL \\ 0, & \text{if } \hat{\gamma}_i > CL \end{cases}$ $S(\hat{\gamma}_i) = \begin{cases} S_t & \text{if } \hat{\gamma}_i \in [UCL_{t-1}, UCL_t) \\ -S_t & \text{if } \hat{\gamma}_i \in [LCL_t, LCL_{t-1}) \end{cases}$ $UCL_t = \mu_0(\hat{\gamma}) + \left(\frac{3t}{k-1}\right)K\sigma_0(\hat{\gamma})$ $LCL_t = \max[0, \mu_0(\hat{\gamma}) - \left(\frac{3t}{k-1}\right)K\sigma_0(\hat{\gamma})]$ $CL = \mu_0(\hat{\gamma})$ $\mu_0(\hat{\gamma}) \simeq \gamma_0[1 + \frac{1}{n}\left(\gamma_0^2 - \frac{1}{4}\right) + \frac{1}{n^2}\left(3\gamma_0^4 - \frac{\gamma_0^2}{4} - \frac{7}{32}\right) + \frac{1}{n^3}(15\gamma_0^2 - \frac{3}{4}\gamma_0^4 - \frac{7}{32}\gamma_0^2 - \frac{19}{128})]$

	$\sigma_0(\hat{\gamma})$ $\simeq \gamma_0 \sqrt{\frac{1}{n}\left(\gamma_0^2+\frac{1}{2}\right)+\frac{1}{n^2}\left(8\gamma_0^4+\gamma_0^2+\frac{3}{8}\right)+\frac{1}{n^3}(69\gamma_0^6+\frac{7}{2}\gamma_0^4+\frac{3}{4}\gamma_0^2+\frac{3}{16})}$
VSI run sum $\overline{X}$ chart (2015)	$UCL_j = \mu_0 + A[\frac{3j}{k-1}](\sigma_0/\sqrt{n})$ $LCL_j = \mu_0 - A[\frac{3j}{k-1}](\sigma_0/\sqrt{n})$ $S(\overline{X}_r) = \begin{cases} +S_j & \text{if } \overline{X}_r \in R_{+j} \\ -S_j & \text{if } \overline{X}_r \in R_{-j} \end{cases}$ where j = 1,2,…,k and r = 1, 2,… $U_r = \begin{cases} 0 & \text{if } \overline{X}_r < CL \\ U_{r-1} + S(\overline{X}_r) & \text{if } \overline{X}_r \geq CL \end{cases}$ $L_r = \begin{cases} 0 & \text{if } \overline{X}_r > CL \\ L_{r-1} + S(\overline{X}_r) & \text{if } \overline{X}_r \leq CL \end{cases}$ $T_{\overline{X}} = \begin{cases} d_1 & \text{if } H/G \leq U_r < H \text{ or } -H < L_r \leq -H/G \\ d_2 & \text{if } 0 \leq U_r < H/G \text{ or } -H/G < L_r \leq 0 \end{cases}$

Table 2: Multivariate run sum charts.

Charts	*Statistics*
Run Sum Hotelling's χ^2chart (2013)	$T_t^2 = n(\overline{X}_t - \mu_0)^T \Sigma_0^{-1} (\overline{X}_t - \mu_0)$ $d = \sqrt{(\mu_1 - \mu_0)^T \Sigma_0^{-1} (\mu_1 - \mu_0)}$ $UCL_j = K \times F_p^{-1}(\alpha_j)$ $\alpha_j = \Phi\left(\frac{3j}{k-1}\right)$ for j = 1, 2, …, k-1 $U_t = \begin{cases} 0 & \text{if } T_t^2 < UCL_0 \\ U_{t-1} + S(T_t^2) & \text{if } T_t^2 \geq UCL_0 \end{cases}$ $S(T_t^2) = S_j$ if $T_t^2 \in [UCL_{j-1}, UCL_j)$
Run Sum multivariate *CV* chart (2017)	$\hat{\gamma} = \left(\overline{x}^T \mathrm{S}^{-1} \overline{x}\right)^{-\frac{1}{2}}$ $UCL_j = F_{\hat{\gamma}}^{-1}(\alpha_j \mid n, v, \delta_0)$ $LCL_j = F_{\hat{\gamma}}^{-1}(1-\alpha_j \mid n, v, \delta_0)$ $\alpha_j = \Phi\left(\frac{3j}{k-1}\right)$ $F_{\hat{\gamma}}^{-1}(\alpha \mid n, v, \delta) = \sqrt{\frac{n(n-v)}{(n-1)v}\left[\frac{1}{F_F^{-1}(1-\alpha \mid n, v, \delta)}\right]}$ $S(\hat{\gamma}_t) = \begin{cases} S_j & \text{if } \hat{\gamma}_i \in [UCL_{j-1}, UCL_j) \\ -S_j & \text{if } \hat{\gamma}_i \in [LCL_j, LCL_{j-1}) \end{cases}$ $U_t = \begin{cases} U_{t-1} + S(\hat{\gamma}_t), & \text{if } \hat{\gamma}_t \geq UCL_0 \\ 0, & \text{if } \hat{\gamma}_t < UCL_0 \end{cases}$ $L_t = \begin{cases} L_{t-1} + S(\hat{\gamma}_t), & \text{if } \hat{\gamma}_t \leq LCL_0 \\ 0, & \text{if } \hat{\gamma}_t > LCL_0 \end{cases}$

5. Conclusions

In this article, various run sum control charts are surveyed. The run sum control charts are gaining popularity due to its simplicity and user friendly in terms of construction. From this survey, the general conclusion that can be made is that most of the univariate run sum control charts have been studied these few years and they are able to perform better compare with those Shewhart-charts. Future research works are suggested to be concentrated more on multivariate run sum control charts even with the contaminated data during simulation studies conducted. The information provided in this article would be beneficial for the researchers to work in this area.

References

Acosta-Mejia, C.A. and Pinatiello, J.J.Jr., 2010. The run sum *R* chart with fast initial response. *Communications in Statistics – Simulation and Computation,* 39, pp. 921– 932.

Aguirre-Torres, V. and Reyes-Lopez, D., 1999. Run sum charts for both $\overline{X}$ and R. *Quality Engineering,* 12, pp.7 – 12.

Alex, J.X. Lim, Michael B.C. Khoo, Teoh, W.L. and Abdul Haq, 2017. Run sum chart for monitoring multivariate coefficient of variation. *Computers and Industrial Engineering*, 109, pp. 84 – 95.

Aparisi, F., Champ, C.W. and Garcia-Diaz, J.C., 2004. A performance analysis of Hotelling χ^2control chart with supplementary runs rules. *Quality Engineering,* 16, pp. 359 – 368.

Champ, C.W. and Rigdon, S.E., 1997. Analysis of the run sum control chart. *Journal of Quality Technology*, 29, pp. 407 – 417.

Chew, X.Y., Michael B.C. Khoo, Teh, S.Y. and Castagliola, P., 2015. The variable sampling interval run sum $\overline{X}$ control chart. *Computers & Industrial Engineering,* 90, pp. 25 –38.

Davis, R.B., Homer, A. and Woodall, W.H., 1990. Performance of the zone control chart. *Communications in Statistics –Theory and Methods,* 19(5), pp. 1581 – 15887.

Davis, R.B., Chun, J. and Guo, Y., 1994. Improving the performance of the zone control chart. *Communications in Statistics – Theory and Methods,* 23(12), pp. 3557 – 3565.

Davis, R.B. and Krehbiel, T.C., 2002. Shewhart and zone control chart performance under linear trend. *Communications in Statistics – Simulation and Computation,* 31, pp. 91 – 96.

Gao, H., Michael B.C. Khoo, Teh , S.Y. and Teoh, W.L., 2019. A study on the Median Run Length Performance of the Run Sum *S* Control Chart. *International Journal of Mechanical Engineering and Robotics Research,* 8(6), pp. 885 – 890

Ho, C.C. and Case, K.E., 1994. An economic design of the zone control chart for monitoring process centering and variation. *Computers and Industrial Engineering*, 26, pp. 213 – 221.

Jaehn, A.H., 1991. The zone control chart. *Quality Progress*, 24, pp. 65 – 68.

Khoo, M.B.C. and Quah, S.H., 2003. Incorporating runs rule into Hotelling χ^2 control chart. *Quality Engineering*, 15, pp. 671 – 675.

Koutras, M.V., Bersimis, S. and Antzoulakos, D.L., 2006. Improving the performance of the chi-square control chart via runs rules. *Methodology and Computing in Applied Probability,* 8, pp. 409 – 426.

Michael B.C. Khoo, Sitt, C.K., Zhang W. and Philippe Castagliola., 2013. A run sum Hotelling's χ^2 control chart. *Computers & Industrial Engineering,* 64, pp. 686 – 695.

Page, E.S., 1954. Control Charts with Warning Lines. *Biometrika*, 42, pp. 243 – 257.

Rakitzis, A.C. and Antzoulakos, D.L., 2011. Chi-square control charts with runs rules. *Computing in Applied Probability*, 13, pp. 657 – 669.

Rakitzis, A.C. and Antzoulakos, D.L., 2016. Run sum control charts for monitoring of process variability. *Quality Technology & Quantitative Management*, 13, pp. 58 – 77.

Reynolds, J.H., 1971. The run sum control chart procedure. *Journal of Quality Technology*, 3, pp. 23 – 27.

Roberts, S.W., 1959. Control charts tests based on geometric moving averages. *Technometrics*, 1, pp. 239 – 250.

Roberts, S.W., 1966. A comparison of some control chart procedures. *Technometrics*, 8, pp. 411 – 430.

Sitt, C.K., Khoo, M.B.C., Shamsuzzaman, M. and Chen, C.H., 2014. The rum sum *t* control chart for monitoring process mean changes in manufacturing. *International Journal of Advanced Manucturing Technology,* 70, pp. 1487 – 1504.

Teoh, W.L., Michael B.C.Khoo, Castagliola, P., Yeong, W.C. and Teh, S.Y., 2017. Run-sum control charts for monitoring the coefficient of variation. *European Journal of Operational Research,* 257, pp. 144 – 158.

A Review on Vehicle Routing Problem

Lam Weng Hoe[a], Lam Weng Siew[a], Liew Kah Fai[a]

[a]Department of Physical and Mathematical Science, Faculty of Science, Universiti Tunku Abdul Rahman, Malaysia. [*]Email (corresponding author): whlam@utar.edu.my

Abstract

Vehicle routing problem is a classical problem and has been gaining popularity nowadays. However, the competition between the transportation industries is very vigorous due to the increasing number of transportation industries. In fact, this industry faces major competition in the local as well as in global markets. In the transportation industry, effective planning is necessary in order to deliver products to customers efficiently. Hence, effective planning is quite important to produce the right product and achieve on-time delivery to meet the customers' demands and expectations. The degree of the customers' satisfaction largely depends on the company's performance. If the company is able to provide better services and products to the customers, then the customers' satisfaction will become higher.

1. Introduction

Nowadays, the ultimate goal of a company is to optimize the profit and minimize the cost. The transportation problem (TP) is an optimization problem with a linear objective function and linear constraints (Mutar et al., 2017). The transportation problem can be solved by using the linear programming mathematical model. Transportation mode plays a central role in achieving competitive advantages through timely responsiveness and cost efficiency by controlling resources, locations, and transportation models (Mutar et al., 2017). Numerous studies can be found on the transportation problem and these problems included inventory routing problem (Bertazzi and Speranza, 2012), bus terminal location problem (Ghanbari and Mahdavi-Amiri, 2011), electric vehicle routing problem (Keskin and Catay, 2016; Montoya et al., 2017), truck loading problem (Yuceer and Ozakca, 2010), convoy routing problem (Goldstein et al., 2010), and vehicle routing problem (Archetti et al., 2016; Braekers et al., 2016; Huang et al., 2017). Among these transportation problems, vehicle routing problem received considerable attention as one of the most common problems in transportation. Therefore, a review on the vehicle routing problem will be discussed in this study. The vehicle routing problem formulation was first introduced by Dantzig and Ramser (1959), as a generalization of the Traveling Salesman Problem (TSP) presented by Flood (1956). Basically, vehicle routing problems always include two important dimensions, they are quality and evolution of information (Psaraftis, 1980). Quality of information reflects the possible uncertainty on the available data (Pillac et al., 2013). For example, when the demand of a customer is only known as a range estimate of its real demand. On the other hand, evolution of information means the information available to the planner may change during the execution of the routes. For instance, the arrival of the new customer's requests (Pillac et al., 2013).

2. Literature Review on Vehicle Routing Problem

Bullnheimer et al. (1999) used metaheuristic to solve the vehicle routing problem with Ant System. They proposed a "hybrid" Ant System algorithm by incorporating the problem-specific information such as capacity utilization and savings. After that, the results of this study are compared with other metaheuristic approaches, including Neural Networks, Simulated Annealing, and Tabu Search. These approaches are compared in terms of run times since run times is an important criterion to determine the quality of an

algorithm. Based on the results, the average deviation of the Tabu Search is 0.77%, which is outperforming the other metaheuristics, followed by Simulated Annealing (2.09%), Ant System (4.43%), and lastly Neural Network (5.30%). According to the authors, there is still room for improvement for Ant System. The superiority of Tabu Search for vehicle routing problems can be explained by two facts. Tabu Search is an excellent method and has been studied and improved a lot since its introduction. Based on the past study, a vast number of the vehicle routing problem-related researches have been done on Tabu Search nowadays (Osman, 1993; Taillard, 1993; Gendreau et al., 1994; Rochat and Taillard, 1995; Rego and Roucairol, 1996). The authors believe that the future work on the Ant System approach will assist to further improve the quality of the vehicle routing.

Prins (2004) proposed a simple yet effective evolutionary algorithm, namely genetic algorithm for the vehicle routing problem. According to the results, this algorithm is able to outperform the most published Tabu Search heuristics on the 14 classical Christofides instances in terms of average solution cost. Hence, effective evolutionary algorithm becomes the best solution method for the large-scale instances generated by Golden et al. (1998).

Bell and McMullen (2004) applied Ant Colony Optimization technique in the vehicle routing problem. They have modified the Ant Colony Optimization algorithm in order to allow the search of the multiple routes of the vehicle routing problem. The results of this study show that the algorithm is able to determine the solutions within 1% of known optimal solutions. Moreover, the advantage of Ant Colony Optimization algorithm is to provide a comparatively competitive solution technique, especially for larger problems. The authors urged that the application of the Ant Colony Optimization techniques should be widely applied to other routing problems with unique clustering features, such as the logistics problem set seen in the research of Ballou (1990).

Erdogan and Miller-Hooks (2012) conducted a study on the Green Vehicle Routing Problem. They have formulated a Green Vehicle Routing Problem and developed solution techniques with alternative fuel-powered vehicle fleets. As a result, in this study, two construction heuristics so-called Modified Clarke and Wright Savings heuristic, and Density-Based Clustering Algorithm are developed. Moreover, a customized improvement technique has been proposed as well in this study. The results indicate that the heuristics are outperformed the exact solution methods. Thus, the heuristics can be used to tackle the large problem instances.

Abdulkader et al. (2015) proposed a hybridized Ant Colony algorithm to comprehend the multi compartment vehicle routing problem. Multi compartment vehicle routing problem is an extension of the classical vehicle routing problem and more sophisticated compared to the classical vehicle routing problem. Multi compartment vehicle routing problem needed to take the type of the goods and products into consideration as they cannot be mixed together due to differences in their individual characteristics. As a result, goods and products have to be stored in different compartments. As a result, this is the main challenging part of this multi compartment vehicle routing problem. Hence, a new hybridized algorithm has been proposed by incorporating the local search procedures with an existent Ant Colony algorithm. The results show that the proposed Ant Colony algorithm gives better results by using less computational time as compared to the existing Ant Colony algorithm.

Karakatic and Podgorelec (2015) resolved the multi depot vehicle routing problem by using the genetic algorithm based solution. In this study, the multi depot vehicle routing problem will be investigated with other existing approaches, both heuristic and exact, and also the genetic algorithm based solutions. The results of this study indicate that the genetic algorithm is on par with other existing approaches. Moreover, genetic algorithm is a very suitable algorithm to tackle this type of problem-solving. This result has also been confirmed in Arostegui et al. (2006) and Youssef et al. (2001), the genetic algorithm is the linear scaling with the growing problem size and therefore is preferred for solving large non-programming problems over exact algorithms or some other heuristic methods.

Yao et al. (2016) have done a study on carton heterogeneous vehicle routing problem with a collection depot by using an improved particle swarm optimization. Carton heterogeneous vehicle routing problem with a collection depot is a quite challenging and complex problem, as we need to pick the cartons

from several carton factories to a collection depot and then from the depot to serve their corresponding customers by using of heterogeneous fleet. In this study, the existing particle swarm optimization has been modified and improved by incorporating a self-adaptive inertia weight and a local search strategy. Based on the results, the proposed particle swarm optimization is able to solve the carton heterogeneous vehicle routing problem with a collection depot, and the multi-depot vehicle routing problem effectively. Moreover, this improved particle swarm optimization is feasible to reduce the required number of vehicles as well as save about 28% in total delivery cost. In summary, the improved particle swarm optimization is very appropriate to be adopted in solving the heterogeneous vehicle routing problem due to its accuracy and quickness.

Yu et al. (2016) proposed a Simulated Annealing algorithm to handle the vehicle routing problem. Initially, they have modeled an open vehicle routing problem with cross-docking as a mixed-integer linear program that minimizes the total cost. The total cost covered transportation cost and vehicle hiring cost. In this study, Simulated Annealing is first verified by solving benchmark instances for the vehicle routing problem with cross-docking and comparing the results with those obtained by CPLEX. According to the results, both Simulated Annealing and CPLEX can obtain optimal solutions to all small and medium instances. However, Simulated Annealing outperforms the CPLEX in terms of computational time and solution value for large instances.

3. Conclusions

In conclusion, vehicle routing problem is a considerable challenging issue and needed to be resolved by a very appropriate and optimal solution. Thus, more and more hybrid models or new models should be proposed and implemented in order to tackle the vehicle routing problem efficiently and effectively. Hence, future work is compulsory to be taken in order to explore more on the vehicle routing problem. Consequently, the transportation cost of the company can be minimized. Furthermore, it will also enhance the company's profit and benefit.

Acknowledements

The authors express gratitude to Universiti Tunku Abdul Rahman (UTAR).

References

Abdulkader, M.M., Gajpal, Y. and ElMekkawy, T.Y., 2015. Hybridized ant colony algorithm for the multi compartment vehicle routing problem. *Applied Soft Computing*, 37, pp. 196 – 203.

Archetti, C., Savelsbergh, M. and Speranza, M.G., 2016. The vehicle routing problem with occasional drivers. *European Journal of Operational Research*, 254 (2), pp. 472 – 480.

Arostegui, M.A., Kadipasaoglu, S.N. and Khumawala, B.M., 2006. An empirical comparison of tabu search, simulated annealing, and genetic algorithms for facilities location problems. *International Journal of Production Economics*, 103 (2), pp. 742 – 754.

Ballou, R.H., 1990. A continued comparison of several popular algorithms for vehicle routing and scheduling. *Journal of Business Logistics*, 11 (1), pp. 111.

Bell, J.E. and McMullen, P.R., 2004. Ant colony optimization techniques for the vehicle routing problem. *Advanced Engineering Informatics*, 18 (1), pp. 41 – 48.

Bertazzi, L. and Speranza, M.G., 2012. Inventory routing problems: an introduction. *EURO Journal on Transportation and Logistics*, 1 (4), pp. 307 – 326.

Braekers, K., Ramaekers, K. and Van Nieuwenhuyse, I., 2016. The vehicle routing problem: state of the art classification and review. *Computers & Industrial Engineering*, 99, pp. 300 – 313.

Bullnheimer, B., Hartl, R.F. and Strauss, C., 1999. *Applying the ant system to the vehicle routing problem*. In Meta-heuristics (pp. 285-296). Boston: Springer.

Dantzig, G. and Ramser, J., 1959. The truck dispatching problem. *Management Science*, 6 (1), pp. 80 – 91.

Erdogan, S. and Miller-Hooks, E., 2012. A green vehicle routing problem. *Transportation Research Part E: Logistics and Transportation Review*, 48 (1), pp. 100 – 114.

Flood, M., 1956. The traveling-salesman problem. *Operations Research*, 4 (1), pp. 61 – 75.

Gendreau, M., Hertz, A. and Laporte, G., 1994. A tabu search heuristic for the vehicle routing problem. *Management Science*, 40 (10), pp. 1276 – 1290.

Ghanbari, R. and Mahdavi-Amiri, N., 2011. Solving bus terminal location problems using evolutionary algorithms. *Applied Soft Computing*, 11 (1), pp. 991 – 999.

Golden, B.L., Wasil, E.A., Kelly, J.P. and Chao, I.M., 1998. *The impact of metaheuristics on solving the vehicle routing problem: algorithms, problem sets, and computational results*. In Fleet management and logistics (pp. 33-56). Boston: Springer.

Goldstein, D., Shehab, T., Casse, J. and Lin, H.C., 2010. On the formulation and solution of the convoy routing problem. *Transportation Research Part E: Logistics and Transportation Review*, 46 (4), pp. 520 – 533.

Huang, Y., Zhao, L., Van Woensel, T. and Gross, J.P., 2017. Time-dependent vehicle routing problem with path flexibility. *Transportation Research Part B: Methodological*, 95, pp. 169 – 195.

Karakatic, S. and Podgorelec, V., 2015. A survey of genetic algorithms for solving multi depot vehicle routing problem. *Applied Soft Computing*, 27, pp. 519 – 532.

Keskin, M. and Çatay, B., 2016. Partial recharge strategies for the electric vehicle routing problem with time windows. *Transportation Research Part C: Emerging Technologies*, 65, pp. 111 – 127.

Montoya, A., Gueret, C., Mendoza, J.E. and Villegas, J.G., 2017. The electric vehicle routing problem with nonlinear charging function. *Transportation Research Part B: Methodological*, 103, pp. 87 – 110.

Mutar, M.L., Aboobaider, B.M. and Hameed, A.S., 2017. Review paper in vehicle routing problem and future research trend. *International Journal of Applied Engineering Research*, 12 (22), pp. 12279 – 12283.

Osman, I.H., 1993. Metastrategy simulated annealing and tabu search algorithms for the vehicle routing problem. *Annals of Operations Research*, 41 (4), pp. 421 – 451.

Pillac, V., Gendreau, M., Gueret, C. and Medaglia, A.L., 2013. A review of dynamic vehicle routing problems. *European Journal of Operational Research*, 225 (1), pp. 1 – 11.

Prins, C., 2004. A simple and effective evolutionary algorithm for the vehicle routing problem. *Computers & Operations Research*, 31 (12), pp. 1985 – 2002.

Psaraftis, H., 1980. A dynamic-programming solution to the single vehicle many-to-many immediate request dial-a-ride problem. *Transportation Science*, 14 (2), pp. 130 – 154.

Rego, C. and Roucairol, C., 1996. *A parallel tabu search algorithm using ejection chains for the vehicle routing problem*. In Meta-Heuristics (pp. 661-675). Boston: Springer.

Rochat, Y. and Taillard, E.D., 1995. Probabilistic diversification and intensification in local search for vehicle routing. *Journal of Heuristics*, 1 (1), pp. 147 – 167.

Taillard, E., 1993. Parallel iterative search methods for vehicle routing problems. *Networks*, 23 (8), pp. 661 – 673.

Yao, B. et al., 2016. An improved particle swarm optimization for carton heterogeneous vehicle routing problem with a collection depot. *Annals of Operations Research*, 242 (2), pp. 303 – 320.

Youssef, H., Sait, S.M. and Adiche, H., 2001. Evolutionary algorithms, simulated annealing and tabu search: a comparative study. *Engineering Applications of Artificial Intelligence*, 14 (2), pp. 167 – 181.

Yu, V.F., Jewpanya, P. and Redi, A.P., 2016. Open vehicle routing problem with cross-docking. *Computers & Industrial Engineering*, 94, pp. 6 – 17.

Yuceer, U. and Ozakca, A., 2010. A truck loading problem. *Computers & Industrial Engineering*, 58 (4), pp. 766 – 773.

Shared-ride Taxi Service for First Mile and Last Mile Travel: An Overview of Issues and Strategies

Azimah Binti Mohd[a], Teoh Lay Eng[b], Khoo Hooi Ling[c]

[a,b]Department of Mathematical and Actuarial Sciences, Lee Kong Chian Faculty of Engineering and Science, Universiti Tunku Abdul Rahman, Malaysia. [*]Email (corresponding author): azimah@utar.edu.my

[c]Department of Civil Engineering, Lee Kong Chian Faculty of Engineering and Science, Universiti Tunku Abdul Rahman, Malaysia.

Abstract

First mile and last mile (FMLM) problem is a major problem for many cities. Many innovations (solutions), such as carsharing, autonomous vehicle, shuttle bus, walking, bicycling, as well as park and ride, had been proposed to solve FMLM problem. The limitations of these innovations are mainly related to travel cost, comfort, convenience, security, safety, route, schedule, distance and time. To tackle these limitations, a better solution should be proposed and developed properly in assuring a sustainable public transportation system. With regard to this, shared-ride taxi service was found to be one of the best alternatives to tackle FMLM problem. Shared-ride taxi service is one-to-many-to-one Pickup and Delivery Problem (PDP) which is a generalization of vehicle routing problem (VRP). This service possesses several advantages, including lower cost, more flexible and also more convenient. It also turns out to be a faster option with a greater opportunity to increase occupancy rates. Correspondingly, this paper aims to provide an overview of FMLM issues and strategies in relation to the existing innovations proposed to solve FMLM problem. In particular, a sustainable shared-ride taxi service will be proposed as a viable alternative. It is expected that this paper could provide some useful insights to the relevant parties in operating a sustainable shared-ride taxi service operating system as an effective alternative to tackle FMLM problem. It is also anticipated that the proposed strategy will be a win-win solution not only to the system operators but also the users (passengers).

1. Introduction

First mile (FM) is the term used to describe the movement of people and goods from the origin location to the transportation hub while last mile (LM) describes the movement of people and goods from the transportation hub to the destination locations (Mineta Transportation Institute, 2009). In overall, the difficulties for the movement of people and goods between transportation hub, origin and destination locations are known as FMLM problem. These difficulties may be due to the deficiency in the transportation mode between transportation hub, origin and destination locations (King, 2016). As such, shared-ride taxi service is proposed as a viable alternative to solve the FMLM problem (Santos and Xavier, 2015; Liang, Correia and van Arem, 2016). Generally, shared-ride taxi service refers as the mode of transportation in which individual traveller shares a taxi for a trip and splits travel costs with others who have similar itineraries and time schedule (Shaheen, et al., 2015).

The aim of this paper is to provide an overview of FMLM issues and strategies in relation to the existing innovations proposed to solve FMLM problem. The rest of the paper is structured as follows. Section 2 reviews the current innovations to solve FMLM problem and the issues of these innovations. Section 3 discusses shared-ride service, the current applications and proposed shared-ride taxi service for FMLM problem. Finally, Section 4 concludes the paper.

2. Literature Review

2.1. Current Innovations

Many innovations such as carsharing (Shaheen, et al., 1999), autonomous vehicle (Liang, Correia and van Arem, 2016), shuttle bus (Wang, et al., 2013), walking and bicycling (Brand, et al., 2017), park and ride (Duncan and Christensen, 2013), had been introduced to FMLM travellers. However, there are many issues concerning the travel cost, route, schedule, distance, time, comfort, convenience, security and safety of these innovations to solve FMLM problem.

For carsharing, a household accesses a fleet of vehicles on an as-needed basis where individuals gain the benefits of private cars without the costs and responsibilities of ownership (Shaheen, et al., 1999). Generally, carsharing systems fall into one of four sharing models: roundtrip (begin and end their trip at the same location), one-way (begin and end their trip at different locations), peer-to-peer (typically privately owned or leased with the sharing system operated by a third-party), or fractional (co-own a vehicle and share its costs and use). In Malaysia, the first carsharing application introduced was Moovby in the Klang Valley (since January 2017), followed by GoCar, SOCAR and Kwikcar (iMoney Editorial, 2018).

Automated vehicle (AV), which is also known as a driverless vehicle or self-driving vehicle, is an advanced type of vehicle which can drive itself on existing roads and can navigate many types of roadways and environmental contexts with reduced direct human input. There are six levels of driving automation from level 0 "no automation" to level 5 "full automation". Currently, there are no companies that are able to offer a fully autonomous vehicle and most of these studies use micro-simulation tools (Liang, Correia and van Arem, 2016) Recently, autonomous buses and taxis have been introduced as an approach of solving FMLM problem in Netherlands and Norway (Liang, Correia and van Arem, 2016; Roche-Cerasi, 2019).

Shuttle bus refers to a bus that travels between two points. The shuttle bus has long been the backbone of high-use locations such as a transportation hub. Shuttle bus is managed privately, sub-contracted through charter bus companies, and in some cases, government-run. Due to unresolved issues of shuttle bus, many studies have looked into improving the traditional shuttle bus by scheduling (Zhibin and Qixiang, 2013), share and shuttle bus (Shen, Zhang and Zhao, 2018), autonomous bus (Roche-Cerasi, 2019) and also merging shuttle bus and technology (Ceder and Yim, 2003). For the study of shared shuttle bus, researchers are looking into how to predict travel requirements and plan dynamic routes on the LM problem (Kong, et al., 2018).

For solving FMLM problem, walking and bicycling has been proposed by Krizek and Stonebraker, (2011); Wasfi, Ross and El-Geneidy (2013) and Brand, et al., (2017). Wasfi, Ross and El-Geneidy (2013) studied the benefit of walking and cycling while Krizek and Stonebraker (2011) studied the improvement of these modes in particular the facilities and policies. Brand, et al., (2017) discussed the aspects and system characteristics that influence integration of bus networks with walking and cycling. Furthermore, Shelat, Huisman and van Oort (2018) proposed e-bicycle and shared-bicycle to solve FMLM problem in Netherlands.

Park and Ride programs have been applied to solve FMLM problem in United States (Duncan and Christensen, 2013). Such services provide a parking spot near the transportation hub where FMLM travellers can use their own personal car. The advantages of these programs allow FMLM traveller to avoid the congestion of city and also as a feasible option for FMLM traveller who do not live within walking distance with the transportation hub (Duncan and Christensen, 2013). The studies of Park and Ride programs are mainly focusing on the demand for Park and Ride facilities, effects on travel behaviour, and the factors related to Park and Ride utilization efficiency (Zhao, et al., 2019).

2.2. Issue of Current Innovations

The main challenges in carsharing innovations are the shortage of car and relocation problem. The users of transportation hub does not have similar origin and destination locations and therefore the relocation of car to these locations emerges as the main problem in all type carsharing models (Shaheen, et al., 1999).

There are still a lot of improvements that need to be considered in AV especially to perform urban driving. (Shen, Zhang and Zhao, 2018; Liang, Correia and van Arem, 2016). According to Dass (2018), the main issue of AV is safety as AV has no ability to make right decision in emergency situations. Furthermore, AV has the issue in route identification as AV driving is difficult in snow, rain and fog weather. In addition, AV is not able to operate smoothly without detailed maps.

There are many issues regarding shuttle bus that make FMLM traveller divert to other alternative that are more user friendly. The most common issues concerning shuttle bus are schedule, route, capacity, comfort, cost, travel and waiting time (Wang, et al., 2013). The scheduling of shuttle bus usually is not based on demand analysis but based on the observations of peak hour's flow which may not be convenient for the users (Wang, et al., 2013). Generally, the route of shuttle bus are fixed with fixed stopping locations that are far from users origin and destination locations. If there are too few passengers, the operation cost of a shuttle bus cannot be covered. On the contrary, too many passengers bring poor travel experiences and security risks (Kong, et al., 2018).

The main issue in integrating walking and cycling to solve FMLM problem is the insufficient and inconvenient facilities of pathway and bicycle lane (Krizek and Stonebraker, 2011). Moreover, walking and cycling have a maximum distance limit, and hence it is not a better choice if the transportation hub is not in walking and cycling distance (Duncan and Christensen, 2013). In addition, these innovations are comfortless and inappropriate since FMLM traveller will be sweating. The capacity of bicycle is also limited and it is not a feasible choice if the number of passengers is more than two.

Park and Ride implemented to solve FMLM problem will be a success if there is a space near to the transportation hub to build a parking area (Zhao, et al., 2019). However, the transportation hub in many cities has been built for a long time. The limited space makes the entrance of transportation hub quite a distance from the parking area. Furthermore, this distance will cause transportation hub user's park illegally near the transportation hub and this is unsafe to other transportation hub users. Moreover, the safety, security and comfort of these innovations users need to be taken into account (Zhao, et al., 2019).

3. Shared-ride Service

Shared-ride service is one of the best innovations developed to resolve the FMLM problem (Shaheen, et al., 2015). The share-ride service can be static or dynamic. For the static shared-ride service, the driver arrangement is computed for a given set of trips. For the dynamic shared-ride service, each trip arrives online and a driver is arranged for an arrived trip without the knowledge of trips in the future (Agatz et al., 2011). Basically, the shared-ride service can be distinguished by four variants namely single rider and single driver arrangements, single driver and multiple rider arrangements, single rider and multiple driver arrangements as well as multiple rider and driver's arrangements (Furuhata, et al., 2015).

Shared-ride service comes at a lower cost, but provide a more flexible, more convenient, and often a faster option (Shen, Zhang and Zhao, 2018). It could be extended to rural or suburban area with the development of new technology. Many studies on shared-ride service focus on social and environmental issues such as vehicle use, ownership, vehicle miles travelled with cost savings and also convenience. Besides, shared-ride service could extend the servicing area of public networks, by connecting the gaps between transportation hub, origin and destination locations by encouraging multi-modal travel.

By considering vehicle capacity for shared-ride service, there is an opportunity to increase the occupancy of vehicle and reduce the transport shortage. Besides, by having the booking in advanced services, the operators might design a better fleet management. And also, shared-ride service could provide economic benefits, such as increased economic activity near the multi-modal hubs, cost savings to users and profitability for the operators (Furuhata, et al., 2015). Shared-ride service has the potential in solving social and environmental issues but it is also important to focus on shared-ride policy challenges in ensuring the users safety and fairness. Thus, a detailed study is needed particularly to operate shared-ride service properly.

3.1. Current Application

Shared-ride service is widely applied today by connecting technology with many types of vehicles such as public transportation, private cars, and autonomous vehicles. There are numerous applications of shared-ride service such as Grab in Malaysia and Singapore, Avego in Ireland, Carticipate, Piggyback, and EnergeticX in United States (Agatz et al., 2011).

For FMLM problem studies, Shen, Zhang and Zhao (2018) proposed and simulated an integrated autonomous vehicle for a public transportation system. They preserved the high demand bus routes and repurposed low-demand bus routes while using the shared autonomous vehicle service on demand as an alternative. Fahnenschreiber, et al., (2016) allowed dynamic shared-ride between two train rides by connecting public transport stations and dynamic shared-ride offers of private car drivers. Kong, et al., (2018) purposed shared shuttle bus to solve the FMLM problem. However, there are still a lot of improvement need to be considered in the above mentioned vehicle especially in urban driving (as discussed in section 2.2).

One of the viable shared-ride services to solve FMLM problem is shared-ride taxi service. While there are numerous applications of shared-ride taxi services, fewer efforts focus on solving FMLM problem. Hosni, Naoum-Sawaya and Artail (2014) formulated the shared-ride taxi problem as a mixed integer program. A lagrangian decomposition approach that exploits the structure of the problem is proposed as a solution methodology. They considered the maximization of profit in their objective function. Besides, Al-Ayyash, Abou-Zeid and Kaysi (2016) evaluated the market demand potential of a shared-ride taxi service in an organization-based context. They presented an integrated choice and latent variable modelling framework for modelling the number of times per week a shared-ride taxi would be used if implemented at an organization. Li, et al., (2016) introduced two stochastic variants of the shared-ride: one with stochastic travel times and one with stochastic delivery locations. They formulated a two-stage stochastic programming model with recourse. Their objective is to maximize the expected profit of serving a set of passengers and parcels by using a set of homogeneous vehicles.

The most well-known shared-ride service in Malaysia is GrabShare. GrabShare is a car shared-ride service that enables passengers to share the ride and fare while driver gain more by picking up several passengers on the same route (Grab, 2019). For GrabShare, there are more than two possible sets of rides. GrabShare uses existing GrabCar applications and makes it possible for passengers to take more than one job per ride in the same manner. It means that passengers can have the opportunity to earn more by receiving more fares from more matches. Besides, Ryde is also another shared-ride services in Malaysia. Ryde passengers pay the cost of each ride and contribute an amount based on distance travelled (Ryde, 2019). This system is still quite new in Malaysia and will take time to grow. Both Grabshared and Ryde service are free-floating service. Apparently, Malaysia's shared-ride taxi service does not integrate the service with the FMLM travel. The shared ride service usually takes place spontaneously in the transport hub. Therefore, a proper planning and policy is crucial in modelling the FMLM shared-ride service.

3.2. Shared-ride Taxi Service for FMLM Problem

3.2.1. A Brief Overview

The most closely associated routing problem to FMLM shared-ride taxi service is Pickup and Delivery Problem (PDP) which is a generalization of Vehicle Routing Problem (VRP) in which people have to be transported between transportation hub, origin and destination locations. Since the VRPs are proved to be NP-hard, therefore PDPs are known to be NP-hard. Consequently, FMLM shared-ride taxi service is NP-hard (Clarke and Wright, 1964).

The PDPs can be classified into three groups: many-to-many problem, one-to-many-to-one problem and one-to-one problem (Berbeglia, et al., 2007). FMLM shared-ride taxi service can be modelled as a one-to-many-to-one PDP and it’s related to slightly to one-to one problem (Berbeglia, et al., 2007). The solution approach to obtain an optimal solution for FMLM shared-ride taxi service is associated with the double-path

solution to the one-to-many-to-one PDP with combined demands (Gribkovskaia, et al., 2007). Double-path solution to the one-to-many-to-one PDP with combined demands can be reduced to the one-to-many-to-one with single demand and backhauls by splitting each vertex into delivery and pickup vertex. The multi-vehicle one-to-many-to-one PDP with single demand and backhauls is usually called the VRP with Backhauls (VRPB) (Clarke and Wright, 1964).

For VRPB, the vehicles capacity could accommodate multiple passengers/objects. Besides each pickup and delivery procedures for VRPB are classified in different commodity. For the solution approach exact, heuristic and metaheuristic had been implemented by the researcher (Berbeglia, et al., 2007). For one-to one PDP problem, there are three well-known studies of static PDP, namely stacker crane problem, VRP with PDP and dial-a-ride problem. For one-to one PDP problem, multiple vehicles, single commodity and exact, heuristic and metaheuristic were used to solve the model (Berbeglia, et al., 2007).

3.2.2. Model Types of Shared-ride Taxi Service

In optimizing shared-ride taxi service for FMLM problem, an appropriate model should be developed in both local-based and network-wide of FMLM travel. In addition, both static and dynamic shared-ride taxi service should be considered.

The most closely associated routing problem to local-based static FMLM shared-ride taxi service is static multi-vehicle 1-M-1-PDP with combined demands (Gribkovskaia, et al., 2007). When considering the stochastic problem, researchers only consider either stochastic demand or stochastic travel time, but not both. The stochastic travel time considered with a soft time window is deterministic and constant. However, there are variable travel times in real life (because of congestion) (Berbeglia, et al., 2007). On the other hand, due to the complexity of the problem, only single vehicle is taken into account.

Local-based dynamic shared-ride taxi service is slightly related to dynamic VRP. In these studies, dynamism is mostly considered with respect to customer requests. While stochastic data (Albareda-Sambola, Fernández and Laporte, 2014) or forecasts data (Ferrucci, Bock and Gendreau, 2013) is available, no information on future requests is assumed. For stochastic travel time, the time window considered to be soft. Backhauls are considered less than average in multi-vehicle and rarely in combination with dynamic or stochastic information. In addition, dynamic VRPB is complex.

Network-wide static shared-ride taxi service is related to Multi-Depot VRP (MDVRP) (Salhi and Nagy, 1999). A better optimal solution with minimum computational time is crucial in solving stochastic demand and travel time with tight time window. The exact algorithms for the MDVRP are rare.

Network-wide dynamic shared-ride taxi service is related to Dynamic Multi-Depot VRP (D-MDVRP) (Psaraftis, 1995). As these problem is dynamic over time, the optimal solutions of D-MDVRP is undetermined from CPLEX software. Therefore, D-MDVRP have to rely on the heuristic approach in order to quickly compute a solution to the current state of the problem. There is no benchmark test problems available for D-MDVRP. Dynamic demand obviously affect the solution because dynamic demand change the problem at the instant the demand arrived at the system (Meesuptaweekoona and Chaovalitwongseb, 2014).

3.2.3. Objective Function and Practical Constraint

According to Furuhata, et al., (2015), a reasonable fare transport that is affordable for the passengers and profitability for the operators must be designed. Therefore, a bi-objective model that maximizes operator profit and passenger cost savings should be considered in order to attain the effectiveness of the shared-ride taxi service.

The uncertainty involved should be captured by taking into account a few factors such as demand, waiting and traveling time of FMLM shared-ride taxi service. It has been addressed that these are the most important factors for the passengers and operators in consuming a shared-ride taxi service (Wang, et al., 2013). To ensure that a feasible FMLM shared-ride taxi service could be provided, the capacity constraint also turns out to be an important constraint (Kong, et al., 2018).

Furthermore, an appropriate fleet size, number of depots, satisfied requests and desired nodes for service should be capture accordingly. Generally, the developed bi-objective FMLM shared-ride taxi service model is an integer programming model since the decision variable that needs to be investigated is an integer (Santos and Xavier, 2015). Besides, mixed integer programing model also can be formed in solving bi-objective FMLM shared-ride taxi service model in view that some of the decision variables are constrained to be integer, while other variables are allowed to be non-integer (Hosni, Naoum-Sawaya and Artail, 2014).

3.2.4. Solution Approach

In finding the optimal solution, exact, heuristic and metaheuristic have been used as the solution approaches (Berbeglia, et al., 2007). To obtain exact solutions, Branch and Bound as well as Branch and Cut are used mainly due to the characteristics of these methods which are more reliable and faster in generating optimal solution (Baldacci and Mingozzi, 2008). These methods have been used to solve very large integer programming problems (Berbeglia, et al., 2007). For heuristic approach, 2-phase and constructive algorithms are used to optimize the model (Clarke and Wright, 1964; Salhi and Nagy, 1999) while for metaheuristics approach, genetic algorithm, adaptive large neighbourhood search, variable neighbourhood search, tabu search and ant colony optimization have been used to determine the expected outputs (Psaraftis, 1995; Berbeglia, et al., 2007).

However, there are still some limitations in the proposed algorithms and the computational programs that should be identified. An appropriate heuristics method with the aid of the programing software such as CPLEX or Python should be applied in the future to solve the local-based and network-wide FMLM static and dynamic shared-ride taxi service (Hosni, Naoum-Sawaya and Artail, 2014).

4. Conclusions

FMLM problem is a crucial problem to operate a sustainable transportation network. A sustainable innovation should be developed to ensure the smoothness of the transportation systems especially in the cities. Thus, a better and efficient operational network that can maximize the savings of passengers should be developed. Moreover, a reasonable fare system that is affordable for the passengers and also profitability to the operators should be designed by taking into account numerous aspects including operating routes, schedule, cost, vehicle capacity and comforts. Besides, a feasible model should be developed for both local-based and network-wide transportation systems, by considering static and dynamic services. Concisely, it is anticipated that a bi-objective optimization model would turn out to be a feasible model in operating a sustainable FMLM shared-ride taxi system.

References

Al-Ayyash, Z., Abou-Zeid, M. and Kaysi, I. (2016). Modeling the demand for a shared-ride taxi service: An application to an organization-based context. *Transport Policy*, 48, pp.169–182.

Albareda-Sambola, M., Fernández, E. and Laporte, G. (2014). The dynamic multiperiod vehicle routing problem with probabilistic information. *Computers & Operations Research*, 48, pp.31–39.

Agatz, N.A.H., Erera, A.L., Savelsbergh, M.W.P. and Wang, X. (2011). Dynamic ride-sharing: A simulation study in metro Atlanta. *Transportation Research Part B: Methodological*, 45(9), pp.1450–1464.

Baldacci, R. and Mingozzi, A. (2008). A unified exact method for solving different classes of vehicle routing problems. *Mathematical Programming*, 120(2), pp.347–380.

Brand, J., van Oort, N., Hoogendoorn, S. and Schalkwijk, B., 2017. Integration of bus networks with walking and cycling. *5th IEEE International Conference on Models and Technologies for Intelligent Transportation Systems (MT-ITS),* pp.750-755.

iMoney Editorial, 2018. Will You Ditch Ride-hailing For Car-sharing? *iMoney Group Articles, Autos.* [Online]. Available at: https://www.imoney.my/articles/car-sharing-malaysians [Accessed 8 October 2019].

Berbeglia, G., Cordeau, J.F., Gribkovskaia, I. and Laporte, G., 2007. Static pickup and delivery problems: a classification scheme and survey. *An Official Journal of the Spanish Society of Statistics and Operations Research*, 15(1), pp. 1–31.

Ceder, A. and Yim, Y.B., 2003. Integrated Smart Feeder/Shuttle Bus Service, *California PATH Working Paper*, Institute of Transportation Studies, University of California, Berkeley.

Clarke, G. and Wright, J.W., 1964. Scheduling of vehicles from a central depot to a number of delivery Points. *Operations Research,* 12 (4), pp 568-581.

Dass, R., 2018. 5 Key Challenges faced by Self-driving cars. *Medium*, [Online]. Available at: https://medium.com/ [Accessed 8 October 2019].

Duncan, M. and Christensen, R.K., 2013. An analysis of park-and-ride provision at light rail stations across the US. *Transport Policy*, 25, pp. 148-157.

Fahnenschreiber, S., Gundling, F., Keyhani, M.H. and Schnee, M., 2016. A multi-modal routing approach combining dynamic shared-ride and public transport. *Transportation Research Procedia*, 13, pp. 176-183.

Ferrucci, F., Bock, S. and Gendreau, M., 2013. A pro-active real-time control approach for dynamic vehicle routing problems dealing with the delivery of urgent goods. *European Journal of Operational Research*, 225(1), pp. 130–141.

Furuhata, M., Dessouky, M., Ordonez, F., Brunet, M., Wang, X. and Koeing, S., 2015. Ridesharing: The state-of-the-art and future directions. *Transportation Research Part B,* pp.28-46.

Grab. 2019. [Online]. Available at:/https://www.grab.com/my/ [Accessed 9 October 2019].

Gribkovskaia, I., Halskau sr,Ø., Laporte, G. and Vlcek, M., 2007.General solutions to the single vehicle routing problem with pickups and deliveries. *European Journal of Operational Research*, 180, pp. 568–584.

Hosni, H., Naoum-Sawaya, J. and Artail, H., 2014. The shared-taxi problem: Formulation and solution methods. *Transportation Research Part B,* 70, pp. 303-318.

Roche-Cerasi, I., 2019. Public acceptance of driverless shuttles in Norway. *Transportation Research Part F: Traffic Psychology and Behaviour*, 66, pp. 162-183.

King, D.A., 2016. What Do We know About the "First Mile/Last Mile" Problem for Transit? *Transportist by David Levinsion* [https://transportist.org/author/davidaking2014/]

Kong, X., Li, M., Tang, T., Tian, K., Moreira-Matias, L. and Xia, F., 2018. Shared subway shuttle bus route planning based on transport data analytics. *IEEE Transactions on Automation Science and Engineering*, pp.1-14.

Krizek, K. J. and Stonebrake, E.W., 2011. Assessing options to enhance bicycle and transit integration. *Transportation Research Record*, 2217, 162–167.

Li, B., Krushinky, D., Woensel T., V. and Reijers, H., A. 2016. The share-a-ride problem with stochastic travel times and stochastic delivery locations. *Transportation Research Part C,* 67, pp. 95–108.

Liang, X., Almeida, G.H. and Arem, C.B., 2016. Optimizing the service area and trip selection of an electric automated taxi system used for the last mile of train trips. *Transportation Research Part E,* 93, pp. 115–129.

Meesuptaweekoona, K. and Chaovalitwongse, P., 2014. Dynamic vehicle routing problem with multiple depots. *Engineering Journal*, 18 (4), pp.135-149.

Psaraftis, H.N., 1995. Dynamic vehicle routing: status and prospects. *Annals of Operations Research,* 61, pp. 143–164.

Ryde, 2019. Available at:https://www.rydesharing.com/ [Accessed 9 October 2019].

Santos, D.O. and Xavier E.C., 2015. Taxi and ride sharing: a dynamic dial-a-ride problem with money as an incentive. *Expert Systems with Applications*, 42, pp. 6728-6737.

Salhi, S. and Nagy, G., 1999. A cluster insertion heuristic for single and multiple depot vehicle routing problems with backhauling. *Journal of the Operational Research Society*, 50, pp. 1034–1042.

Shelat, S., Huisman, R. and van Oort, N., 2018. Analysing the trip and user characteristics of the combined bicycle and transit mode. *Research in Transportation Economics*, 69, pp. 68-76.

Shen, Y., Zhang, H. and Zhao, J., 2018. Integrating shared autonomous vehicle in public transportation system: A supply-side simulation of the first-mile service in Singapore. *Transportation Research Part A: Policy and Practice*, 113, pp. 125-136.

Shaheen, Susan, Sperling, Daniel, Wagner and Conrad, 1999. A short history of carsharing in the 90's. *Journal of World Transport Policy & Practice*, 5(3), pp.18-40.

Mineta Transportation Institute, *Using Bicycles for the First and Last Mile of a Commute*, pp. 1-56, 2009.

Wang, B., Zhao, L., Pang, Y., Zhang, D. and Yang, X., 2013. Analysis of passenger's choice between shuttle bus and illegal taxi. *Procedia - Social and Behavioral Sciences*, 96, pp. 1948 – 1960.

Wasfi, R.A., Ross, N.A. and El-Geneidy, A.M. (2013). Achieving recommended daily physical activity levels through commuting by public transportation: Unpacking individual and contextual influences. *Health & Place*, 23, pp.18–25.

Zhoa, X., Chen, P., Jiao, J., Chen, X. and Bischak, C., 2019. How does 'park and ride' perform? An evaluation using longitudinal data. *Transport Policy,* 74, pp. 15-23.

Zhibin, J. and Qixiang, H., 2013. A service-based method to generate shuttle bus timetable in accordance with rail transit timetable. *Procedia - Social and Behavioral Sciences*, 96, pp.1890-1897.

CMS Events

January

Date : 09 January 2019 (Wednesday)

Time : 2:30pm - 4:00pm

Venue : KB100, UTAR (Sungai Long Campus)

Speaker : Mr. Kelvin Hii Chee Yun
(MSIG Insurance (Malaysia) Bhd.)

Organizer : Department of Mathematical and Actuarial Sciences (DMAS),
Centre for Mathematical Sciences (CMS)

IAP Talk For Final Year Students

February

MetLife's Actuarial Industrial Talk

Date : 26 February 2019 (Tuesday)

Time : 8:30am - 10:00am

Venue : KB209, UTAR (Sungai Long Campus)

Speakers : Tim Braswell, Stephanie McGovern, Nick Walters, Des Thomas, Rick Butler & Micky Kuo (MetLife, Inc.)

Organizer : Department of Mathematical and Actuarial Sciences (DMAS), Centre for Mathematical Sciences (CMS)

March

Understanding of Actuarial Sciences Studies and Its Applications

Date : 25 March 2019 (Monday)

Time : 10:00am - 11:00am

Venue : KB214, UTAR (Sungai Long Campus)

Speakers : Mr Goh Chek Heong, Ms Sasa Tan Yuin Joo
(Great Eastern Life Assurance (M) Bhd.)

Organizer : Department of Mathematical and Actuarial Sciences (DMAS),
Centre for Mathematical Science (CMS)

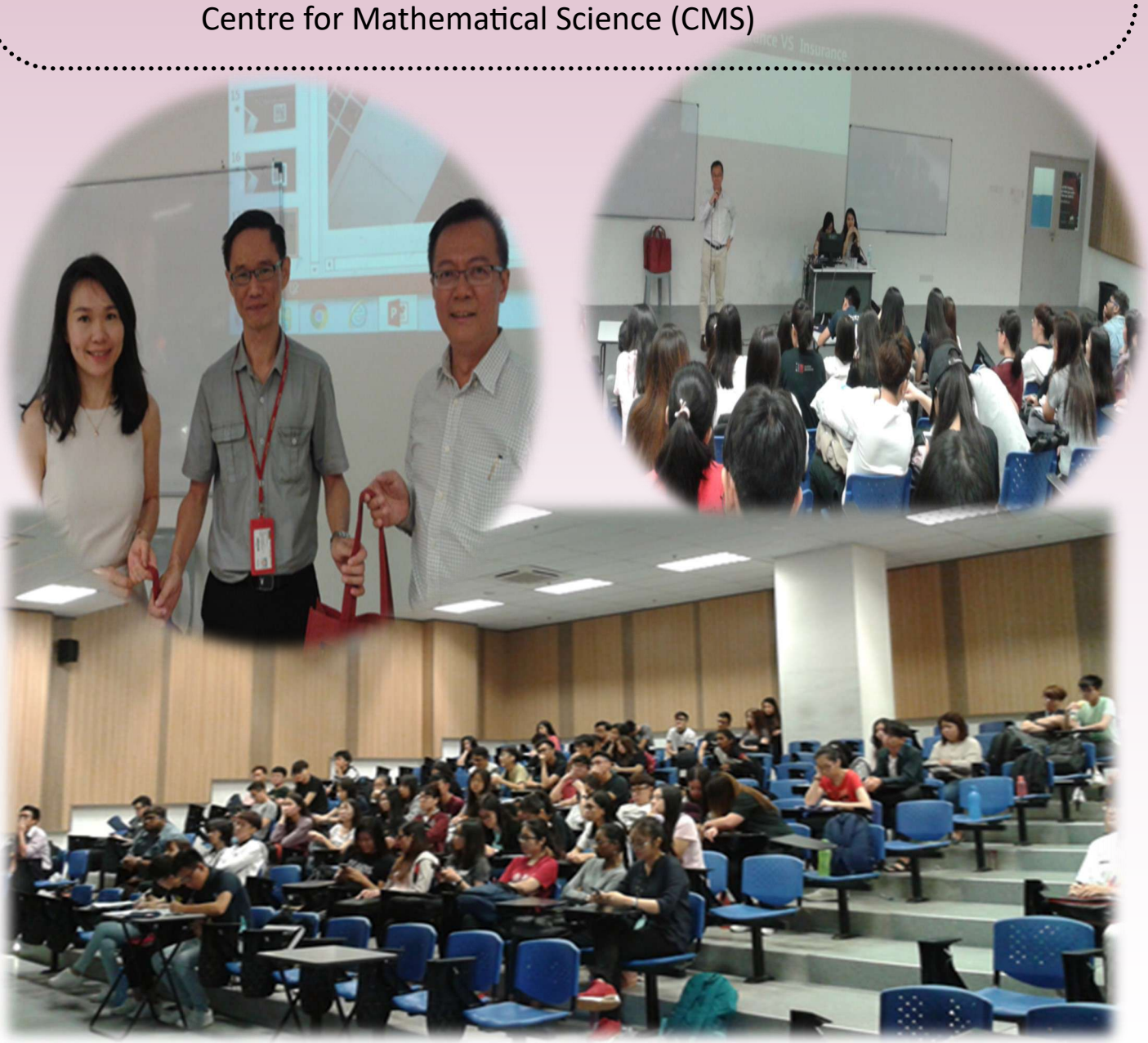

April

CMS One-Day Research Seminar

Date : 19 April 2019 (Friday)

Time : 8:50am - 5:00pm

Venue : KB110, UTAR
(Sungai Long Campus)

Speakers :

- Prof. Pooi Ah Hin
- Dr. Goh Yong Kheng
- Dr. Sim Hong Seng
- Dr. Chang Yun Fah
- Prof. Chia Gek Ling

April

Workshop on Python in Statistical Modelling

Date : 22 & 23 April 2019

Trainer : Mr. Chin Ching Herny (CMS, UTAR)

Facilitator : Dr. Mahboobeh Zangeneh Sirdari (CMS, UTAR)

Organizer : Institute for Mathematical Research (INSPEM), Universiti Putra Malaysia

Co-organizer: Centre for Mathematical Sciences (CMS)

May

Robust Tensor Completion and Its Application

Date : 15 May 2019 (Wednesday)

Time : 3:30pm - 4:30pm

Venue : KB520, UTAR (Sungai Long Campus)

Speaker : Prof Michael Ng Kwok Po (Hong Kong Baptist University)

Organizer : Department of Mathematical and Actuarial Sciences (DMAS), Centre for Mathematical Sciences (CMS)

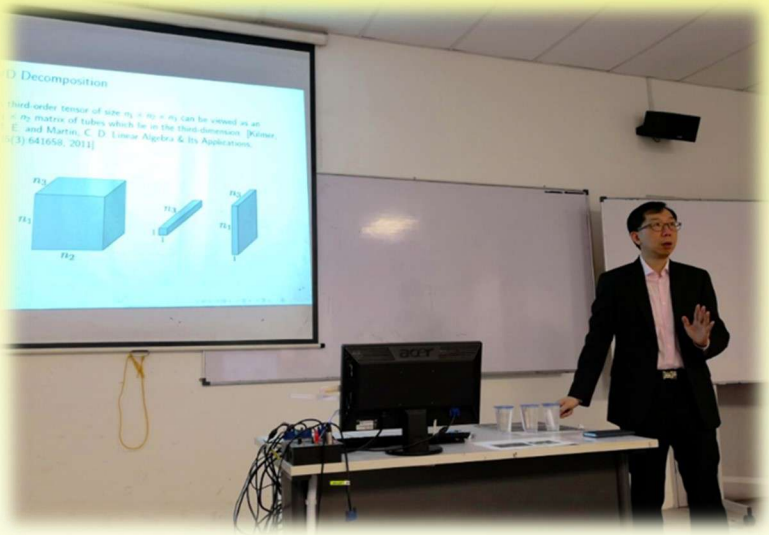

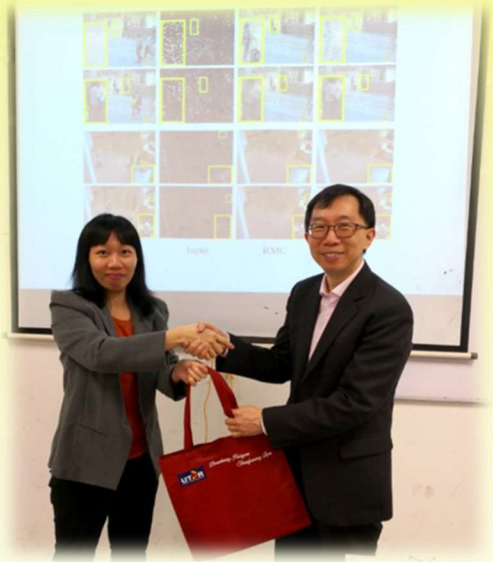

May

Effective Teaching Skills in Mathematic for Engineering Students

Date : 24 May 2019 (Friday)

Time : 10:00am - 11:00am

Venue : D121, UTAR (Kampar Campus)

Speaker : Mr Chong Fook Seng (FSc, UTAR)

Organizer : Centre for Mathematical Sciences (CMS)

June

Applications of Graph Theory in Data Science

Date : 24 June 2019 (Monday)

Time : 9.30am - 11.30am

Venue : KA600D, UTAR (Sungai Long Campus)

Speaker : Dr. Gobithaasan Rudrusamy
(Universiti Malaysia Terengganu)

Organizer : Centre for Mathematical Sciences (CMS)

July

Industry Talk by Alliance Bank

Date : 05 July 2019 (Friday)

Time : 9:00am - 5:00pm

Venue : KB313 & KB323, UTAR (Sungai Long Campus)

Speakers : Ms Heng Ai Lee, Ms Hor Jiun Ru (Alliance Bank Malaysia Berhad)

Organizer: Department of Mathematical and Actuarial Sciences (DMAS), Centre for Mathematical Sciences (CMS)

July

Preparation on the Application for Anugerah Akademik Negara (AAN) - Anugerah Pengajaran

Date : 12 July 2019 (Friday)

Time : 10:00am - 11:00am

Venue : D121, UTAR (Kampar Campus)

Speaker : Mr Chong Fook Seng (FSc, UTAR)

Organizer : Centre for Mathematical Sciences (CMS)

August

Technical Talk for Lanzhou Jiaotong University, China

Date : 5 & 9 August 2019

Time : 11:00am - 1:00pm & 9:00am - 11:00am

Venue : E010 & KB315, UTAR (Kampar Campus, Sungai Long Campus)

Speakers : Encik Khairul Rizuan bin Suliman (UTAR, Kampar Campus) & Ts Dr Teoh Lay Eng (UTAR, Sungai Long Campus)

Organizer : Faculty of Engineering and Green Technology (FEGT), UTAR

August

Deep-Learning Solution to Portfolio Selection with Serially-Dependent Returns

Date : 16 August 2019 (Friday)

Time : 3:30pm - 4:30pm

Venue : KB208, UTAR (Sungai Long Campus)

Speaker : Professor Wong Hoi Yin (The Chinese University of Hong Kong)

Organizer : Department of Mathematical and Actuarial Sciences (DMAS), Centre for Mathematical Sciences (CMS)

August

Matrix Visualization:
New Generation of Exploratory Data Analysis

Date : 19 August 2019 (Monday)

Time : 2:00pm - 3:00pm

Venue : KB211, UTAR (Sungai Long Campus)

Speaker : Dr Chun-houh Chen (Academia Sinica, Taiwan)

Organizer : Department of Mathematical and Actuarial Sciences (DMAS), Centre for Mathematical Sciences (CMS)

August

On Lifetime Data Modelling and Model Selection With Extended Weibull Distribution

Date : 19 August 2019 (Monday)

Time : 3:00pm - 4:00pm

Venue : KB211, UTAR (Sungai Long Campus)

Speaker : Professor Xie Min (City University of Hong Kong)

Organizer : Department of Mathematical and Actuarial Sciences (DMAS), Centre for Mathematical Sciences (CMS)

August

Currency Hedging and Fair Premiums in Life Insurance Guaranty Schemes

Date :	20 August 2019 (Tuesday)
Time :	3:00pm - 4:00pm
Venue :	KB107, UTAR (Sungai Long Campus)
Speaker :	Professor Bill Chang Shih-Chieh (National Chengchi University, Taiwan)
Organizer :	Department of Mathematical and Actuarial Sciences (DMAS), Centre for Mathematical Sciences (CMS)

October

LKCFES
Postgraduate Research Colloquium 2019

Date : 11 October 2019 (Friday)

Time : 9.30am - 5.00pm

Venue : MPH, UTAR (Sungai Long Campus)

Speakers : LKCFES Postgraduate Students

Organizer : Lee Kong Chian Faculty of Engineering and Science (LKCFES), CPAMR, CPSE, CRIE, CCS, CCIS, CCSN, CMS, CDRR, CHST, CVT, COSA

November

Professional Talks by Invited Speakers from Universiti Putra Malaysia (UPM)

Date : 08 November 2019 (Friday)

Time : 2:30pm - 4:30pm

Venue : KB213, UTAR (Sungai Long Campus)

Speakers : Dr Chen Chuei Yee, Dr Yow Kai Siong, Dr Lim Fong Peng (Universiti Putra Malaysia)

Organizer : Department of Mathematical and Actuarial Sciences (DMAS), Centre for Mathematical Sciences (CMS)

November

Talk 1: Stochastic Control Application to Energy Tolling Agreements

Talk 2: Dependence in Binary Outcomes: A Quadratic Exponential Model Approach

Date : 27 November 2019 (Wednesday)

Time : 2:00pm - 4:00pm

Venue : KB213, UTAR (Sungai Long Campus)

Speakers : Talk 1: Dr Leyla Ranjbari

Talk 2: Dr Mahboobeh Zangeneh Sirdari

Organizer : Department of Mathematical and Actuarial Sciences (DMAS), Centre for Mathematical Sciences (CMS)

November

CMS Research Sharing Seminar 2019

Date : 29 November 2019 (Friday)

Time : 10:00am - 4:00pm

Venue : IDK 5, 7 & 8 (UTAR, Kampar Campus)

Speakers : Grant Holders & Postgraduate Students

Organizer : Department of Mathematical and Actuarial Sciences (DMAS), Centre for Mathematical Sciences (CMS)

Memorable Events


THANK YOU
FOR YOUR SERVICES
AND CONTRIBUTIONS
IN THE YEAR 2019
DR CHANG YUN FAH
CENTRE FOR MATHEMATICAL SCIENCES
(CMS)
UNIVERSITI TUNKU ABDUL RAHMAN

ACKNOWLEDGEMENTS

Thank you for your contributions!

Universiti Tunku Abdul Rahman

Institute of Postgraduate Studies and Research (IPSR), UTAR

Lee Kong Chian Faculty of Engineering and Science, UTAR

Department of Mathematical and Actuarial Sciences, UTAR

Actuarial Science Society, UTAR

CMS Committee Members

Research Collaborators

Event Participants

Industry Partners

Invited Speakers

Sponsors

Alumni

Let's move on hand-in-hand closely towards a great 2020!